

**CONSTRUCTABILITY AND
DURABILITY OF CONCRETE
PAVEMENTS**

Final Report

PROJECT SPR 823



Oregon Department of Transportation

CONSTRUCTABILITY AND DURABILITY OF CONCRETE PAVEMENTS

Final Report

PROJECT SPR 823

by

David Trejo, Ph.D., P.E.

Pavan Vaddey, Ph.D.

Gokul Dev Vasudevan

O. Burkan Isgor, Ph.D., P.E.

Armen Amirkhonian, Ph.D.

for

Oregon Department of Transportation

Research Section

555 13th Street NE, Suite 1

Salem OR 97301

and

Federal Highway Administration

1200 New Jersey Avenue SE

Washington, DC 20590

January 2022

1. Report No. FHWA-OR-RD-22-10	2. Government Accession No.	3. Recipient's Catalog No.	
4. Title and Subtitle Constructability and Durability of Concrete Pavements		5. Report Date January 2022	
		6. Performing Organization Code	
7. Author(s) David Trejo, 0000-0001-8647-8096 Naga Pavan Vaddey ¹ , 0000-0002-1999-0003 Gokul Dev Vasudevan, 0000-0002-3310-2535 O. Burkan Isgor, 0000-0002-0554-3501 Armen Amirkhanian, 0000-0002-8436-8958		8. Performing Organization Report No.	
9. Performing Organization Name and Address School of Civil and Construction Engineering Oregon State University 101 Kearney Hall Corvallis, Oregon 97331		10. Work Unit No. (TRAIS)	
		11. Contract or Grant No.	
12. Sponsoring Agency Name and Address Oregon Dept. of Transportation Research Section 555 13 th Street NE, Suite 1 Salem, OR 97301		13. Type of Report and Period Covered: Final Report	
		14. Sponsoring Agency Code	
15. Supplementary Notes			
16. Abstract: Concrete for pavements must be proportioned so that the concrete is economical and durable. Because ordinary Portland cement (OPC) is the most costly component and is generally less durable than the aggregates, the OPC should be minimized. OPC significantly contributes to CO ₂ during manufacturing. Therefore, minimizing the OPC will also make the concrete greener. This research developed a mixture proportioning method to minimize the OPC content. This is achieved by characterizing the aggregates that will be use in the concrete to minimize the voids in the aggregates (fine and coarse). This will result in lower OPC requirements. This research assessed concretes proportioned with the new method. All concretes met edge slump and surface void requirements. All concretes met compressive and flexural strength requirements. Most concretes met formation factor requirements. Select testing indicates that shrinkage, as measured with shrinkage rings, is likely dependent on paste content; lower paste contents lead to lower shrinkage, but more research is needed. Select concretes did not perform well in freeze-thaw testing, however void spacing and size were not assessed.			
17. Key Words: Pavements; concrete, mixture proportioning; sustainability; resilience, aggregate void, paste volume		18. Distribution Statement Copies available from NTIS, and online at www.oregon.gov/ODOT/TD/TP_RES/	
19. Security Classification (of this report): Unclassified	20. Security Classification (of this page): Unclassified	21. No. of Pages 217	22. Price

SI* (MODERN METRIC) CONVERSION FACTORS

APPROXIMATE CONVERSIONS TO SI UNITS					APPROXIMATE CONVERSIONS FROM SI UNITS				
Symbol	When You Know	Multiply By	To Find	Symbol	Symbol	When You Know	Multiply By	To Find	Symbol
<u>LENGTH</u>					<u>LENGTH</u>				
in	inches	25.4	millimeters	mm	mm	millimeters	0.039	inches	in
ft	feet	0.305	meters	m	m	meters	3.28	feet	ft
yd	yards	0.914	meters	m	m	meters	1.09	yards	yd
mi	miles	1.61	kilometers	km	km	kilometers	0.621	miles	mi
<u>AREA</u>					<u>AREA</u>				
in ²	square inches	645.2	millimeters squared	mm ²	mm ²	millimeters squared	0.0016	square inches	in ²
ft ²	square feet	0.093	meters squared	m ²	m ²	meters squared	10.764	square feet	ft ²
yd ²	square yards	0.836	meters squared	m ²	m ²	meters squared	1.196	square yards	yd ²
ac	acres	0.405	hectares	ha	ha	hectares	2.47	acres	ac
mi ²	square miles	2.59	kilometers squared	km ²	km ²	kilometers squared	0.386	square miles	mi ²
<u>VOLUME</u>					<u>VOLUME</u>				
fl oz	fluid ounces	29.57	milliliters	ml	ml	milliliters	0.034	fluid ounces	fl oz
gal	gallons	3.785	liters	L	L	liters	0.264	gallons	gal
ft ³	cubic feet	0.028	meters cubed	m ³	m ³	meters cubed	35.315	cubic feet	ft ³
yd ³	cubic yards	0.765	meters cubed	m ³	m ³	meters cubed	1.308	cubic yards	yd ³
~NOTE: Volumes greater than 1000 L shall be shown in m ³ .									
<u>MASS</u>					<u>MASS</u>				
oz	ounces	28.35	grams	g	g	grams	0.035	ounces	oz
lb	pounds	0.454	kilograms	kg	kg	kilograms	2.205	pounds	lb
T	short tons (2000 lb)	0.907	megagrams	Mg	Mg	megagrams	1.102	short tons (2000 lb)	T
<u>TEMPERATURE (exact)</u>					<u>TEMPERATURE (exact)</u>				
°F	Fahrenheit	(F-32)/1.8	Celsius	°C	°C	Celsius	1.8C+32	Fahrenheit	°F

*SI is the symbol for the International System of Measurement

ACKNOWLEDGEMENTS

The authors gratefully acknowledge the individuals that assisted with making this research successful and implementable. The following individual provided guidance, assistance, and experience to the project team. Undergraduate research students at Oregon State University included Nicholas Ole Peterson, Eric Daniel Moreno Rangel, Thanh Dat Mai, Kevin M Davis, and Rafael Ramirez Vargas. Graduate students at Oregon State University included Keshav Bharadwaj Ravi (regarding TP119 testing) and Dr. Siva Teja Chopperla (regarding dimensional stability and testing). Greyson Teremi, Jeff Gent, and James Batti, technicians and machinists at Oregon State University, were instrumental in assisting with instrumentation, fabrication of specimens, and general troubleshooting. This research would not have been possible without the assistance of Oregon Department of Transportation personnel, including Justin Moderie, Austin Johnson, Norris Shippen, Scott Nelson, Daniel Schiller, and Cristhian Galvez. Special thanks go to our industry partners that assisted with providing the field perspective for the research: Greg Wong (Knife River Corporation), Jon Berger (Concrete Placing Co., Inc.), and Jim Powell (American Concrete Pavement Association). Special thanks to Jon Berger and Dave Burg (AshGrove Cement) for providing aggregates and cementitious materials for the project.

DISCLAIMER

This document is disseminated under the sponsorship of the Oregon Department of Transportation and the United States Department of Transportation in the interest of information exchange. The State of Oregon and the United States Government assume no liability of its contents or use thereof.

The contents of this report reflect the view of the authors who are solely responsible for the facts and accuracy of the material presented. The contents do not necessarily reflect the official views of the Oregon Department of Transportation or the United States Department of Transportation.

The State of Oregon and the United States Government do not endorse products of manufacturers. Trademarks or manufacturers' names appear herein only because they are considered essential to the object of this document.

This report does not constitute a standard, specification, or regulation.

TABLE OF CONTENTS

1.0	INTRODUCTION.....	1
1.1	RESEARCH OBJECTIVES AND APPROACH.....	2
1.2	OUTLINE OF REPORT	2
2.0	LITERATURE REVIEW	5
2.1	AGGREGATE GRADATION PARTICLE PACKING MODELS.....	5
2.2	STANDARD GRADATION CHARTS	6
2.2.1	<i>0.45 power chart</i>	6
2.2.2	<i>Haystack plot</i>	7
2.2.3	<i>Tarantula chart</i>	9
2.3	PAVING CONCRETE SPECIFICATIONS FOR DIFFERENT SHAS.....	10
2.3.1	<i>Oregon DOT (ODOT)</i>	11
2.3.2	<i>Texas DOT (TxDOT)</i>	12
2.3.3	<i>Pennsylvania DOT (PennDOT)</i>	13
2.3.4	<i>California DOT (Caltrans)</i>	14
2.3.5	<i>Iowa DOT</i>	16
2.3.6	<i>Illinois DOT (IDOT)</i>	17
2.4	COMPARISON OF AGGREGATE GRADATIONS FROM DIFFERENT SHAS.....	18
2.5	PERFORMANCE OF PAVING MIXTURES	24
2.5.1	<i>Influence of aggregate type and gradation</i>	24
2.5.2	<i>Influence of paste volume, binder type, w/cm, and air entrainment</i>	25
2.6	SUMMARY	27
3.0	PROJECT BACKGROUND.....	29
3.1	AGGREGATE GRADATIONS FOR PRELIMINARY STUDY	29
3.2	TESTING AND RESULTS FROM PRELIMINARY STUDY	34
3.2.1	<i>Mixing and Standard Fresh Properties</i>	35
3.2.2	<i>The Box Test</i>	35
3.2.3	<i>Hardened concrete properties</i>	36
3.3	RESULTS AND DISCUSSION FROM PRELIMINARY STUDY	39
3.3.1	<i>Fresh concrete characteristics</i>	39
3.3.2	<i>Box Test</i>	40
3.4	HARDENED CONCRETE PROPERTIES.....	42
3.4.1	<i>Strength Properties</i>	42
3.4.2	<i>Formation Factor</i>	43
3.5	SUMMARY OF FINDINGS FROM PRELIMINARY STUDY	45
4.0	METHODOLOGY FOR DETERMINING OPTIMUM PASTE CONTENT.....	47
4.1	STEP 1. CHARACTERIZE COARSE AND FINE AGGREGATES.....	48
4.2	STEP 2. PERFORM AASHTO T 19M (2014A) TEST AND DETERMINE AV_{MIN}	48
4.3	STEP 3. DETERMINE IF COMBINED AGGREGATE GRADATION MEETS PROJECT REQUIREMENTS	50
4.4	STEP 4. DETERMINE PASTE AND AGGREGATE VOLUMES.....	50
4.5	STEP 5. DETERMINE W/CM AND BINDER QUANTITY:.....	53

4.6	STEP 6. DETERMINE FINE AGGREGATE AND COARSE AGGREGATE QUANTITIES:	54
4.7	STEP 7. CHECK CALCULATIONS AND PERFORM TRIAL MIXTURES:	55
4.8	SUMMARY	56
5.0	EXERIMENTAL PROGRAM AND MATERIALS	57
5.1	PHASE 1 – AGGREGATE CHARACTERIZATION	57
5.2	PHASE 2	58
5.2.1	<i>Phase 2A-Identifying Required WR and Paste Volumes for Placeability</i>	58
5.2.2	<i>Phase 2B-Identifying Influence of Paste Volume on Placeability</i>	60
5.2.3	<i>Phase 2C-Assessment of Fresh and Hardened Characteristics</i>	62
5.2.4	<i>Materials</i>	66
5.3	SUMMARY	72
6.0	RESULTS AND DISCUSSION	73
6.1	PHASE 1 - IDENTIFYING AV_{MIN}	73
6.1.1	<i>Comparison between AASHTO T 19M (2014a) and packing models</i>	75
6.1.2	<i>Combined gradations at AV_{min} and Comparison with Models</i>	76
6.1.3	<i>Summary of Phase 1</i>	87
6.2	PHASE 2A – DETERMINING WR REQUIREMENTS	88
6.2.1	<i>Summary of Phase 2A</i>	92
6.3	PHASE 2B – DETERMINING PV/AV	92
6.3.1	<i>Summary of Phase 2B</i>	95
6.4	PHASE 2C – ASSESSMENT OF CONCRETES USING VARYING PV/AV VALUES	95
6.4.1	<i>Test Results and Discussions</i>	97
6.4.2	<i>Effects of paste volume and total binder content</i>	101
6.4.3	<i>Effect of binder type</i>	124
6.4.4	<i>Effect of w/cm</i>	134
7.0	CONCLUSIONS, RECOMMENDATIONS, AND NEEDED RESEARCH.....	139
7.1	CONCLUSIONS.....	140
7.2	RECOMMENDATIONS.....	141
7.3	NEEDED RESEARCH	142
8.0	REFERENCES.....	145
	APPENDIX.....	A-1

LIST OF TABLES

Table 2.1:	ODOT Percent-passing Limits for Coarse Aggregates.	11
Table 2.2:	ODOT Percent-passing Limits for Fine Aggregates.	11
Table 2.3:	ODOT Percent-passing Limits for Combined Aggregates.....	12
Table 2.4:	TxDOT Percent-passing Limits for Coarse Aggregates.....	13
Table 2.5:	TxDOT Percent-passing Limits for Fine Aggregates.....	13
Table 2.6:	PennDOT Percent-passing Limits for Coarse Aggregates.	14
Table 2.7:	PennDOT Percent-passing Limits for Fine Aggregates	14
Table 2.8:	Gradation Limits Specified for Different Individual Sieves.....	15

Table 2.9: Caltrans Percent-passing Limits for Coarse Aggregates Specified as ‘Operating Range.’	15
Table 2.10: Caltrans Percent-passing Limits for Fine Aggregates Specified as ‘Operating Range.’	16
Table 2.11: Caltrans Percent-passing Limits for Combined Aggregates.....	16
Table 2.12: Iowa DOT Percent-passing Limits for Coarse Aggregates.	17
Table 2.13: Iowa DOT Percent-passing Limits for Fine Aggregates.	17
Table 2.14: IDOT Percent-passing Limits for Coarse Aggregates.	18
Table 2.15: IDOT Percent-passing Limits for Fine Aggregates.	18
Table 2.16: Comparison of Coarse Aggregate Gradations from Different SHAs.	19
Table 2.17: Comparison of Fine Aggregate Gradations from Different SHAs.	19
Table 2.18: ODOT Percent-passing Limits for Combined Aggregates.....	19
Table 3.1: Control Sieves for Bailey Method for both Coarse and Fine Gradations.....	30
Table 3.2: Recommended Ranges for Bailey Mixture Design Ratios (Vavrik et al. 2002, 2001).	31
Table 3.3: Bailey Gradation Parameters for Mixtures Tested.	31
Table 3.4: Index of Particle Size and Texture Values for each Sieve Size and Aggregate Source.	32
Table 3.5: Weighted Particle Indexes for the Three Gradations used in this Study.	32
Table 3.6: Mixture Designs used in this Study. All units in lbs/yd ³ (kg/m ³).....	34
Table 3.7: Standard Fresh Properties of Tested Mixtures.....	39
Table 3.8: Comparison of Grid Overlay and Visual Assessment Values for Surface Voiding Characterization.	41
Table 3.9: Calculated Formation Factor Values for each Mixture.	44
Table 5.1: Aggregate Types and Sources.	57
Table 5.2: Combined Aggregate Systems Tested in Phase 2A.....	59
Table 5.3: Details of Different Mixtures Evaluated as Part of Phase 2A.	59
Table 5.4: Systems Evaluated in Phase 2B.....	60
Table 5.5: Details of Different Mixtures Evaluated in Phase 2B.	61
Table 5.6: Mixtures Evaluated in Phase 2C.....	64
Table 5.7: Groups of Concrete Mixtures used for Assessing Different Study Parameters.....	65
Table 5.8: List of Physical Tests Conducted as Part of Phase 2C	65
Table 5.9: Coarse Aggregate Characteristics.....	67
Table 5.10: Fine Aggregate Characteristics.....	67
Table 5.11: Chemical Compositions of the Different Cementitious Materials, %.	72
Table 6.1: F/C _{opt} and AV _{min} for Different Systems.....	75
Table 6.2: A Summary of Admixture Requirements and Fresh Characteristics for Mixtures Evaluated in Phase 2A.	89
Table 6.3: Results from Phase 2b Test Program.....	94
Table 6.4: Groups of Concrete Mixtures used for Assessing Different Study Parameters.....	96
Table 6.5: Summary of Admixture Dosages, Fresh Characteristics, Paste Volumes, Binder Contents, and PV/AV Values Recorded for Phase 2C Concrete Mixtures.....	98
Table 6.6: Summary of Average Test Values Estimated for Different Hardened Properties of Phase 2C Concrete Mixtures.....	100
Table 6.7: Predicted RCP Test Classification for Phase 2C Mixtures.....	101

Table 6.8: p-values Generated from ANOVA Testing of Compressive Strength Data within Different Mixture Groups.	110
Table 6.9: p-values Generated from ANOVA Testing of Flexural Strength Data within Different Mixture Groups.	116
Table 6.10: p-values Generated from ANOVA Testing of Drying Shrinkage Data within Different Mixture Groups.	122

LIST OF FIGURES

Figure 2.1: 0.45 power chart for aggregates with different nominal maximum size.	7
Figure 2.2: Different gradations compared to haystack plot (Richardson 2005).	8
Figure 2.3: Another example for unacceptable gradation (Richardson 2005).	9
Figure 2.4: The tarantula curve limits as reported in Cook et al. (2013).	10
Figure 2.5: Comparison of percent-passing limits of coarse aggregates between ODOT and TxDOT (note: ODOT upper is the same as TxDOT Grade 2 upper).	20
Figure 2.6: Comparison of percent-passing limits of fine aggregates between ODOT and TxDOT.	20
Figure 2.7: Comparison of percent-passing limits of coarse aggregates between ODOT and PennDOT.	21
Figure 2.8: Comparison of percent-passing limits of fine aggregates between ODOT and PennDOT.	21
Figure 2.9: Comparison of percent-passing limits of combined aggregates between ODOT and Caltrans.	22
Figure 2.10: Comparison of percent-passing limits of coarse aggregates between ODOT and Iowa DOT.	22
Figure 2.11: Comparison of percent-passing limits of fine aggregates between ODOT and Iowa DOT.	23
Figure 2.12: Comparison of percent-passing limits of coarse aggregates between ODOT and IDOT.	23
Figure 2.13: Comparison of percent-passing limits of fine aggregates between ODOT and IDOT.	24
Figure 2.14: RCPT results for 100% OPC, 80% OPC + 20% Class C ash, 80% OPC + 20% Class F ash, and 60% OPC + 40% slag mixtures (Taylor et al. 2014).	26
Figure 3.1: Aggregate gradations of the 1.5 (38 mm) inch to #4 (a), 1 inch (25.4 mm) to #4 (b), and sand (c) sources used in this preliminary study. Gradations shown represent as-received conditions.	30
Figure 3.2: Proposed aggregate gradations with “tarantula” upper and lower bounds (Ley et al. 2012).	33
Figure 3.3: Proposed aggregate gradations plotted on a 0.45-power curve.	33
Figure 3.4: The proposed gradations plotted on a Shilstone workability chart.	34
Figure 3.5: Schematic (a) of the edge slump measurement, E , and image of base mixture edge slump (b).	36
Figure 3.6: Four-category surface voiding assessment template for the Box Test (Cook et al. 2014).	36

Figure 3.7: Comparison of SAM number and the ACI201.2R recommended spacing factor (Welchel, 2012).....	40
Figure 3.8: Comparison of Box Test edge slump values to standard AASHTO T 119M (2018) slump values. Line of unity shown for comparative purposes. Note: 1 inch = 25.4 mm.	42
Figure 3.9: Results of compressive (a) and flexural (b) testing for all mixtures. Tests were conducted at an age of 28 days and were in a lime bath until the time of testing.	43
Figure 3.10: Comparison of unit weight measurements obtained via vacuum saturation. See note on mixture 3.	44
Figure 3.11: Comparison of formation factor measurements at different locations in each Box Test specimen. See note on mixture 3.	45
Figure 4.1: Aggregate voids (AV) as a function of F/C.	50
Figure 4.2: Example of anticipated results from Step 4.....	51
Figure 5.1: Target gradation considered for coarse aggregates.	58
Figure 5.2: Aggregates considered for SPR 823.....	67
Figure 5.3: Measured gradation for QR 1.5- ¾ inch (38-19 mm).	68
Figure 5.4: Measured gradation for QR ¾ inch (19 mm) - #4.....	68
Figure 5.5: Measured gradation for CG 1.5 - ¾ inch (38-19 mm).	69
Figure 5.6: Measured gradation for CG ¾ inch (19 mm) - #4.....	69
Figure 5.7: Measured gradation for G 1.5 - ¾ inch (38-19 mm).	70
Figure 5.8: Measured gradation for G ¾ inch (19 mm) - #4.	70
Figure 5.9: Measured gradation for coarse sand.	71
Figure 5.10: Measured gradation for fine sand.	71
Figure 6.1: F/C versus aggregate void content for different systems.	74
Figure 6.2: Comparison of optimized gradations for systems containing quarry rock and fine sand.	76
Figure 6.3: Comparison of optimized gradations for systems containing gravel and fine sand. ...	77
Figure 6.4: Comparison of the ODOT combined gradation limits to 0.45 power curve.	78
Figure 6.5: Comparison of the combined gradations of quarry rock plus coarse sand to 0.45 power curve (CAG: Coarse aggregate gradation; c: coarse; i: intermediate; and f: fine).....	78
Figure 6.6: Comparison of the combined gradations of quarry rock plus fine sand to 0.45 power curve (CAG: Coarse aggregate gradation; c: coarse; i: intermediate; and f: fine).....	79
Figure 6.7: Comparison of the combined gradations of crushed gravel plus coarse sand to 0.45 power curve (CAG: Coarse aggregate gradation; c: coarse; i: intermediate; and f: fine).....	79
Figure 6.8: Comparison of the combined gradations of crushed gravel plus fine sand to 0.45 power curve (CAG: Coarse aggregate gradation; c: coarse; i: intermediate; and f: fine).....	80
Figure 6.9: Comparison of the combined gradations of gravel plus coarse sand to 0.45 power curve (CAG: Coarse aggregate gradation; c: coarse; i: intermediate; and f: fine).....	80
Figure 6.10: Comparison of the combined gradations of gravel plus fine sand to 0.45 power curve (CAG: Coarse aggregate gradation; c: coarse; i: intermediate; and f: fine).....	81
Figure 6.11: Comparison of the combined gradations of quarry rock plus coarse sand to 8-18 band (CAG: Coarse aggregate gradation; c: coarse; i: intermediate; and f: fine).....	81
Figure 6.12: Comparison of the combined gradations of quarry rock plus fine sand to 8-18 band (CAG: Coarse aggregate gradation; c: coarse; i: intermediate; and f: fine).	82
Figure 6.13: Comparison of the combined gradations of crushed gravel and coarse sand to 8-18 band (CAG: Coarse aggregate gradation; c: coarse; i: intermediate; and f: fine).....	82

Figure 6.14: Comparison of the combined gradations of crushed gravel and fine sand to 8-18 band (CAG: Coarse aggregate gradation; c: coarse; i: intermediate; and f: fine).....	83
Figure 6.15: Comparison of the combined gradations of gravel and coarse sand to 8-18 band (CAG: Coarse aggregate gradation; c: coarse; i: intermediate; and f: fine).	83
Figure 6.16: Comparison of the combined gradations of gravel and fine sand to 8-18 band (CAG: Coarse aggregate gradation; c: coarse; i: intermediate; and f: fine).	84
Figure 6.17: Comparison of the combined gradations of quarry rock plus coarse sand to tarantula curve (CAG: Coarse aggregate gradation; c: coarse; i: intermediate; and f: fine).....	85
Figure 6.18: Comparison of the combined gradations of quarry rock plus fine sand to tarantula curve (CAG: Coarse aggregate gradation; c: coarse; i: intermediate; and f: fine).....	85
Figure 6.19: Comparison of the combined gradations of crushed gravel plus coarse sand to tarantula curve (CAG: Coarse aggregate gradation; c: coarse; i: intermediate; and f: fine).	86
Figure 6.20: Comparison of the combined gradations of crushed gravel plus fine sand to tarantula curve (CAG: Coarse aggregate gradation; c: coarse; i: intermediate; and f: fine).....	86
Figure 6.21: Comparison of the combined gradations of gravel plus coarse sand to tarantula curve (CAG: Coarse aggregate gradation; c: coarse; i: intermediate; and f: fine).....	87
Figure 6.22: Comparison of the combined gradations of gravel plus fine sand to tarantula curve (CAG: Coarse aggregate gradation; c: coarse; i: intermediate; and f: fine).	87
Figure 6.23: Influence of aggregate type on WR requirements.....	90
Figure 6.24: Influence of combined aggregate gradation on WR requirements.....	91
Figure 6.25: Influence of air-entrainment on WR requirements.....	91
Figure 6.26: Relationship between slump and edge-slump.	92
Figure 6.27: Required binder content versus AV_{min}	96
Figure 6.28: Effect of paste volume and binder content on WR dosage (Mixtures 1, 2, 3).	102
Figure 6.29: Effect of paste volume and binder content on WR dosage (Mixtures 4, 5, 6).	103
Figure 6.30: Effect of paste volume and binder content on WR dosage (Mixtures 7, 8, 9).	103
Figure 6.31: Effect of paste volume and binder content on WR dosage (Mixtures 10, 11, 12).	104
Figure 6.32: Effect of paste volume and binder content on WR dosage (Mixtures 13, 14, 15).	104
Figure 6.33: Effect of paste volume and binder content on WR dosage (Mixtures 16, 17, 18).	105
Figure 6.34: Effect of paste volume and binder content on WR dosage (Mixtures 19, 20, 21).	105
Figure 6.35: Effect of paste volume and binder content on compressive strength (Mixtures 1, 2, 3).	107
Figure 6.36: Effect of paste volume and binder content on compressive strength (Mixtures 4, 5, 6).	107
Figure 6.37: Effect of paste volume and binder content on compressive strength (Mixtures 7, 8, 9).	108
Figure 6.38: Effect of paste volume and binder content on compressive strength (Mixtures 10, 11, 12).	108
Figure 6.39: Effect of paste volume and binder content on compressive strength (Mixtures 13, 14, 15).	109
Figure 6.40: Effect of paste volume and binder content on compressive strength (Mixtures 16, 17, 18).	109
Figure 6.41: Effect of paste volume and binder content on compressive strength (Mixtures 19, 20, 21).	110
Figure 6.42: Scatter plot of 28-day compressive strength results as a function of paste volume and binder content.....	111

Figure 6.43: Scatter plot of 56-day compressive strength results as a function of paste volume and binder content.....	112
Figure 6.44: Effect of paste volume and binder content on flexural strength (Mixtures 1, 2, 3).	113
Figure 6.45: Effect of paste volume and binder content on flexural strength (Mixtures 4, 5, 6).	113
Figure 6.46: Effect of paste volume and binder content on flexural strength (Mixtures 7, 8, 9).	114
Figure 6.47: Effect of paste volume and binder content on flexural strength (Mixtures 10, 11, 12).	114
Figure 6.48: Effect of paste volume and binder content on flexural strength (Mixtures 13, 14, 15).	115
Figure 6.49: Effect of paste volume and binder content on flexural strength (Mixtures 16, 17, 18).	115
Figure 6.50: Effect of paste volume and binder content on flexural strength (Mixtures 19, 20, 21).	116
Figure 6.51: Scatter plot of 28-day flexural strength results as a function of paste volume and binder content.....	117
Figure 6.52: Scatter plot of 56-day flexural strength results as a function of paste volume and binder content.....	117
Figure 6.53: Drying shrinkage as a function of the paste volume and total binder content (Mixtures 1, 2, 3).	118
Figure 6.54: Drying shrinkage as a function of the paste volume and total binder content (Mixtures 4, 5, 6).	119
Figure 6.55: Drying shrinkage as a function of the paste volume and total binder content (Mixtures 7, 8, 9).	119
Figure 6.56: Drying shrinkage as a function of the paste volume and total binder content (Mixtures 10, 11, 12).	120
Figure 6.57: Drying shrinkage as a function of the paste volume and total binder content (Mixtures 13, 14, 15).	120
Figure 6.58: Drying shrinkage as a function of the paste volume and total binder content (Mixtures 16, 17, 18).	121
Figure 6.59: Drying shrinkage as a function of the paste volume and total binder content (Mixtures 19, 20, 21).	121
Figure 6.60: Restrained shrinkage strain for mixture 1.	123
Figure 6.61: Restrained shrinkage strain for mixture 3.	124
Figure 6.62: Effect of binder type on water-reducer dosage (Mixtures 1, 2, 3, 7, 8, 9).	125
Figure 6.63: Effect of binder type on water-reducer dosage (Mixtures 10, 11, 12, 16, 17, 18).	125
Figure 6.64: Effect of binder type on water-reducer dosage (Mixtures 17, 11, 25).	126
Figure 6.65: Effect of binder type on 28-day compressive strength (Mixtures 1, 2, 3, 7, 8, 9)..	127
Figure 6.66: Effect of binder type on 56-day compressive strength (Mixtures 1, 2, 3, 7, 8, 9)..	127
Figure 6.67: Effect of binder type on 28-day compressive strength (Mixtures 10, 11, 12, 16, 17, 18).	128
Figure 6.68: Effect of binder type on 56-day compressive strength (Mixtures 10, 11, 12, 16, 17, 18).	128
Figure 6.69: Effect of binder type on compressive strength (Mixtures 17, 11, 25).	129

Figure 6.70: Effect of binder type on 28-day flexural strength (Mixtures 1, 2, 3, 7, 8, 9).	130
Figure 6.71: Effect of binder type on 56-day flexural strength (Mixtures 1, 2, 3, 7, 8, 9).	130
Figure 6.72: Effect of binder type on 28-day flexural strength (Mixtures 10, 11, 12, 16, 17, 18).	131
Figure 6.73: Effect of binder type on 56-day flexural strength (Mixtures 10, 11, 12, 16, 17, 18).	131
Figure 6.74: Effect of binder type on flexural strength (Mixtures 17, 11, 25).	132
Figure 6.75: Effect of binder type on drying shrinkage (Mixtures 1, 2, 3, 7, 8, 9).....	133
Figure 6.76: Effect of binder type on drying shrinkage (Mixtures 10, 11, 12, 16, 17, 18).....	133
Figure 6.77: Effect of binder type on drying shrinkage (Mixtures 17, 11, 25).....	134
Figure 6.78: Effect of w/cm on water-reducer dosage (Mixtures 22, 11, 23).....	135
Figure 6.79: Effect of w/cm on compressive strength results (Mixtures 22, 11, 23).....	135
Figure 6.80: Effect of w/cm on flexural strength results (Mixtures 22, 11, 23).	136
Figure 6.81: Effect of w/cm on drying shrinkage results (Mixtures 22, 11, 23).	136
Figure 6.82: Durability factor of specimens subjected to 300 FT cycles (Mixtures 10, 11, 12). 137	
Figure 6.83: Durability factor of specimens subjected to 300 FT cycles (Mixtures 16, 17, 18). 137	
Figure 6.84: Edge slump versus binder content.....	138
Figure A.1: Surface-void profile for one of the sides of box test specimen (Mixture 1).....	A-1
Figure A.2: Overview of box test specimen (Mixture 1).....	A-1
Figure A.3: Result from slump testing (Mixture 1)	A-2
Figure A.4: Concrete finished- surface after screeding and troweling (Mixture 1).....	A-2
Figure A.5: Surface-void profile for one of the sides of box test specimen (Mixture 2).....	A-3
Figure A.6: Result from slump testing (Mixture 2)	A-3
Figure A.7: Concrete finished surface after screeding and troweling (Mixture 2).....	A-4
Figure A.8: Surface-void profile for one of the sides of box test specimen (Mixture 3).....	A-5
Figure A.9: Overview of box test specimen (Mixture 3).....	A-5
Figure A.10: Result from slump testing (Mixture 3)	A-6
Figure A.11: Concrete finished surface after screeding and troweling (Mixture 3).....	A-6
Figure A.12: Surface-void profile for one of the sides of box test specimen (Mixture 4).....	A-7
Figure A.13: Overview of box test specimen (Mixture 4).....	A-7
Figure A.14: Result from slump testing (Mixture 4)	A-8
Figure A.15: Concrete finished surface after screeding and troweling (Mixture 4).....	A-8
Figure A.16: Surface-void profile for one of the sides of box test specimen (Mixture 5).....	A-9
Figure A.17: Overview of box test specimen (Mixture 5).....	A-9
Figure A.18: Result from slump testing (Mixture 5)	A-10
Figure A.19: Concrete finished surface after screeding and troweling (Mixture 5).....	A-10
Figure A.20: Surface-void profile for one of the sides of box test specimen (Mixture 6).....	A-11
Figure A.21: Overview of box test specimen (Mixture 6).....	A-11
Figure A.22: Result from slump testing (Mixture 6)	A-12
Figure A.23: Concrete finished surface after screeding and troweling (Mixture 6).....	A-12
Figure A.24: Surface-void profile for one of the sides of box test specimen (Mixture 7).....	A-13
Figure A.25: Result from slump testing (Mixture 7)	A-13
Figure A.26: Concrete finished surface after screeding and troweling (Mixture 7).....	A-14
Figure A.27: Surface-void profile for one of the sides of box test specimen (Mixture 8).....	A-15
Figure A.28: Result from slump testing (Mixture 8)	A-15
Figure A.29: Concrete finished surface after screeding and troweling (Mixture 8).....	A-16

Figure A.30: Surface-void profile for one of the sides of box test specimen (Mixture 9).....	A-17
Figure A.31: Result from slump testing (Mixture 9).....	A-17
Figure A.32: Concrete finished surface after screeding and troweling (Mixture 9).....	A-18
Figure A.33: Surface-void profile for one of the sides of box test specimen (Mixture 10).....	A-19
Figure A.34: Result from slump testing (Mixture 10).....	A-19
Figure A.35: Concrete finished surface after screeding and troweling (Mixture 10).....	A-20
Figure A.36: Surface-void profile for one of the sides of box test specimen (Mixture 11).....	A-21
Figure A.37: Result from slump testing (Mixture 11).....	A-21
Figure A.38: Concrete finished surface after screeding and troweling (Mixture 11).....	A-22
Figure A.39: Surface-void profile for one of the sides of box test specimen (Mixture 12).....	A-23
Figure A.40: Result from slump testing (Mixture 12).....	A-23
Figure A.41: Concrete finished surface after screeding and troweling (Mixture 12).....	A-24
Figure A.42: Surface-void profile for one of the sides of box test specimen (Mixture 13).....	A-25
Figure A.43: Result from slump testing (Mixture 13).....	A-25
Figure A.44: Concrete finished surface after screeding and troweling (Mixture 13).....	A-26
Figure A.45: Surface-void profile for one of the sides of box test specimen (Mixture 14).....	A-27
Figure A.46: Result from slump testing (Mixture 14).....	A-27
Figure A.47: Concrete finished surface after screeding and troweling (Mixture 14).....	A-28
Figure A.48: Surface-void profile for one of the sides of box test specimen (Mixture 15).....	A-29
Figure A.49: Result from slump testing (Mixture 15).....	A-29
Figure A.50: Concrete finished surface after screeding and troweling (Mixture 15).....	A-30
Figure A.51: Surface-void profile for one of the sides of box test specimen (Mixture 16).....	A-31
Figure A.52: Concrete finished surface after screeding and troweling (Mixture 16).....	A-31
Figure A.53: Surface-void profile for one of the sides of box test specimen (Mixture 17).....	A-32
Figure A.54: Result from slump testing (Mixture 17).....	A-32
Figure A.55: Concrete finished surface after screeding and troweling (Mixture 17).....	A-33
Figure A.56: Surface-void profile for one of the sides of box test specimen (Mixture 18).....	A-34
Figure A.57: Surface-void profile for one of the sides of box test specimen (Mixture 18).....	A-34
Figure A.58: Concrete finished surface after screeding and troweling (Mixture 18).....	A-35
Figure A.59: Surface-void profile for one of the sides of box test specimen (Mixture 20).....	A-36
Figure A.60: Surface-void profile for one of the sides of box test specimen (Mixture 21).....	A-37
Figure A.61: Surface-void profile for one of the sides of box test specimen (Mixture 22).....	A-38
Figure A.62: Result from slump testing (Mixture 22).....	A-38
Figure A.63: Concrete finished surface after screeding and troweling (Mixture 22).....	A-39
Figure A.64: Surface-void profile for one of the sides of box test specimen (Mixture 23).....	A-40
Figure A.65: Result from slump testing (Mixture 23).....	A-40
Figure A.66: Concrete finished surface after screeding and troweling (Mixture 23).....	A-41

1.0 INTRODUCTION

Slipform concrete construction is commonly adopted for constructing pavements by many state highway agencies (SHAs) in the U.S. This is often a result of high productivity and excellent durability. One of the many factors that influence the long-term performance of the concrete pavement is the design of concrete mixtures. As an example, it is generally recommended that a low slump concrete be used for concrete in paving projects as the concrete needs to hold its shape after the slip-form paver has passed and until the concrete achieves its final set. Specifications related to the concrete paving mixtures generally focus on the material constituents and the mixture design, or proportioning parameters. While most states, including Oregon, specify general requirements for Portland cement concrete (PCC) that are applicable for paving projects, some states, such as Pennsylvania and Iowa, provide specific requirements for concrete used in pavements.

Oregon has a long history with constructing asphalt pavements. Concrete pavements, and their long service lives, have garnered interest. Although recent projects have been successful, some challenges have been observed. These challenges included some early-age cracking and in some cases, excessive edge-slumping of the concrete. These issues highlighted the need for developing strategies for improving the constructability and long-term performance of these concrete pavements. In addition to constructability and durability, the Oregon Department of Transportation (ODOT) is engaged in making their systems more sustainable. The ODOT Sustainability Program states that ODOT will lead efforts “to conserve resources and protect and enhance the environment.” Therefore, in addition to constructability and durability, this research will enhance the sustainability of concrete paving mixtures by developing a methodology to minimize the ordinary Portland cement (OPC) in paving mixtures, while achieving required performance requirements.

OPC is a vital and strategic commodity material and the annual global cement production has now reached up to 3.6 billion tons (Imbabi, Carrigan, and McKenna (2012). With increasing infrastructure and building demands, a sustainable, durable, constructable, and economical concrete is needed (Monteiro, Miller, & Horvath, 2017). Unfortunately, approximately 0.9 tons of CO₂ are released for each ton of OPC produced (He, Zhu, Wang, Mu, & Wang, 2019). This results in over 2.7 billion tons of CO₂ emitted as a result of OPC production each year (or 5 to 7% of all CO₂ production) (Naik, 2005). To enhance sustainability, the research team has developed a methodology to minimize the OPC content in paving mixtures, based on the aggregates used, while ensuring constructability. Some durability was performed.

It is estimated that ODOT uses approximately 65,000 cy of concrete annually. Assuming a cubic yard contains 610 pounds of OPC, this concrete contributes about 18,000 tons of CO₂ annually. If the OPC can be minimized, up to 4000 tons of CO₂ can be eliminated. Additional OPC can be removed from the concrete with the addition of supplementary cementitious material (SCM)s. This research evaluated concretes that reduced the OPC using the new proportioning method and with the addition of SCMs. These mixtures contained about 40% less OPC than the current

content recommended by ODOT. Reducing the OPC to these levels would result in a reduction of CO₂ pollutants by over 7000 tons per year. Minimizing OPC content, while ensuring constructability and durability, will enhance the sustainability of concrete pavements and will optimize value to the Oregon taxpayers.

1.1 RESEARCH OBJECTIVES AND APPROACH

The objective of this research is to develop concrete mixture proportioning guidelines to minimize paste content (i.e., cement content) while ensuring performance of concrete used for pavements. The report focuses on a new mixture proportioning methodology and generates data for concrete mixtures using materials locally available in Oregon. To optimize concrete mixture performance, it is critical to generate information on the coarse aggregate, fine aggregate, combined aggregate gradation, air-void content of the aggregates, and necessary paste volume necessary to achieve required constructability characteristics. Information on constituent materials, such as SCM type, SCM replacement level, and water-to-cementitious materials ratio (w/cm) are also needed. Having this information will allow for the prediction of the fresh characteristics and hardened properties of concretes used for paving projects.

This research was executed in three separate phases and one preliminary phase. A preliminary phase evaluated the use of the Box Test, a procedure used to quantify the consolidation behavior of concrete paving mixtures (M. D. Cook, Ley, & Ghaeezadah, 2014). Some limited concrete characteristics were assessed as part of this preliminary phase. It should be noted that the preliminary phase research was a separate project and is reported here for completeness. Phase 1 consisted of characterizing coarse and fine aggregates and combining these aggregates at different fine to coarse aggregate ratios (F/C) to identify an optimal F/C, F/C_{opt} , that results in a minimum aggregate air-void (AV_{min}) content of the combined aggregates. Three coarse aggregates and 2 fine aggregates were evaluated in Phase 1. Phase 2 of the research included three (3) sub-phases: 2A, 2B, and 2C. Phase 2A consisted of assessing mixtures containing a water-reducer (WR) to identify reasonable mixture proportions that can be used for concrete pavements. Phase 2B identified ratios of paste volumes (PV) to aggregate void-volumes (AV_{min}), or PV/AV_{min} , necessary to achieve the desired fresh characteristics for several cementitious material types. Using the information from Phases 1, 2A, and 2B, Phase 2C included a comprehensive assessment of the fresh and hardened concrete characteristics of mixtures containing different PV/AV_{min} values. One objective was to identify minimum paste contents (and minimum OPC content) for concrete mixtures while ensuring these mixtures meet constructability and performance criteria. Minimizing OPC content while ensuring constructability and performance will provide environmental benefits.

1.2 OUTLINE OF REPORT

This report consists of seven chapters. Chapter 1 provides an introduction, objectives of the research, and a brief description of what is included in each chapter. Chapter 2 presents a review of methods used to optimize aggregate packing (minimize air voids in aggregate), current state highway agency practices regarding aggregate requirements, and concrete pavement performance. Chapter 3 provides an overview of a previous preliminary research task. Chapter 4 provides details on the experimental program and materials used in the project. Descriptions of the experimental test matrix, testing scope, and test procedures are provided in this chapter.

Chapter 5 presents the methodology used to assess aggregates and proportion concrete to minimize paste content in paving mixtures. Chapter 6 presents the experimental results and main findings from the different phases of the research program. The effects of the different study parameters on the fresh and hardened concrete characteristics are presented in this chapter. Chapter 7 summarizes the research needs and findings, presents the main conclusions of the research program, and provides recommendation for implementation.

2.0 LITERATURE REVIEW

This chapter provides an overview of the current literature and current practices on aggregate gradations and packing. Optimizing aggregate packing will minimize aggregate voids, which in turn can minimize the amount of paste, and OPC, required for the concrete mixtures. A review of current practices by SHAs is also provided, including a comparison of these practices and requirements. Concrete requirements for concrete pavements is then presented.

2.1 AGGREGATE GRADATION PARTICLE PACKING MODELS

Several models are reported in the literature that can be used to determine the particle packing density of the aggregate systems. The models reported in the literature can be classified as either discrete models or continuous models. In discrete models, it is assumed that an aggregate system is composed of two or more discrete size ranges of particles. The voids of the coarsest particles are filled by smaller particles and the voids of these smaller particles are filled by the even finer particles. Continuous models assume that all possible sizes are present in the particle distribution system and that no gaps exist between the different aggregate size ranges. This document provides a brief review of some particle packing models reported in the literature. The particle packing models commonly used include:

1. Furnas model (Furnas, 1929): This model can be used to estimate the particle packing density of a binary system (e.g., coarse + fine aggregates) if the packing densities of the individual aggregates are known. The model assumes that all particles are spherical in shape and neglects the particle sizes of the individual aggregates.
2. Aim and Goff model (Aim & Le Goff, 1968): This model is used to estimate the particle packing density of binary systems. Unlike the Furnas model, this model considers the effects of particle size. The fraction of fine particles that results in maximum packing density is first estimated using the maximum diameters and the packing densities of the individual aggregates. Using this, the maximum packing density of the combined aggregate system is estimated.
3. Modified Toufar model (Goltermann, Johansen, & Palbøl, 1997): This model assumes that the aggregate matrix consists of two systems: one mostly composed of densely packed coarse particles and the other consisting of areas of packed fine particles with discretely distributed coarse particles. This model also assumes that particles are spherical in shape. Use of this model requires information on the volume fractions and packing densities of individual aggregates. In addition, information of two empirical factors is needed and this requires knowledge of the characteristic diameters of individual aggregates. A procedure to estimate the values of these factors is provided in the referenced article.

4. Compressible Packing Model (CPM): This model, originally developed by (De Larrard, 1999), is based on the principal that the process of compaction influences the packing density. In addition to information on individual aggregates, a compaction index (based on the compaction method) must be specified to estimate the packing density.

A comprehensive review on the mathematics of different packing models can be found in (Mamirov, 2019). In addition to the models specified above, Powers model (Powers, 1968), linear packing density model (LPDM) (Stovall, De Larrard, & Buil, 1986), Fuller and Thomson model (Fuller & Thompson, 1907), and Andreassen model (Mangulkar & Jamkar, 2013) are other models that are reported in the literature. All models listed here except the Fuller and Thompson model and the Andreassen model are discrete models.

2.2 STANDARD GRADATION CHARTS

In addition to the particle packing models, standard gradation charts such as 0.45 power, 18-8 or haystack plot, and tarantula curve charts are available for optimizing aggregate gradations. These are commonly adopted by SHAs. A brief description of these charts follows.

2.2.1 0.45 power chart

The 0.45 power chart is a mathematically derived cumulative passing gradation that was originally developed by the Federal Highway Administration (FHWA) in the early 1960s, following the concepts reported in (Fuller & Thompson, 1907). The 0.45 power curve has been historically used to design hot mix asphalt mixtures. However, this curve has become increasingly common for designing PCC mixtures. Mixtures with gradations that are closer to the 0.45 power curve are generally referred to as well-graded or dense-graded mixtures and are anticipated to have maximum densities. The arrangement of aggregate particles for a dense-graded system is assumed to be optimal; that is, the smaller particles will occupy the voids created by the larger particles, resulting in low aggregate void (AV) contents. However, limited information is available on whether the aggregate gradations optimized following the 0.45 power curve correlate with the aggregate gradations developed experimentally (e.g., ASTM International C29 (2017), or American Association of State Highway and Transportation Officials (AASHTO) T 19M (2014a)). A review by (Richardson, 2005) indicated that optimizing gradations with the 0.45 power curve may not always result in maximum density and can increase the harshness of concrete mixtures.

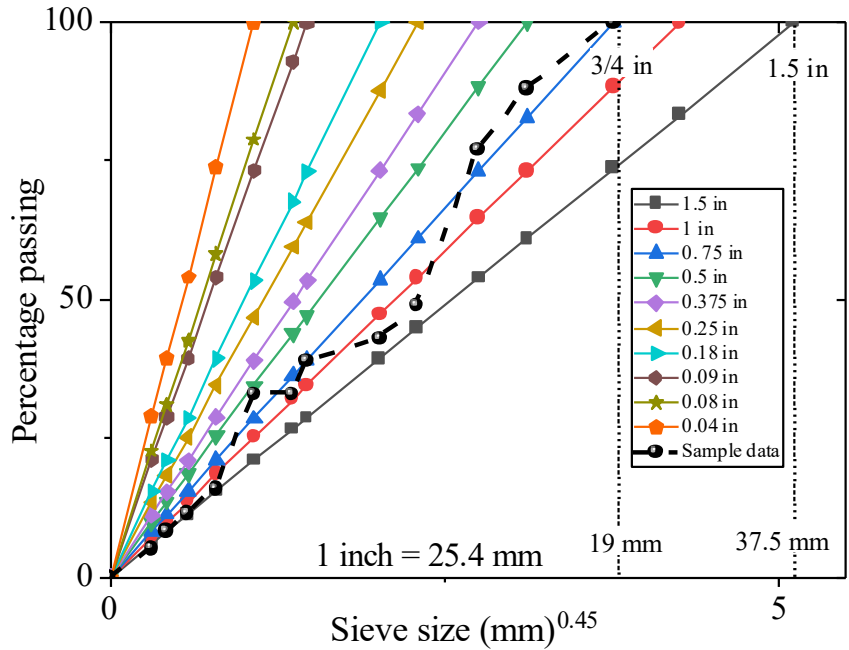


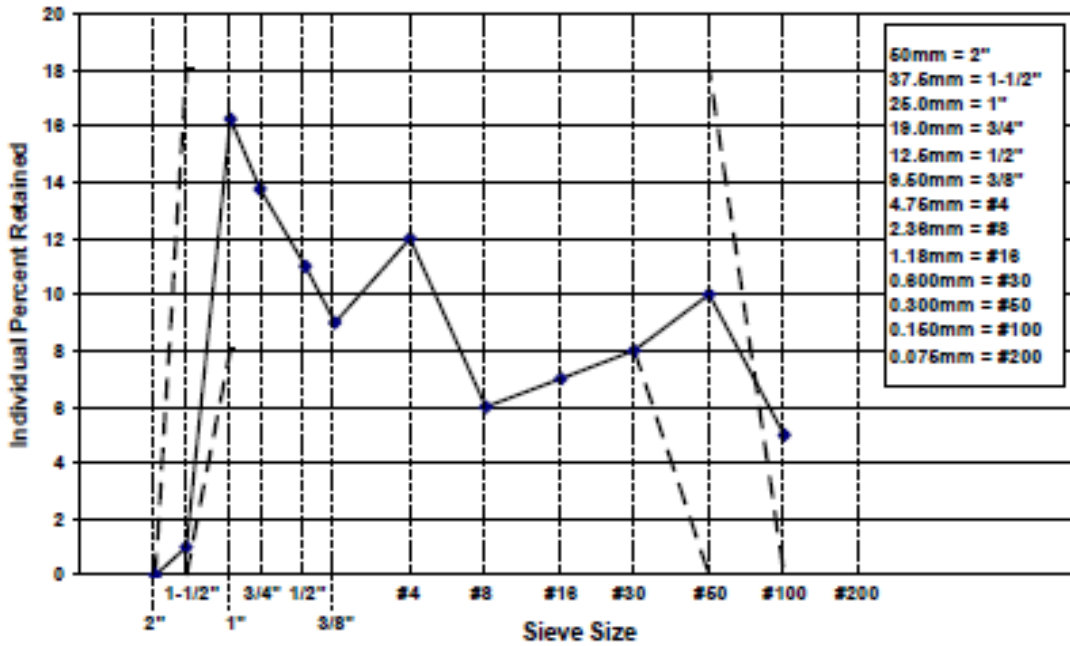
Figure 2.1: 0.45 power chart for aggregates with different nominal maximum size.

2.2.2 Haystack plot

The 8-18 band or haystack plot was originally proposed by (Holland, 1990) to attempt to force the gradation into more of a “haystack” shape. The 18-8 limits were defined to obtain a more unified individual percent retained values between the sieve sizes of the nominal maximum aggregate size and 0.023 in. (0.595mm; U.S. sieve size #30). These limits were reportedly based on field experience. To meet the requirements of the haystack plot, the aggregate systems must have the percent retained values between 8 and 18 percent for the sieve sizes one size below the nominal maximum size aggregate (NMSA), that is, 1 inch (25 mm) for ODOT aggregates for paving through 0.023 in. (0.595mm; U.S. sieve size #30). Also, the percent retained values for all sizes must be below 18 percent. Aggregate gradation following the haystack shape will have greater percentage of particles with intermediate sizes and smaller percentage of particles with extreme sizes. (Richardson, 2005) performed a comprehensive review of aggregate optimization procedures used by different SHAs and reported the following points relating to the haystack chart:

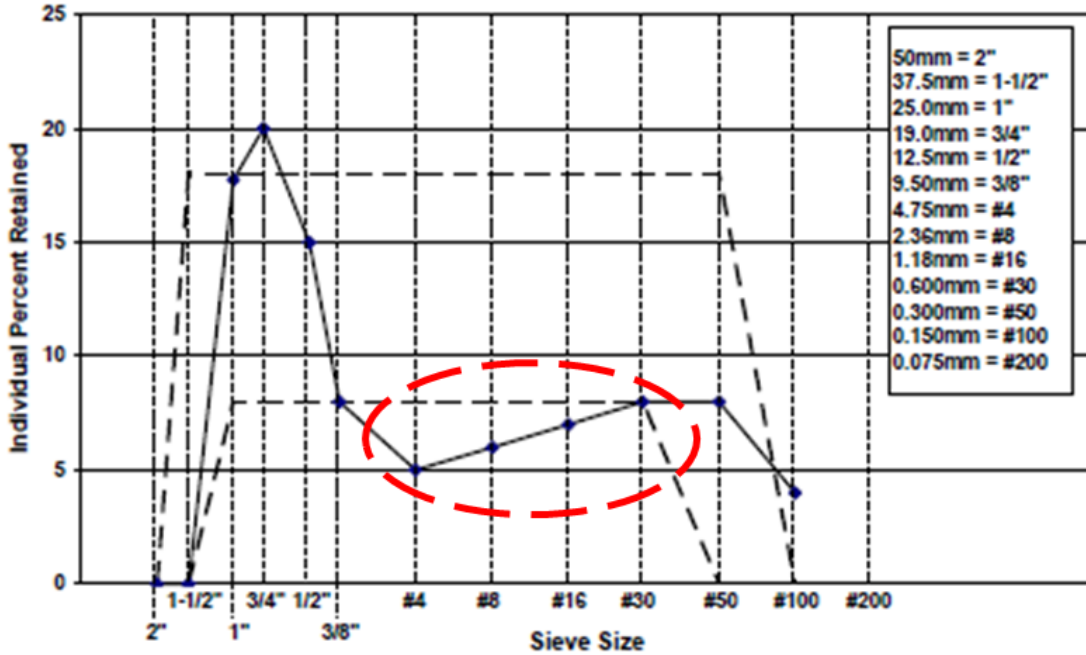
1. When plotted on the haystack chart, the combined gradation curve should not have a significant valley between the 0.375 in. (9.5 mm) sieve and the lowest specified sieve size. A significant valley is where the percent retained values is less than 8% for more than two sieve sizes (at least three). Examples for acceptable and unacceptable gradations when compared to the 8-18 band are shown in Figure 2.2. The significant valley, and thus unacceptable gradation, is highlighted by a dotted ellipse.

Individual Percent Retained



(a) An example for acceptable gradation

Individual Percent Retained



(b) An example for unacceptable gradation

Figure 2.2: Different gradations compared to haystack plot (Richardson 2005).

- Aggregate systems for which the percent retained values on two successive sieves are more than 18% may also be concerning. Consider the example gradation shown in Figure 2.3. For this example, the aggregate system has an excess of larger stones. A concrete mixture with such gradation will tend to segregate upon vibration and will exhibit poor finish ability due to excessive voids.

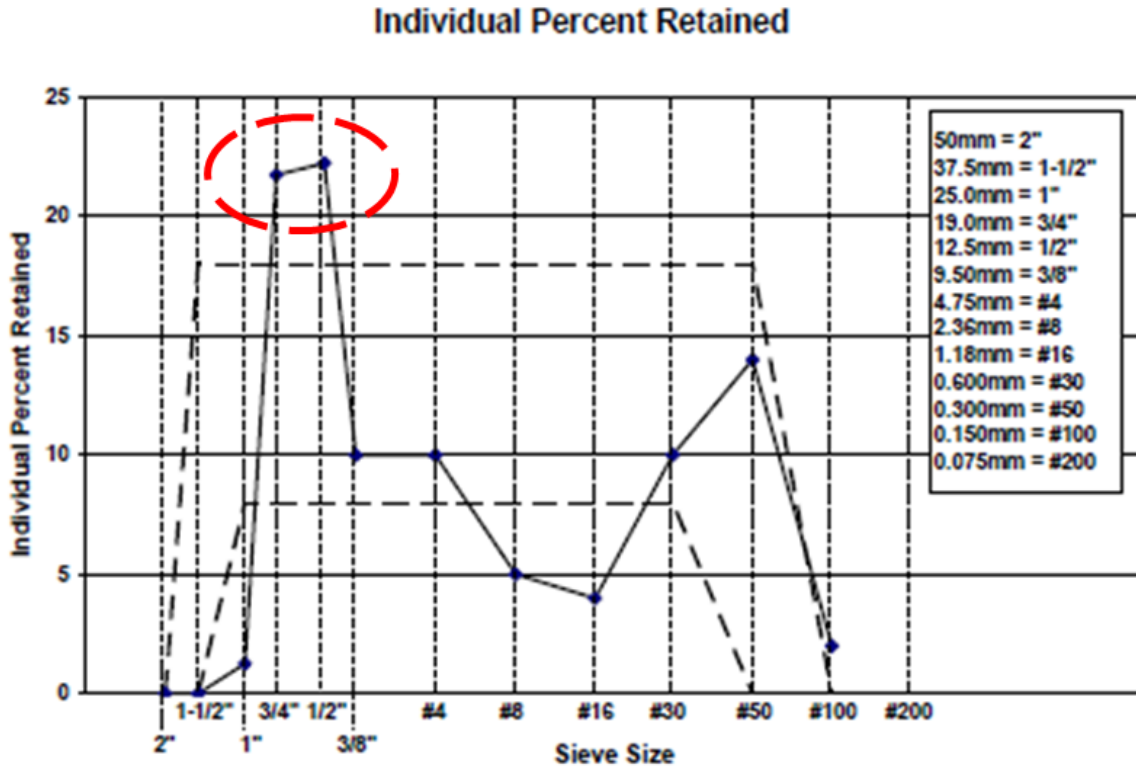


Figure 2.3: Another example for unacceptable gradation (Richardson 2005).

2.2.3 Tarantula chart

The tarantula chart was developed and reported by D. M. Cook, Ghaeezadeh, Ley, and Russell (2013). The concrete mixtures investigated by Cook et al. to develop the tarantula gradation limits had the same w/cm (0.45) and the same combined volume of binder and water (24.2%). All mixtures had a Class C fly ash (20% by mass of total binder), an NMSA of 1 in. (25.2 mm), and the total binder content was 423 lb/yd³ (251 kg/m³). In other words, the volume of combined aggregates was held constant among all mixtures. The volumes of the coarse, intermediate, and fine aggregates varied among different mixtures. The following criteria were used to generate the limits for the tarantula curve: 1) The average surface voids on a Box Test specimen is less than 30%, 2) The dosage of the lignosulfate-based mid-range water reducer is less than 12 fl oz/cwt (780 ml/100 kg), and 3) A small number of passes with a hand float are required to finish the concrete surface. Aggregate gradations of the mixtures that exhibited satisfactory performance in the fresh state were then used to develop the upper and lower limits of the tarantula chart, as shown in Figure 2.4. Note that these limits were developed without any packing or void characteristics of the aggregates. Figure 2.4 provides the lower and upper limits for various individual sieve sizes ranging between 1 in. (25.4 mm) and 0.003 in. (0.074 mm, U.S. sieve size

No. 200) and summarizes the potential issues faced while exceeding the proposed limits. A comprehensive discussion of the development of these limits can be found in D. M. Cook et al. (2013).

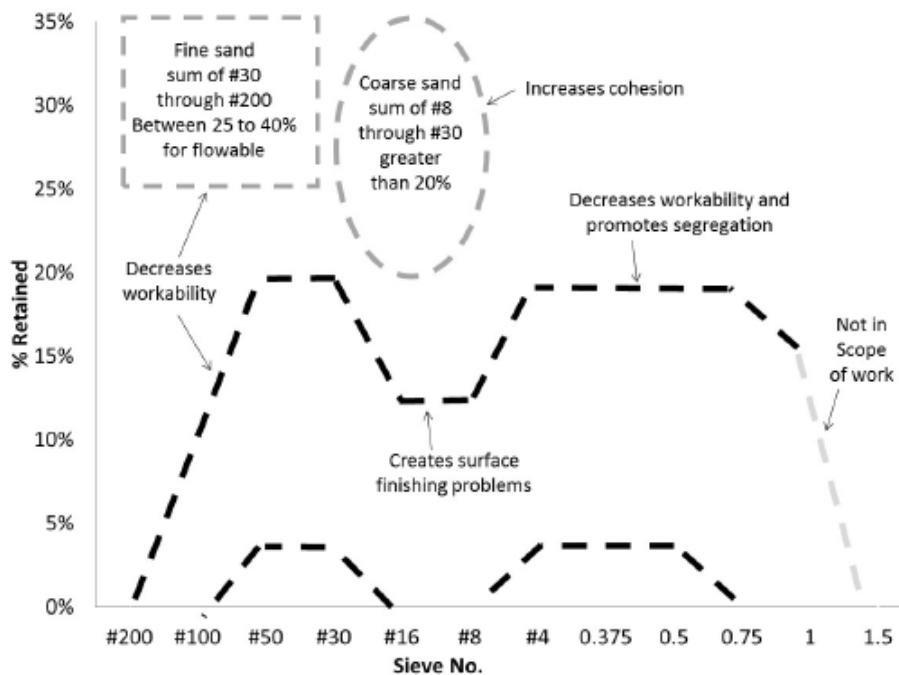


Figure 2.4: The tarantula curve limits as reported in Cook et al. (2013).

The gradation charts discussed thus far can be used to rank various aggregate gradations and suggest proportioning when attempting to meet other criteria. Limited information is available on whether meeting the criteria with the gradation charts result in an aggregate gradation that results in minimum aggregate void content and minimum paste and cement contents.

The literature contains information on packing of aggregates with the objective of minimizing aggregate voids. However, aggregate characteristics can vary significantly and “general” guidelines on aggregate packing may not always result in maximum packing, minimum aggregate voids, and minimum cementitious materials paste content.

2.3 PAVING CONCRETE SPECIFICATIONS FOR DIFFERENT SHAs

This section summarizes paving concrete specification documents from different SHAs. The SHAs considered here include Oregon, Texas, Pennsylvania, California, Iowa, and Illinois. The requirements of concrete for paving generally include requirements for aggregate characteristics (maximum size, gradation, and fracture), concrete strength, binder requirements, w/cm, and air content. The reference to each specific requirement (e.g., §02690.20(e) in ODOT specification that specifies requirements for aggregate fracture) is also provided. Aggregate gradation requirements specified by ODOT are also compared with other SHA gradation requirements.

2.3.1 Oregon DOT (ODOT)

ODOT specifies the use of coarse aggregates with at least two fractured faces on at least 50 percent of the particles retained on the 0.38 in. (9.5 mm), 0.5 in. (12.7 mm), 0.75 in. (19.1 mm), 1 in. (25.4 mm), and 1.5 in. (38.1 mm) sieves for paving concrete (§02690.20(e)). ODOT also requires 4000 psi (27.6 MPa) concrete with NMSA of 1.5 in. (38.1 mm) (§00755.11). The current ODOT specification document does not report requirements on gradation for paving aggregates, however, the requirements specified in section 02690.20(g) for structural concrete are commonly adopted. More recently, ODOT has developed project-specific gradation requirements for coarse aggregates, fine aggregates, and combined aggregates for paving concrete (Table 02690-3; I84 special provisions contract document; contract number 15090). These requirements are summarized here in Table 2.1, Table 2.2, and Table 2.3.

A maximum w/cm value of 0.44 is also specified. The specified target air entrainment values for moderate and severe exposures are 4.5 and 5%, respectively. The field measured air-entrainment values shall be $\pm 1.5\%$ of the specified target values (§02001.20). An ASTM C150 (2021) type I/II cement is specified for paving concrete. Modifiers such as fly ash (12 to 18%), ground granulated blast furnace slag (20 to 35%), and silica fume (3 to 5%) may be used separately or in combinations as approved by the engineer (§02001.31). If the paving concrete is designed as high-performance concrete (HPC), the minimum absolute volume of coarse aggregate shall be 0.46 yd³ (0.35 m³) per 1 yd³ (0.76 m³) of concrete (§02001.31). The minimum flexural strength of paving concrete at 28 days is also specified to be 600 psi (4.1 MPa) (§02001.33).

Table 2.1: ODOT Percent-passing Limits for Coarse Aggregates.

Sieve ID, customary	Sieve size, in. (mm)	Percent passing (%)
2 inch	2 (50.8)	100
1½ inch	1.5 (38.1)	85 - 100
1 inch	1 (25.4)	
¾ inch	0.75 (19.1)	35 - 65
½ inch	0.5 (12.7)	
⅜ inch	0.38 (9.5)	10 - 30
#4	0.19 (4.75)	0 - 5
#8	0.09 (2.36)	

Table 2.2: ODOT Percent-passing Limits for Fine Aggregates.

Sieve ID, customary	Sieve size, in. (mm)	Percent passing (%)
⅜ inch	0.38 (9.5)	100
#4	0.19 (4.75)	90 - 100
#8	0.09 (2.36)	70 - 100
#16	0.046 (1.19)	50 - 85
#30	0.023 (0.595)	25 - 60
#50	0.012 (0.297)	5 - 30
#100	0.006 (0.149)	0 - 10
#200	0.003 (0.074)	0 - 4

Table 2.3: ODOT Percent-passing Limits for Combined Aggregates.

Sieve ID, customary	Sieve size, in. (mm)	Percent passing (%)
2 inch	2 (50.8)	100
1½ inch	1.5 (38.1)	90 - 100
1 inch	1 (25.4)	70 - 85
¾ inch	0.75 (19.1)	60 - 78
⅜ inch	0.38 (9.5)	44 - 57
#4	0.19 (4.75)	30 - 41
#8	0.09 (2.36)	23 - 32
#16	0.046 (1.19)	15 - 29
#30	0.023 (0.595)	8 - 29
#50	0.012 (0.297)	2 - 12
#100	0.006 (0.149)	0 - 4
#200	0.003 (0.074)	0 - 1.5

2.3.2 Texas DOT (TxDOT)

TxDOT specifies a ‘Grade 2’ or ‘Grade 3’ coarse aggregate type for pavements (Texas Department of Transportation, 2014). The percent passing limits for both grades are summarized here in Table 2.4. Both grade types have a NMSA requirement of 1.5 in. (38.1 mm) (Item 421, §4.2.1 and §2.6.1). TxDOT does not report specific requirements on aggregate fracture for paving concrete. The fine aggregate gradation requirements specified by TxDOT for hydraulic cement concrete are summarized here in Table 2.5. TxDOT requires the fineness modulus of fine aggregate to fall between 2.3 and 3.1. TxDOT also requires that concrete for pavements be class ‘P’ or class ‘HES’ (high early-age strength) concrete. Class ‘P’ concrete must be designed to meet a minimum average compressive strength of 3200 psi (22.1 MPa) and flexural strength of 470 psi (3.2 MPa) at 7 days or a minimum average compressive strength of 4000 psi (27.6 MPa) and flexural strength of 570 psi (3.9 MPa) at 28 days. Class ‘HES’ concrete must be designed to meet a minimum average compressive strength of 3200 psi (22.1 MPa) and flexural strength of 450 psi (3.1 MPa) in 24 hours (Item 360, §2.1). Class ‘P’ and class ‘HES’ concretes are required to have a maximum w/cm of 0.5 and 0.45, respectively (Item 421, §4.2.1).

TxDOT allows partial replacements of OPC with Class F or C fly ash (20 to 35%), slag cement (35 to 50%), and silica fume (<10%) for paving concrete. More information on the different mixture design options for paving concrete can be found in Item 421, §4.2.6. The cementitious material content must not exceed 700 lb/yd³ (415 kg/m³), unless otherwise specified or approved (Item 421, §4.2). If the cementitious material content does not exceed 520 lb/yd³ (309 kg/m³), class C fly ash may be used instead of class F fly ash (Item 421, §4.21, Table 2.8). TxDOT specifies a minimum air-entrainment of 3% for all classes of concrete except class ‘P’ concrete. Although air-entrainment is required for paving concrete, an acceptable range is not specified in the document. The coefficient of thermal expansion for paving concrete must not more than 5.5 x 10⁻⁶ in./in./°F (Item 360, §2.1).

Table 2.4: TxDOT Percent-passing Limits for Coarse Aggregates.

Sieve ID, customary	Sieve size, in. (mm)	Grade 2	Grade 3
2 inch	2 (50.8)	100	100
1½ inch	1.5 (38.1)	95 - 100	95 - 100
1 inch	1 (25.4)		
¾ inch	0.75 (19.1)	35 - 70	60 - 90
½ inch	0.5 (12.7)		25 - 60
⅜ inch	0.38 (9.5)	10 - 30	
#4	0.19 (4.75)	0 - 10	0 - 10
#8	0.09 (2.36)		

Table 2.5: TxDOT Percent-passing Limits for Fine Aggregates

Sieve ID, customary	Sieve size, in. (mm)	Percent passing (%)
⅜ inch	0.38 (9.5)	100
#4	0.19 (4.75)	95 - 100
#8	0.09 (2.36)	80 - 100
#16	0.046 (1.19)	50 - 85
#30	0.023 (0.595)	25 - 65
#50	0.012 (0.297)	10 - 35
#100	0.006 (0.149)	0 - 10
#200	0.003 (0.074)	0 - 3

2.3.3 Pennsylvania DOT (PennDOT)

PennDOT requires the use of class ‘AA’ concrete or HES concrete for rigid pavements (Pennsylvania Department of Transportation, 2017). PennDOT specifies ASTM gradations requirements of No. 57, No. 67, or No. 8 for concrete. The percent passing limits for these grades are summarized in Table 2.6. For paving, the solid volume of coarse aggregate must fall between 11 ft³ (0.31 m³) to 13.1 ft³ (0.37 m³) per 1 yd³ of concrete. PennDOT does not specify requirements on fracture of aggregate faces. The specification requires that the minimum amount of coarse aggregates passing the 0.5 in. (12.7 mm) sieve must be 35% (§704.1(b)). PennDOT requires use of Type A fine aggregates for concrete. Table 2.7 summarizes the percent passing limits specified by PennDOT for fine aggregates in PCC paving mixtures. The fineness modulus of fine aggregates must fall between 2.3 and 3.15 (§703.1(c)). PennDOT requires use of class AA concrete or HES concrete for rigid pavements (§501.2).

PennDOT also requires that the edge slump of paving concrete in its plastic state must not exceed 0.125 in. (3.18 mm) between adjacent lanes or between lanes and ramps. The edge slump must not exceed 0.25 in. (6.35 mm) between lanes and shoulders and between ramps and shoulders. For class AA concrete, the minimum and maximum required cementitious material contents are 587.5 lb/yd³ (348 kg/m³) and 752 lb/yd³ (446 kg/m³), respectively. A 28-day design strength of 3500 psi (24.1 MPa) and the maximum allowable w/cm is 0.47 are required for class AA concrete (§704.1(b)). If HES cement concrete is adopted, then the minimum and maximum cementitious material contents are 752 lb/yd³ (446 kg/m³) and 846 lb/yd³ (502 kg/m³). A 28-day design strength of 3500 psi (24.1 MPa) is required and the maximum allowable w/cm is 0.40

(§704.1(b)). PennDOT allows use of pozzolans for cement concrete but does not specify the replacement levels (§704.1(b)). PennDOT allows a design air content of 6% for all classes of concrete. The measured air content in the field can vary by $\pm 1.5\%$ (§703.1(c)).

Table 2.6: PennDOT Percent-passing Limits for Coarse Aggregates.

Sieve ID, customary	Sieve size, in. (mm)	Percent Passing		
		No. 57	No. 67	No. 8
2 inch	2 (50.8)			
1½ inch	1.5 (38.1)	100		
1 inch	1 (25.4)	95 - 100	100	
¾ inch	0.75 (19.1)		90 - 100	
½ inch	0.5 (12.7)	25 - 60		100
⅜ inch	0.38 (9.5)		20 - 55	85 - 100
#4	0.19 (4.75)	0 - 10	0 - 10	10 - 30
#8	0.09 (2.36)	0 - 5	0 - 5	0 - 10
#16	0.046 (1.19)			0 - 5

Table 2.7: PennDOT Percent-passing Limits for Fine Aggregates

Sieve ID, customary	Sieve size, in. (mm)	Percent passing
⅜ inch	0.38 (9.5)	100
#4	0.19 (4.75)	95 - 100
#8	0.09 (2.36)	70 - 100
#16	0.046 (1.19)	45 - 85
#30	0.023 (0.595)	25 - 65
#50	0.012 (0.297)	10 - 30
#100	0.006 (0.149)	0 - 10
#200	0.003 (0.074)	

2.3.4 California DOT (Caltrans)

Caltrans specifies gradation requirements for aggregates for use in PCC (Caltrans, 2018). These requirements are also applicable for concrete mixtures used for pavements. Unlike other SHAs, Caltrans specifies a range of percent passing limit values for a certain set of individual sieve sizes. The sieve sizes for which the ranges are specified are different for different aggregate size ranges (§90-1.02C(4)(a)). These details are summarized here in Table 2.8. Table 2.9 and Table 2.10 summarize the percent passing limits specified by Caltrans for coarse and fine aggregates, respectively. The owner or contractor can choose a specific value for ‘X’ such that final percent passing value on a particular individual sieve falls in the range specified in Table 2.8 (§90-1.02C(4)(b) and §90-1.02C(4)(c)). In addition to the gradation requirements for individual size ranges, Caltrans specifies aggregate gradations for combined aggregate size ranges (§90-1.02C(4)(d)). These are summarized in Table 2.11. Caltrans requires 1.5 in. (38.1 mm) or 1 in. (25.4 mm) NMSA, unless otherwise specified. Note that the percent passing limits for different sieve sizes of combined coarse aggregates are fixed.

For the combined aggregate gradation, the difference between the percent passing value of the 0.38 in. (9.5 mm) and the percent passing value of the 0.09 in. (2.36 mm) sieve must not be less than 16 percent of the total aggregate (§40-1.02B(3)). Caltrans allows usage of gravel or crushed rock for PCC (§90-1.02C(2)). There are no specific requirements for aggregate fracture for paving concrete. Caltrans specifies a range of 505 lb/yd³ (300 kg/m³) to 675 lb/yd³ (400 kg/m³) of cementitious material for PCC (§40-1.02B(2)). Caltrans allows use of SCMs in concrete, however, it does not specify the range of partial replacement levels for each. More information on the requirements for SCMs are provided in §90-1.02B(3) of the specification document. There are no limits specified for w/cm or air entrainment for PCC.

Table 2.8: Gradation Limits Specified for Different Individual Sieves.

Aggregate size range, customary	Aggregate size range	Individual sieve size, in. (mm)	Limits of gradation (% passing)
1.5 – ¾ inch	1.5 in. (38.1 mm) to 0.75 in. (19.1mm)	1 (25.4)	19 - 41
1 inch – #4	1 in. (25.4 mm) to 0.19 in. (4.75 mm)	0.75 (19.1)	52 - 85
1 inch – #4	1 in. (25.4 mm) to 0.19 in. (4.75 mm)	0.38 (9.5)	15 - 38
½ inch – #4	0.5 in. (12.7 mm) to 0.19 in. (4.75 mm)	0.38 (9.5)	40 - 78
⅜ inch – #8	0.38 in. (9.5 mm) to 0.09 in. (2.36 mm)	0.38 (9.5)	50 - 85
#4 – 0	0.19 in. (4.75 mm) to 0	0.046 (1.19)	55 - 75
#4 – 0	0.19 in. (4.75 mm) to 0	0.023 (0.595)	34 - 46
#4 – 0	0.19 in. (4.75 mm) to 0	0.012 (0.297)	16 - 29

Table 2.9: Caltrans Percent-passing Limits for Coarse Aggregates Specified as ‘Operating Range.’

Sieve ID, customary	Sieve size, in. (mm)	Aggregate size range, customary			
		1½ – ¾ inch	1 inch – #4	½ inch – #4	⅜ inch – #8
2"	2 (50.8)	100			
1½ "	1.5 (38.1)	88 – 100	100		
1"	1 (25.4)	X±18	88 - 100		
¾"	0.75 (19.1)	0 – 17	X±15	100	
½"	0.5 (12.7)			82 - 100	100
⅜"	0.38 (9.5)	0 – 17	X±15	X±15	X±20
#4	0.19 (4.75)		0 - 16	0 - 15	0 - 28
#8	0.09 (2.36)		0 - 6	0 - 6	0 - 7

Table 2.10: Caltrans Percent-passing Limits for Fine Aggregates Specified as ‘Operating Range.’

Sieve ID, customary	Sieve size, in. (mm)	Percent passing (%)
$\frac{3}{8}$ inch	0.38 (9.5)	100
#4	0.19 (4.75)	95 - 100
#8	0.09 (2.36)	65 - 95
#16	0.046 (1.19)	X±10
#30	0.023 (0.595)	X±9
#50	0.012 (0.297)	X±6
#100	0.006 (0.149)	2 - 12
#200	0.003 (0.074)	0 - 8

Table 2.11: Caltrans Percent-passing Limits for Combined Aggregates.

Sieve ID, customary	Sieve size, in. (mm)	NMSA, in. (mm)			
		1.5 (38.1)	1 (25.4)	0.5 (12.7)	0.38 (9.5)
2 inch	2 (50.8)	100			
1½ inch	1.5 (38.1)	90 - 100	100		
1 inch	1 (25.4)	50 - 86	90 - 100		
$\frac{3}{4}$ inch	0.75 (19.1)	45 - 75	55 - 100	100	
$\frac{1}{2}$ inch	0.5 (12.7)			90 - 100	100
$\frac{3}{8}$ inch	0.38 (9.5)	38 - 55	45 - 75	55 - 86	50 - 100
#4	0.19 (4.75)	30 - 45	35 - 60	45 - 63	45 - 63
#8	0.09 (2.36)	23 - 38	27 - 45	35 - 49	35 - 49
#16	0.046 (1.19)	17 - 33	20 - 35	25 - 37	25 - 37
#30	0.023 (0.595)	10 - 22	12 - 25	15 - 25	15 - 25
#50	0.012 (0.297)	4 - 10	5 - 15	5 - 15	5 - 15
#100	0.006 (0.149)	1 - 6	1 - 8	1 - 8	1 - 8
#200	0.003 (0.074)	0 - 3	0 - 4	0 - 4	0 - 4

2.3.5 Iowa DOT

Iowa DOT requires use of Grade 3, Grade 4, or Grade 5 coarse aggregates for concrete mixtures for paving (Iowa Department of Transportation, 2015). The requirements specified by Iowa DOT for coarse and fine aggregates are summarized here in Table 2.12 and Table 2.13. Iowa DOT allows class ‘A’, class ‘C’, or class ‘M’ concrete mixtures for paving. Among these two classes, class ‘A’ concrete is considered as a primary paving mixture. The class-A mixture has lower cement content and lower ultimate strength compared to the class-C mixture (I.M. 529). Limits on cementitious material content are not specified. The minimum and maximum w/cm values for class ‘A’ mixtures are 0.474 and 0.532, respectively. The minimum and maximum w/cm values for class ‘C’ mixtures are 0.43 and 0.488, respectively. (Materials I.M. 529). For slip-form paving concrete, Iowa DOT allows a target air content of 8% with a tolerance level of ±2% (§2301.02B). The maximum allowable replacement levels specified for fly ash and slag are 20 and 35%, respectively. The maximum allowable total SCM replacement level is 40% (§2301.02B).

Table 2.12: Iowa DOT Percent-passing Limits for Coarse Aggregates.

Sieve ID, customary	Sieve size, in. (mm)	Grade 3	Grade 4	Grade 5
1½ inch	1.5 (38.1)	100	100	
1 inch	1 (25.4)	95 - 100	50 - 100	100
¾ inch	0.75 (19.1)		30 - 100	90 - 100
½ inch	0.5 (12.7)	25 - 60	25 - 75	
⅜ inch	0.38 (9.5)		5 - 55	20 - 55
#4	0.19 (4.75)	0 - 10	0 - 10	0 - 10
#8	0.09 (2.36)	0 - 5	0 - 5	0 - 5
#200	0.003 (0.08)	0 - 1.5	0 - 1.5	0 - 1.5

Table 2.13: Iowa DOT Percent-passing Limits for Fine Aggregates.

Sieve ID, customary	Sieve size, in. (mm)	Percent passing (%)
⅜ inch	0.38 (9.5)	100
#4	0.19 (4.75)	90 - 100
#8	0.09 (2.36)	70 - 100
#16	0.046 (1.19)	
#30	0.023 (0.595)	10 - 60
#50	0.012 (0.297)	
#100	0.006 (0.149)	
#200	0.003 (0.074)	0 - 1.5

2.3.6 Illinois DOT (IDOT)

IDOT specifies to use the grades CA7, CA11, CA14 or combinations of CA5 and CA11, and CA7 and CA11 for coarse aggregates for paving concrete (Illinois Department of Transportation, 2016). The gradation requirements for the individual size ranges are summarized in Table 2.14. IDOT allows three different fine aggregate gradations for PCC (§1003.02). These limits are summarized in Table 2.15. IDOT specifies class ‘PV’ concrete for pavements. The minimum and maximum allowable cementitious material contents are 585 lbs/yd³ (347 kg/m³) and 705 lbs/yd³ (418 kg/m³), respectively. The minimum and maximum allowable w/cm values are 0.32 and 0.42, respectively. The target air content should be between 5 and 8%. Class F fly ash, Class C fly ash, and blast furnace slag are allowed for producing class ‘PV’ concrete. The maximum allowable replacement levels for class C fly ash, class F fly ash, and slag are 25, 30, and 35%, respectively.

Table 2.14: IDOT Percent-passing Limits for Coarse Aggregates.

Sieve ID, customary	Sieve size, in. (mm)	CA5	CA7	CA11	CA14
2 inch	2 (50.8)	100			
1½ inch	1.5 (38.1)	95 - 100	100		
1 inch	1 (25.4)	15 - 65	90 - 100	100	
¾ inch	0.75 (19.1)			84 - 100	
½ inch	0.5 (12.7)	0 - 10	30 - 60	30 - 60	90 - 100
⅜ inch	0.38 (9.5)				25 - 65
#4	0.19 (4.75)	0 - 6	0 - 10	0 - 12	0 - 6
#8	0.09 (2.36)		0 - 5		
#16	0.046 (1.19)			0 - 6	

Table 2.15: IDOT Percent-passing Limits for Fine Aggregates.

Sieve ID, customary	Sieve size, in. (mm)	FA1	FA2	FA3
⅜ inch	0.38 (9.5)	100	100	100
#4	0.19 (4.75)	95 - 100	95 - 100	95 - 100
#8	0.09 (2.36)			60 - 100
#16	0.046 (1.19)	45 - 85	45 - 85	35 - 65
#30	0.023 (0.595)			
#50	0.012 (0.297)	3 - 29	0 - 30	8 - 30
#100	0.006 (0.149)	0 - 10	0 - 10	3 - 17
#200	0.003 (0.074)			0 - 8

2.4 COMPARISON OF AGGREGATE GRADATIONS FROM DIFFERENT SHAs

The gradations for different aggregate size ranges specified by different SHAs are compared here. Based on the information provided so far, it can be concluded that some SHAs have requirements for NMSA for paving aggregates, while some SHAs do not. For the purpose of comparisons, only the gradation limits of coarse aggregate with NMSA of 1.5 in. (38.1 mm) or 1 in. (25.4 mm) are shown. Table 2.16 compares the coarse aggregate gradation limits between ODOT and other SHAs. Note that Caltrans does not specify the gradation limits for the size range of 1.5 in. (38.1 mm) to 0.19 in. (4.75 mm) and hence, is excluded from the list of SHAs shown in the table. Table 2.17 compares the fine aggregate gradation limits among different SHAs. Among all SHAs, only ODOT (the special provision contract document) and Caltrans specify gradation limits for the combined aggregate size range of 1.5 in. (38.1 mm) to 0.003 in. (0.074 mm). These limit values are summarized in Table 2.18. Figure 2.5 through Figure 2.13 show comparisons of aggregate gradations between ODOT and other SHAs.

Table 2.16: Comparison of Coarse Aggregate Gradations from Different SHAs.

Sieve ID, customary	ODOT	TxDOT		PennDOT	Iowa DOT		IDOT CA5
		Grade 2	Grade 3		Grade 3	Grade 4	
2"	100	100	100				100
1½"	85 - 100	95 - 100	95 - 100	100	100	100	95 - 100
1"				95 - 100	95 - 100	50 - 100	15 - 65
¾"	35 - 65	35 - 70	60 - 90			30 - 100	
½"			25 - 60	25 - 60	25 - 60	25 - 75	0 - 10
⅜"	10 - 30	10 - 30				5 - 55	
#4	0 - 5	0 - 10	0 - 10	0 - 10	0 - 10	0 - 10	0 - 6
#8				0 - 5	0 - 5	0 - 5	

Table 2.17: Comparison of Fine Aggregate Gradations from Different SHAs.

Sieve ID, customary	ODOT	TxDOT	PennDOT	Caltrans	Iowa DOT	IDOT	
						FA2	FA3
⅜ inch	100	100	100	100	100	100	100
#4	90 - 100	95 - 100	95 - 100	95 - 100	90 - 100	95 - 100	95 - 100
#8	70 - 100	80 - 100	70 - 100	65 - 95	70 - 100		60 - 100
#16	50 - 85	50 - 85	45 - 85	55 - 75		45 - 85	35 - 65
#30	25 - 60	25 - 65	25 - 65	34 - 46	10 - 60		
#50	5 - 30	10 - 35	10 - 30	16 - 29		0 - 30	8 - 30
#100	0 - 10	0 - 10	0 - 10	2 - 12		0 - 10	3 - 17
#200	0 - 4	0 - 3		0 - 8	0 - 1.5		0 - 8

Table 2.18: ODOT Percent-passing Limits for Combined Aggregates.

Sieve ID, customary	ODOT	Caltrans
2 inch	100	100
1½ inch	90 - 100	90 - 100
1 inch	70 - 85	50 - 86
¾ inch	60 - 78	45 - 75
⅜ inch	44 - 57	38 - 55
#4	30 - 41	30 - 45
#8	23 - 32	23 - 38
#16	15 - 29	17 - 33
#30	8 - 29	10 - 22
#50	2 - 12	4 - 10
#100	0 - 4	1 - 6
#200	0 - 1.5	0 - 3

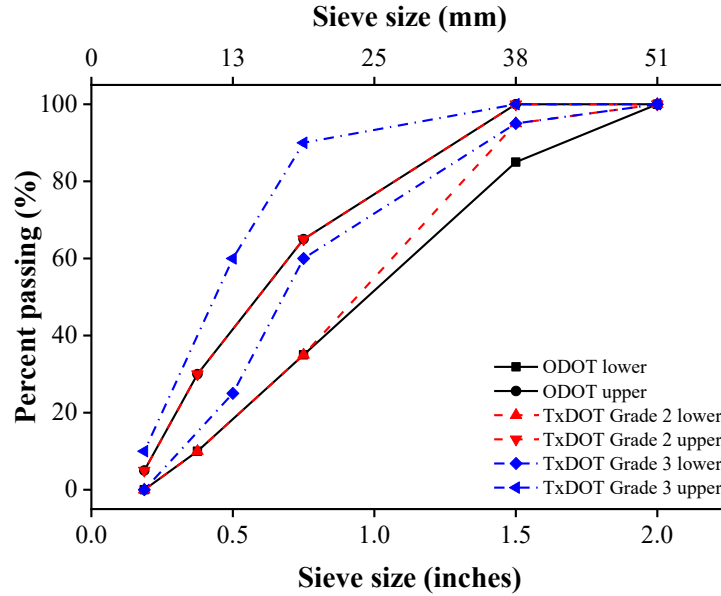


Figure 2.5: Comparison of percent-passing limits of coarse aggregates between ODOT and TxDOT (note: ODOT upper is the same as TxDOT Grade 2 upper).

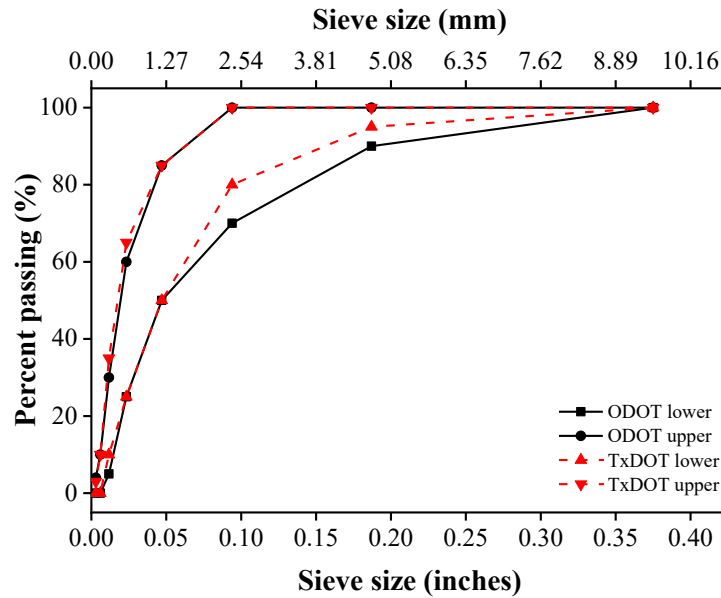


Figure 2.6: Comparison of percent-passing limits of fine aggregates between ODOT and TxDOT.

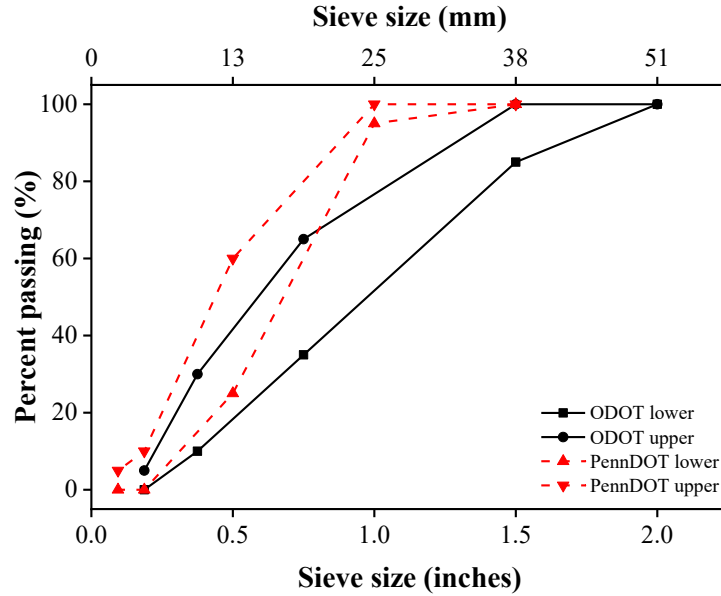


Figure 2.7: Comparison of percent-passing limits of coarse aggregates between ODOT and PennDOT.

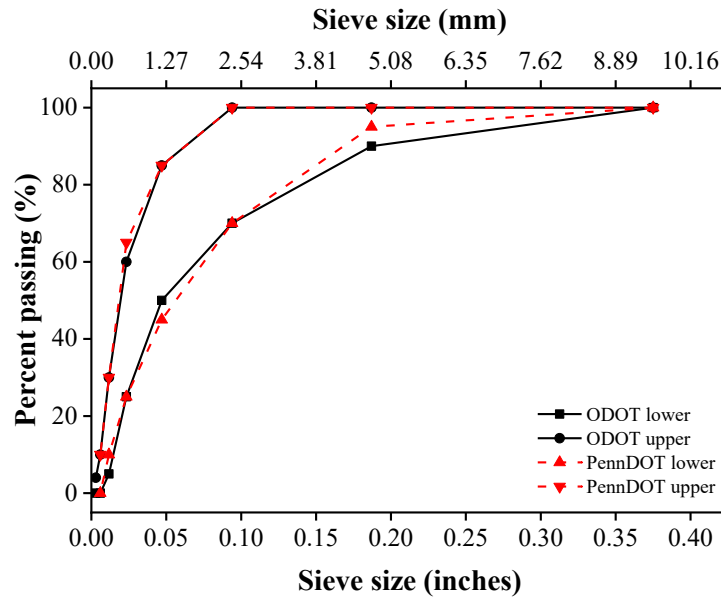


Figure 2.8: Comparison of percent-passing limits of fine aggregates between ODOT and PennDOT.

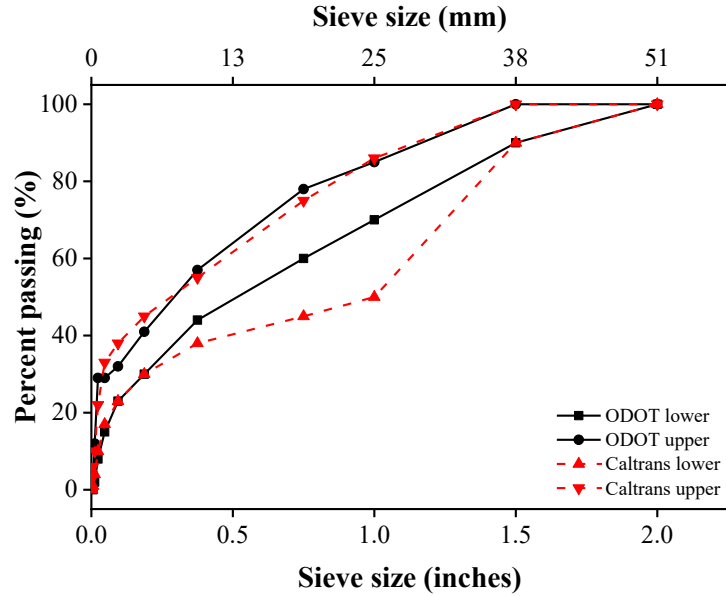


Figure 2.9: Comparison of percent-passing limits of combined aggregates between ODOT and Caltrans.

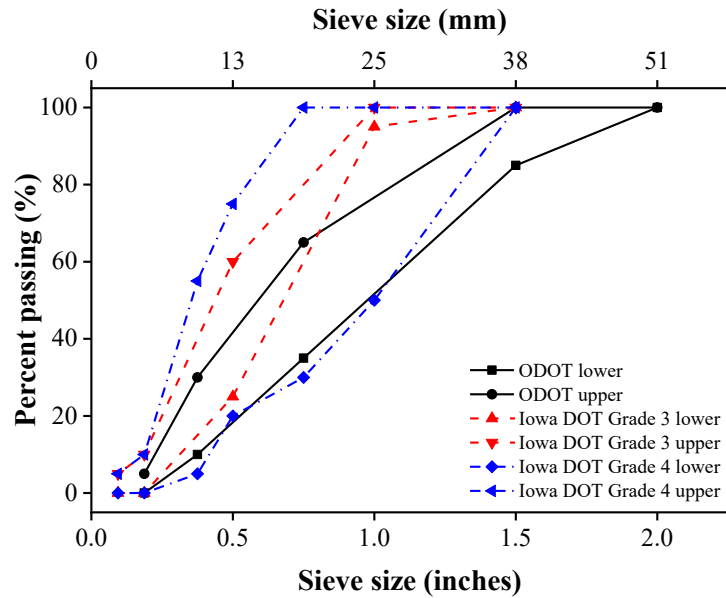


Figure 2.10: Comparison of percent-passing limits of coarse aggregates between ODOT and Iowa DOT.

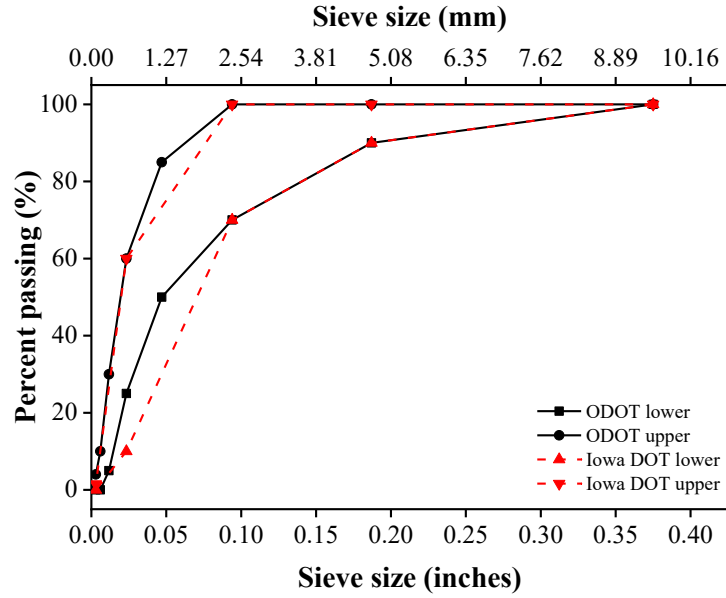


Figure 2.11: Comparison of percent-passing limits of fine aggregates between ODOT and Iowa DOT.

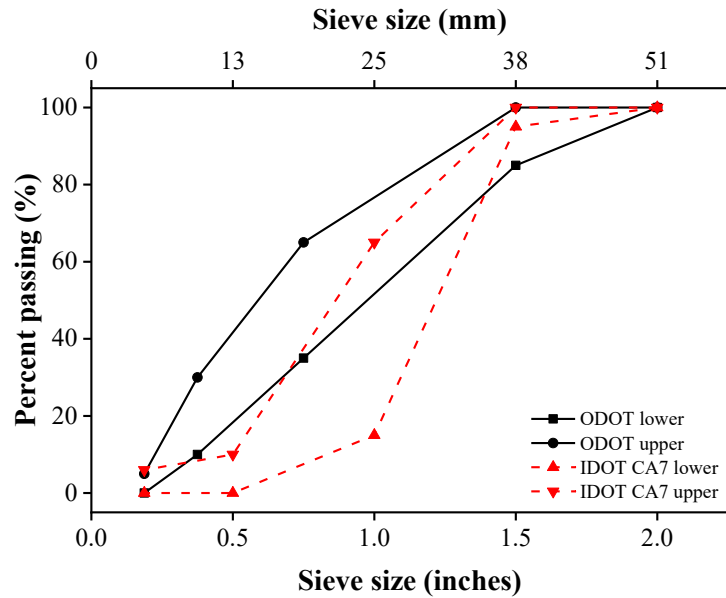


Figure 2.12: Comparison of percent-passing limits of coarse aggregates between ODOT and IDOT.

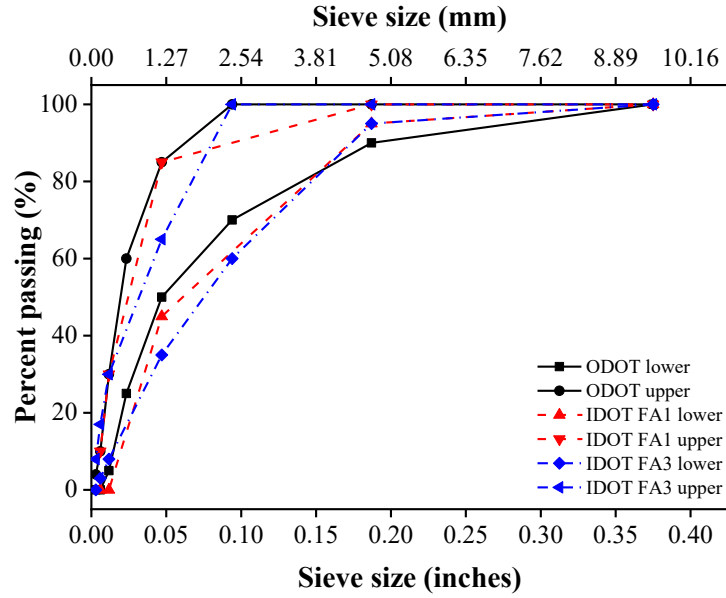


Figure 2.13: Comparison of percent-passing limits of fine aggregates between ODOT and IDOT.

2.5 PERFORMANCE OF PAVING MIXTURES

This section presents a literature review on the effects of various concrete mixture parameters on the performance of paving concrete. From this point forward, the paste volume and the aggregate void content in a concrete mixture are referred by the acronyms PV and AV, respectively.

2.5.1 Influence of aggregate type and gradation

Cramer, Hall, and Parry (1995) and Cramer and Carpenter (1999) studied the effects of aggregate type and aggregate gradation on the performance of paving concrete. In these studies, the optimized gradation was developed based on Shilstone and 0.45 power charts, and the gap gradation was developed by minimizing the aggregate particles in the size range of No. 4 to No. 16 in the combined aggregate systems. The authors reported that considering an optimized gradation generally resulted in an increased compressive strength and decreased water demand at similar slumps and F/C requirements when compared to gap gradations. Similar observations were made in other studies (Jerath & Hanson, 2007). Cramer and Carpenter (1999) also reported an increase in AASHTO T 277 (2015b) rapid chloride permeability test (RCPT) results with changes in gradation from optimized to gap-graded and with changes in aggregate types from gravel to crushed stone. However, the effects for Oregon aggregates are unknown.

D. M. Cook et al. (2013) performed a comprehensive investigation on the effect of aggregate gradation on performance of paving concrete in fresh states. The outcome of this work led to development of the tarantula curve that is currently being used by different SHAs. The authors reported a maximum percent retained value of 20% for sieve sizes ranging from 0.75 in. (19.1 mm) to 0.023 in. (0.595 mm) to avoid workability issues. Also reported is maximum percent-retained value of 12% on 0.09 in. (2.36 mm) and 0.046 in. (1.19 mm) sieves to avoid surface

finishing issues. All mixtures considered in D. M. Cook et al. (2013) had the same PV, same w/cm, and no air entrainment.

2.5.2 Influence of paste volume, binder type, w/cm, and air entrainment

Concrete mixtures with higher paste volumes are generally prone to higher shrinkage cracking compared with mixtures with lower paste volumes. Hence, minimizing the paste volume is critical for designing paving concrete mixtures. In this regard, it is beneficial to define the paste volume of a concrete mixture as a factor of aggregate void content.

The paste volume for a concrete mixture can be defined as the sum of volume of paste required for filling the aggregate-voids and the volume of paste required for covering the surfaces of aggregate particles for a defined consistency. Although the concept of considering paste volume to aggregate void ratio for proportioning concrete mixture constituents was initially proposed for self-compacting concrete (Skarendahl & Petersson, 1999), its application has become increasingly common in designing other concrete systems. It is understood that increasing the PV of a mixture will increase the overall consistency at a fixed aggregate void content (up to a certain volume). However, for minimizing the overall shrinkage in a mixture, it is important to minimize paste content while maintaining sufficient paste to achieve satisfactory workability. The following discussion provides a brief review on work performed in this area.

Jacobsen and Arntsen (2008) investigated the consistency of various mortar mixtures that had no air-entrainment. The authors defined a parameter called paste-aggregate void saturation ratio (k), which essentially is the ratio of volume of paste and volume of aggregate voids. The authors reported that a k value of 1.15 is a good start when designing mortar or concrete mixtures. However, this value is very dependent on the aggregate characteristics and proportions of fine and coarse aggregates. The authors also reported that the k correlates well with mixture consistency when air is included as part of the paste.

Rudy (2012) investigated the effect of binder type on the fresh characteristics and mechanical properties of paving concrete. The author suggested the combined volume of cement and water to range from 21.5 to 23.25% for mixtures with binary binder systems (i.e., cement + fly ash or cement + slag) for ensuring proper workability. These values correspond to total cementitious material contents of 469 to 507 lb/yd³ at a w/cm of 0.44 and approximately 6.5% air. The author however did not report the AV values for the aggregate systems considered for the investigation, which can vary significantly and is an important for minimizing OPC content.

Yurdakul, Taylor, Ceylan, and Bektas (2013) investigated the effect of the ratio of paste to aggregate void contents (PV/AV), w/cm, and binder type on the performance of non-air entrained mixtures. A high-range water reducer (HRWR) was used in this study, when needed for improving the workability. The authors reported that the PV/AV required for a mixture is dependent on the w/cm of the mixture. Analysis of the data reported in this study indicates that, at a maximum recommended HRWR dosage, the PV/AV values required to achieve a slump value of 1 in. (25.4 mm) were approximately 1.6 at a w/cm of 0.4 and 1.4 at a w/cm of 0.45 (significantly different than the k -values reported by Jacobsen and Arntsen. The optimum PV/AV seems to be dependent on the aggregate type, texture, NMSA, and gradation. Mixtures with fly ash showed improved workability compared to the control and slag mixtures. The

authors also reported that the rapid chloride permeability test (RCPT) results generally increase with an increase in PV/AV, as shown in Figure 2.14. This is important to note: increasing paste content can lead to higher transport rates of aggressive ions into the concrete, which can reduce service lives of the concrete system. The rate of increase in RCPT value with PV/AV is dependent on the type of binder. In this regard, concrete systems with slag were found to provide satisfactory results followed by concrete systems with fly ash and OPC concrete systems at an age of 90 days. ODOT currently adopts a maximum RCPT value of 1500 coulombs at an age of 90 days for paving concrete. Figure 2.14 indicates that this requirement can be met at PV/AV values as low as 1.25. However, the HRWR dosage levels considered by the researchers were significantly higher than the maximum recommended dosage levels. Recent research at OSU has shown that air-entrainment can have a significant impact on the water-reducer used in a concrete mixture. However, more testing is needed to determine the minimum PV/AV that can be achieved by using admixtures at dosage levels below the maximum recommended levels and that can provide satisfactory performance.

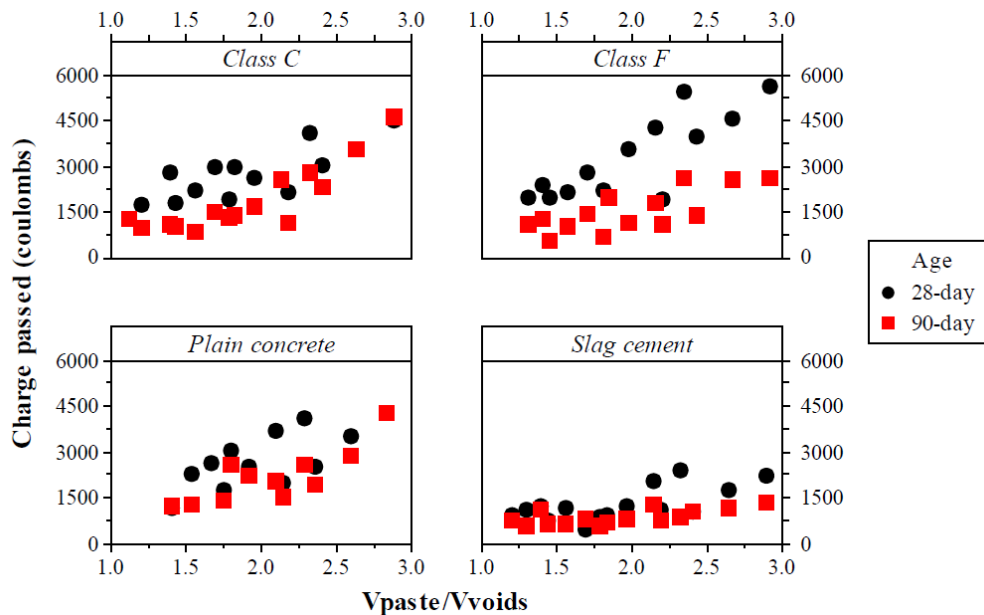


Figure 2.14: RCPT results for 100% OPC, 80% OPC + 20% Class C ash, 80% OPC + 20% Class F ash, and 60% OPC + 40% slag mixtures (Taylor et al. 2014).

Yurdakul et al. (2013) provided good insight on PV and performance; however, this study did not consider air-entrainment for concrete mixtures. Most SHAs require air-entrainment for concrete paving mixtures. The OSU research group anticipates that using an air-entraining admixture along with water-reducers (at recommended dosage levels) can assist in achieving low PV/AV values. Research studies performed by Cramer and Carpenter (1999), D. M. Cook et al. (2013), Rudy (2012), and Yurdakul et al. (2013) show that the paving mixtures, irrespective of the type of aggregate gradation and binder, generally show satisfactory freeze-thaw durability if air-entrainment is included. However, limited information is available on whether low PV/AV air-entrained mixtures provide satisfactory results towards parameters such as shrinkage and RCPT. Research is needed.

2.6 SUMMARY

Based on the information provided, the following general conclusions can be made regarding the current practice of specifying aggregate gradations for paving concretes:

1. The gradations specified by TxDOT, PennDOT, and Iowa DOT for coarse aggregates can be finer when compared to the gradation specified by ODOT.
2. The gradations specified by IDOT for coarse aggregates are coarser when compared to the gradation specified by ODOT.
3. The gradations specified by TxDOT and PennDOT for fine aggregates are like that of ODOT, although both can be a slightly finer than the gradation specified by ODOT.
4. The gradations specified by Iowa DOT and IDOT for fine aggregates are less restrictive (some sieve size limits are not specified) than ODOT specifications, and these fine aggregates can be slightly coarser than the gradation specified by ODOT.
5. The gradations specified by Caltrans for fine aggregate have tighter ranges (#4, #16, #30, and #50) than the ranges specified by the ODOT specifications. The mean fineness modulus for the specified fine aggregates for both ODOT and Caltrans are similar.
6. The gradation specified by Caltrans for combined aggregates is slightly coarser than the gradation specified by ODOT.

Regarding paste volume, aggregate gradation, and concrete performance, the following general conclusions can be drawn:

1. The optimum PV/AV is dependent on the aggregate type, texture, and gradation and minimizing this value while achieving the required concrete characteristics should lead to improved performance and better economy.
2. Optimized aggregate gradation, i.e., minimizing the AV, can result in increased compressive strength and decreased water demand.
3. Minimizing PV/AV can result in lower RCPT results, and improved performance.

3.0 PROJECT BACKGROUND

Prior to beginning this research project, ODOT initiated a small study to assess a concrete mixture used on a paving project. The preliminary research assessed the pavement mixture, but also assessed variants of the mixture. Aggregate gradation and cementitious materials content were modified to assess how these modification influence consolidation and stability, two key constructability characteristics for concrete pavements. Results are presented here to provide the reader with background.

3.1 AGGREGATE GRADATIONS FOR PRELIMINARY STUDY

The aggregate used in this study is from an ODOT approved source and met all agency requirements with the exception of the larger-sized aggregates, which in many cases did not meet the required two-face fracture. Aggregate was provided by ODOT. The aggregate gradation has been reported to significantly impact the consolidation behavior of concrete mixtures. Using ODOT's base mixture aggregate gradation as a reference, additional mixture aggregate gradations were designed to be coarser and finer. The determination of what constitutes a coarse and fine aggregate gradation was accomplished using the Bailey method (Vavrik, Pine, & Carpenter, 2002). While predominantly used for asphalt concrete gradation design, the Bailey method has been shown to be practical when a specific aggregate structure is desired as it provides a partially mechanistic procedure to quantify the gradation and blend of multiple aggregate sources. The individual aggregate gradations received and used for the study are shown in Figure 3.1. The 1.5 inch (38 mm) to #4 and 1 inch (25.4 mm) to #4 aggregate materials were proportioned in different fractions to modify the gradations.

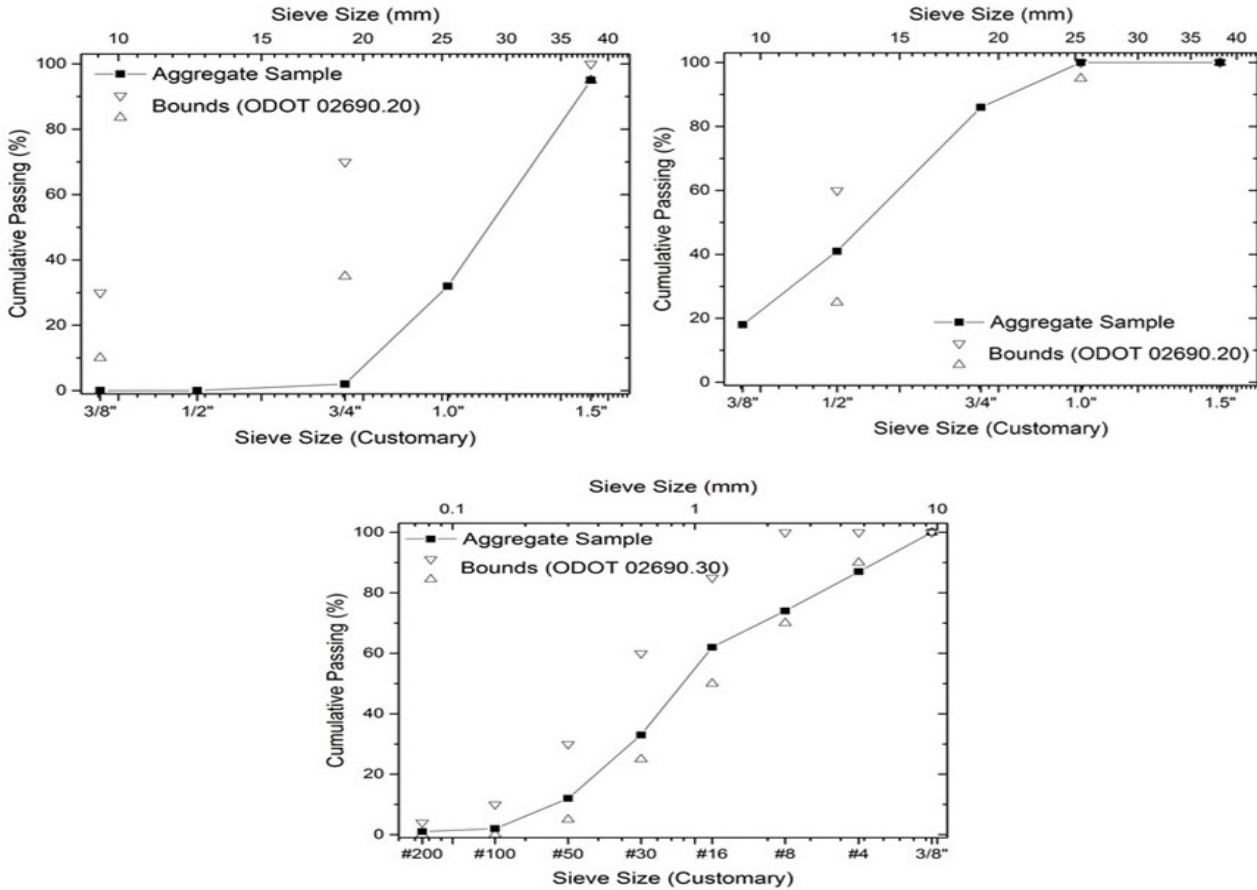


Figure 3.1: Aggregate gradations of the 1.5 (38 mm) inch to #4 (a), 1 inch (25.4 mm) to #4 (b), and sand (c) sources used in this preliminary study. Gradations shown represent as-received conditions.

The general procedure of the Bailey method is to assign control sieves to the gradation range desired and then calculate bounds based on those sieves. The control sieves vary depending on the NMSA, which was 1.5 inches (38 mm), per ODOT requirements, for all gradations. The control sieves based on the NMSA of 1.5 inches (38 mm) are shown in Table 3.1 for both coarse and fine gradations.

Table 3.1: Control Sieves for Bailey Method for both Coarse and Fine Gradations.

	Coarse Gradation	Fine Gradation
Primary Control Sieve (PCS)	3/8 inch (9.5 mm)	#8 (2.36 mm)
Half sieve (HS)	3/4 inch (19.0 mm)	#4 (4.75 mm)
Secondary Control Sieve (SCS)	#8 (2.36 mm)	#30 (0.60 mm)
Tertiary Control Sieve (TCS)	#30 (0.60 mm)	#100 (0.15 mm)

The control sieves can be used to calculate three ratios: CA, FA_c, and FA_f. The CA ratio describes the interlock and packing that can be achieved above the PCS. Generally, as the CA ratio increases, the voids in the aggregate increase. The FA_c ratio describes the interlock and

packing that can be achieved in the fine aggregate. The SCS is defined as the dividing line between aggregate particles that create voids (interceptors) and the aggregate particles that fill the voids (pluggers). As the FA_c ratio increases, the voiding in the aggregate decreases. The FA_f ratio describes the efficiency of the fine portion of the fine aggregate to fill voids. As the FA_f ratio increases, voids decrease. Based on empirical testing and field experience (Vavrik et al. 2002, 2001), a range of values for all three ratios can be established for what is considered a coarse gradation and fine gradation (Table 3.2).

Table 3.2: Recommended Ranges for Bailey Mixture Design Ratios (Vavrik et al. 2002, 2001).

Ratio	Coarse	Fine
CA	0.80 – 0.95	0.60 – 1.0
FA_c	0.35 – 0.50 ¹	0.35 – 0.50 ¹
FA_f	0.35 – 0.50 ¹	0.35 – 0.50 ¹

¹Recommended to have a value greater than 0.40 if possible

The ratios can be calculated using Eqs. 3-1 to 3-3, where the control sieve designations indicate the cumulative percent passing values. The Bailey parameters for each of the mixtures are shown in Table 3.3 which shows ODOT’s base mixture (based on the Bailey parameters) is a coarse mixture. The fine mixtures used in this preliminary study (Mixtures 2 and 4) have low FA_f ratios due to the low amounts of fine material on the #100 (0.15 mm) and #200 (0.075 mm) sieves of the source aggregates.

$$CA = \frac{HS - PCS}{100\% - HS} \tag{3-1}$$

$$FA_c = \frac{SCS}{PCS} \tag{3-2}$$

$$FA_f = \frac{TCS}{SCS} \tag{3-3}$$

Table 3.3: Bailey Gradation Parameters for Mixtures Tested.

	Base Mixture	Mixture 1	Mixture 2	Mixture 3	Mixture 4
Type	Coarse	Coarse	Fine	Coarse	Fine
CA Ratio	1.110	0.846	0.693	0.846	0.693
FA_c Ratio	0.586	0.554	0.448	0.554	0.448
FA_f Ratio	0.451	0.453	0.059	0.453	0.059

The original and proposed gradations were also characterized using ASTM D3398 (2006) (Table 3.4 and Table 3.5). The method is used to determine a particle index for each sieve size for each aggregate source and is based on work done on aggregate characterization in the 1960s (Huang, 1962). While the ASTM specification has been withdrawn, it still provides a useful technique to characterize the particle interactions (Jamkar & Rao, 2004). The gradation information is used to calculate a type of weighted average of the particle index, I_a . Since the 1.5 inch (38 mm) to #4 aggregate and the 1 inch (25.4 mm) to #4 aggregate sources are similar in terms of geological characteristics and source, with the only difference being their percentages in the aggregate mixture, the characterization of the two gradation ranges overlap and are similar.

Table 3.4: Index of Particle Size and Texture Values for each Sieve Size and Aggregate Source.

Retained Sieve	Source Aggregate	Absorption [%]	BSG, OD	I_a
1 inch (25.4 mm)	Coarse	2.1	2.656	14.3 ¹
0.75 inch (19.0 mm)	Coarse	2.0	2.650	14.3
0.5 inch (12.5 mm)	Coarse	2.0	2.655	14.1
0.375 inch (9.5 mm)	Coarse	2.5	2.598	11.9
#4 (4.75 mm)	Coarse	2.9	2.552	10.4
#4 (4.75 mm)	Sand	4.5	2.443	4.8
#8 (2.36 mm)	Sand	5.3	2.342	3.0
#16 (1.18 mm)	Sand	6.0	2.225	2.9
#30 (0.60 mm)	Sand	8.0	2.122	4.7

¹This value was assumed based on the 0.75 inch (19.0 mm) measurements

Table 3.5: Weighted Particle Indexes for the Three Gradations used in this Study.

Gradation	Weighted Particle Index	Overall Gradation Described by Index [%]
Base	10.2	85.2
Coarse	11.1	89.8
Fine	9.4	83.0

The use of the Bailey and ASTM D3398 (2006) procedures to classify aggregate gradations can be useful in quantifying gradation parameters. Although useful, proposed gradations may still require that proper bounds be met for qualification and specification purposes. There are numerous pavement gradation workability charts available for agencies to use for gradation qualification. For this preliminary study, the so-called tarantula curve (M. D. Cook et al., 2014) is used to assess bounds for the proposed gradations (Figure 3.2). All three proposed gradations are well within the bounds described by the tarantula curve.

For reference, the 0.45-power curve and Shilstone charts are provided in Figure 3.3 and Figure 3.4, respectively. The coarse and fine proposed gradations are clearly below and above the 0.45-power curve, respectively. Additionally, the Shilstone chart indicates that the coarse gradation could result in workability issues. Namely, the coarse gradation is in the portion of the chart that predicts a rocky mixture. However, previous researchers have indicated that the Shilstone chart may have poor predictive capability for certain mixtures (Ley, Cook, & Fick, 2012; Yurdakul et al., 2013).

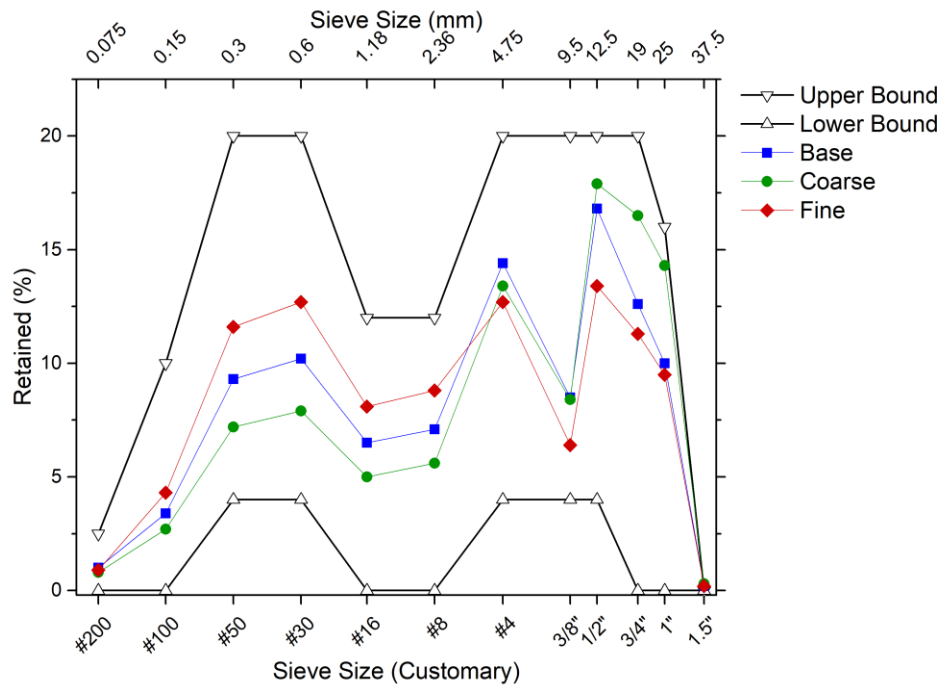


Figure 3.2: Proposed aggregate gradations with “tarantula” upper and lower bounds (Ley et al. 2012).

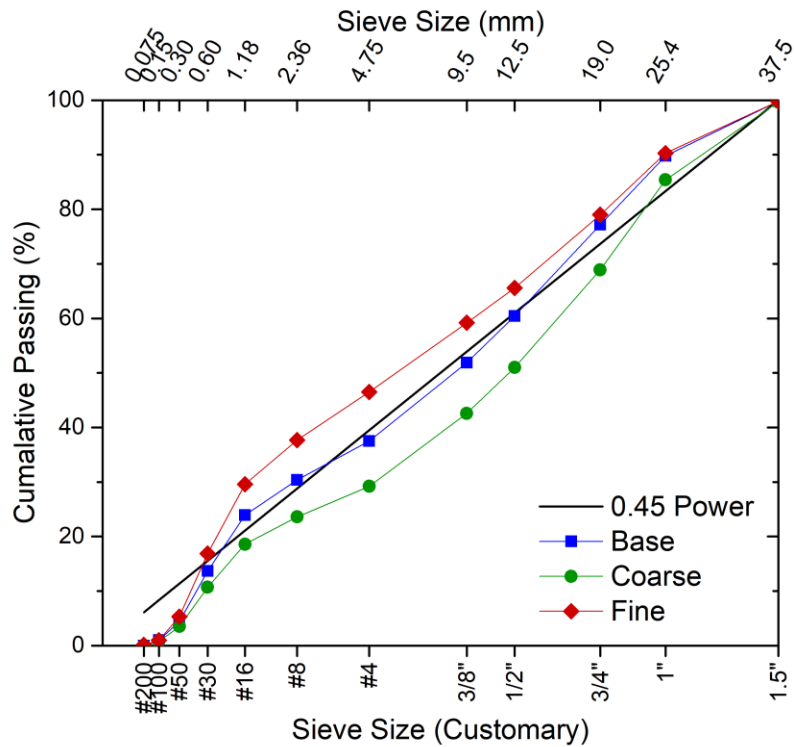


Figure 3.3: Proposed aggregate gradations plotted on a 0.45-power curve.

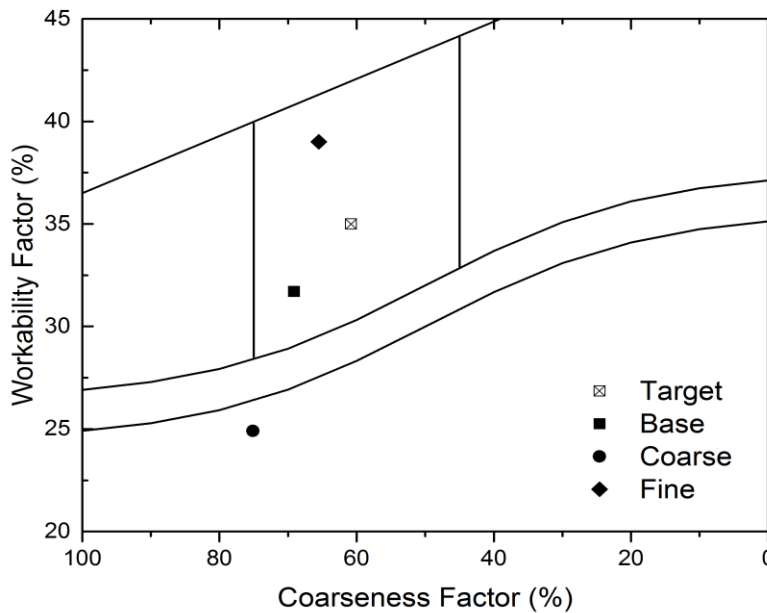


Figure 3.4: The proposed gradations plotted on a Shilstone workability chart.

3.2 TESTING AND RESULTS FROM PRELIMINARY STUDY

Five concrete mixtures were cast and tested for this project (Table 3.6). The base mixture was the mixture used by ODOT and some issues have been reported in the field. Based on this mixture, four additional mixtures were proportioned with input from ODOT and the effects of aggregate gradation and cementitious materials content were assessed. Mixtures 1 and 2 have the same cementitious content as the base mixture but have coarser and finer aggregate gradations, respectively. Mixtures 3 and 4 have a reduced cementitious content and the same coarser and finer aggregate gradations as mixtures 1 and 2. Note that no systematic approach is used here to minimize cementitious materials (and paste) content; this will be addressed in the main research program. Three admixtures were used in all mixtures: MasterAir AE90 (1.6 fl oz/cwt [104 mL/100 kg]), MasterPozzoloth 80 (4.9 fl oz/cwt [319 mL/100 kg]), and MasterSet Delvo (2.9 fl oz/cwt [189 mL/100 kg]).

Table 3.6: Mixture Designs used in this Study. All units in lbs/yd³ (kg/m³).

Material	Base Mixture	Mixture 1	Mixture 2	Mixture 3	Mixture 4
OPC	458 (273)	458 (273)	458 (273)	435 (259)	435 (259)
GGBFS ¹	153 (91)	153 (91)	153 (91)	145 (86)	145 (86)
Water	235 (140)	235 (140)	235 (140)	223 (133)	223 (133)
1.5" - #4 Agg.	561 (334)	880 (524)	561 (334)	897 (534)	572 (340)
1" - #4 Agg.	1293 (769)	1278 (760)	975 (580)	1303 (775)	994 (591)
Sand	1264 (752)	981 (584)	1565 (931)	1000 (595)	1595 (949)

¹Ground granulated blast furnace slag

Note: 1 inch = 25.4 mm

3.2.1 Mixing and Standard Fresh Properties

Prior to mixing, each aggregate source was dried and fractioned. This allowed for careful control of the gradation during batching and removed inconsistencies that could be present in the supplied materials. During batching, the fractioned materials were recombined to achieve the target gradation. The chemical admixtures were mixed in the batch water immediately prior to mixing to ensure uniform dispersion. The mixing procedure followed typical field conditions. The mixing and dwell times were chosen to simulate a batch plant with concrete transported via dump truck to the jobsite. In this way, the measured fresh properties would be similar to those that would be seen at the paving train in the jobsite compared to the just mixed properties at a batch plant. The following standard test were performed for each concrete mixture: slump test (AASHTO, 2018), unit weight (AASHTO, 2019), air content (AASHTO, 2017c), and super air meter (SAM) number (AASHTO, 2017c).

3.2.2 The Box Test

The Box Test (M. D. Cook et al., 2014) can be performed to quantify the “quality” of slipform paving mixtures. The test addresses some of the shortcomings that a standard AASHTO T 119M (2018) slump test has with slipform paving operations. Mainly, the Box Test introduces a known amount of energy through vibration to simulate the area of influence that the vibrator rack has on a slipform paver and the amount of consolidation that can be expected. All five mixtures were tested using the Box Test procedure. The concrete was shoveled into the box, which is a cube (1 ft³ [0.028 m³]), to a height of 9 inches (22.9 cm). Care was taken to evenly distribute the concrete in the box while minimizing any compactive effort. Once the concrete was at a level height of 9 inches (22.9 cm), a Wyco 994 square-head vibrator was used to introduce the consolidation energy. The vibrator was slowly and steadily inserted into the concrete sample within 3 seconds and then slowly and steadily withdrawn from the sample within 3 seconds.

After withdrawal of the vibrator, one side of the box form is removed and the edge slump, E , is measured, if any, by using the box itself as a vertical reference point (Figure 3.5). Once measured, the remaining sides of the box are carefully removed and the percent surface voids on each side is assessed. The literature for the Box Test (Cook et al. 2014; Ley et al. 2012) provides a four-category guideline to follow for assessing surface voiding (Figure 3.6). A comparison between the completely visual assessment (Figure 3.6) and the grid overlay procedure results are shown in Table 3.8.

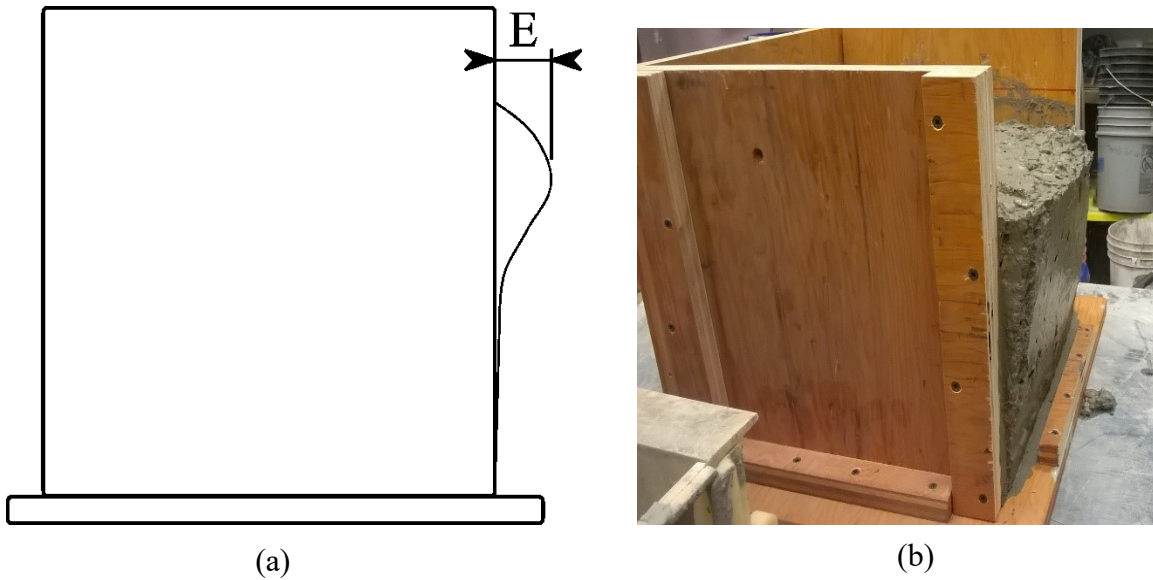


Figure 3.5: Schematic (a) of the edge slump measurement, E , and image of base mixture edge slump (b).

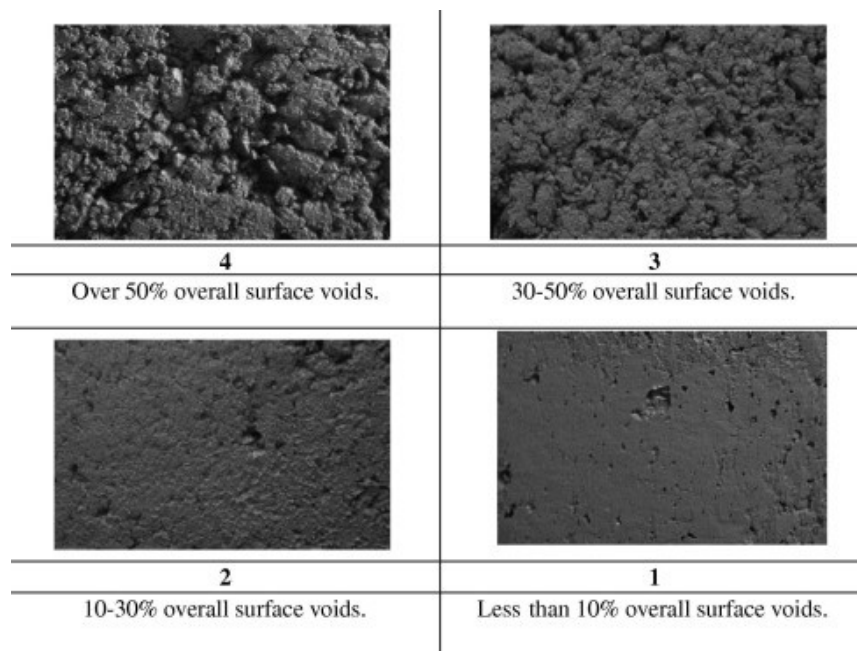


Figure 3.6: Four-category surface voiding assessment template for the Box Test (Cook et al. 2014).

3.2.3 Hardened concrete properties

Standard compressive and flexural strength tests were performed on the concrete mixtures. Additionally, the Box Test specimens were retained, cored after a minimum of 28 days of sealed curing, and then tested for unit weight and formation factor.

The compressive strength of each mixture was measured using three 6 inch by 12 inch (150 mm by 300 mm) cylinders following AASHTO T 22 (2017a). Upon demolding at 24 hours, specimens were placed in a lime water bath at 73.4°F±3.6°F (23°C±2°C) for 27 days. The flexural strength of each mixture was measured using three 6 inch square by 21 inch (150 mm square by 533 mm) long beams following AASHTO T 97 (2017b). The beams were cured in the same manner as the compressive strength specimens and tested at an age of 28 days.

3.2.3.1 Resistivity and Formation Factor

Numerous researchers have used electrical resistivity measurements of concrete to estimate the set time of concrete mixtures (Li, Xiao, & Wei, 2007) or correlate to various transportation properties of concrete (Andrade, 1993; Nokken & Hooton, 2008; Riding, Poole, Schindler, Juenger, & Folliard, 2008; Rupnow & Icenogle, 2012; Tumidajski, Schumacher, Perron, Gu, & Beaudoin, 1996). A standardized procedure to assess chloride ingress on concrete structures using surface resistivity is outlined in AASHTO T 358 (2019c). The AASHTO method outlines the procedure for surface resistivity measurements. With cores and cylinders, it is also possible to measure the bulk resistivity (AASHTO, 2015a). The two types of measures are not identical but can be interconverted with a geometric correction factor.

Another parameter that can be calculated from resistivity measurements is a formation factor. The formation factor, F , of a porous material, as determined using resistivity measurements (Archie 1942), describes the porosity and connectivity of the pore structure. It is simply defined as the ratio of the bulk resistivity, ρ , and the pore solution resistivity, ρ_o , as shown in Eq. 3-4. The formation factor can also be described in terms of porosity, ϕ , and connectivity, β .

$$F = \frac{\rho}{\rho_o} \cong \frac{1}{\phi} \cdot \frac{1}{\beta} \tag{3-4}$$

The formation factor of a concrete material can be calculated at any degree of saturation (DOS). However, this work compared the formation factors determined at the nick point of the concrete moisture state. The nick point is the DOS that corresponds to the filling of gel and capillary porosity.

3.2.3.2 Experimental Procedure

The Box Test specimens were sealed with sheet plastic for a minimum of 28 days at 73.4°F±3.6°F (23°C±2°C). Each specimen was then cored in several locations. A core was taken of the center portion where the vibrator entered the specimen. Cores were also taken at the four corners of the hardened Box Test specimen in order to assess the differences in consolidation and pore structure development. The cores were air-dried for 2 days and then the ends were saw cut to provide a uniform surface free of surface irregularities and edge effects.

An initial resistivity and mass measurement were taken of the air-dried specimens. An RCON2 resistivity unit from Giatec was used for all resistivity measurements. The frequency was 1kHz and the temperature of the specimen was measured during each test. After the samples were initially measured, they were then submerged in buckets containing simulated pore solution. A simulated pore solution was used to prevent alkali leaching during the re-saturation of the specimens (Bu & Weiss, 2014).

Temperature changes can significantly influence resistivity readings. Several temperature correction methods exist in the literature and the activation energy approach (A. Coyle, Spragg, Amirkhanian, & Weiss, 2016; Elkey & Sellevold, 1995; Sant, Ferraris, & Weiss, 2008) was chosen for this project. The equation is an Arrhenius based approach as follows:

$$\rho_{T_{ref}} = \rho_T \cdot e^{\left[\frac{-E_a}{R} \left(\frac{1}{T} - \frac{1}{T_{ref}} \right) \right]} \quad (3-5)$$

where:

$\rho_{T_{ref}}$ is the resistivity corrected to the reference temperature,

T_{ref} , ρ_T is the resistivity at temperature T ,

R is the universal gas constant, and

E_a is the activation energy of conduction.

Because the specimens were sealed, an activation energy of conduction of 23 kJ/mol (A. T. Coyle, 2017) was assumed for all mixtures to correct for temperature effects.

The simulated pore solution is calculated using the online NIST pore solution calculator (<https://ciks.cbt.nist.gov/poresolncalc.html>) which is based on prior published work (Bentz, 2007; Snyder, Feng, Keen, & Mason, 2003). The alkali content of the OPC was available through the provided mill sheet. Slag alkali content was estimated as no information on this was available. Based on the calculations, the simulated pore solution is comprised of 0.22M NaOH and 0.18M KOH with 2 grams of lime added per liter to form a saturated lime solution. Mass gain and electrical resistivity measurements were taken, at a minimum, at the following times from the start of the test: 2 hours, 4 hours, 1, 2, and 7 days.

The formation factor calculation requires knowledge of the pore solution resistivity. The most direct way to obtain this is to perform a pore solution extraction. Due to the significant difficulties of extracting pore solution from concrete older than 28 days, an estimated value obtained from the previously mentioned NIST calculator was used. Mixtures 1, 2, and the base had an estimated pore solution resistivity of 0.0040 kOhm*in

(0.0102 kOhm*cm) and mixes 3 and 4 had an estimated pore solution resistivity of 0.0048 kOhm*in (0.0122 kOhm*cm).

3.3 RESULTS AND DISCUSSION FROM PRELIMINARY STUDY

3.3.1 Fresh concrete characteristics

A summary of the fresh concrete characteristics is shown in Table 3.7. The base mixture had a target slump of 1.5±0.5 inches (38.1 mm ±12.7 mm). Mixtures 2 and 4 exhibited lower slump values.

Table 3.7: Standard Fresh Properties of Tested Mixtures.

Mixture	Slump [in]	Unit Weight [lbs/ft ³]	Air Content ¹ [%]	SAM Number	Temperature [°F]	Paste [%, vol.]
Base	2.00	143.3	8.3	0.24	68.4	25.7
1	1.25	141.5	8.7	0.26	72.7	25.7
2	0.75	144.6	6.9	0.42	73.4	25.7
3	2.00	144.1	8.7	1.21	72.0	24.4
4	0.25	147.7	5.3	0.24	72.6	24.4

¹Measured using the Super Air Meter.

Note: 1 lb/ft³ = 16.02 kg/m³ and °F = °C*9/5 + 32

The air content of the mixtures varied from 5.3% to 8.7%, even though all mixtures used the same air-entraining dosage rate. The combined effects of gradation and cementitious content can explain some of these differences. Mixtures 2 and 4 had the lowest air contents and had the highest sand percentage. It has been reported that gradation and the amount of sand can have a substantial impact on the effectiveness of the air-entraining admixture and thus the measured air content (Gaynor, 1963; Du & Folliard, 2005). The minimum specified air content for ODOT pavements is 4.5% and 5.0% for moderate (<1000 feet elevation) and severe (>1000 feet elevation) exposure conditions, respectively. All of the tested mixtures exceed these minimum values. However, air content as a function of paste plus aggregate volume alone does not provide a complete characterization of the freeze-thaw durability of a particular concrete mixture, especially when paste contents vary. The size and spacing of the air bubbles is an important factor. ASTM C457 (2016) is a method used to analyze the void size and spacing but is labor intensive and requires hardened concrete specimens. Another test method, AASHTO T 348 (2013b), uses an Air Void Analyzer (AVA) which is a timing method to assess bubble size AASHTO T 84 (2013a). However, that method was found to have highly variable results. In one case, two properly run tests with the same operator and device had values that differed by 43% (Distlehorst & Kurgan, 2007). Furthermore, using two separate devices on the same material produced values that differed by 53%.

The SAM was developed to address some of the shortcomings of measuring void spacing and size on fresh concrete (Ley & Tabb, 2013). It is similar to a standard air meter test except that after applying the first pressure to the concrete, two more over-pressures are applied and the responses are measured. This test is run twice on the same concrete specimen and the difference in the final over-pressures is calculated as a SAM number. Based on testing, a SAM number was

developed that offers some qualitative prediction of freeze-thaw durability (Figure 3.7) by correlating the pressure difference of two over-pressures with the ACI 201.2R recommendation for the air void spacing factor. A concrete mixture that has a SAM number at or below 0.20 is considered to have good freeze-thaw resistance (Ley & Tabb, 2013). More recent literature suggests that moving the threshold to 0.30 could reduce the number of false negatives (Tanesi, Kim, Beyene, & Ardani, 2016). By this metric, the base mixture, mixture 1, and mixture 4 all should have relatively good freeze-thaw resistance. Mixtures 2 and 3 do not appear to have ideal air bubble spacing.

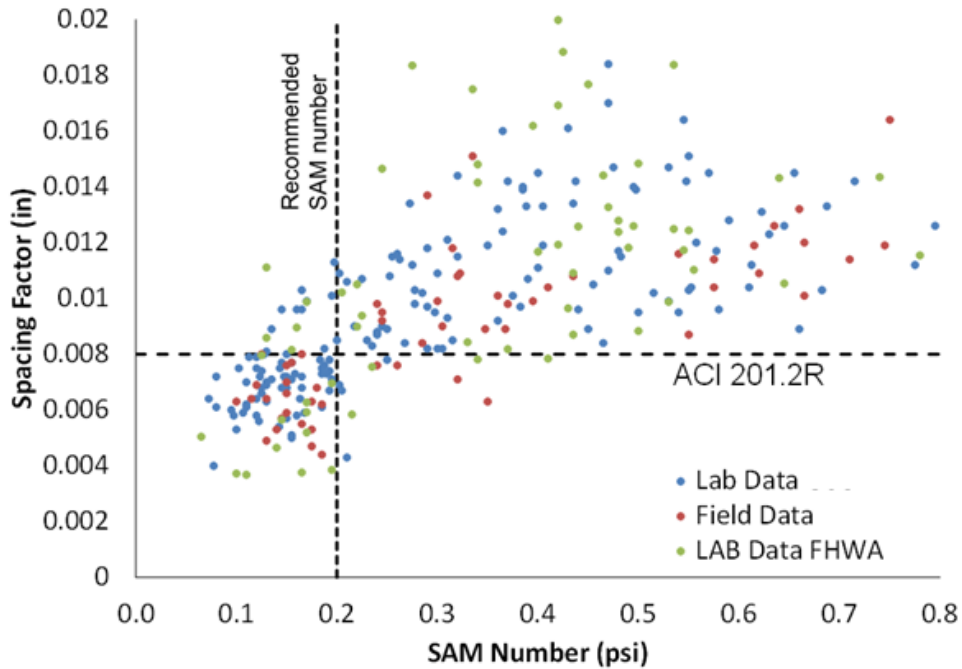


Figure 3.7: Comparison of SAM number and the ACI201.2R recommended spacing factor (Welchel, 2012).

3.3.2 Box Test

The Box Test was conducted on all five mixtures and the results from the image and visual assessment analysis are shown in Table 3.8. The edge slump values are shown in parenthesis for each mixture. Examining the surface consolidation first, it appears that the base mixture, mixture 1, mixture 2, and mixture 3 have good consolidation characteristics. The test indicated minimal voiding on the surface. Mixture 4 exhibited significant voiding and poor consolidation characteristics. The leaner cementitious content and larger sand fraction likely led to a mixture that did not form enough paste relative to the increase in the surface area of the overall mixture.

Table 3.8: Comparison of Grid Overlay and Visual Assessment Values for Surface Voiding Characterization.

Mixture	Side	Grid Overlay [%]	Visual Assessment [%]
Base Mixture (1 inch)	1	6	10-30
	2	2	<10
	3	2	<10
	4	3	<10
	Average	3	
Mixture 1 (1.5 inch)	1	3	<10
	2	7	10-30
	3	3	<10
	4	3	<10
	Average	4	
Mixture 2 (0.25 inch)	1	7	<10
	2	5	<10
	3	6	<10
	4	4	<10
	Average	6	
Mixture 3 (1.25 inch)	1	8	10-30
	2	5	<10
	3	13	10-30
	4	7	<10
	Average	8	
Mixture 4 (0 inch)	1	41	30-50
	2	20	10-30
	3	27	30-50
	4	29	30-50
	Average	29	

Note: 1 inch = 25.4 mm

Edge slump values for each mixture are also provided in parentheses.

While the base mixture, mixture 1, mixture 2, and mixture 3 specimens had good consolidation characteristics, only mixture 2 had sufficient stiffness to maintain its shape upon removal of the formwork (i.e., edge slump). The other three mixtures had edge slumps that were at least 1 inch (25.4 mm). According to ODOT construction specifications, 00755.49(a) and 00756.49(a), the edge slump on continuously reinforced concrete pavements (CRCP) and jointed plain concrete pavements (JPCP) should be no greater than 0.25 inches (6.35 mm) and thus the base mixture, mixture 1, and mixture 3 would fail the specification regardless of the pavement type.

When the values of the Box Test edge slump are compared to the standard slump test (AASHTO T 119M (2018)) there appears to be no significant trend between the two (Figure 3.8). Generally, the standard slump test seems to over-predict the amount of edge slump. Both tests fail to account for the thickness, and thus outward pressure generated by the weight of the concrete pavement is not included in the test and care must be used when using these results. However,

due to the shape, the Box Test appears to be a better indication of the field performance compared to the sloped edges of the standard slump test.

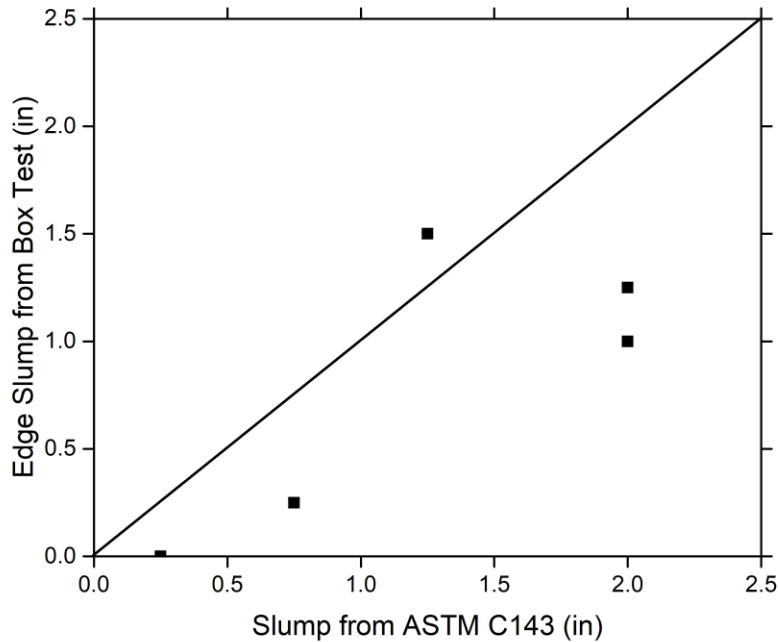
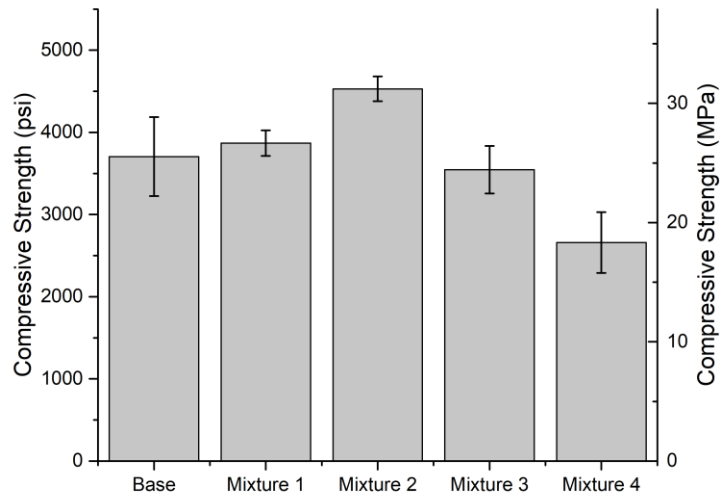


Figure 3.8: Comparison of Box Test edge slump values to standard AASHTO T 119M (2018) slump values. Line of unity shown for comparative purposes. Note: 1 inch = 25.4 mm.

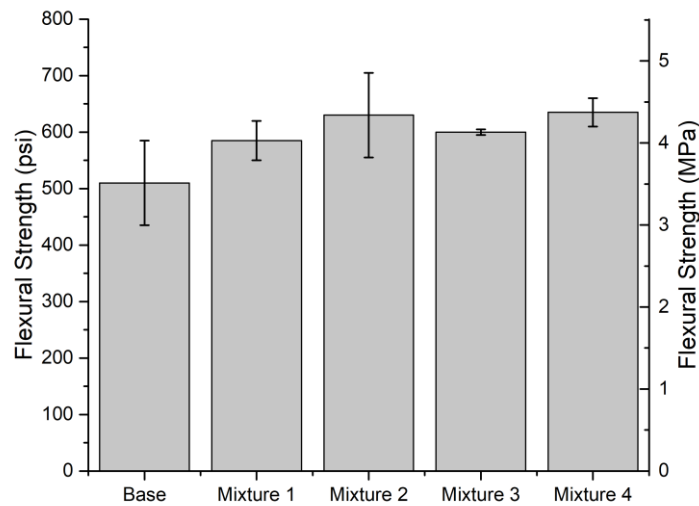
3.4 HARDENED CONCRETE PROPERTIES

3.4.1 Strength Properties

The results of the compressive and flexural testing procedures are shown in Figure 3.9. According to ODOT 00754.60(b), the concrete compressive strength must have a minimum compressive strength of 3000 psi (20.7 MPa) for traffic opening. For compliance, according to ODOT 02001.20(a), the pavement requires a minimum 28-day compressive strength of 4000 psi (27.6 MPa). Based on the test data, only mixture 2 would meet the compressive strength requirement (this mixture also met requirements of the Box Test). Documents provided by ODOT indicate that the base mixture met the compressive strength requirement when tested. However, documents indicated that the field mixture had 4.6% air and the laboratory mixture had 8.3% air. The reason for the difference is unknown.



(a)



(b)

Figure 3.9: Results of compressive (a) and flexural (b) testing for all mixtures. Tests were conducted at an age of 28 days and were in a lime bath until the time of testing.

3.4.2 Formation Factor

The formation factors were calculated using Eq.3-4 and are shown in Table 3.9 and Figure 3.10 and Figure 3.11. While each mixture only had one center core tested, four corner cores were extracted and averaged. The Box Test specimen with Mixture 3 broke after the first corner core was removed and as such, only one corner specimen was obtained. As expected, the formation factor is higher in the center cores for all the mixtures compared to the cores from the corner

locations. A higher formation factor indicates a more tortuous and refined pore structure. Looking at the standard deviations, it appears that the base mixture and mixture 1 had significantly different formation factors for the center and corner locations. This suggests that the mixtures may not consolidate evenly and may develop different pore structures depending on the distance from the vibrator. The resistivity values used in the calculation have been corrected for temperature. Mixtures 1, 2, and the base mixture had a pore solution resistivity of 0.0040 kOhm-in (0.0102 kOhm-cm) and mixtures 3 and 4 had a pore solution resistivity of 0.0048 kOhm-in (0.0122 kOhm-cm).

Table 3.9: Calculated Formation Factor Values for each Mixture.

Mixture	Location	Formation Factor	Unit Weight ¹ , lbs/ft ³	Voids, %	Air Content, %
Base Mixture	Center	1018	148.5	21.8	8.3
	Corners	783	147.2	23.2	
Mixture 1	Center	1104	149.4	21.6	8.7
	Corners	939	146.6	24.0	
Mixture 2	Center	973	148.7	20.8	6.9
	Corners	918	147.8	21.5	
Mixture 3	Center	859	148.8	21.9	8.7
	Corners	808	147.1	24.1	
Mixture 4	Center	800	151.2	19.4	5.3
	Corners	728	150.7	19.4	

¹Measured using vacuum saturation but functionally equivalent to ASTM C642 (2013).

Note: 1 lb/ft³ = 16.02 kg/m³

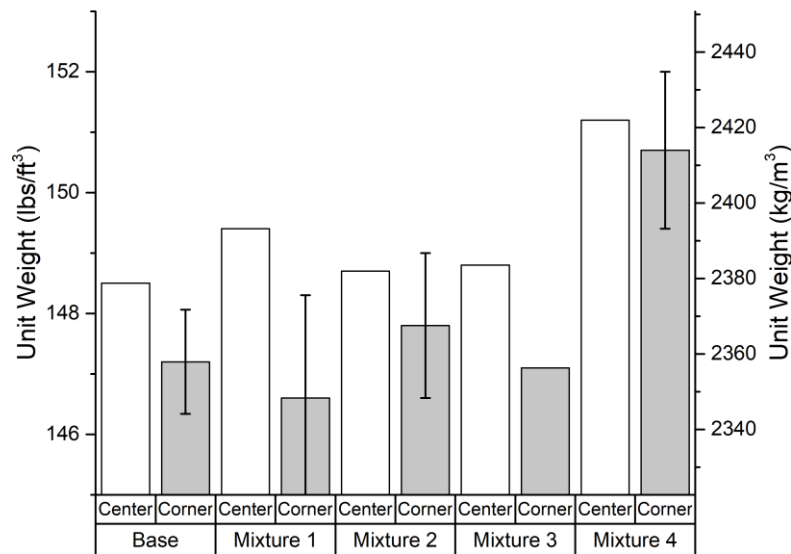


Figure 3.10: Comparison of unit weight measurements obtained via vacuum saturation. See note on mixture 3.

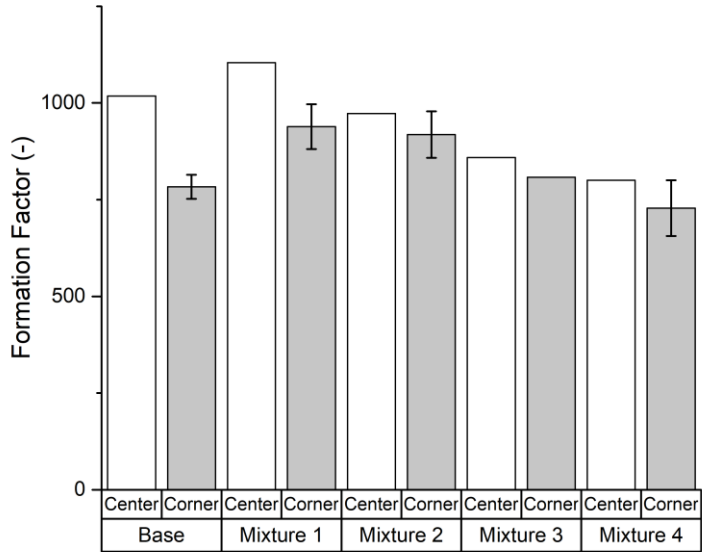


Figure 3.11: Comparison of formation factor measurements at different locations in each Box Test specimen. See note on mixture 3.

One apparent anomaly in the data is mixture 4. Results for the Box Test indicate that the mixture was extremely harsh and experienced significant surface voiding. Due to the harshness, the edge slump was zero. The unit weight data indicates that the box consolidated somewhat evenly. However, the formation factor data, while similar between the center and corner locations, was the lowest of the tested mixtures. This indicates a higher permeability than the other mixtures.

3.5 SUMMARY OF FINDINGS FROM PRELIMINARY STUDY

Five mixtures were tested as part of this preliminary research. One of the mixtures was a replicate of the field mixture that ODOT experienced challenges with previously. The other four mixtures assessed the effects of gradation and cementitious materials content. Mixtures were made with both coarser and finer aggregate gradations than the original mixture and the cementitious content was reduced to examine the possibility of a more sustainable pavement design. The Bailey method and ASTM D3398 (2006) was used to quantify the changes in the gradation.

The Box Test was used to estimate edge surface voiding and edge slump values. When the original mixture was tested, it indicated similar edge slump issues as reported with the field mixture. Several other mixtures experienced edge slump above the maximum values allowed by ODOT. While these other mixtures were not used in the field, it is expected that the Box Test could provide information on workability and consolidation for concrete slipform paving operations. These edge slump issues cannot be predicted or examined by the standard slump test and little correlation between the standard slump test and the Box Test was identified. The mixture that met all of the ODOT specifications was a modified mixture that had a finer

gradation than the original mixture. This mixture, mixture 2, had approximately 50% coarse and 50% intermediate/sand proportions by weight.

The SAM was used to measure the air content and estimate freeze-thaw durability. While mixture 2 met the fresh concrete requirements, the somewhat high SAM number indicated that the mixture may have some freeze-thaw durability issues. Further testing is needed to confirm this.

Formation factor was used to assess the pore structure development of each Box Test specimen. Results indicate that a very general trend may result: the greater the surface voiding, the lower the formation factor. There seems to be no trend in edge slump and formation factor. The testing also indicates that mixture 2, in addition to having low edge slump and low surface voiding, exhibited a uniform formation factor value regardless of location within the specimen. A uniform formation factor is ideal as it represents a consistent and even consolidation throughout the sample and this would be expected in the field during slipform paving operations.

Preliminary testing indicates that resistivity, and thus formation factor, measurements may be a good complement to the Box Test. However, the number of samples tested is small.

Additional assessment is needed to determine if the Box Test should be required for concrete pavements. Preliminary testing indicates that this test may provide guidance on constructability. Although preliminary tests indicate that the Box Test may provide an indication of the constructability of the concrete pavement mixture, little information is available on cementitious content required to achieve this workability/constructability. Therefore, a methodology is needed to quantify aggregate voids for various aggregate gradations. Using this information, additional testing should be performed to determine required paste content necessary to achieve constructability requirements. The research described in the following sections addresses these needs.

4.0 METHODOLOGY FOR DETERMINING OPTIMUM PASTE CONTENT

This chapter provides a detailed step-by-step procedure for designing paving concrete mixtures based on a “optimized-paste-volume” approach. Optimum paste content is generally defined as the minimum paste content associated with the aggregate void content that can achieve required fresh and hardened characteristics. However, in some cases where AV_{\min} occurs at low or high fine aggregate contents, the minimum paste content may be associated with an AV not at the minimum voids. The premise for this research is that the required paste content is dependent on the aggregates used for the concrete and characterizing these aggregates prior to developing the mixture proportions can provide valuable information to minimize the paste content of the concrete. Minimizing the paste content can result in environmental and economic benefits. Also, Yurdakul et al. (2013) reported that strength is independent of paste volume (assuming the concrete is workable) and that permeability increases with increased paste volumes. Piasta and Zarzycki (2017) reported that lower paste contents result in lower shrinkage values. Therefore, in addition to environmental and economic benefits, durability benefits are also possible. A standard methodology is needed.

The first step in this methodology involves the characterization of the coarse and fine aggregates. The second step involves conducting AASHTO T 19M (2014a) test on different combined samples of coarse and fine aggregates. The objective here is to establish a relationship between aggregate void content (AV) and the fine to coarse aggregate ratio values by mass (F/C) to identify an optimum F/C (F/C_{opt}) that results in the lowest AV (AV_{\min}) value. The third step is to determine whether the optimized combined gradation meets the project specification requirements. For example, past research has shown that F/C_{opt} values can be greater than 1 for aggregate systems composed of quarry rock (Hendrix (2015)). However, most SHAs have historically used F/C values below 1, often due to lack of availability or higher costs associated with procuring good quality sand (i.e., fine aggregate). If the optimized aggregate gradation developed in step 2 fail to meet specification requirements, one of the following two options must be implemented. The gradation of the combined aggregates must be modified per specification requirements and re-evaluated for AV per AASHTO T 19M (2014a) or the optimized gradation must be approved for the out-of-specification gradation before implementing it for batching of concrete.

The fourth step is to determine the initial paste volume for conducting trial mixtures. The total paste volume (PV) required for a concrete mixture is the sum of paste volume (cementitious materials, water, and air) required to fill the voids in the combined aggregate system and the additional paste volume required to achieve a required workability. For this project, workability requirements are for a typical paving concrete (i.e., low slump). The initial PV for assessing workability is dependent on aggregate type, texture, size, shape and can be determined from experience and/or past data. Yurdakul et al. (2013) recommended a value of 1.5 times the aggregate void content. This research indicates the required PV is very dependent on both the coarse and fine aggregate characteristics. For example, quarry rock required, on average, a PV/AV of 1.7; crushed gravel required an average PV/AV of about 1.9, and gravel required an average PV/AV of 1.7. Also, when a sand with a finer FM was used an average PV/AV was almost 1.9 and when a coarse sand was used an average PV/AV of 1.55 was required. A better estimate of the initial PV will result in fewer trial mixtures.

Therefore, with the AV known from testing, the ratio of PV and AV (PV/AV) must be determined via testing for the combined aggregates. Because the total paste volume required in a mixture is always greater than the minimum paste volume required to fill in the aggregate voids, the ratio of PV/AV (or PV/AV_{min}) is always greater than 1. Depending on a specific PV/AV or PV/AV_{min} value (e.g., 1.5), the volumetric proportions of paste volume and overall aggregate volume per cubic yard of concrete can be determined in this step.

The fifth step involves determining the water to cementitious material ratio (w/cm) value and the type of binder required for meeting the specified prescriptive or performance requirements for concrete. The sixth step involves determining the individual mass proportions of water, cement, SCMs, coarse and fine aggregates. If two types of coarse aggregates are used, then the total coarse aggregate (TCA) quantity needs to be determined first. The seventh step involves batching of trial concrete using estimated constituent mass proportions. The dosages of different admixtures (e.g., water-reducer, air-entraining agent, hydration stabilizer) can also be determined during this step. If it is determined that the trial mixture requires high dosage of water-reducer to achieve a desired workability, and if this dosage level exceeds the project specification requirement, the PV/AV value may be increased to reduce the water-reducer dosage. Alternately, if the PV/AV value is determined to be too high for a water-reducer dosage, the PV/AV value can be reduced, and the new trial mixture can be evaluated for performance. Steps four, five, six, and seven specified above must be repeated until the trial mixture meets the project-specified requirements in both fresh and hardened states.

The following sections outline the steps necessary for the methodology.

4.1 STEP 1. CHARACTERIZE COARSE AND FINE AGGREGATES

Select coarse and fine aggregates that meet the specification requirements. It is not uncommon to mix coarse aggregates of two different size ranges (e.g., ‘1.5 – 0.75 inch’ and ‘0.75 inch - #4’) during concrete batching. If coarse aggregates of two different sizes are anticipated for use in concrete, then coarse aggregates from each of the specified size ranges must meet the specification requirements, and the combined coarse aggregate gradation must meet the gradation requirements, if any, specified for the project. Information on the aggregate characteristics is generally provided by the supplier. In case this information is not provided by the supplier, the following test procedures must be conducted, results of which are required for conducting AASHTO T 19M (2014a) testing:

- AASHTO T 27 (2020a), Standard Test Method for Sieve Analysis of Fine and Coarse Aggregates;
- AASHTO T 84 (2013a), Standard Test Method for Density, Relative Density (Specific Gravity), and Absorption of Coarse Aggregate;
- AASHTO T 85 (2014b), Standard Test Method for Density, Relative Density (Specific Gravity), and Absorption of Fine Aggregate.

4.2 STEP 2. PERFORM AASHTO T 19M (2014A) TEST AND DETERMINE AV_{MIN}

Perform the AASHTO T 19M (2014a) test with different F/C values. An initial F/C value of 1.0 or less is recommended for testing. If the coarse aggregate is crushed gravel or gravel,

conduct testing at F/C intervals of 0.1 below the initial value. If coarse aggregate is crushed quarry rock, the F/C range of 1.0 or higher should potentially be investigated. The process of blending can impact the outcome of AASHTO T 19M (2014a) test. It is recommended that the guidelines of AASHTO T 2 (1991) be followed to obtain test samples. The F/C should be adjusted during testing until an AV_{\min} value for the combined aggregate system is identified, as shown in Figure 4.1. The AV content of the combined aggregate system can be determined using the following equation specified in AASHTO T 19M (2014a):

$$AV = 100 \times \frac{(SG_{com.agg}) \times (\rho_w) - DRUW}{(SG_{com.agg}) \times (DRUW)} \quad (4-1)$$

where:

DRUW is the dry rodded unit weight (lb/ft³ or kg/m³) of the combined aggregate as determined by the AASHTO T 19M (2014a) test,

ρ_w is the density of water (62.4 lb/ft³ or 1000 kg/m³), and

$SG_{com.agg}$ is the weighted average of the combined aggregates' oven dried specific gravity.

$SG_{com.agg}$ can be calculated using the following equation:

$$\frac{100}{SG_{com.agg}} = \frac{x_1}{SG_{A1}} + \frac{x_2}{SG_{A2}} + \frac{x_3}{SG_{A3}} \quad (4-2)$$

where:

x_1 , x_2 , and x_3 are the percentage mass fractions of individual aggregates and

A1, A2, and A3 are the different aggregates used in the blend.

Note here that the sum of the percentage mass fractions is 100. The relationship between AV_{\min} and F/C_{opt} can be influenced by the gradation of the coarse aggregates. Results from the Phase 1 study also indicate that targeting a coarser gradation for combined coarse aggregates of two different size fractions generally result in lower AV_{\min} values, which will be discussed in more detail later.

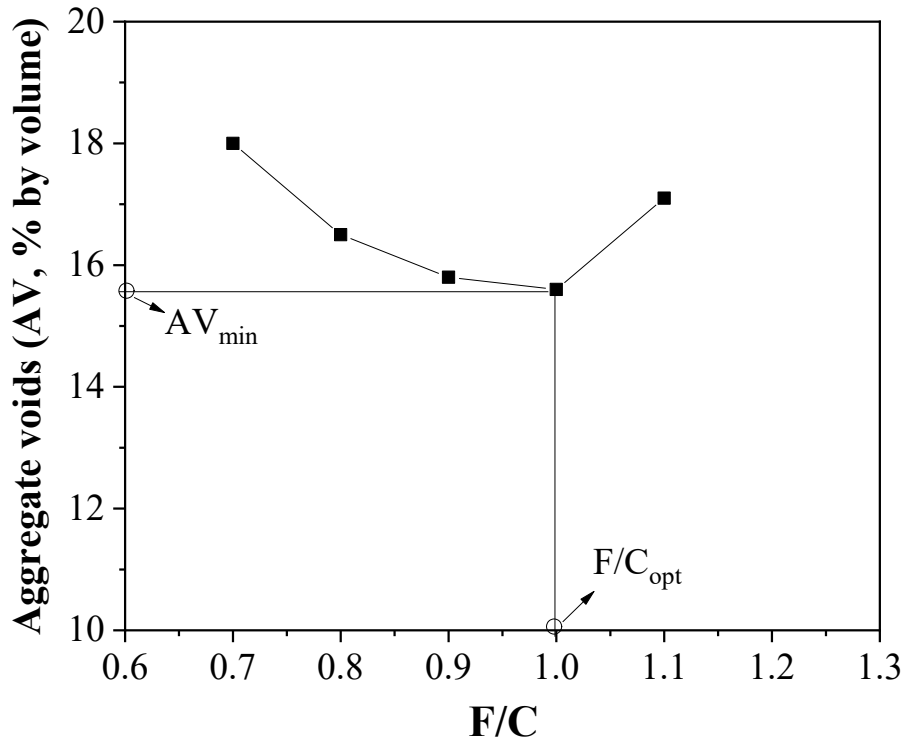


Figure 4.1: Aggregate voids (AV) as a function of F/C.

4.3 STEP 3. DETERMINE IF COMBINED AGGREGATE GRADATION MEETS PROJECT REQUIREMENTS

The estimated F/C_{opt} from testing may or may not fall in the range of F/C values specified for a project. For instance, ODOT has historically considered F/C values ranging between 0.48 and 0.79. However, test results from the Phase 1 study of this project indicate an F/C_{opt} of 1 or greater for most of the combined aggregate systems investigated. If F/C is governed by the project specification, and if the optimized combined aggregate gradation does not meet the gradation specifications, it is recommended to test combined aggregate system at the specified F/C to determine AV content. An alternative would be to obtain prior approval to use out-of-specification aggregates.

4.4 STEP 4. DETERMINE PASTE AND AGGREGATE VOLUMES

The volumes of paste and aggregate are determined in step 4. In general, this is performed for a target PV/AV_{min} and PV/AV_{min} values lower and higher than the target value. The objective of this step is to identify a range of PV/AV_{min} values to generate a plot showing edge slump (or some other specified criteria) versus PV/AV as shown in Figure 4.2. Note that in the figure an actual PV/AV would range between 1.5 and 1.64, because the limit on edge slump is 0.25 inches (6 mm) and PV/AV values higher than 1.64 do not meet this requirement (the shaded area indicates edge slump values that are less than the specified value of 0.25 inch (6.3 mm)).

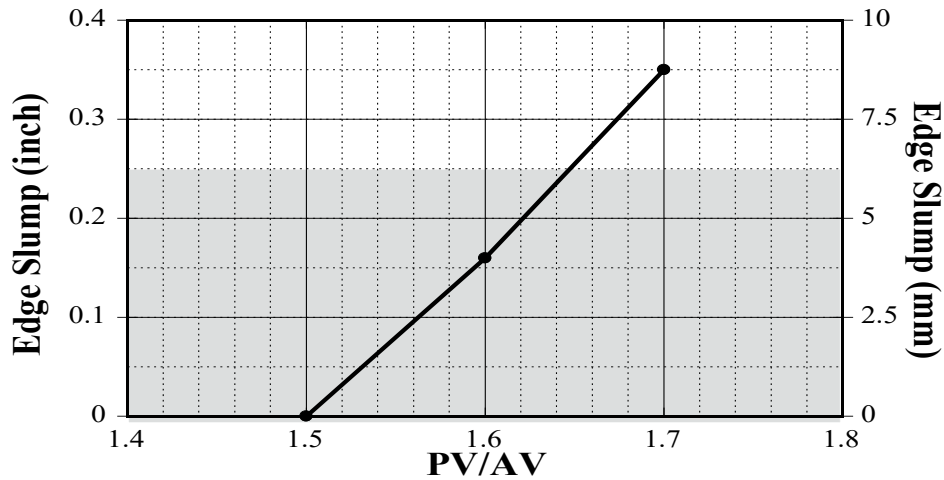


Figure 4.2: Example of anticipated results from Step 4.

For a fixed bulk volume of combined aggregates, the total paste volume is first calculated using the pre-defined PV/AV_{min} value and the AV_{min} value estimated in step 2 via aggregate testing. In this method, the volume of entrapped or entrained air is considered as part of the total paste volume. If the bulk volume of combined aggregates is assumed as 27 ft^3 , the solid volume of combined aggregates can be determined using the equation below:

$$Volume \text{ of combined aggregates} = 27 \times \frac{(100 - AV_{min})}{100} \quad (4-3)$$

where;

AV_{min} is a percentage. Note that the AV_{min} is a measure of the voids in the aggregate and the required paste content must be greater than this to achieve adequate flow (Hendrix, 2015).

Increasing the paste volume beyond AV_{min} increases the flowability of the mixture. However, increasing the paste volume beyond a high value can lead to instability, poor compressive strength, and volume change issues in concrete (Yurdakul et al., 2013). Therefore, it is critical to identify an optimal PV/AV_{min} ratio based on a set of trial mixtures. The data generated from the trial mixtures can be used to identify a range of paste volumes required for designing a paving mixture. However, to produce trial mixtures, some understanding on the typical range of PV/AV_{min} is required for the aggregate system being evaluated. For the combined aggregate systems evaluated in this research project, these ranges were identified in the Phase 2B and Phase 2C studies. The volume of paste required, for a known PV/AV_{min} (e.g., 1.7) and AV_{min} , can be estimated using the equation below:

$$Volume \text{ of paste} = PV / AV_{min} \times \left(27 \times \frac{AV_{min}}{100} \right) \quad (4-4)$$

Note that the sum of the calculated volumes of paste and combined aggregates is now greater than 27 ft³ (or some unit volume) because of the additional paste volume necessary to achieve the concrete's fresh characteristic requirements (e.g., edge slump, surface voids). To make the concrete mixture yield, the paste and combined aggregate volume shall be adjusted to a total concrete volume of 27 ft³ (i.e., 1 yd³ or other unit volume). The volume of combined aggregates per one cubic yard of concrete ($V_{com.agg}$) can be calculated using the following equation:

$$V_{com.agg} = \left[\frac{27 \times \frac{(100 - AV_{min})}{100}}{[(PV / AV_{min}) \times (27 \times \frac{AV_{min}}{100})] + [27 \times \frac{(100 - AV_{min})}{100}]} \right] \times 27 \quad (4-5)$$

where:

PV/AV_{min} is the ratio determined (or estimated) earlier and

AV_{min} is a percentage.

This equation can be further simplified as follows:

$$V_{com.agg} = \frac{(100 - AV_{min}) \times 27}{[(PV / AV_{min}) \times (AV_{min})] + [100 - AV_{min}]} \quad (4-6)$$

This unit of this value is cubic feet per cubic yard. The volume of paste per one cubic yard of concrete (V_P) can now be calculated by subtracting the value determined from Equations 5-5 or 5-6 from 27 or using the following equation:

$$V_P = \left[\frac{(PV / AV_{min}) \times (27 \times \frac{AV_{min}}{100})}{[(PV / AV_{min}) \times (27 \times \frac{AV_{min}}{100})] + [27 \times \frac{(100 - AV_{min})}{100}]} \right] \times 27 \quad (4-7)$$

This equation can be further simplified as follows:

$$V_P = \frac{(PV / AV_{min}) \times (AV_{min}) \times 27}{[(PV / AV_{min}) \times (AV_{min})] + [100 - AV_{min}]} \quad (4-8)$$

To summarize, in step 4, the volumes of both the combined aggregates and paste are calculated for 1 unit, in this case a cubic yard, of concrete. The two key parameters that are used for these calculations are AV_{min} and PV/AV_{min} . AV_{min} is determined in step 2 using the AASHTO T 19M (2014a) method and an initial estimate of PV/AV_{min} , greater than 1, is

selected to assess workability and/or constructability. Using the estimated total paste and combined aggregate volumes, the mass proportions of the main constituents (i.e., binder, water, coarse aggregates, and fine aggregates) are then determined using steps 5 and 6 (shown next). If the fresh characteristics of the trial mixture produced during step 7 meet specification requirements, it is recommended to lower the PV/AV_{min} and evaluate the new trial mixture based on this modified PV/AV_{min}. If the performance of the trial mixture based on initial PV/AV_{min} does not meet specification requirements, it is recommended to modify PV/AV_{min} based on the workability observed for the mixture. That is, if the mixture is harsh and unstable, PV/AV_{min} should be increased. Alternately, if the mixture is very flowable and is deemed unlikely to form a vertical edge during construction of slip-form pavement, PV/AV_{min} should be reduced. Different PV/AV_{min} values and the performance of the corresponding trial mixtures must be evaluated to determine the optimal PV/AV_{min} that meets all project specifications, in this case for paving concrete in both fresh and hardened states.

4.5 STEP 5. DETERMINE W/CM AND BINDER QUANTITY:

With the volume of combined aggregates (V_{CA}) and volume of paste (V_P) content values determined for one unit volume, the next step is to identify the w/cm and the quantity of binder required. The target w/cm is typically based on the compressive strength requirements of concrete. Several methods can be used to select an appropriate w/cm that meets project requirements and the user is encouraged to use the equation most appropriate for the conditions in which they are working. As an example, ACI 211 provides a table of target strength values as a function of w/c as follows:

$$\text{Target } w/cm = 1.163 \times e^{-0.0001776(\text{target strength [psi]})} \quad (4-9)$$

Note that other equations may be more applicable and the user should use the most appropriate equation. The weight of water (W_{t_{water}}) can be estimated using the following equation:

$$W_{t_{water}} = \frac{(V_P - (\%Air / 100 \times V_C)) \times (\rho_w)}{1 + \frac{1}{(w/cm) \times (SG_{bin})}} \quad (4-10)$$

where:

%Air is the percentage of design air specified for concrete,

V_c is the unit volume of concrete (27 ft³ or 1 yd³), and

SG_{bin} is the specific gravity of the binder.

Note here that if multiple cementitious or pozzolanic materials are used in the binder, a weighted average of the specific gravities of the cementitious materials can be used to calculate SG_{bin}. SG_{bin} can be calculated using the following equation:

$$\frac{100}{SG_{bin}} = \frac{y_1}{SG_{cem}} + \frac{y_2}{SG_{SCM1}} + \frac{y_3}{SG_{SCM2}} \quad (4-11)$$

where:

y_1 , y_2 , and y_3 are the percentage mass fractions of the cement and

SCMs. SCM_1 and SCM_2 are the different SCMs used in the ternary blend.

Note here that the sum of the percentage of mass fractions must be 100. Following this, the weight of the binder (Wt_{bin}) can be determined using the following equation:

$$Wt_{bin} = \frac{(V_P - (\%Air / 100 \times V_C)) \times (\rho_w)}{1 + \frac{1}{(w/cm) \times (SG_{bin})}} \times (w/cm)^{-1} \quad (4-12)$$

Once the weight of the binder (Wt_{bin}) is determined, the weights of the cement (Wt_{cem}) and SCMs (Wt_{SCM}) can also be determined. Wt_{SCM1} and Wt_{SCM2} can be calculated by multiplying the mass fractions with the weight of the binder as shown in the following equation:

$$Wt_{SCM1} = \frac{y_2}{100} \times Wt_{bin} \quad (4-13)$$

$$Wt_{SCM2} = \frac{y_3}{100} \times Wt_{bin} \quad (4-14)$$

Finally, the weight of the cement (Wt_{cem}) can be calculated by subtracting the weight of SCM (Wt_{SCM}) from the total binder content (Wt_{bin}), as shown in the following equation:

$$Wt_{cem} = Wt_{bin} - Wt_{SCM1} - Wt_{SCM2} \quad (4-15)$$

Now the weights of water, cement, and SCM(s) are now known and can be documented.

4.6 STEP 6. DETERMINE FINE AGGREGATE AND COARSE AGGREGATE QUANTITIES:

The remaining quantities left to be determined are the weights of the fine and coarse aggregates. F/C_{opt} , determined in step 2, is one of the key parameters to calculate the quantities of aggregates. The weight of total coarse aggregates (Wt_{TCA}) can be determined based on the following equation:

$$Wt_{TCA} = \frac{(V_C - V_P) \times (\rho_w) \times (SG_{TCA})}{1 + \left(\frac{SG_{TCA}}{SG_{FA}} \right) \times (F/C_{opt})} \quad (4-16)$$

where:

SG_{TCA} and SG_{FA} are the specific gravities of the total coarse aggregates and fine aggregates, respectively.

SG_{TCA} , assuming two aggregates are used, can be calculated using the following equation:

$$\frac{100}{SG_{TCA}} = \frac{z}{SG_{CA1}} + \frac{1-z}{SG_{CA2}} \quad (4-17)$$

where:

z is the percentage mass fraction of CA1.

SG_{CA1} and SG_{CA2} are the specific gravities of CA1 and CA2 respectively.

The weight of CA1 (Wt_{CA1}) and CA2 (Wt_{CA2}) can be calculated based on the following equations:

$$Wt_{CA1} = Wt_{TCA} \times \frac{z}{100} \quad (4-18)$$

$$Wt_{CA2} = Wt_{TCA} - Wt_{CA1} \quad (4-19)$$

Subsequently, the weight of the fine aggregates (Wt_{FA}) can be calculated based on the following equation:

$$Wt_{FA} = Wt_{CA} \times (F/C_{opt}) \quad (4-20)$$

At the end of this step, the weights of the coarse and fine aggregates are known and can be documented.

4.7 STEP 7. CHECK CALCULATIONS AND PERFORM TRIAL MIXTURES:

Once the weights of different constituent materials are computed, the user must check to confirm that the sum of volume of all the ingredients equals 27 ft³ (or some unit volume).

Once the mixture design is finalized, trial mixtures are batched and investigated for adequate workability. The dosages of chemical admixtures such as water reducers and air entrainers are also determined at this step. From a sustainability standpoint, it is recommended to use minimal binders and maximum water reducers (within the manufacturer's recommendation) to achieve the workability target. If the target workability is not achieved at recommended admixture dosages, then the PV/AV_{min} of the mixture must be modified and investigated via batching. Repeat steps 4 to 7 until a mixture design is arrived at that meets all project specification requirements.

4.8 SUMMARY

This chapter provided a step by step approach to proportion a concrete that meets the fresh and hardened characteristic requirements at the lowest achievable paste content. The lowest achievable paste content will require the lowest amount of cement, which is generally more economical, sustainable, and resilient.

5.0 EXPERIMENTAL PROGRAM AND MATERIALS

The experimental program of this research study (not including the preliminary study in the project background) was executed in two different phases—Phase 1 and Phase 2. The objectives and test program for each phase are presented next.

5.1 PHASE 1 – AGGREGATE CHARACTERIZATION

Because one of the objectives of this research is to identify a minimum required paste volume for concrete mixtures used for pavements and the paste volume is dependent on the voids in the aggregate system, the effects of different concrete aggregate parameters on AV content was first evaluated.

Parameters considered in this phase included coarse aggregate shape, coarse aggregate gradation, sand fineness, and the F/C. Note that the gradation of combined aggregates is dependent on coarse aggregate gradation, fine aggregate gradation, and the F/C. Essentially, the effect of coarse aggregate shape and combined aggregate gradation on AV was investigated in Phase 1. Three different gradations, coarse (c), intermediate (i), and fine (f) are targeted for coarse aggregate gradations, as shown in Figure 5.1. The coarse and fine gradations for the coarse aggregates met the lower and upper gradation limits specified by ODOT for the aggregates falling in the size range 0.187 in. (4.75 mm) to 1.5 in. (38.1 mm).

Three different coarse aggregate types and two different sands available in Oregon were evaluated. Because ODOT requires using a nominal maximum aggregate size of 1.5 in. (38.1 mm) for paving concrete mixtures, a size range of 1.5 in. (38.1 mm) to 0.187 in. (4.75 mm) was adopted for all coarse aggregates. Coarse aggregates from two different size ranges, 1.5 in. (38.1 mm) to 0.75 in. (19.1 mm) and 0.75 in. (19.1 mm) to 0.187 in. (4.75 mm), were combined to achieve the full range of sizes. Two different natural sands with different fineness moduli were considered. The type and source for each coarse and fine aggregate considered in this study are shown in Table 5.1.

Table 5.1: Aggregate Types and Sources.

Aggregate ID	Aggregate type	Source
QR	Quarry rock	Pleasant Valley, OR
CG	Crushed gravel	Knife River, Corvallis, OR
G	Gravel	
CS	Concrete sand; Fineness modulus (FM) > 3.0	Pleasant Valley, OR
FS	Concrete sand; FM < 3.0	Knife River, Corvallis, OR

The gradation of the combined aggregate system is dependent on the ratio of relative proportions of coarse and fine aggregates, a parameter that is commonly referred as F/C in the literature (Hendrix & Trejo, 2017). To identify the AV_{min}, four (4) to six (6) F/C values were tested for each of the eighteen (18) different systems (3 CA types x 3 coarse aggregate gradations x 2 FA types). The AV values of the combined aggregate systems with different

F/C values were determined following AASHTO T 19M (2014a) test procedure. The optimal value of F/C (F/C_{opt}), where the minimum value of AV (AV_{min}) is achieved, is identified for each of the eighteen (18) different combined aggregate systems. Results from Phase 1 testing are presented later.

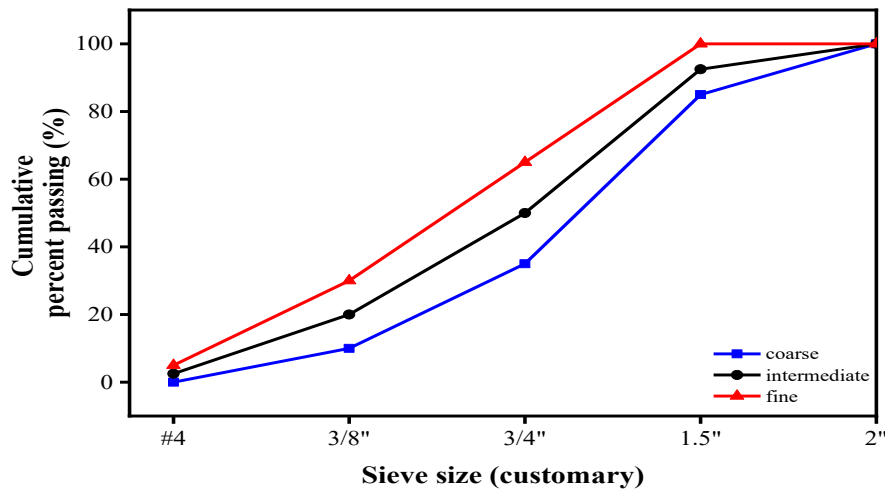


Figure 5.1: Target gradation considered for coarse aggregates.

5.2 PHASE 2

Information summarized in section 2.5.2 indicates that aggregate type, aggregate gradation, binder type, paste volume, and admixtures can influence both the fresh characteristics and hardened properties of concrete mixtures. However, the review indicates research gaps. Research studies that investigated the effect of aggregate type and/or gradation on concrete performance considered the same paste volume for all mixtures. Research studies that investigated the effect of binder type on concrete performance considered the same aggregate gradation and air-entrainment for all mixtures. Finally, research studies that investigated the effect of paste volume on concrete performance considered the same aggregate gradation and no air-entrainment for all mixtures. To better design the concrete mixtures for paving, it is important to understand the effect of aggregate type, aggregate gradation, binder type, and paste volume on the fresh and hardened concrete characteristics. Because ODOT requires air-entrainment, these mixtures should be assessed with air-entrainment. These mixtures have been comprehensively evaluated in Phase 2. Given the larger scope of Phase 2, testing was executed in three different sub-phases—Phase 2A, Phase 2B, and Phase 2C, details of which are discussed next.

5.2.1 Phase 2A-Identifying Required WR and Paste Volumes for Placeability

To generate data on how the paste volume, aggregate type, aggregate gradation, and chemical admixtures influence the fresh characteristics of concrete, the OSU research team initially produced and investigated twenty-one (21) different mixtures. The objective of this phase was to identify a general range of PV/AV values, using reasonable amounts of water-reducer, where the concrete could meet edge slump and surface voids required specified in the Box Test. Each of the mixtures evaluated were proportioned using one of the three different combined aggregate systems shown in Table 5.2. The ratio of paste volume to minimum aggregate void-volume (PV/AV_{min}) and total binder content used for all mixtures are

summarized in Table 5.3. The information on AV_{min} and F/C_{opt} was determined in the Phase 1 testing. All mixtures had a w/cm of 0.41 and aggregate quantities are based on oven-dried conditions. An OPC meeting ASTM C150 (2021) Type I/II requirements was used for all mixtures and no SCMs were used. MasterPozzoloth 80 (water-reducing admixture) and Masterair AE 90 (air-entraining admixture) were used on select mixtures. More information on the characteristics of these materials is presented later.

Table 5.2: Combined Aggregate Systems Tested in Phase 2A.

Aggregate system	Coarse aggregate type	Coarse aggregate gradation	Sand type	AV_{min} (%)	F/C_{opt}
1	Quarry rock	Coarse	Fine	18.78	1
2	Quarry rock	Fine	Coarse	25.09	1.25
3	Gravel	Coarse	Fine	18.23	0.75

Table 5.3: Details of Different Mixtures Evaluated as Part of Phase 2A.

Mix #	Agg. system	Design air-content (%)	Design PV/ AV_{min}	OPC content (lb/yd ³)	CA: 1.5"-0.75" (lb/yd ³)	CA: 0.75"-0.187" (lb/yd ³)	Fine agg. (lb/yd ³)	Water content (lb/yd ³)	Water reducer added?						
1	1	1	1.25	496	1109	624	1733	203	No						
2									Yes						
3									1.5	573	1062	597	1659	235	No
4															Yes
5									1.75	644	1018	573	1591	264	No
6															Yes
7	2	1	1.25	660	419	978	1747	271	No						
8									Yes						
9									1.5	751	396	924	1650	308	No
10															Yes
11									1.75	833	375	875	1563	341	No
12															NT
13	3	1	1.25	482	1274	627	1426	198	No						
14									Yes						
15									1.5	557	1221	601	1366	229	No
16															Yes
17									1.75	627	1172	577	1312	257	No
18															Yes
19	6	1	1.55	459	1213	598	1358	188	Yes						
20			1.82	531	1163	573	1301	218	Yes						
21			2.08	597	1116	550	1249	245	Yes						

All mixtures were evaluated using the Box Test (M. D. Cook et al., 2014) and slump test (AASHTO, 2018). The final dosage level of the WR was determined by the mixture's ability to pass the Box Test. To pass the Box Test, an average edge-slump is 0.25 in. (6.35 mm) or less and a percent surface-void area of 30% or less on all sides of the box-test specimen were set as criterion. An initial dosage of WR was fixed based on manufacturer's recommendations, which was thoroughly dissolved in mix water prior to concrete mixing. If required, additional dosage of WR was added during the concrete mixing process or after the

initial results from Box Test. The additional dosage of WR was added until the mixture passed the Box Test (M. D. Cook et al., 2014). The dosage of air-entraining admixture was chosen to achieve a target air-content of 6%. Air content (AASHTO, 2019b) was measured for mixtures that passed the Box Test requirements. For mixtures containing air-entraining admixture, a predefined amount of the admixture was added to the mixing water before the mixing process. This was done to increase the uniformity of the distribution of entrained air in the mixture. After the mixture passed the Box Test, it was tested for slump (AASHTO, 2018) and air-content (AASHTO, 2017c).

5.2.2 Phase 2B-Identifying Influence of Paste Volume on Placeability

The objective of Phase 2B testing was to identify a range of acceptable PV/AV_{min} values for concrete mixtures containing different aggregate systems. Acceptable PV/AV_{min} values are defined as values that pass the Box Test and meet required characteristics. Four different systems with varying aggregate types, aggregate gradations, and binder types were investigated. Details of these systems are shown in Table 5.4. It was determined from Phase 1 testing that a coarser gradation for the coarse aggregates and a sand of higher sand fineness will generally result in lower AV_{min} values. Hence, these conditions were considered for all systems. The coarse aggregate types for systems 1, 2, and 4 were quarry rock, crushed gravel, and gravel, respectively. Phase 1 testing indicated that, for a coarser gradation of the coarse aggregate and a finer sand, crushed gravel systems exhibited an AV_{min} value at an F/C_{opt} of 0.5. The initial thinking of the OSU research team was that concrete mixtures with a low F/C value, such as 0.5, may exhibit workability issues as there may be insufficient fine aggregate particles. To identify the effect of F/C on the WR requirements and fresh characteristics of concrete, system 3 was included in the test plan. The materials used for systems 2 and 3 were similar (crushed gravel meeting coarse gradation requirements, fine sand, and 70% OPC + 30% slag binder). Because the AV and F/C of system 3 do not represent the AV_{min} and F/C_{opt} of the crushed gravel (coarse) system with fine sand, the F/C and AV values for system 3 have been listed separately in Table 5.4.

Table 5.4: Systems Evaluated in Phase 2B.

System type	Coarse aggregate type	Coarse aggregate gradation	Sand type	Binder type	AV_{min} (%)	F/C_{opt}	AV (%)	F/C
1	Quarry rock	Coarse	Fine	70% OPC + 30% fly ash	18.78	1.25	–	–
2	Crushed gravel	Coarse	Fine	70% OPC + 30% slag	17.57	0.5	–	–
3	Crushed gravel	Coarse	Fine	70% OPC + 30% slag	–	–	18.09	0.75
4	Gravel	Coarse	Fine	100% OPC	18.23	0.75	–	–

Thirteen different mixtures were designed using the four different systems and were evaluated for surface voids and edge slump (Box Test), slump, and air-content. All mixtures had a w/cm of 0.41. Fly ash meeting Class F requirements and slag were used at 30% mass replacement levels for concrete mixtures containing quarry rock and crushed gravel, respectively. Information on the SCMs used in this study follow. All mixtures were designed with a target air-content of 5%. The admixtures used in this phase were the same as the admixtures used in Phase 2A. The system type and the design PV/AV_{min} values for different mixtures are summarized in Table 5.5.

Table 5.5: Details of Different Mixtures Evaluated in Phase 2B.

System	CA type	Mix #	Design PV/AV _{min} or PV/AV	Target air (%)	OPC content (lb/yd ³)	Fly ash content (lb/yd ³)	Slag content (lb/yd ³)	Total binder content (lb/yd ³)	Water content (lb/yd ³)	CA: 1.5"-0.75" (lb/yd ³)	CA: 0.75"-0.187" (lb/yd ³)	FA (lb/yd ³)
1	Quarry rock	1	1.55	5	338	145	–	483	198	1053	592	1645
		2	1.7	5	367	157	–	524	215	1026	577	1604
		3	1.85	5	395	169	–	564	231	1002	564	1565
		4	2	5	421	180	–	601	246	978	550	1528
2	Crushed gravel	5	1.65	5	337	–	144	481	197	1481	650	1066
		6	1.8	5	364	–	156	520	213	1447	635	1041
		7	1.95	5	390	–	167	558	229	1415	621	1018
3		8	1.7	5	358	–	153	511	209	1242	545	1340
		9	1.85	5	385	–	165	550	225	1213	532	1309
		10	2	5	411	–	176	587	241	1185	520	1279
4	Gravel	11	1.6	5	493	–	–	493	202	1259	553	1359
		12	1.75	5	534	–	–	534	219	1229	539	1326
		13	1.9	5	573	–	–	573	235	1200	527	1295

Note: 1 lb./cy = 0.59 kg/m³.

5.2.3 Phase 2C-Assessment of Fresh and Hardened Characteristics

The objective of Phase 2C study was to evaluate the performance of concrete mixtures designed using the new proportioning methodology; these mixtures had varying levels of paste volumes, aggregate types, aggregate gradations, SCMs, and SCM replacement levels. Details of the different mixtures evaluated as part of Phase 2C are shown in Table 5.6.

Mixtures 1, 2, and 3 were designed with the same binder type (30% fly ash replacement), same coarse aggregate type (quarry rock), same constituent volumetric proportions for aggregates (coarser coarse aggregate gradation and sand of lower fineness modulus), and same design air content (5%). The lower percent-passing limits specified by ODOT for the aggregate size ranges of 1.5 inch to 0.75 inch (38 mm to 19 mm) and 0.75 inch to 0.187 inch (19 mm to 4.7 mm) were considered in developing the coarser gradation for coarse aggregates. The only parameter that varied among these mixtures was the paste volume. The PV/AV values for mixtures 1 to 3 ranged from 1.7 to 1.9 and these were considered based on the preliminary test results generated from Phase 2B. Tests results from the Phase 2B study indicated that, for quarry rock mixtures with a coarser gradation of coarse aggregates, fine sand, and 30% ash replacement, a minimum PV/AV value of 1.7 is required to produce a stable concrete mixture with an edge-slump closer to zero (0.06 inch [1.5 mm]). Results also indicated that a PV/AV of 1.9 results in a mixture for which the edge-slump equalled the maximum limit (0.25 inch [32 mm]). Because the objective of this project is to evaluate the performance of paving concrete mixtures with a reasonable edge-slump, a focused PV/AV range of 1.7 to 1.9 was considered. The range of PV/AV values considered for mixtures 7, 8, and 9 was the same as the range considered for mixtures 1, 2, and 3. Note that the only variation between these mixture groups was the type of binder used; mixtures 7, 8, and 9 were designed without any fly ash replacement. The dosages of water-reducer required for mixtures 7, 8, and 9 were higher compared to their companion mixtures with 30% fly ash, as expected, which will be discussed in more detail in later sections. Similar design approaches were considered for developing mixtures 10, 11 and 12, and 16, 17, and 18. These mixtures composed of crushed gravel, a coarser gradation for the coarse aggregate, sand of lower fineness modulus, 30% slag replacement, and a design air content of 5%. A PV/AV range of 1.85 to 2.15 was considered for this mixture group (10, 11, 12) based on the edge-slump test results generated in Phase 2B study. Mixtures 16, 17, and 18 were designed without any slag replacement but with the same PV/AV values of mixtures 10, 11, and 12, respectively. Only three mixtures were considered with gravel as the coarse aggregate type (i.e., mixtures 19, 20, and 21). The PV/AV for this group mixtures was also based on the results generated in Phase 2B study.

Mixtures 4, 5, 6 and 13, 14, and 15 were designed to investigate how varying the aggregate gradation effects the performance of concrete. A finer gradation of coarse aggregates (i.e., the upper percent-passing limits specified by ODOT for aggregate size ranges 1.5 inch to 0.75 inch (38 mm to 19 mm) and 0.75 inch to 0.187 inch (19 mm to 4.7 mm) and sand of higher fineness modulus were adopted for these mixtures. Note that the ranges of PV/AV values considered for both groups of mixtures are significantly different compared to their companion groups with similar aggregate gradations, due to variations in AV of the different aggregate systems. Lastly, mixtures 22, 23, 24, and 25, were designed to evaluate the effects of w/cm and binder type (binary versus ternary) on concrete performance. A list of different study parameters and the group of mixtures designed to evaluate each of the study parameters are listed in Table 5.7.

The initial dosage of water-reducer considered for different mixtures was based on the experience the authors gained from the Phase 2A and 2B studies. Additional dosages of WR were added, if required, to make the concrete achieve the desired workability. The overall dosage was limited based on the mixture meeting the edge-slump requirement of 0.25 inches (6.4 mm). The dosage of air-entraining admixture was based on achieving a target plastic air content of $5\% \pm 1.5\%$.

Details of the different test methods used to evaluate the different concretes and their modifications considered for evaluating the fresh and hardened specimens are shown in Table 5.8.

One of the objectives of this study is to identify optimal ranges, or minimum paste volumes where concrete exhibits lower shrinkage values while meeting the requirements set by ODOT for other concrete properties, such as strength and chloride penetration resistance. Hence, experimental data generated from compressive tests, flexural tests, and unrestrained length change tests were compared to ODOT prescriptive limits specified for these tests. The minimum limits specified by ODOT for compression and flexural strengths for paving concrete mixtures were 4000 psi (27.6 MPa) and 600 psi (4.1 MPa), respectively. ODOT specifications do not specify a maximum unrestrained length change limit for paving concrete mixtures. However, specifications do specify a maximum limit of -0.045% (i.e., 450 microstrain) for high performance concrete (HPC) mixtures. Since SCMs, such as slag and fly ash were considered in the majority of paving mixtures of the past, the limit specified for HPC mixtures was considered to evaluate the paving mixtures in this study. The limit values for different tests are highlighted in different data plots shown.

It should be noted that the ODOT unrestrained length change is based on specimens wet cured for 28 days. Because a 7-day wet cure is considered in this study, as shown in Table 5.8, the specified ODOT limit is not applicable to the tested mixtures and the data generated from testing will likely exceed the limit value. These data are provided for comparison. However, the ODOT limit is shown on all unrestrained length change data plots for comparison purposes.

Table 5.6: Mixtures Evaluated in Phase 2C.

Mixture ID	Coarse aggregate type	Target coarse aggregate gradation	Fine Aggregate fineness modulus	AV _{min} or AV	OPC (lb/yd ³)	Fly ash (lb/yd ³)	Slag (lb/yd ³)	Total binder (lb/yd ³)	Water (lb/yd ³)	Coarse aggregate 1.5"-0.75" (lb/yd ³)	Coarse aggregate 0.75"-0.187" (lb/yd ³)	Fine aggregate (lb/yd ³)	w/cm	Design Paste volume (%)	Design PV/AV
1	QR	ODOT-C	2.91		367	157	–	524	215	1026	577	1604	0.41	28.2	1.70
2	QR	ODOT-C	2.91		385	165	–	551	226	1010	568	1578	0.41	29.4	1.80
3	QR	ODOT-C	2.91		403	173	–	576	236	993	559	1552	0.41	30.5	1.90
4	QR	ODOT-F	3.64		413	177	–	590	242	409	955	1704	0.41	31.1	1.35
5	QR	ODOT-F	3.64		438	188	–	625	256	400	933	1666	0.41	32.7	1.45
6	QR	ODOT-F	3.64		461	198	–	659	270	391	912	1629	0.41	34.2	1.55
7	QR	ODOT-C	2.91		538	–	–	538	221	1026	577	1604	0.41	28.2	1.70
8	QR	ODOT-C	2.91		565	–	–	565	232	1010	568	1578	0.41	29.4	1.80
9	QR	ODOT-C	2.91		591	–	–	591	242	993	559	1552	0.41	30.5	1.90
10	CG	ODOT-C	2.91		385	–	165	550	225	1213	532	1309	0.41	29.0	1.85
11	CG	ODOT-C	2.91		411	–	176	587	241	1185	520	1279	0.41	30.6	2.00
12	CG	ODOT-C	2.91		436	–	187	623	255	1158	508	1250	0.41	32.2	2.15
13	CG	ODOT-F	3.64		426	–	182	608	250	261	1045	1632	0.41	31.6	1.65
14	CG	ODOT-F	3.64		456	–	196	652	267	254	1015	1587	0.41	33.5	1.80
15	CG	ODOT-F	3.64		485	–	208	693	284	247	987	1544	0.41	35.3	1.95
16	CG	ODOT-C	2.91		556	–	–	556	228	1217	532	1309	0.41	29.0	1.85
17	CG	ODOT-C	2.91		594	–	–	594	243	1185	520	1279	0.41	30.6	2.00
18	CG	ODOT-C	2.91		630	–	–	630	258	1158	508	1250	0.41	32.2	2.15
19	G	ODOT-C	2.91		493	–	–	493	202	1185	583	1326	0.41	26.3	1.60
20	G	ODOT-C	2.91		521	–	–	521	214	1165	574	1305	0.41	27.5	1.70
21	G	ODOT-C	2.91		548	–	–	548	225	1147	565	1284	0.41	28.6	1.80
22	CG	ODOT-C	2.91		428	–	184	612	233	1185	520	1279	0.38	30.6	2.00
23	CG	ODOT-C	2.91		395	–	169	564	248	1185	520	1279	0.44	30.6	2.00
24	QR	ODOT-C	2.91		388	83	83	554	227	1010	568	1578	0.41	29.4	1.80
25	CG	ODOT-C	2.91		408	87	87	582	239	1185	520	1279	0.41	30.6	2.00

Note: 1 lb/cy = 0.59 kg/m³.

Table 5.7: Groups of Concrete Mixtures used for Assessing Different Study Parameters

Study parameter	Groups of different mixtures considered for assessing study parameter
Paste volume and total binder content	(1, 2, 3); (4, 5, 6); (7, 8, 9); (10,11,12); (13, 14, 15); (16, 17, 18); (19, 20, 21)
Binder type	(1, 7); (2, 8); (3, 9); (10, 16); (11, 17); (12, 18); (2, 8, 24); (11, 17, 25)
w/cm	(11, 22, 23)
Aggregate type ^s	(9, 17)
Aggregate gradation ^s	(3, 4); (12, 13)

Table 5.8: List of Physical Tests Conducted as Part of Phase 2C

Concrete property	Reference standard	Concrete age(s), days	Curing conditions (Temperature/RH)	Modifications
Slump	AASHTO T 119	--	--	--
Unit weight / Density	AASHTO T 121	--	--	--
Air content	AASHTO T 152	--	--	--
Edge-slump	AASHTO PP 84	--	--	--
Compressive strength	AASHTO T 22	28 and 56	73°F/100%RH until test	--
Flexural strength	AASHTO T 97	28 and 56	73°F/100%RH until test	--
Unrestrained length change	AASHTO T 160*	28	73°F/100%RH for 7 days; 73°F/50%RH for 21 days	7-day moist cure was considered instead of 28-day moist cure
Restrained shrinkage	AASHTO T 334*	28	73°F/50%RH	Concrete ring thickness of 5.5 inches was considered instead of 3 inches
Bulk resistivity	AASHTO TP 119*	28 and 56	73°F/100%RH until test	Specimens were cured on shelves in moist room instead of immersion in lime water
Bulk resistivity for formation factor	AASHTO TP 119*	63	73°F/100%RH	Specimens were moist cured for 56-days followed by 7-day immersion in calcium hydroxide-saturated pore solution until test
Freeze-thaw resistance	AASHTO T 161	--	73°F/100% RH until test	--
Formation factor	AASHTO PP 84	63	--	A curing age of 63 days was considered instead of 91 days

To further evaluate the hypothesis on the effect of paste volume on shrinkage, modified AASHTO T 334 (2008) testing was conducted on mixtures 1 and 3. The modification involved using a 5.5-inch (14 cm) ring thickness over the 3-inch (7.6 cm) standard ring thickness specified by the standard. This thicker specimen was used to ensure that the thickness of the concrete was greater than three times the NMSA used in the concrete (i.e., 1.5 inches [38 mm]). Restrained shrinkage strains were monitored for a period of 28 days after casting.

Testing for formation factor was conducted to determine whether mixtures meet the AASHTO PP 84 (2020b) minimum formation factor limit of 1000 units for paving concrete mixtures. Since a 63-day curing time (56-day moist cure followed by 7-day cure in simulated saturated $\text{Ca}(\text{OH})_2$ pore solution) was considered in this study as opposed to 91-day cure time required by AASHTO PP 84 (2020b), the test results generated in this study are referred to as “modified AASHTO PP 84 (2020b) formation factor values.” A pore solution resistivity value of 0.127 ohm-m was considered for estimating the formation factor, per AASTHO PP 84 (2020b). Test results indicated that 78% of mixtures tested for formation factor met the AASHTO PP 84 (2020b) limit at 63-day test age, which will be discussed in more detail later. ODOT specifies limit requirements for chloride penetration resistance of HPC mixtures based on RCP testing (AASHTO T 277 (2015b)). As such, an attempt was made to rank the different mixtures based on AASHTO T 277 (2015b) RCP classification criteria using formation factor values. Information reported by Weiss, Spragg, Isgor, Ley, and Van Dam (2018) was used for this purpose.

Lastly, select mixtures were evaluated for freeze-thaw resistance following AASHTO T 161 (2017e) requirements. Mixtures evaluated for this testing included 10, 11, 12, 16, 17, and 18. The specimens were cured for 56 days and stored in a freezer until the time of testing.

5.2.4 Materials

Figure 5.2 shows the different aggregates assessed in this project. Three different coarse aggregates (CA), quarry rock (QR), crushed gravel (CG), and gravel (G), and two different fine aggregates (FA), coarse sand (CS) and fine sand (FS), are considered. Both the fine aggregates are concrete sands with different fineness modulus (FM) values. Table 5.9 and Table 5.10 report the characteristics of the coarse and fine aggregates, respectively. Testing for specific gravity, absorption, fineness modulus, and particle size index testing followed the requirements of AASHTO T 84 (2013a), AASHTO T 85 (2014b), AASHTO T 27 (2020a), and ASTM D3398 (2006).

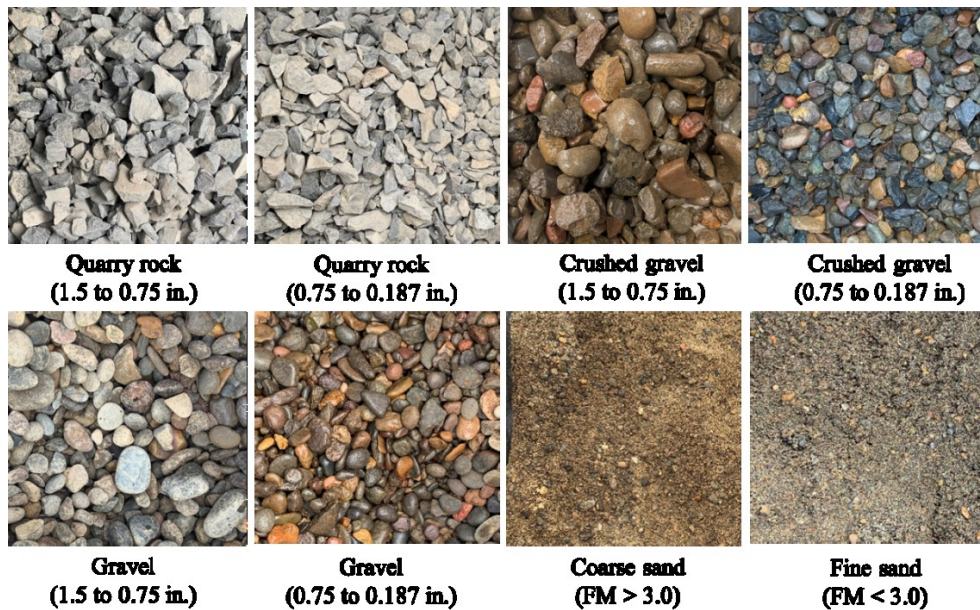


Figure 5.2: Aggregates considered for SPR 823

Table 5.9: Coarse Aggregate Characteristics.

Coarse aggregate type	Size range	Bulk dry SG	Saturated surface-dry SG	Apparent SG	Absorption, %	Weighted particle size index (I_a)
QR	1.5 inch - 3/4"	2.85	2.88	2.93	1.04	13.9
	3/4 inch - #4	2.86	2.89	2.85	1.15	12.3
CG	1.5 inch - 3/4"	2.64	2.68	2.75	1.51	10.2
	3/4 inch - #4	2.59	2.64	2.71	1.60	8.0
G	1.5 inch - 3/4"	2.55	2.60	2.69	2.07	5.9
	3/4 inch - #4	2.44	2.52	2.64	3.00	1.6

Table 5.10: Fine Aggregate Characteristics.

Fine aggregate type	Bulk dry SG	Saturated surface-dry SG	Apparent SG	Absorption, %	Weighted particle size index (I_a)	Fineness modulus
CS	2.5	2.57	2.68	2.69	7.69	3.64
FS	2.48	2.56	2.69	3.29	7.2	2.91

Figure 5.3 through Figure 5.10 show the particle size distribution curves for different aggregate types and size ranges. Testing for particle-size distribution followed AASHTO T 27 (2020a) requirements. Three representative samples, referred in the figures below as samples 1, 2, and 3, are tested for each aggregate size range and the results are compared to lower and upper limits specified in ODOT specifications. Note that the repeatability of the gradation results is good.

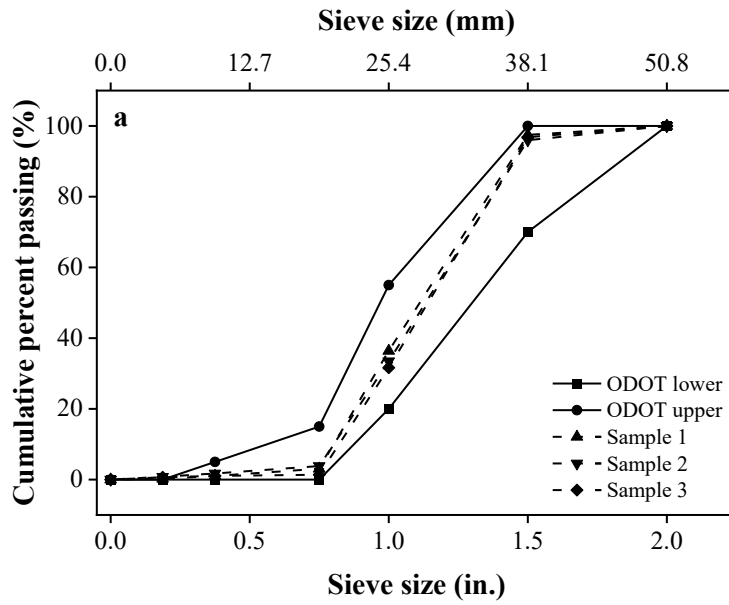


Figure 5.3: Measured gradation for QR 1.5- 3/4 inch (38-19 mm).

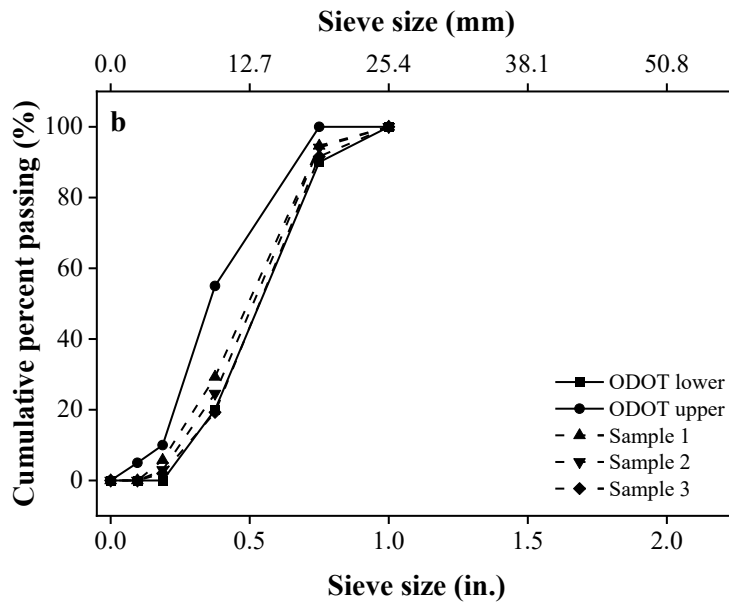


Figure 5.4: Measured gradation for QR 3/4 inch (19 mm) - #4.

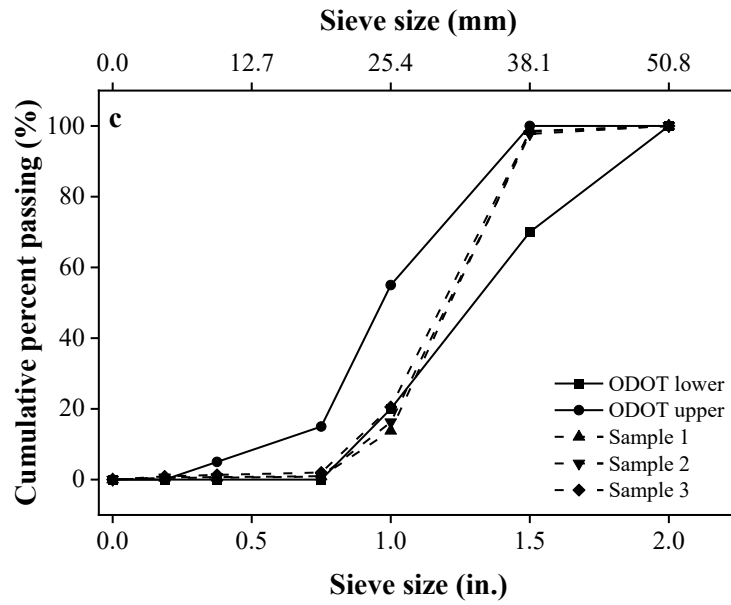


Figure 5.5: Measured gradation for CG 1.5 - 3/4 inch (38-19 mm).

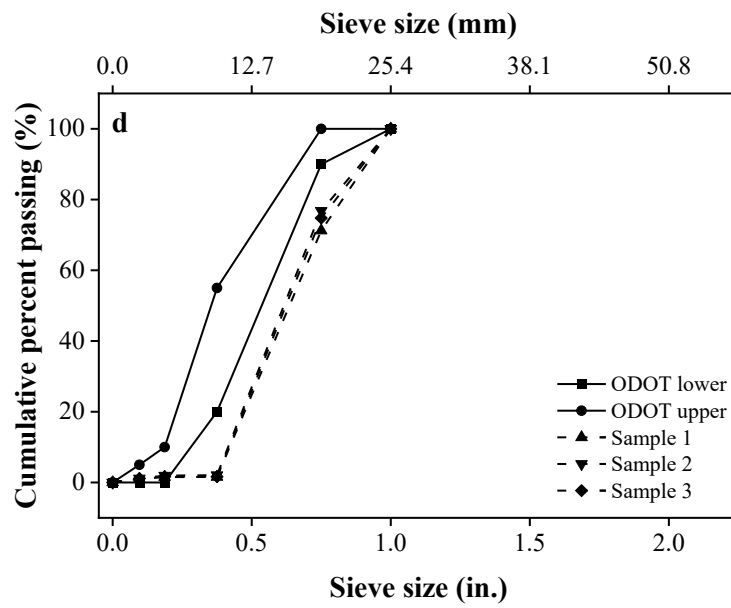


Figure 5.6: Measured gradation for CG 3/4 inch (19 mm) - #4.

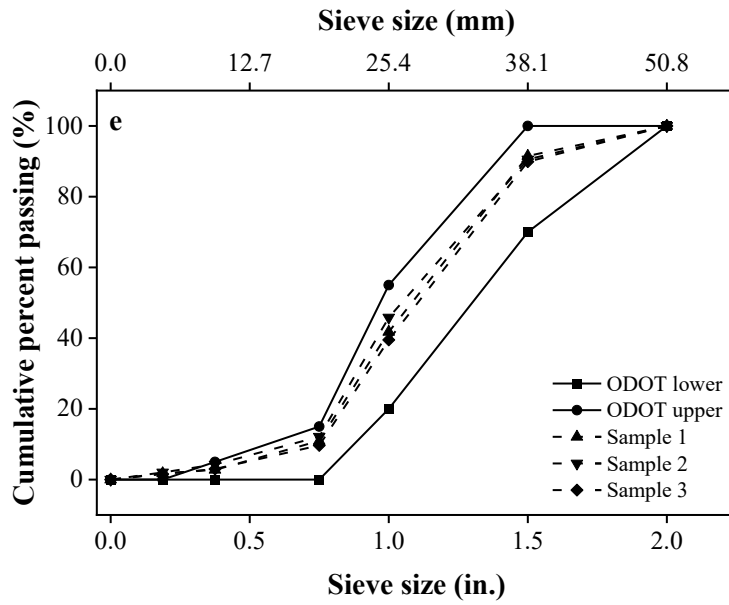


Figure 5.7: Measured gradation for G 1.5 - 3/4 inch (38-19 mm).

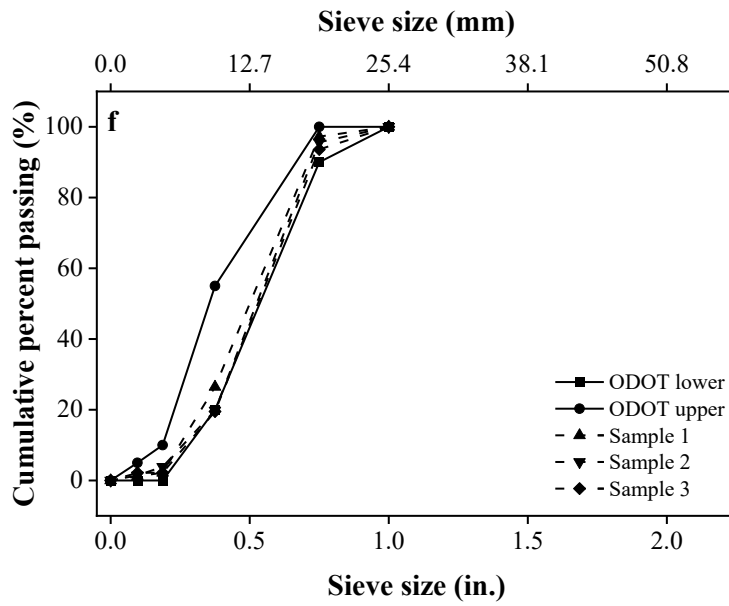


Figure 5.8: Measured gradation for G 3/4 inch (19 mm) - #4.

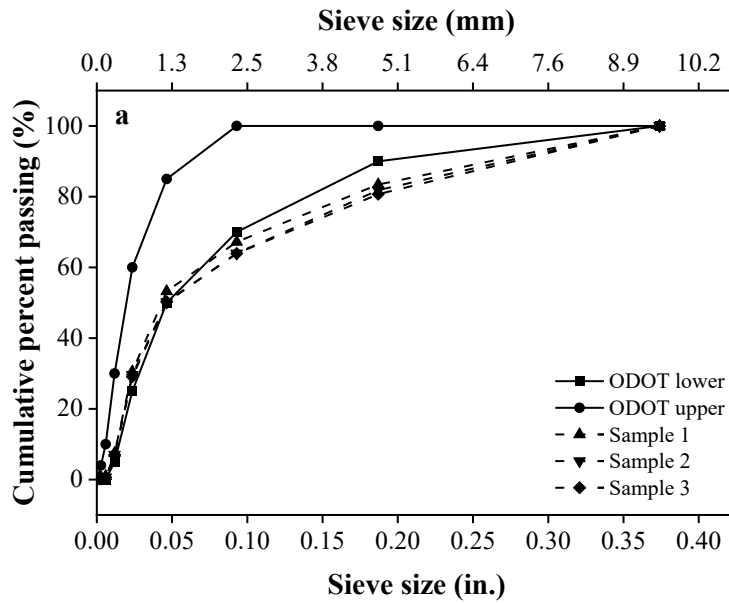


Figure 5.9: Measured gradation for coarse sand.

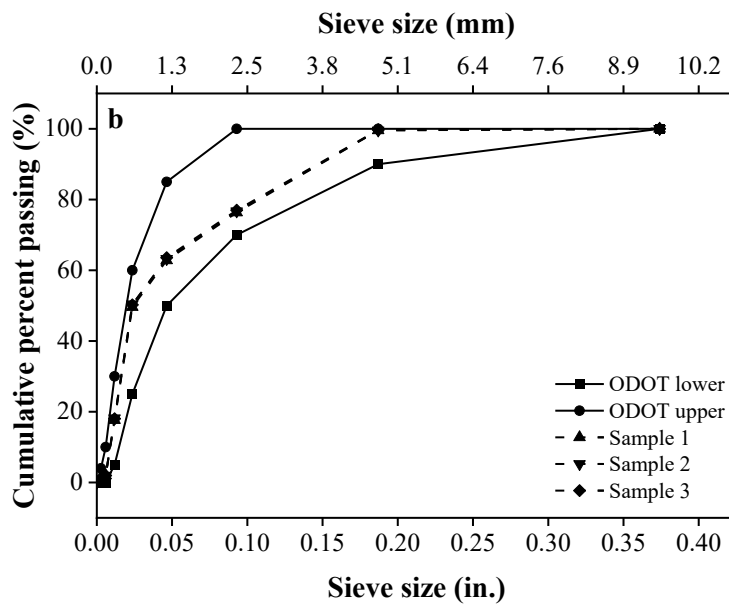


Figure 5.10: Measured gradation for fine sand.

Table 5.11 reports the chemical composition data obtained from material suppliers for the different cementitious materials used in this study.

Table 5.11: Chemical Compositions of the Different Cementitious Materials, %.

Parameter	Cementitious Material Type		
	OPC	Fly Ash	Slag
SiO ₂	21.0	48.4	29.91
Al ₂ O ₃	3.7	16.4	14.99
Fe ₂ O ₃	3.2	6.3	0.33
CaO	62.6	14	37.61
MgO	4.0	5.3	8.41
SO ₃	2.4	0.9	4.28
Na ₂ O	0.25	--	0.39
K ₂ O	0.45	--	0.54
TiO ₂	0.28	--	1.76
P ₂ O ₅	0.13	--	0.01
Mn ₂ O ₃	0.07	--	0.43
SrO	--	--	0.08
ZnO	--	--	0.22
Na ₂ O _{eq}	0.56	5.22	0.75
Loss on Ignition	2.0	0.33	0.00

OPC and slag were procured from Ash Grove, Oregon. Fly ash was procured from Lafarge, Washington. A mid-range water reducer, MasterPozzolith 80, was used in select mixtures. The maximum WR dosage recommended by the manufacturer was 10 fl-oz/cwt (650 ml/100 kg). Masterair AE 90 was the AEA used in this study. For trial mixtures, an initial dosage ranging between 0.25 fl-oz/cwt (16 ml/100 kg) and 4 fl-oz/cwt (250 ml/100 kg) was initially added and then increased as needed.

5.3 SUMMARY

Aggregates used for concrete paving vary widely. To quantify how aggregate shape, gradation, texture, and fineness influence aggregate void content, various combinations of different aggregates should be assessed. This experimental program includes the assessment of three different coarse aggregates and two different sands typical in Oregon.

Phase 1 of the research includes characterizing these aggregates to quantify the aggregate void content. Lower aggregate void contents should result in lower paste contents in concrete paving mixtures. After the minimum aggregate void content is identified in Phase 1, concrete mixtures are assessed in Phase 2. The Phase 2 research includes three sub-phases: 2A, 2B, and 2C. The purpose of Phase 2A is to identify required water-reducing admixture contents necessary for concrete paving mixtures containing aggregates with minimum void contents. Phase 2B quantifies the general amount of cementitious paste, or more specifically, the paste to aggregate void ratio, necessary to achieve workable paving concrete. Phase 2C includes the assessment of paving mixtures developed in Phases 2A and 2B.

6.0 RESULTS AND DISCUSSION

Results and discussion from the Phase 1, 2a, 2b, and 2c research tasks are presented next. Note that the results from the preliminary study are not presented here as they were presented earlier. The results from each phase are presented in separate sub-headings.

6.1 PHASE 1 - IDENTIFYING AV_{\min}

This section reports experimental test data generated as part of optimizing the gradations of different aggregates locally available in Oregon. As noted, the optimization is based on minimizing the aggregate voids in the aggregate system. The purpose of estimating the minimum void content is to identify the ratio of fine to coarse aggregate that results in the minimum amount of paste required to fill the aggregate voids. This value, in addition to aggregate shape, can be considered as a baseline for determining additional paste volume required to achieve an intended workability.

Figure 6.1 summarizes the F/C versus AV values for different aggregate systems. The data points circled on each plot represent the AV_{\min} values observed for different systems at a certain F/C, referred herein as F/C_{opt} .

The AV_{\min} and the corresponding F/C_{opt} for different aggregate systems are summarized in Table 6.1. Note the difference between the low (17.57 percent) and high (25.09 percent) AV values in the table. Assuming a 0.41 water-cement ratio, 20% air in the paste, and a PV/AV of 1, the difference in OPC resulting from the gradation that results in the lower AV would be about 140 lbs/cy (83 kg/cm) of OPC. This indicates that optimizing aggregate gradation can result in a significant reduction in OPC. The following general comments can be made from the data:

1. Changing the gradation of coarse aggregates from fine to coarse was found to decrease the AV_{\min} , irrespective of the type of sand used.
2. Decreasing the FM of the sand resulted in a decrease in the AV_{\min} , irrespective of the coarse aggregate type and coarse aggregate gradation.
3. The influence of coarse aggregate type is found to be more pronounced when a coarser sand (higher FM) is used in the system.
4. Irrespective of the coarse aggregate type, the aggregate system with coarser coarse aggregates and fine sand exhibited the lowest AV_{\min} and the system with finer coarse aggregates and coarse sand was identified as having the highest AV_{\min} .

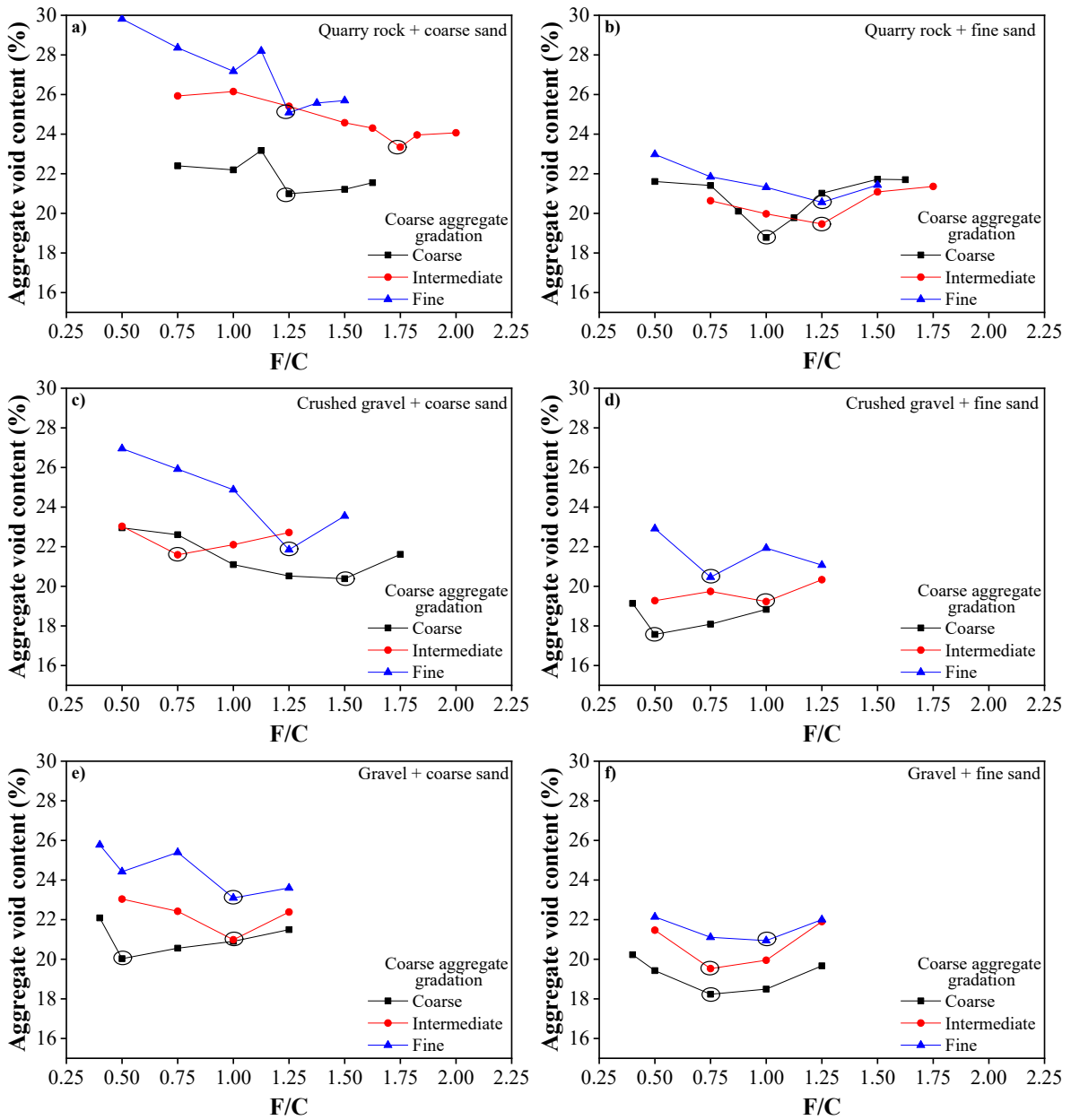


Figure 6.1: F/C versus aggregate void content for different systems.

Table 6.1: F/C_{opt} and AV_{min} for Different Systems

Coarse aggregate type	Coarse aggregate gradation	Sand	F/C _{opt}	AV _{min} (%)
Quarry	Coarse	Coarse	1.25	20.99
Quarry	Intermediate	Coarse	1.75	23.35
Quarry	Fine	Coarse	1.25	25.09
Quarry	Coarse	Fine	1	18.78
Quarry	Intermediate	Fine	1.25	19.46
Quarry	Fine	Fine	1.25	20.56
Crushed gravel	Coarse	Coarse	1.5	20.38
Crushed gravel	Intermediate	Coarse	0.75	21.59
Crushed gravel	Fine	Coarse	1.25	21.84
Crushed gravel	Coarse	Fine	0.5	17.57
Crushed gravel	Intermediate	Fine	1	19.23
Crushed gravel	Fine	Fine	0.75	20.46
Gravel	Coarse	Coarse	0.5	20.03
Gravel	Intermediate	Coarse	1	20.98
Gravel	Fine	Coarse	1	23.10
Gravel	Coarse	Fine	0.75	18.23
Gravel	Intermediate	Fine	0.75	19.53
Gravel	Fine	Fine	1	20.94

6.1.1 Comparison between AASHTO T 19M (2014a) and packing models

The optimized aggregate gradations established using AASHTO T 19M (2014a) testing were compared with aggregate optimization developed through software platforms. In this comparison study, the optimized gradation and the voids ratio for the combined aggregates were estimated using the particle packing models for two different aggregate systems, quarry rock and fine sand, and gravel and fine sand. The COMPASS software was used for optimization, which provides analyses based on the Toufar, Dewar, and De Larrard particle packing models. To use these models, information on the aggregate gradation, packing density, and voids ratio for different individual size ranges is needed as input. Voids ratio (VR) is defined as the ratio of the volume of voids to the volume of solids. For the aggregates in dry condition,

$$VR = V_v / (100 - V_v) \quad (6-1)$$

where:

V_v is the volume of voids divided by the total volume expressed in percentage.

It should be noted that the packing density and voids ratio could be different for aggregate systems subjected to different modes of compaction. For the purpose of the preliminary comparisons, the packing density and voids ratio estimated under dry rodded condition are considered for packing models since AASHTO T 19M (2014a) recommends dry-rodded compaction for NMSA of 1.5 in. (38.1 mm) or less. The information obtained from packing models was then compared with the experimental test results of AASTHO T 19M (2014a). This is presented next.

Table 6.2 and Table 6.3 show the comparisons of “optimized” aggregate gradations developed using AASHTO T 19M (2014a) and three different particle-packing models of COMPASS software for two different aggregate systems. For the Toufar and DeLarrard models, the VR values are also generated as output for combined aggregates. For the aggregate systems under investigation, the VR values and the corresponding V_v values estimated using Equation 6.1 are also shown in the figures. COMPASS software does not generate VR values for the Dewar model and hence these are not shown. Ideally if the AASHTO T 19M (2014a) testing and particle packing models were to provide similar output, the combined aggregate gradations and the AV_{min} and V_v values should be similar.

These results indicate that the De Laarand model and AASHTO T 19M (2014a) provide more or less similar gradation curves. However, AV_{min} determined using AASHTO T 19M (2014a) and the V_v estimated using the packing models can be significantly different. This is important as the amount of paste is dependent on the AV_{min} . This indicates that aggregate testing following AASHTO T 19M (2014a) should be performed to generate realistic values and minimized cement contents. The V_v estimated using particle packing models is approximately 63 to 95% higher than the AV_{min} estimated using AASHTO T 19M (2014a). Similar findings have been reported in Cook et al. (2016).

6.1.2 Combined gradations at AV_{min} and Comparison with Models

Using the F/C_{opt} and the individual gradations of coarse and fine aggregates, the combined aggregate gradation corresponding to AV_{min} were established for different combinations of coarse and fine aggregates. The following sections highlight the combined aggregate gradations on the 0.45 power, 8-18 (haystack), and tarantula charts.

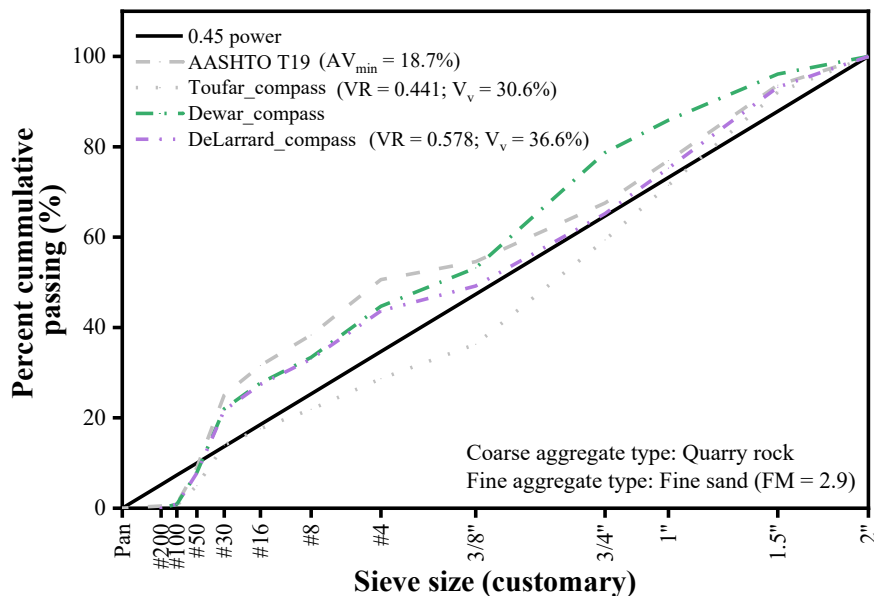


Figure 6.2: Comparison of optimized gradations for systems containing quarry rock and fine sand.

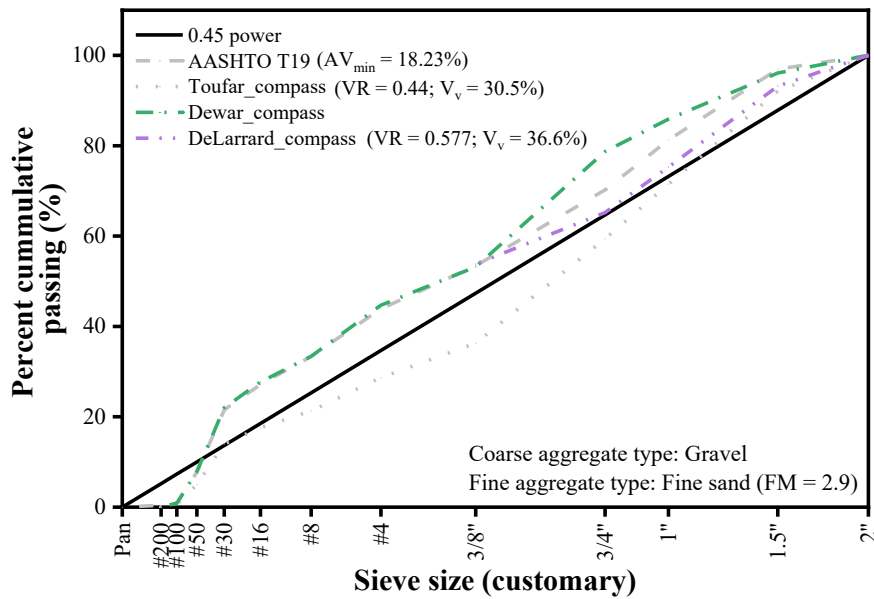


Figure 6.3: Comparison of optimized gradations for systems containing gravel and fine sand.

6.1.2.1 The 0.45 power chart

Figure 6.4 compares the combined aggregate gradation limits specified in the ODOT special provisions document (contract number 15090) with the 0.45 power curve. The ODOT lower gradation limit is relatively close to the 0.45 power curve when compared to the ODOT upper gradation limit. Figure 6.5 to Figure 6.10 represent the combined aggregate gradations, at which AV_{min} values are observed for different aggregate systems. Each figure presents three combined aggregate systems that correspond to three different gradations of coarse aggregates (i.e., coarse, intermediate, and fine gradations). Based on the figures, the following general conclusions can be made:

1. Excluding the aggregate system of crushed gravel and coarse sand, the gradation curve representing the lowest AV_{min} is closer to 0.45 power curve for the remaining five systems. Data recorded from the Phase 1 testing support the concept of the 0.45 power curve, that is, aggregate gradations closer to 0.45 power curve exhibit lower AV contents.
2. Most combined gradation curves that represent AV_{min} values do not fall within the ODOT aggregate gradation limits. When out of the specified limits, the combined gradations are generally finer when compared to the ODOT limit.
3. The combined gradations necessary to achieve AV_{min} for systems with quarry rock are finer compared to the systems prepared with crushed gravel or gravel. This is due to the high F/C_{opt} observed in quarry rock systems.

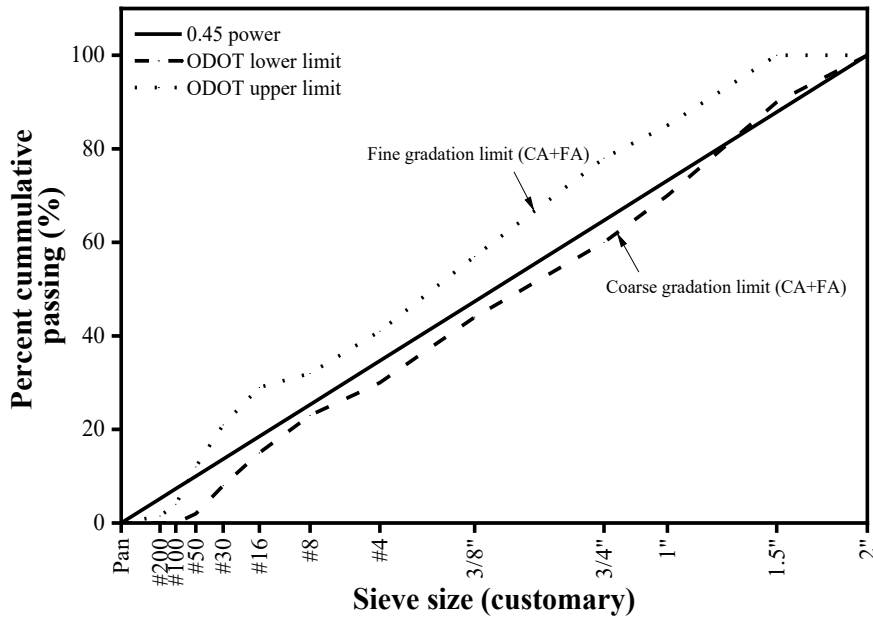


Figure 6.4: Comparison of the ODOT combined gradation limits to 0.45 power curve.

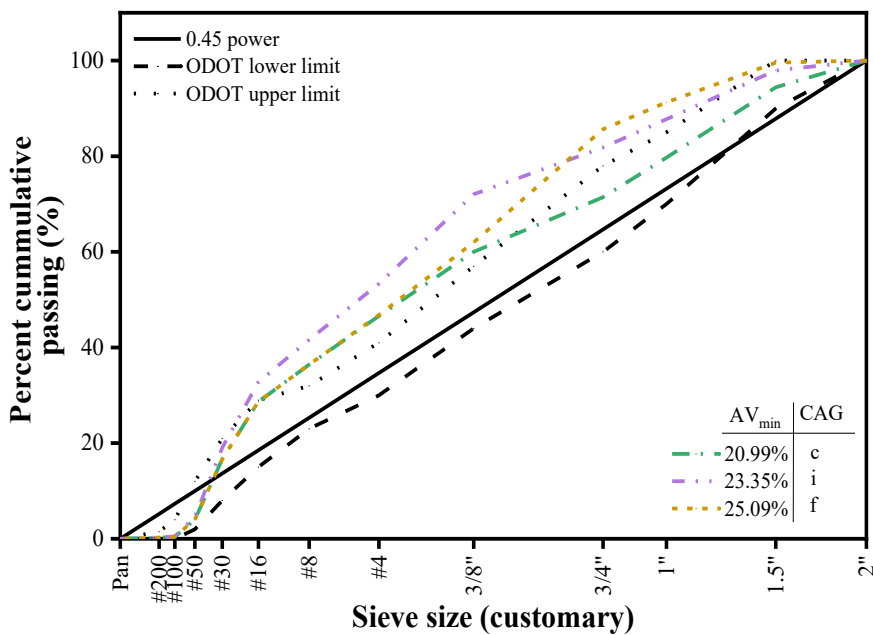


Figure 6.5: Comparison of the combined gradations of quarry rock plus coarse sand to 0.45 power curve (CAG: Coarse aggregate gradation; c: coarse; i: intermediate; and f: fine).

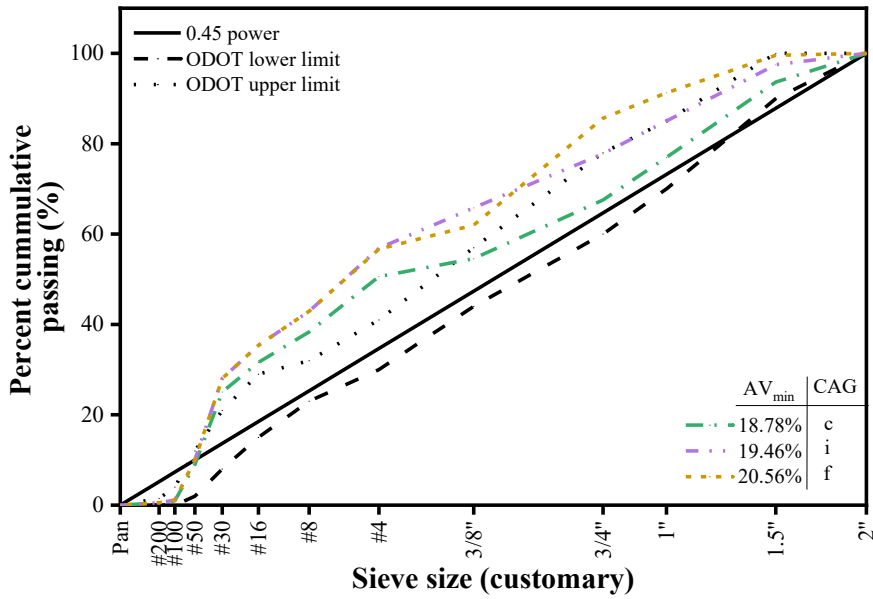


Figure 6.6: Comparison of the combined gradations of quarry rock plus fine sand to 0.45 power curve (CAG: Coarse aggregate gradation; c: coarse; i: intermediate; and f: fine).

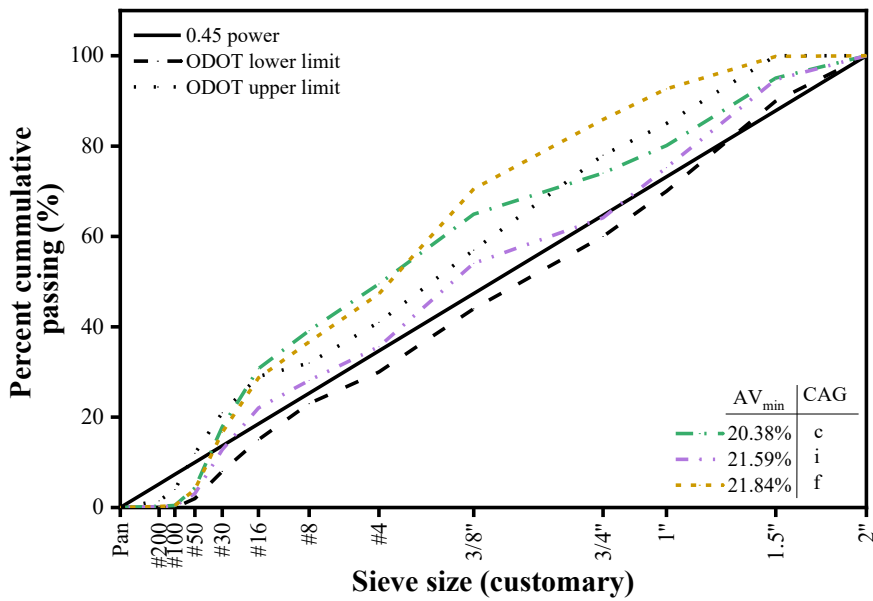


Figure 6.7: Comparison of the combined gradations of crushed gravel plus coarse sand to 0.45 power curve (CAG: Coarse aggregate gradation; c: coarse; i: intermediate; and f: fine).

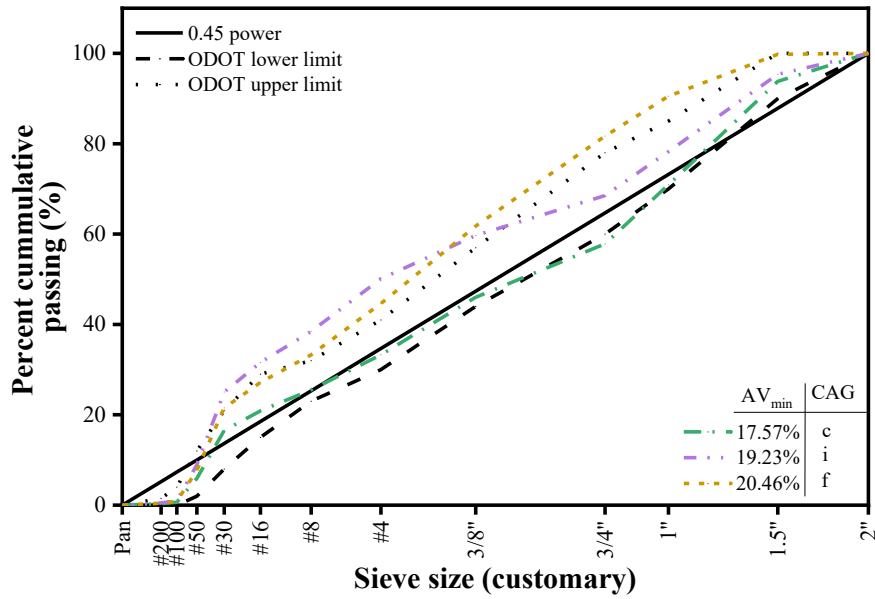


Figure 6.8: Comparison of the combined gradations of crushed gravel plus fine sand to 0.45 power curve (CAG: Coarse aggregate gradation; c: coarse; i: intermediate; and f: fine).

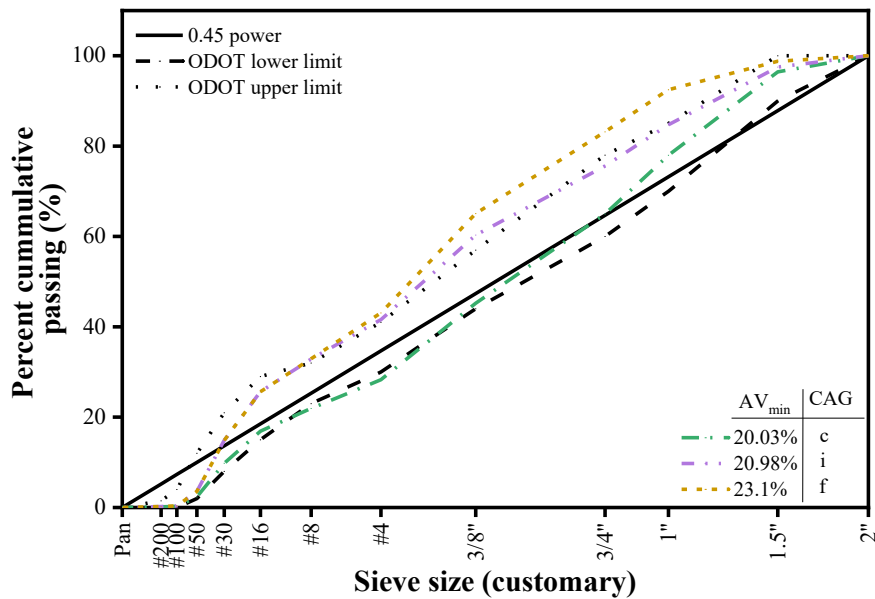


Figure 6.9: Comparison of the combined gradations of gravel plus coarse sand to 0.45 power curve (CAG: Coarse aggregate gradation; c: coarse; i: intermediate; and f: fine).

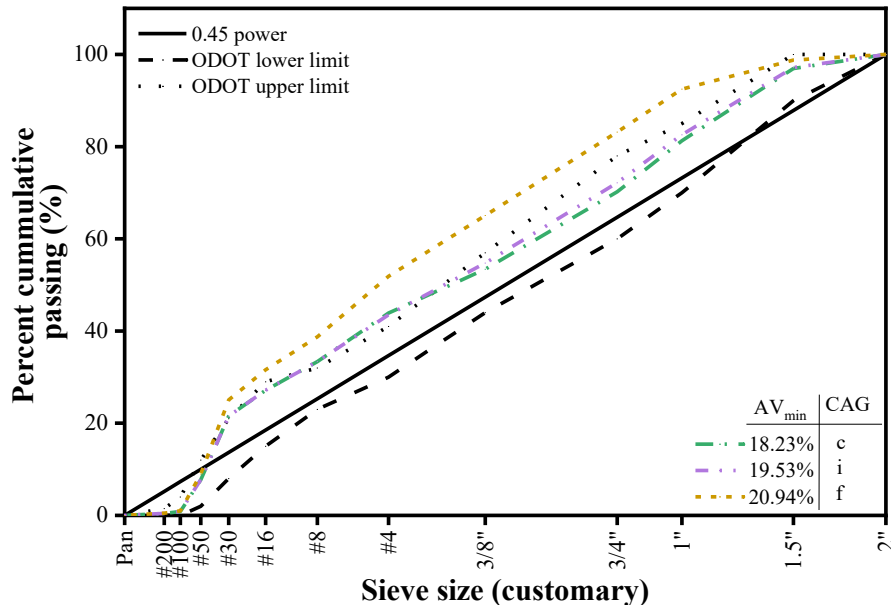


Figure 6.10: Comparison of the combined gradations of gravel plus fine sand to 0.45 power curve (CAG: Coarse aggregate gradation; c: coarse; i: intermediate; and f: fine).

6.1.2.2 The 8-18 band or haystack chart

Figure 6.11 to Figure 6.16 show a comparison of the different combined gradations, at which AV_{min} values are shown with the haystack plot. Also shown in the figures are the 0.45 power curve and ODOT limits. Analyses show that all gradations that represent AV_{min} for different systems meet the two criteria reported by Richardson (2005) for the haystack plot.

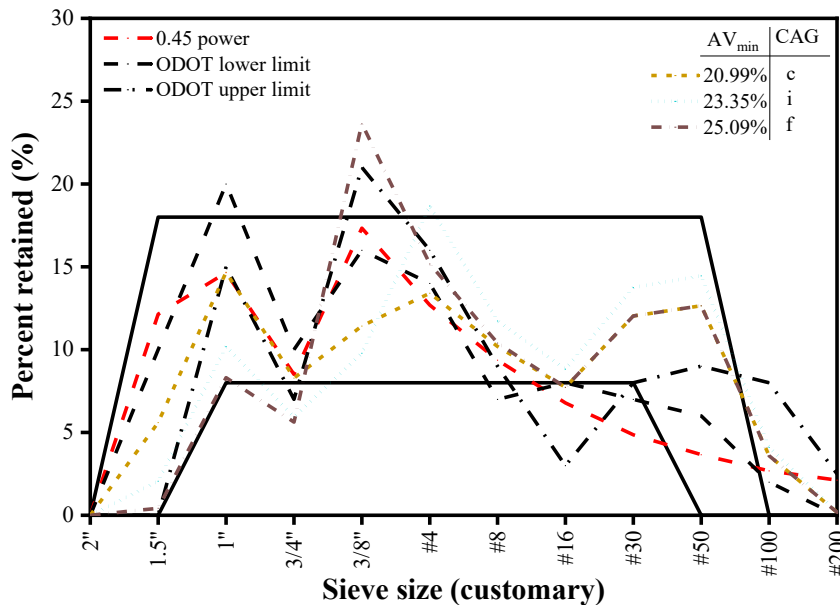


Figure 6.11: Comparison of the combined gradations of quarry rock plus coarse sand to 8-18 band (CAG: Coarse aggregate gradation; c: coarse; i: intermediate; and f: fine).

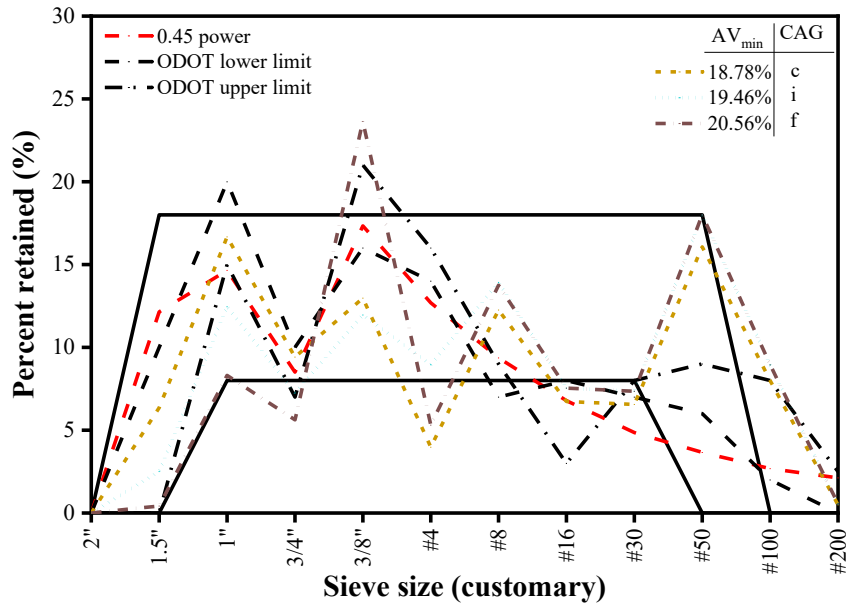


Figure 6.12: Comparison of the combined gradations of quarry rock plus fine sand to 8-18 band (CAG: Coarse aggregate gradation; c: coarse; i: intermediate; and f: fine).

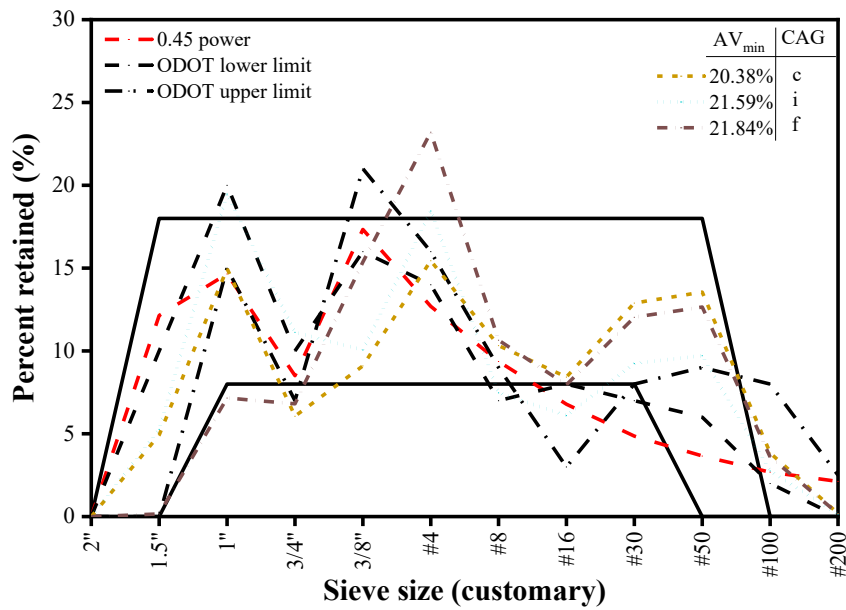


Figure 6.13: Comparison of the combined gradations of crushed gravel and coarse sand to 8-18 band (CAG: Coarse aggregate gradation; c: coarse; i: intermediate; and f: fine).

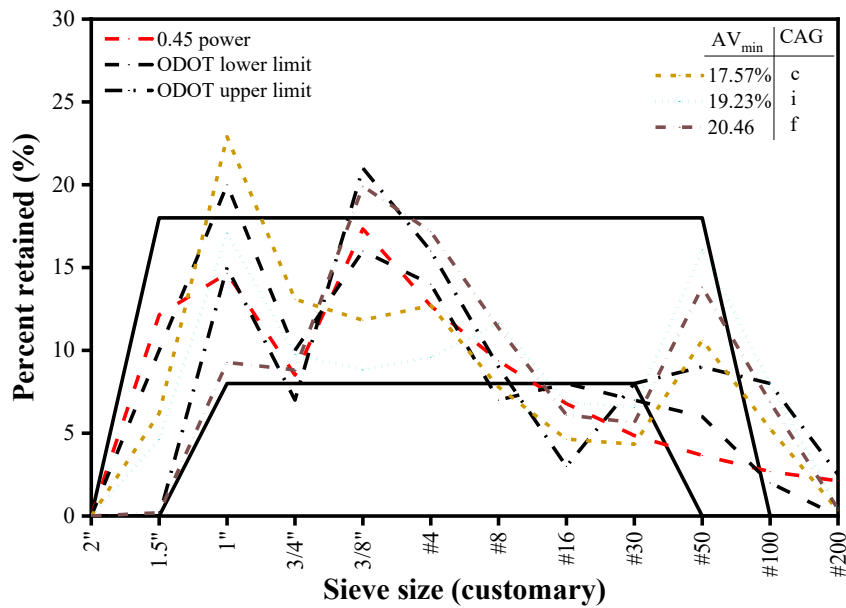


Figure 6.14: Comparison of the combined gradations of crushed gravel and fine sand to 8-18 band (CAG: Coarse aggregate gradation; c: coarse; i: intermediate; and f: fine).

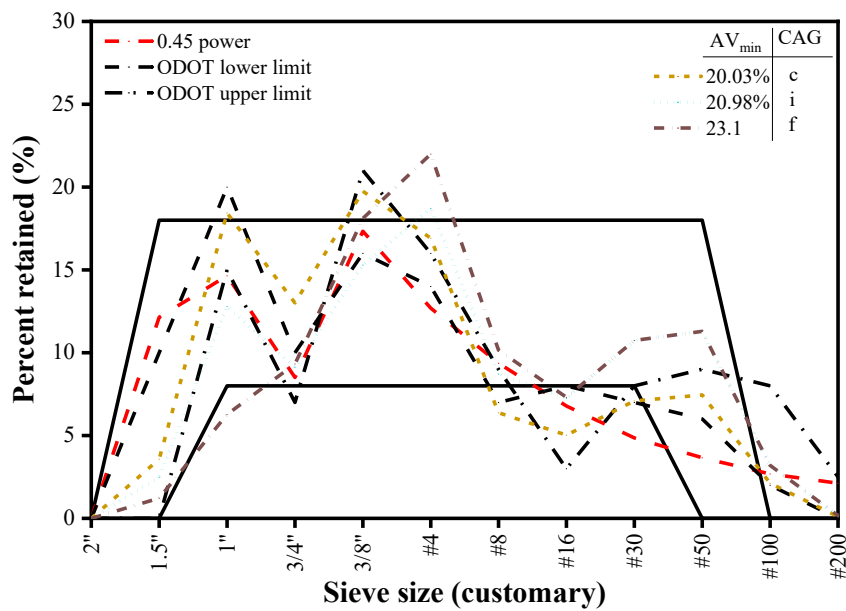


Figure 6.15: Comparison of the combined gradations of gravel and coarse sand to 8-18 band (CAG: Coarse aggregate gradation; c: coarse; i: intermediate; and f: fine).

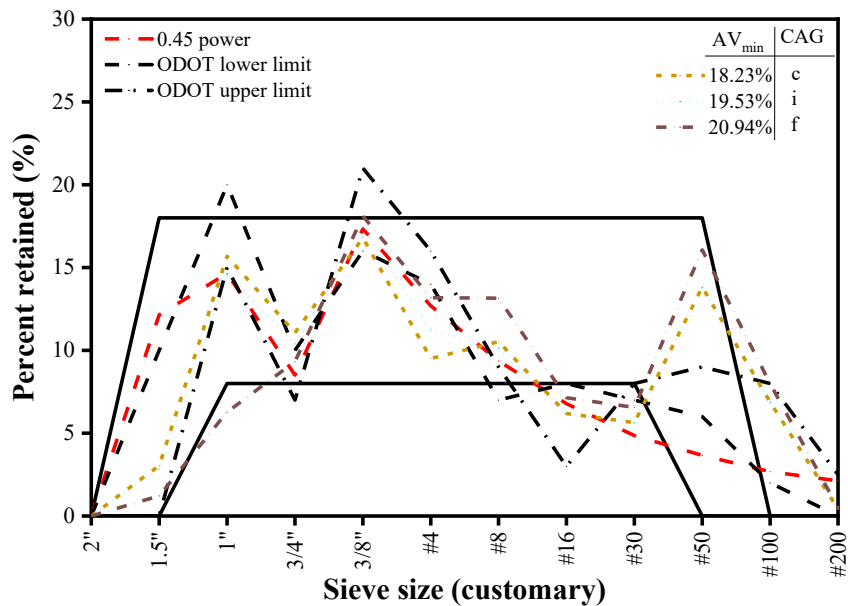


Figure 6.16: Comparison of the combined gradations of gravel and fine sand to 8-18 band (CAG: Coarse aggregate gradation; c: coarse; i: intermediate; and f: fine).

6.1.2.3 Tarantula curve

Figure 6.17 to Figure 6.22 compare the combined gradation curves observed at different AV_{min} values for the different systems with the tarantula curve. Also shown on the figures are the ODOT gradation limits and the 0.45 power curve. It should be noted that the research study behind the development of tarantula curves considered aggregate systems with a nominal maximum size of 1 inch (25.4 mm) while ODOT requires a nominal maximum size of 1.5 in. (38.1 mm) for paving concrete. Hence, the actual percent retained values at 1.5 inch (38.1 mm) may be neglected while comparing the combined aggregate gradations to tarantula curve limits. Under this assumption, the following general conclusions can be made for the different combined aggregate gradations:

1. The ODOT gradation limits and 0.45 power curve also meet the tarantula curve limits.
2. The crushed gravel considered in this study have little or no particles retained on the 0.375-inch (9.5 mm) sieve. Hence, all the combined aggregate gradations for crushed gravel systems (6 in total) failed to meet the tarantula lower limits.
3. Among the remaining systems, quarry rock (intermediate gradation) plus coarse sand, gravel (fine gradation) plus coarse sand, and gravel (fine gradation) plus fine sand failed to meet the tarantula limits. Among the 18 different combinations, aggregate systems representing 9 combinations failed to meet the tarantula curve limits.

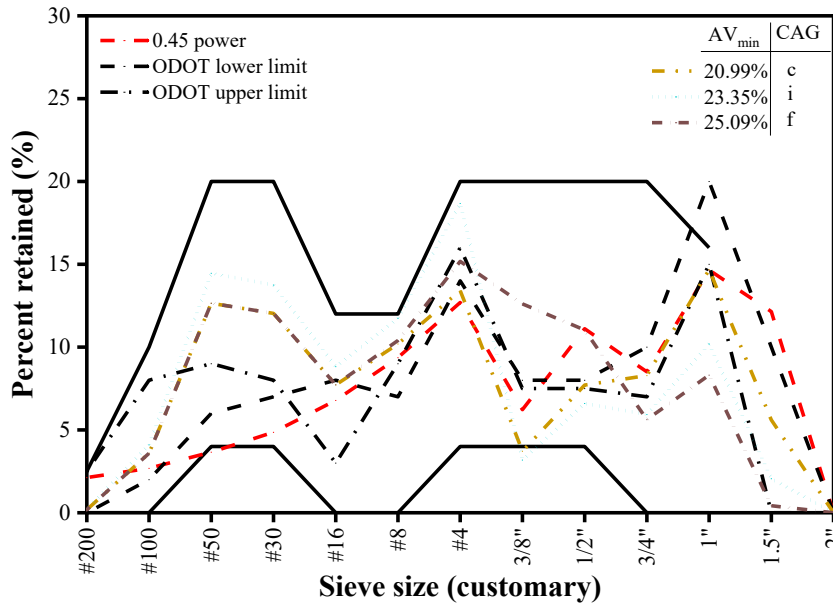


Figure 6.17: Comparison of the combined gradations of quarry rock plus coarse sand to tarantula curve (CAG: Coarse aggregate gradation; c: coarse; i: intermediate; and f: fine).

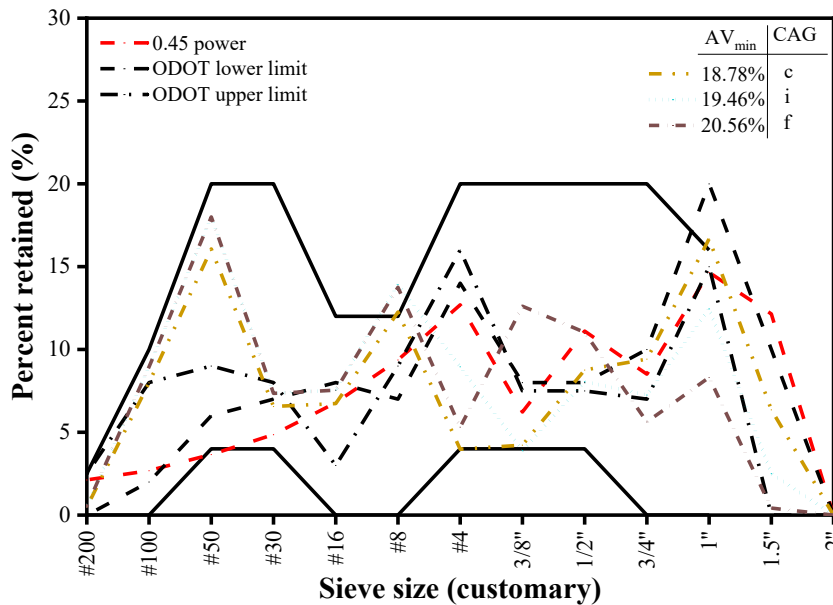


Figure 6.18: Comparison of the combined gradations of quarry rock plus fine sand to tarantula curve (CAG: Coarse aggregate gradation; c: coarse; i: intermediate; and f: fine).

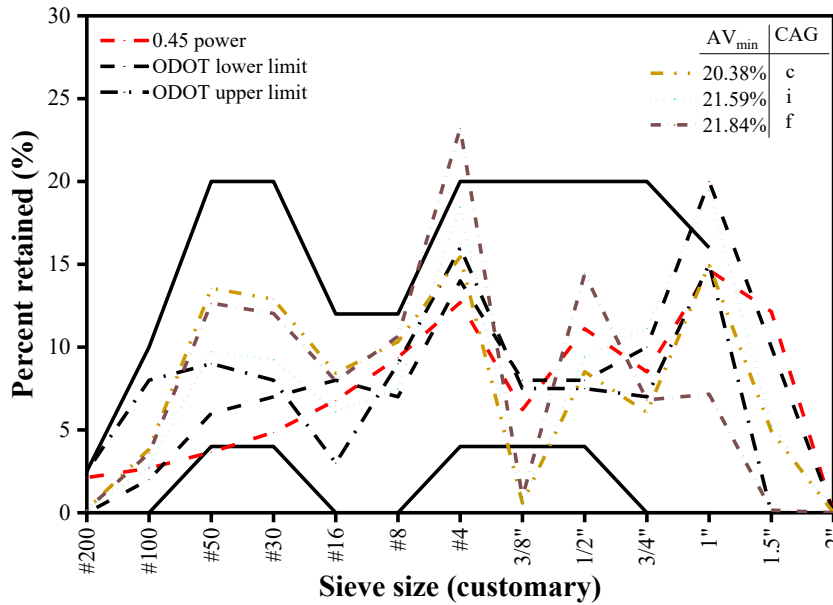


Figure 6.19: Comparison of the combined gradations of crushed gravel plus coarse sand to tarantula curve (CAG: Coarse aggregate gradation; c: coarse; i: intermediate; and f: fine).

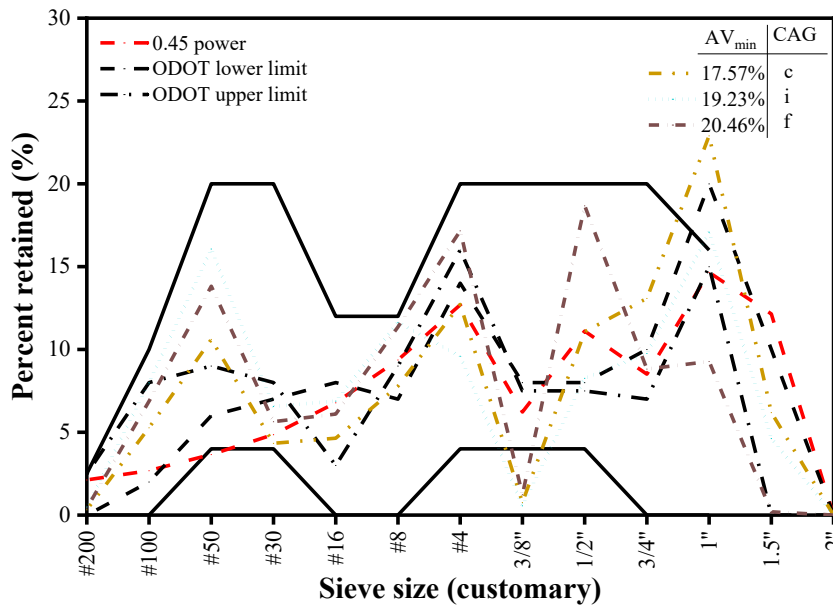


Figure 6.20: Comparison of the combined gradations of crushed gravel plus fine sand to tarantula curve (CAG: Coarse aggregate gradation; c: coarse; i: intermediate; and f: fine).

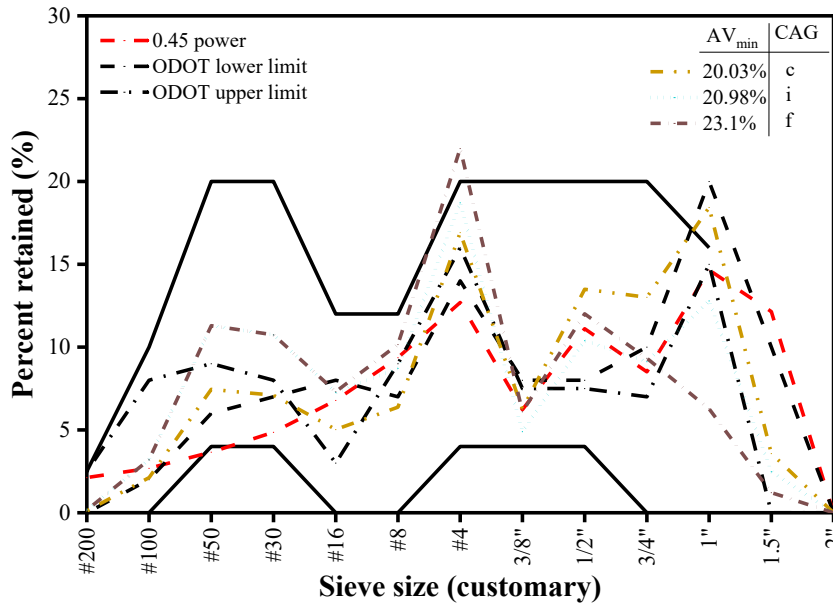


Figure 6.21: Comparison of the combined gradations of gravel plus coarse sand to tarantula curve (CAG: Coarse aggregate gradation; c: coarse; i: intermediate; and f: fine).

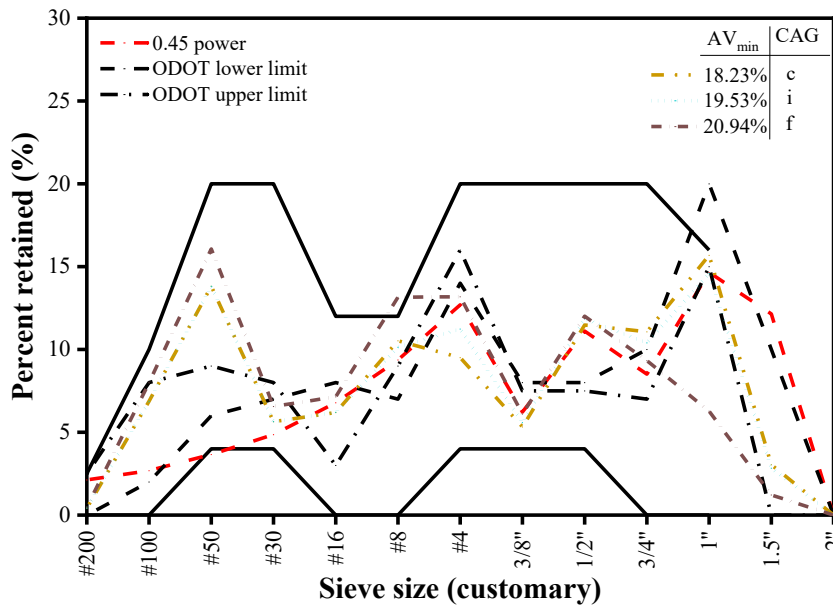


Figure 6.22: Comparison of the combined gradations of gravel plus fine sand to tarantula curve (CAG: Coarse aggregate gradation; c: coarse; i: intermediate; and f: fine).

6.1.3 Summary of Phase 1

A summary of AV_{min} data and the corresponding combined aggregate gradations generated from Phase 1 are presented here. The following conclusions can be made:

1. Increasing the coarseness of coarse aggregates and/or increasing the fineness of the fine aggregates were found to minimize the void-content of the combined aggregate system.

2. Aggregate systems with the lowest AV_{\min} values have their gradation curves closer to 0.45 power curve. For the aggregates evaluated in this research, higher AV_{\min} values were associated with finer gradations of combined aggregates.
3. The combined aggregate gradations representing the AV_{\min} of the different aggregate systems from Phase 1 are found to meet the criteria reported by Richardson (2005) for the haystack chart.
4. Six out of eighteen different combined aggregate systems evaluated as part of Phase 1 of SPR 823 failed to meet the tarantula curve limits. However, the performance of paving mixtures prepared with these aggregate systems is yet to be evaluated.
5. For the aggregates assessed, the minimum AV was recorded with the crushed gravel, coarser coarse aggregate gradation, and a finer sand at a low F/C.
6. The highest AV was observed with the quarry rock, a finer coarse aggregate gradation, and a coarser sand at a 1.25 F/C.

In summary, using the voids content values for aggregate systems estimated using available software platforms on the internet could result in high estimates of void contents when compared to the actual results from AASHTO T 19M (2014a) testing. The void ratio values estimated using packing models could therefore be impractical for estimating the minimum paste required for concrete mixtures. For example, at a V_v of 36.6%, the required minimum cementitious content required would be 847 lbs for one cubic yard (502 kg/m^3) of concrete at a w/cm of 0.41. The OSU research group believes that using the void content data generated from AASHTO T 19M (2014a) is more reliable than the voids ratio estimated from the software packages (as these do not consider aggregate shape). Moreover, estimating the minimum void content using AASHTO T 19M (2014a) for the aggregate materials that are locally available for a paving project can better assist in controlling the paste volume in a mixture.

6.2 PHASE 2A – DETERMINING WR REQUIREMENTS

The objective of this phase of the research is to identify WR requirements for a range of PV/AV_{\min} values that result in the concrete passing the edge slump and surface voids requirements specified in the Box Test. This information will provide a general range of required paste volumes so that a more comprehensive test program can be performed. Table 6.2 shows the results from the test program for this phase.

Table 6.2: A Summary of Admixture Requirements and Fresh Characteristics for Mixtures Evaluated in Phase 2A.

Mixture number	Aggregate system	Design air-content (%)	Design PV/AV _{min}	OPC content (lb/yc ³)	Water reducer added?	Water reducer dosage (% of suggested maximum)	Air - entraining admixture dosage (% of suggested maximum)	Measured air-content (%)	Passed the Box Test?	Average edge-slump (in.)	Average surface voids (%)	Slump (in.)	
1	1	1	1.25	496	No	—	—	—	No	Test invalid		0	
2					Yes	492	—	0.9	No	0.19	10-30	0.25	
3			1.5	573	No	—	—	—	No	Test invalid		0	
4					Yes	279	—	1.3	Yes	0.19	10-30	1.25	
5			1.75	644	No	—	—	—	No	Test invalid		0	
6					Yes	118	—	1.6	Yes	0.06	10-30	0.25	
7	2	1	1.25	660	No	—	—	—	No	Test invalid		0	
8					Yes	242	—	1.2	Yes	0.06	10-30	0.5	
9			1.5	751	No	—	—	—	No	0.06	50-100	0	
10					Yes	91	—	1.5	Yes	0.06	10-30	0.5	
11			1.75	833	No	—	—	—	1.3	Yes	0.25	10-30	2.25
12					NT	NT	NT	NT	NT	NT	NT	NT	NT
13	3	1	1.25	482	No	—	—	—	No	Test invalid		0	
14					Yes	380	—	1.1	Yes	0.13	10-30	0.5	
15			1.5	557	No	—	—	—	No	Test invalid		0	
16					Yes	123	—	1	Yes	0.13	10-30	0.5	
17			1.75	627	No	—	—	—	No	0.19	30-50	0.5	
18					Yes	58	—	1.4	Yes	0.13	10-30	1.5	
19	6	1	1.55	459	Yes	114	158	6.5	Yes	0.19	10-30	1	
20			1.82	531	Yes	55	164	5.5	Yes	0.06	10-30	1.25	
21			2.08	597	Yes	29	170	6.5	No	0.44	10-30	3	

Agg. System 1: Coarse graded QR with fine sand; Agg. System 2: Fine graded QR with coarse sand; Agg. System 3: Coarse graded G with fine sand (NT = Not Tested; If the Box Test specimen collapsed during the test, the test was considered invalid)

Analyses of the data from different mixtures in Phase 2A indicates that:

1. The WR dosage requirement for a mixture is dependent on the aggregate type. This can be concluded by comparing the results from mixtures 2, 4, 6, 14, 16 and 18. Note that the F/C_{opt} and AV_{min} values of mixtures 2, 4, and 6 are different when compared to mixtures 14, 16, and 18. However, the PV/AV_{min} values are similar. A comparison of PV/AV_{min} versus WR requirements for these mixtures is shown in Figure 6.23. The numbers next to the data points refer to the mixture number. At a given PV/AV_{min} and no air entrainment, the WR requirement for quarry rock mixtures is higher when compared to gravel mixtures.

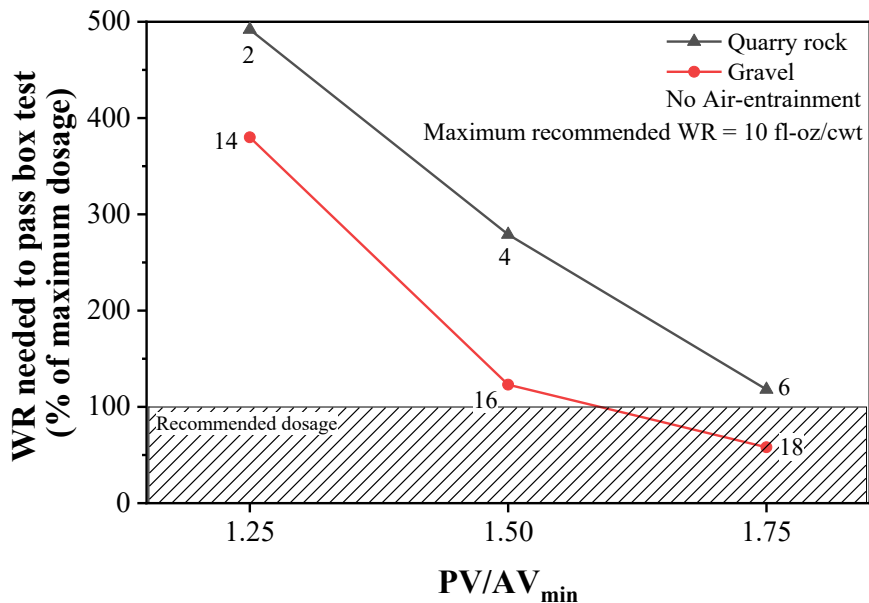


Figure 6.23: Influence of aggregate type on WR requirements.

2. A change in combined aggregate gradation in a mixture can influence the WR requirements. A comparison of the WR requirements for mixtures 2, 4, 6, 8, 10 and 11 is summarized in Figure 6.24. Note that different combined aggregate gradations for the same coarse and fine aggregate types can change the AV_{min} and the total surface area of the aggregates. The differences in WR requirements could be due to either of these factors. The AV_{min} for mixtures 2, 4, and 6 (coarser gradation for coarse aggregates and fine sand) is 18.78% while the AV_{min} for mixtures 8, 10, and 11 (finer gradation for coarse aggregates and coarse sand) is 25.09%. Because the PV of the mixture is normalized to the AV_{min} , the total binder contents (shown in Figure 6.24) were significantly higher for mixtures 8, 10, 11 when compared to the mixtures 2, 4, and 6. The low WR requirements for mixtures 8, 10, and 11 could therefore be due to the higher binder contents in the mixtures.

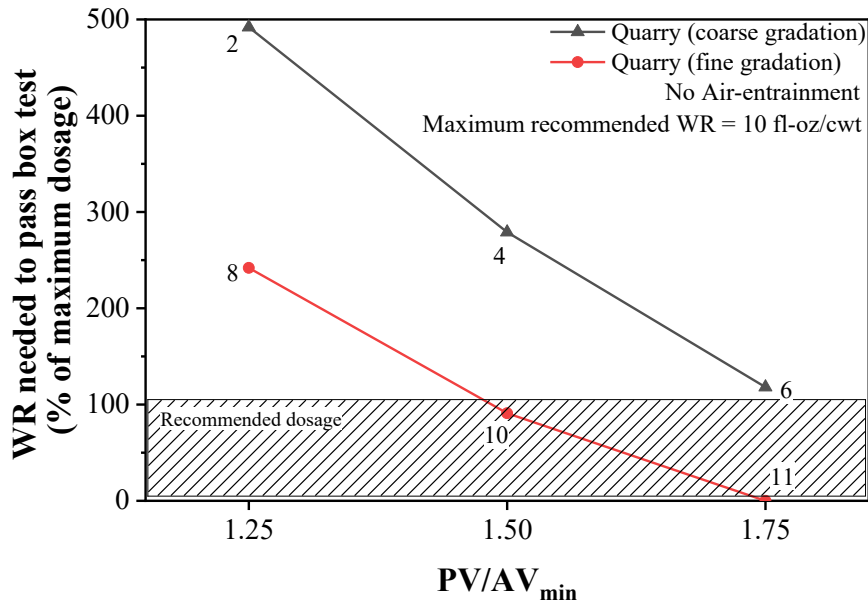


Figure 6.24: Influence of combined aggregate gradation on WR requirements.

3. A comparison of the data from the mixtures 14, 16, 18, 19, 20, and 21 indicates that the WR requirement for a mixture with no air-entrainment can be higher than the WR requirement for a mixture with air-entrainment. A comparison of data from these mixtures is shown in Figure 6.25. Note that the binder contents between mixtures 14 and 19, mixtures 16 and 20, and mixtures 19 and 21 are similar.

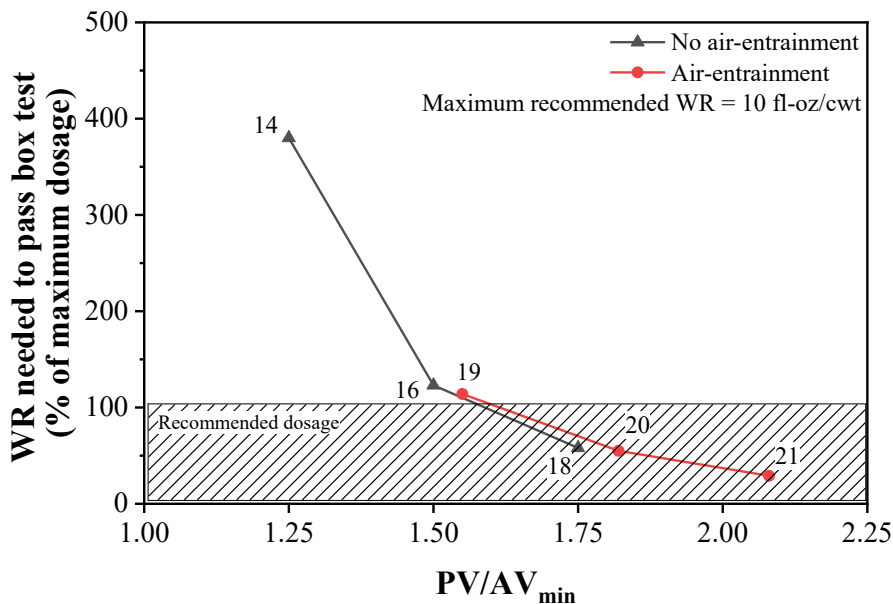


Figure 6.25: Influence of air-entrainment on WR requirements.

4. The PV/AV_{min} for air-entrained mixtures was higher than the PV/AV_{min} for non air-entrained mixtures on average by 0.3 units. Although it would be expected that the addition of an air-entrainer should reduce the required PV necessary to pass the Box Test, the volume of entrained air is included the overall paste volume and this increase results in the higher PV/AV_{min}.

5. Figure 6.26 shows results from edge slump versus slump. No clear trend was observed between slump and edge-slump values when the slump ranged from 0 in. (0 mm) to 1.25 in. (31.8 mm). This lack of correlation was also observed in the preliminary study. Although limited data are available, for slump values greater than 1.25 in. (31.8 mm), the edge-slump seemingly increases linearly. More research would be needed to validate this correlation.

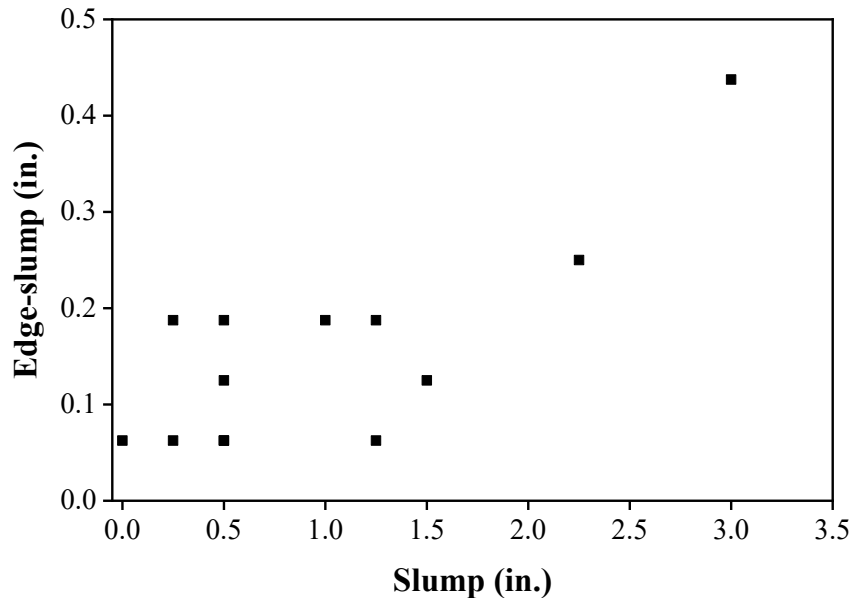


Figure 6.26: Relationship between slump and edge-slump.

6.2.1 Summary of Phase 2A

The amount of WR necessary to pass the Box Test decreases with increasing PV/AV_{\min} values. Coarse aggregate type and aggregate gradation also influence the amount of required WR to pass the Box Test. Increasing the WR dosage above typical values used in the field can result in lower PV/AV_{\min} values, which could result in lower cementitious materials contents. For paving concrete mixtures, consideration of using higher WR dosages may result in lower cementitious materials contents in concrete mixtures, and possibly improved performance.

6.3 PHASE 2B – DETERMINING PV/AV

The objective of the Phase 2B testing program is to identify a range of acceptable PV/AV_{\min} values for concrete mixtures containing different aggregate systems. Acceptable PV/AV_{\min} values are defined as values that pass the Box Test and meet required concrete characteristics.

Results from the Phase 2b test program are shown in Table 6.3. Note that the QR mixtures required a PV/AV_{\min} of 1.7 to pass the surface void requirements and a PV/AV_{\min} of less than 2 to pass the edge slump requirements. The CG concrete mixture with an F/C of 0.5 (AV of 17.57%) required a PV/AV_{\min} of 1.95 to pass the Box Test (a paste content of 34.26%, or 9.25 cf [0.262 cubic meters]). Increasing the F/C to 0.75 for this aggregate increased the AV to 18.09%, which would indicate that more paste would be required. However, at a F/C of 0.75, the PV/AV necessary to pass the Box Test was 1.7 (a paste content of 30.75%, or 8.3 cf [0.235 cubic meters]). This is an important finding. Although the minimum aggregate void

content was identified at a F/C of 0.5, significantly more paste was required to achieve the passing requirements of the Box Test when compared with the mixture with more sand. This indicates that although AV_{\min} should be the first choice for developing mixture proportions, in some cases AV_{\min} will not result in the lowest paste volume.

It should be noted that the PV/AV_{\min} value of concrete after mixing can be different from the PV/AV_{\min} value initially assumed during the proportioning (referred to as the target PV/AV_{\min}). This can occur when there are differences in the design and measured air-content values. Table 7.5 provides a summary of actual PV/AV_{\min} (or PV/AV) values, the air-content measured from the fresh concrete, the binder and water contents based on the actual PV/AV_{\min} (or PV/AV), admixture dosages, and results from slump and Box Tests. The following criteria were used to identify if a mixture is acceptable: 1) The measured air-content must be $\pm 1.5\%$ of the target value (i.e., 5%), 2) The WR dosage must meet the ODOT requirements (i.e., maximum dosage = 80% of maximum recommended limit by manufacturer), and 3) the mixture must pass the Box Test.

Table 6.3: Results from Phase 2b Test Program.

Aggregate System	Coarse aggregate type	Mixture number	Design PV/AV _{min} or PV/AV ^a	Target air-content (%)	OPC content (lb/yd ³)	Fly ash content (lb/yd ³)	Slag content (lb/yd ³)	Total binder content (lb/yd ³)	Water content (lb/yd ³)	Water reducer dosage (% of maximum)	Air - entraining admixture dosage (% of maximum)	Passed the box test?	Edge-slump (in.)	Surface voids (%)	Slump (in.)
1	Quarry rock	1	1.55	5	338	145	–	483	198	76	70	No	0	30-50	0
		2	1.7	5	367	157	–	524	215	40	58	Yes	0.25	10-30	1.75
		3	1.85	5	395	169	–	564	231	52	65	Yes	0.13	10-30	0.5
		4	2	5	421	180	–	601	246	0	61	No	0.75	10-30	4
2	Crushed gravel	5	1.65	5	337	–	144	481	197	73	61	No	0.19	30-50	0.25
		6	1.8	5	364	–	156	520	213	89	74	No	0	30-50	0.5
		7	1.95	5	390	–	167	558	229	79	81	Yes	0.13	10-30	0.5
3		8	1.7	5	358	–	153	511	209	87	70	Yes	0.06	10-30	0.25
		9	1.85	5	385	–	165	550	225	60	70	Yes	0.13	10-30	0
		10	2	5	411	–	176	587	241	55	65	Yes	0.06	10-30	0.75
4	Gravel	11	1.6	5	493	–	–	493	202	60	74	Yes	0.13	10-30	1.25
		12	1.75	5	534	–	–	534	219	24	72	Yes	0.19	10-30	1.75
		13	1.9	5	573	–	–	573	235	0	75	No	0.38	10-30	3

Agg. System 1: Coarse graded QR with fine sand; Agg. System 2: Coarse graded CG with fine sand and F/C=0.5; Agg. System 3: Coarse graded CG with fine sand and F/C=0.75; Agg. System 4: Coarse graded gravel with fine sand.

a. Aggregate system 3 is not at PV/AV_{min} (F/C=0.75) and therefore is referred to as PV/AV.

6.3.1 Summary of Phase 2B

The following conclusions can be drawn from the Phase 2B test data:

1. For concrete mixtures containing coarse-graded quarry rock and fine sand, the design PV/AV_{\min} ranged from 1.7 to approximately 1.9. Within this PV/AV_{\min} range and with WR, the mixture passed the requirements of the Box Test.
2. Concrete mixtures containing crushed gravel (coarse gradation) and fine sand where the F/C was 0.5 failed to meet the target air-content at all PV/AV_{\min} levels investigated here. Increasing the F/C from 0.5 to 0.75 resolved this issue. For concrete mixtures containing crushed gravel (coarse gradation) and fine sand and with a F/C of 0.75, design PV/AV_{\min} values ranged from 1.7 to approximately 2.0; within this range the mixtures with WR passed the Box Test requirements.
3. For some aggregate combinations (coarse + fine), in some cases where F/C values are far from unity, the minimum paste content necessary to pass the Box Test may not be associated with AV_{\min} ; in these cases, judgement is needed to select a more appropriate F/C and the corresponding A/V. More research is needed to assess this.
4. For concrete mixtures containing gravel (coarse gradation) and fine sand, a design PV/AV_{\min} value ranging from 1.6 to approximately 1.8 can pass the Box Test at acceptable WR dosage levels.

Based on the results from the research in Phase 2B, acceptable ranges of PV/AV values were identified. Using this information, the OSU research team finalized the 2C experimental program.

6.4 PHASE 2C – ASSESSMENT OF CONCRETES USING VARYING PV/AV VALUES

This section reports the analyses and discussions of the experimental data generated as part of Phase 2C study. Results from the test program are presented. After the results are presented, analyses on the effects of the different parameters will be performed. As already reported, the objective this study is to evaluate the performance of concrete mixtures designed using the new proportioning methodology. Information on these mixture constituent materials have been already provided. The varying levels of paste volumes, aggregate types, aggregate gradations, SCMs, and SCM replacement levels in the fresh and hardened states are varied. Twenty-five (25) concrete mixtures, as shown in Table 5.6, were mixed and evaluated. Among these mixtures, only mixture 24 was deemed too harsh and unstable, likely due to limited amount of paste. Specimens from mixture 24 were not assessed.

It should also be noted that the initial assumption that the required paste content will decrease with decreasing AV_{\min} content has not yet been confirmed. Figure 6.27 shows the required binder content for the mixtures assessed in Phase 2C versus the AV_{\min} . The figure clearly shows that lower AV_{\min} values result in lower binder contents.

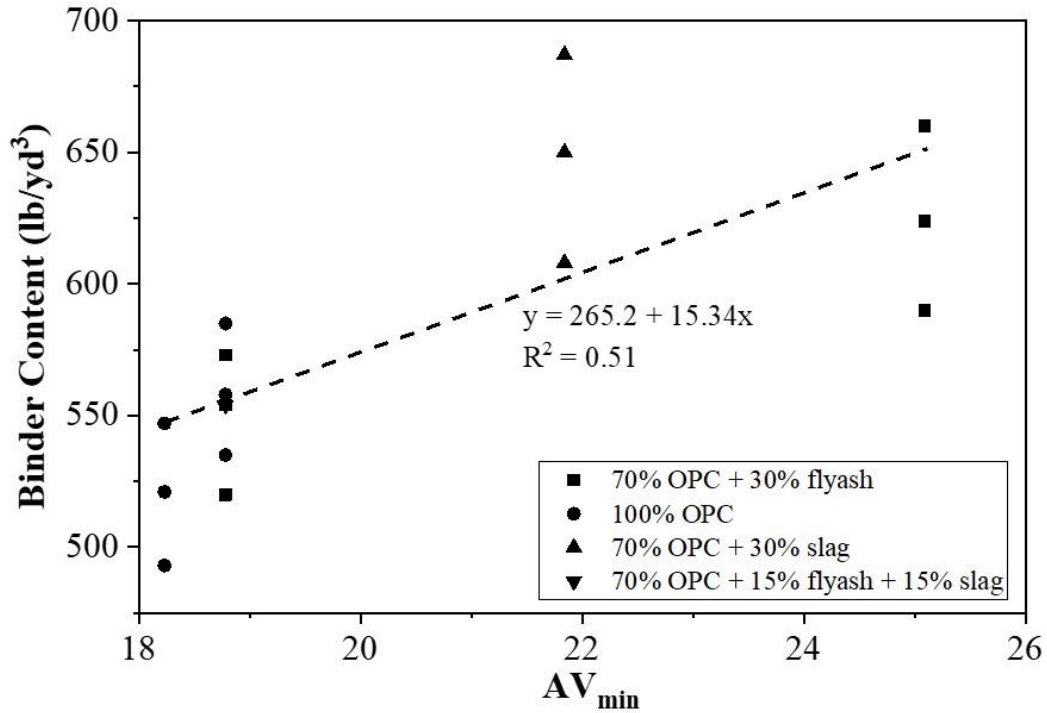


Figure 6.27: Required binder content versus AV_{min}.

To accomplish the objective of this phase, different groups of mixtures were considered for evaluating different study parameters. Test data for mixtures within each group were compared to assess the effects of the respective study parameter on concrete properties. Details of different groups of mixtures considered for assessing different parameters are summarized in Table 6.4. The groups within the paragraphs are used for comparisons.

Table 6.4: Groups of Concrete Mixtures used for Assessing Different Study Parameters.

Study parameter	Groups of different mixtures considered for assessing study parameter
Paste volume and total binder content	(1, 2, 3); (4, 5, 6); (7, 8, 9); (10,11,12); (13, 14, 15); (16, 17, 18); (19, 20, 21)
Binder type	(1, 7); (2, 8); (3, 9); (10, 16); (11, 17); (12, 18); (11, 17, 25)
w/cm	(11, 22, 23)
Aggregate type	(9, 17)
Aggregate gradation	(3, 4); (12, 13)

Statistical analyses were conducted to evaluate the significance of the effects of study parameters on concrete performance. Tools such as two sample t-test and one-way ANOVA were adopted as reported by Park (2009). A confidence level of 0.05 was chosen for all tests and the following criteria were set for outcome of the statistical tests (i.e., p-value):

- Strong evidence of significant effect for ‘p-value < 0.01’;

- Moderate evidence of significant effect for ' $0.01 < p\text{-value} < 0.05$ ';
- No evidence of significant effect for ' $p\text{-value} > 0.05$ '.

6.4.1 Test Results and Discussions

Table 6.5 summarizes the required admixture dosages for the different concrete mixtures and their fresh characteristics measured from testing. Also listed in the table are the adjusted amounts of paste volume, PV/AV, and total binder contents based on the measured plastic air contents. The dosage of water reducer was adjusted for each mixture with an intention of limiting the edge-slump (M. D. Cook et al., 2014) as tested using the Box Test to 0.25 inches (6.3 mm). The dosage of air-entraining admixture was based on achieving a target plastic air content of $5\% \pm 1.5\%$ following AASHTO T 152 (2019b) test procedure. For the mixtures tested in this study, the air-entraining dosage values ranged between 2.18 and 2.92 fl-oz/cwt.

Among the twenty-four (24) mixtures investigated, two mixtures (18 and 19) did not meet the requirements on plastic air content and two mixtures (18 and 23) did not meet edge-slump requirements. A discussion on the effect of different study parameters on admixture dosage requirements is provided in following write-up. Because the performance of concrete in both fresh and hardened states can depend on the actual paste volume and actual total binder content of the batched concrete, the adjusted paste volumes and adjusted total binder content values shown in Table 6.5 are used in all data plots in this section for comparing test data among different mixtures.

Table 6.5: Summary of Admixture Dosages, Fresh Characteristics, Paste Volumes, Binder Contents, and PV/AV Values Recorded for Phase 2C Concrete Mixtures.

Mix ID	Admixture dosages		Fresh concrete characteristics					Actual total binder content (lbs/yd ³)	Actual Paste volume (%)	Actual PV/AV
	WR (fl-oz/cwt)	AEA (fl-oz/cwt)	Plastic air content (%)	Unit weight (lbs/ft ³)	Slump (in.)	Edge slump (in.)	Surface voids (%)			
1	3.27	2.18	5.8	146.7	1	0.06	10-30	520	28.8	1.75
2	4.06	2.34	4.5	149.1	0.75	0.19	10-30	554	29.0	1.77
3	1.49	2.32	5.5	150.4	0.75	0.25	10-30	573	30.9	1.93
4	3.88	2.46	5	149.2	0.75	0.13	10-30	590	31.1	1.35
5	2.74	2.52	5.2	150.4	0.75	0.22	10-30	624	32.8	1.46
6	2.17	2.39	4.8	149.6	1.25	0.16	10-30	660	34.0	1.54
7	5.58	2.92	5.5	149.3	0.5	0.19	10-30	535	28.6	1.73
8	6.83	2.78	6.2	149.2	1	0.13	10-30	558	30.3	1.88
9	5.32	2.66	6	148.7	0.25	0.22	10-30	585	31.3	1.97
10	4.68	2.6	5	147.1	0.5	0.13	10-30	550	29	1.85
11	3.65	2.68	5.4	144.8	0.75	0.19	10-30	584	30.9	2.03
12	2.76	2.76	4.8	144.6	1.5	0.25	10-30	624	32.1	2.14
13	7.65	2.73	5	146.2	0.25	0.13	10-30	608	31.6	1.65
14	6.14	2.41	5.2	146.6	0.5	0.16	10-30	650	33.6	1.81
15	4.95	2.68	5.8	141.3	1.5	0.25	10-30	687	35.8	2.00
16	6.69	2.57	4.8	146.7	0.25	0	10-30	557	28.9	1.84
17	4.33	2.65	5	145.8	0.5	0	10-30	594	30.6	2.00
18	3.09	2.71	7	141.4	1.75	0.38	10-30	617	33.6	2.29
19	4.06	2.61	7.5	149	2.25	0.20	10-30	493	26.3	1.60
20	1.65	2.47	NA	147.2	0.75	0.07	10-30	521	27.5	1.71
21	0	2.61	5.2	148.6	0.5	0.11	10-30	547	28.6	1.80
22	4.67	2.57	5	147	0.5	0.19	10-30	612	30.6	2.00
23	2.54	2.78	6.5	149.3	2.25	0.31	10-30	555	31.7	2.11
25	3.83	2.81	5.4	150.3	1	0.24	10-30	580	30.9	2.03

*Imperial to SI units conversion factors: 1 lb/yd³ = 0.59 kg/m³, 1 lb/ft³ = 16 kg/m³, 1 inch = 0.0254 m, 1 fl oz = 29.57 mL.

The average measured test values for different hardened concrete properties are summarized in Table 6.6. The mean compressive strength values at 56 days for mixtures 1, 9, and 21 were observed to be lower than 28-day compressive strength results, but a two-sample t-test between the 28- and 56-day test results revealed no significant difference between the mean strengths for each of these mixtures. The p-values observed from t-tests between 28- and 56-day compressive strength results for mixtures 1, 9, and 21 were 0.166, 0.797, and 0.95, respectively. Similar observations were made in case of flexural strength test results for mixtures 10, 18, 21, and 22, respectively. While the mean 56-day strengths were lower compared to the mean 28-day strengths, no significant differences were identified between the mean outcomes. The p-values observed from t-tests between the 28- and 56-day flexural strength results for mixtures 10, 19, 21, and 22, were 0.451, 0.128, 0.790, and 0.130, respectively. The effects of different study parameters on admixture dosages and fresh characteristics will be discussed in more detail in the following sections. Pictures of testing on fresh characteristics for different mixtures are included in Appendix.

Table 6.6: Summary of Average Test Values Estimated for Different Hardened Properties of Phase 2C Concrete Mixtures.

Mixture ID	Average compressive strength, psi		Average flexural strength, psi		Durability characteristics		
	28-days	56-days	28-days	56-days	Modified AASHTO PP 84 formation factor	AASHTO PP 84 drying shrinkage (μm)	AASHTO T 161 durability factor
1	4502	4333	585	706	763	379	NITP
2	4893	5454	592	712	876	300	NITP
3	5164	5671	665	722	1016	277	NITP
4	5495	6046	744	776	907	397	NITP
5	5249	6386	741	749	1256	352	NITP
6	5285	6303	747	792	1429	380	NITP
7	5898	6387	768	788	1531	280	NITP
8	5572	5819	745	941	991	380	NITP
9	6669	6472	754	809	1127	356	NITP
10	6055	6537	754	695	1655	528	63
11	6433	6780	803	808	1378	584	64
12	5986	6382	668	831	1667	600	54
13	6586	7681	727	805	1557	548	NITP
14	6886	7841	713	803	1579	628	NITP
15	5939	6850	702	717	1537	592	NITP
16	6395	6995	698	777	1780	538	54
17	6205	6596	687	690	1273	615	58
18	5630	6326	797	745	1086	464	58
19	4291	5128	679	761	1291	308	NITP
20	4488	4628	823	853	Not Tested	467	NITP
21	4983	4922	852	839	754	538	NITP
22	6625	7486	818	889	1721	503	NITP
23	4599	5136	745	731	2010	527	NITP
25	5323	6415	655	809	1278	421	NITP

*NITP = Not in test program; Imperial to SI units conversion factors: 1 micron = 39.37 microinch, 1 psi = 0.00689 MPa.

The formation factor values shown in Table 6.6 are based on the testing of specimens subjected to 56-day curing period. This curing was selected due to time constraints. AASHTO PP 84 (2020b) specifies a 91-day curing period for assessing the formation factor. The test results generated in this study are referred as modified AASHTO PP 84 (2020b) formation factor values. A pore solution resistivity value of 0.127 ohm-m has been considered for estimating the formation factor, per AASHTO PP 84 (2020b). It is anticipated that the AASHTO PP 84 (2020b) formation factor values for concrete mixtures investigated in this study to be higher than the formation factor results shown in Table 6.6 due to improvements in concrete pore structure

characteristics associated with longer curing times. AASHTO PP 84 (2020b) reports a minimum formation factor limit of 1000 for performance engineered paving mixtures. With a 56-day curing regime, 18 out of 23 tested mixtures met this limit requirement.

Weiss et al. (2018) reported the correlations between formation factor and Rapid Chloride Permeability (RCP) test results for different classifications of AASHTO T 277 (2015b). These correlations are shown in Table 6.7. Also shown in the table are the lists of different concrete mixtures that met different classification criteria. The majority of the tested mixtures met the RCP test ‘low’ classification requirements with a few falling under the ‘moderate’ classification, which agrees well with literature (Ramezaniapour, Pilvar, Mahdikhani, & Moodi, 2011; Wee, Suryavanshi, & Tin, 2000).

Table 6.7: Predicted RCP Test Classification for Phase 2C Mixtures.

RCP test classification	Total charge passed, coulombs	Formation factor	List of Phase 2C mixtures that meet the criteria
High	>4000	<520	--
Moderate	2000 – 4000	520-1040	1, 2, 4, 8, 21
Low	1000 – 2000	1040-2080	3, 5, 6, 7, 9, 10, 11, 12, 13, 14, 15, 16, 17, 18, 19, 22, 23, 25
Very low	100 – 1000	2080 – 20800	--
Negligible	<100	>20800	--

The drying shrinkage values reported in Table 6.6 are based on AASHTO T 160 (2017d) testing (AASHTO, 2017d) with modifications in curing and drying times as suggested by AASHTO PP 84 (i.e., 7-day moist cure followed by 21-day drying). The unrestrained length change limit reported by AASHTO PP 84 (2020b) is 420 microstrain. The ODOT construction specification document requires a 28-day wet cure followed by 28-day drying period. Because of this, the ODOT drying shrinkage limit for high performance concrete mixtures, 450 microstrain, is not applicable here. Test results indicate that mixtures containing 30% fly ash met the AASHTO PP 84 (2020b) unrestrained shrinkage limit requirements. Based on these preliminary test results, it is initially hypothesized that the binary or ternary mixtures considered in this study with slag likely require extended curing times, which should reduce drying shrinkage values; but this requires further testing.

Due to time and budget constraints associated with this project, only a limited number of concrete mixtures were evaluated for AASHTO T 161 (2017e) durability factor. A discussion on the effects of different study parameters on concrete properties, including the durability factor, is provided in the following sections.

6.4.2 Effects of paste volume and total binder content

6.4.2.1 Water reducer dosage

Figure 6.28: Effect of paste volume and binder content on WR dosage (Mixtures 1, 2, 3) Figure 6.28 to Figure 6.34 show the effects of paste volume and total binder content on the required WR dosage to meet the requirements of the Box Test for the different

mixture groups. Note that the range of labels of the x-axes are different for the different figures. Except for mixture groups (1, 2, 3) and (7, 8, 9), results indicate the concrete mixture requires less WR with an increase in paste volume for a fixed workability requirement (i.e., edge-slump < 0.25 inches). The addition of more paste to the concrete mixture is generally anticipated to contribute towards the enhancement of concrete's workability, therefore limiting the corresponding requirement of the WR dosage. Data from mixture groups (1, 2, 3) and (7, 8, 9) exhibited similar trends, although the requirement of WR dosage increased with an increase in paste volume for recorded paste volumes below ~30%. Above this 30% threshold, the requirement of WR dosage decreased with an increase in paste volume. This finding was contrary to the general assumption of the relationship between paste volume and water-reducer dosage, which requires further investigation (Hover, 1998).

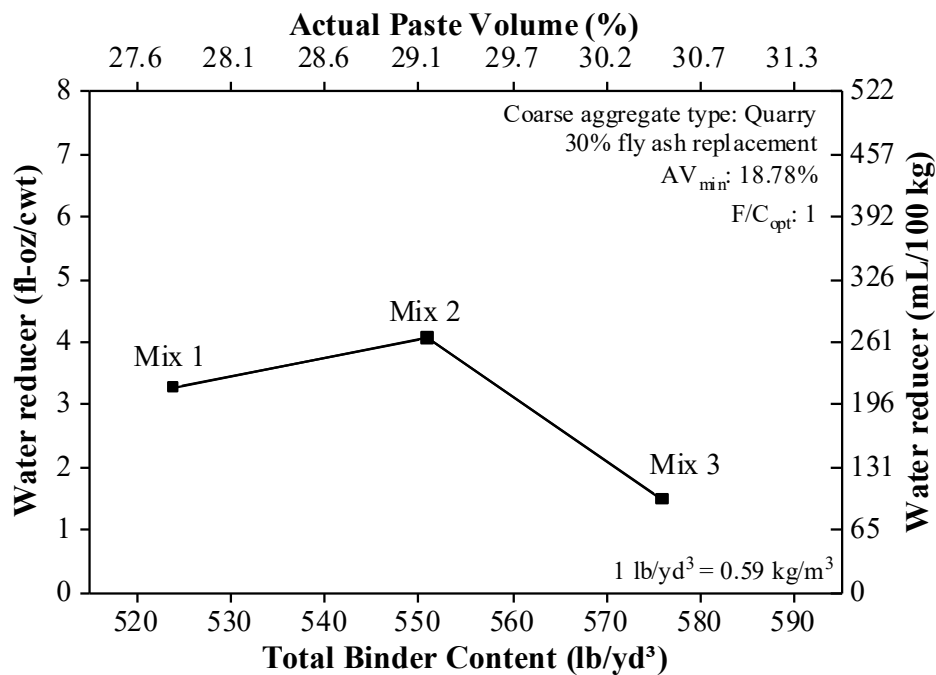


Figure 6.28: Effect of paste volume and binder content on WR dosage (Mixtures 1, 2, 3).

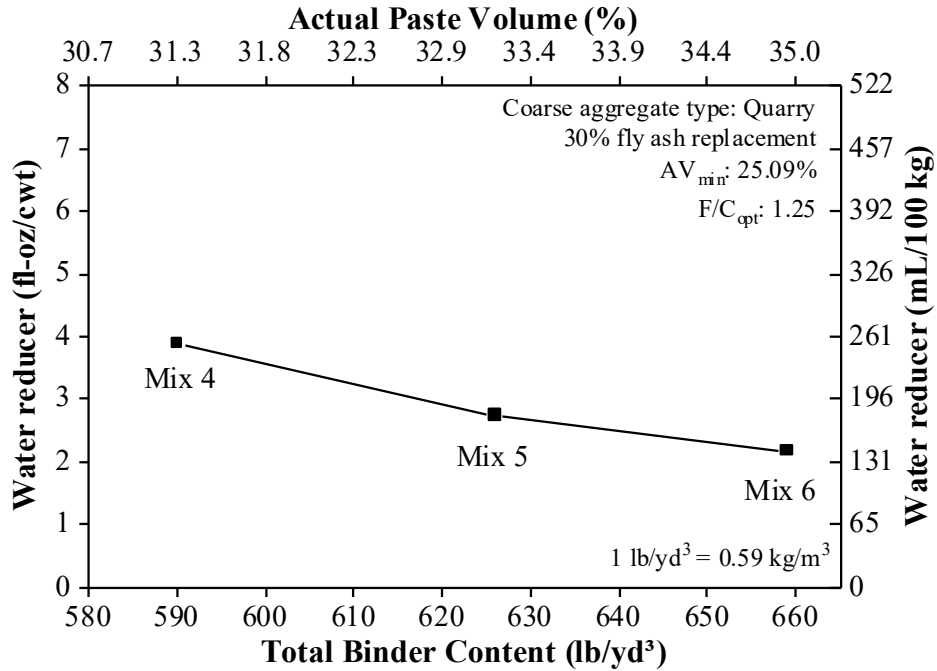


Figure 6.29: Effect of paste volume and binder content on WR dosage (Mixtures 4, 5, 6).

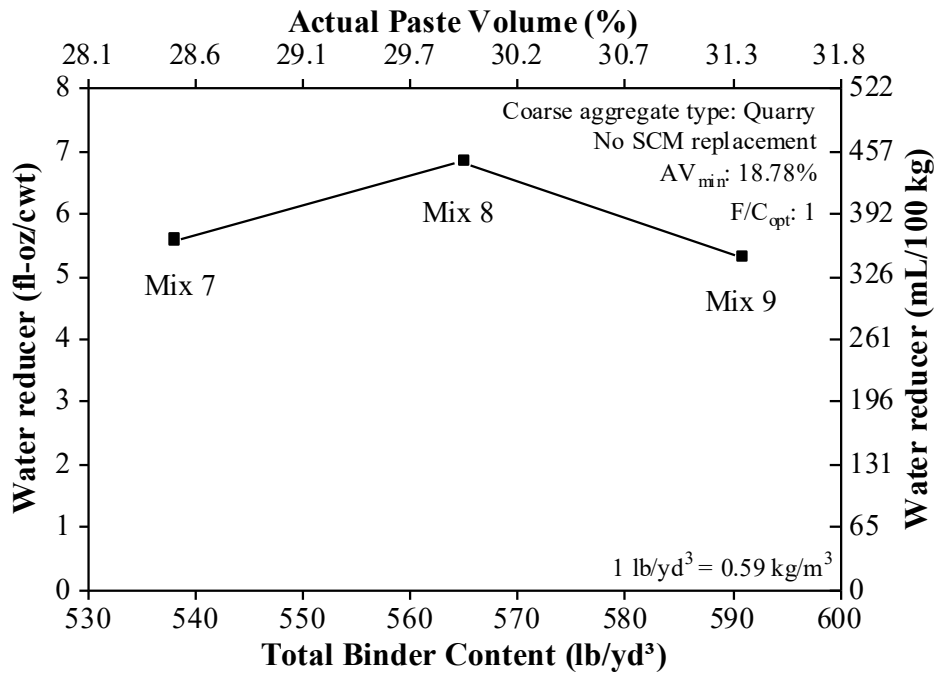


Figure 6.30: Effect of paste volume and binder content on WR dosage (Mixtures 7, 8, 9).

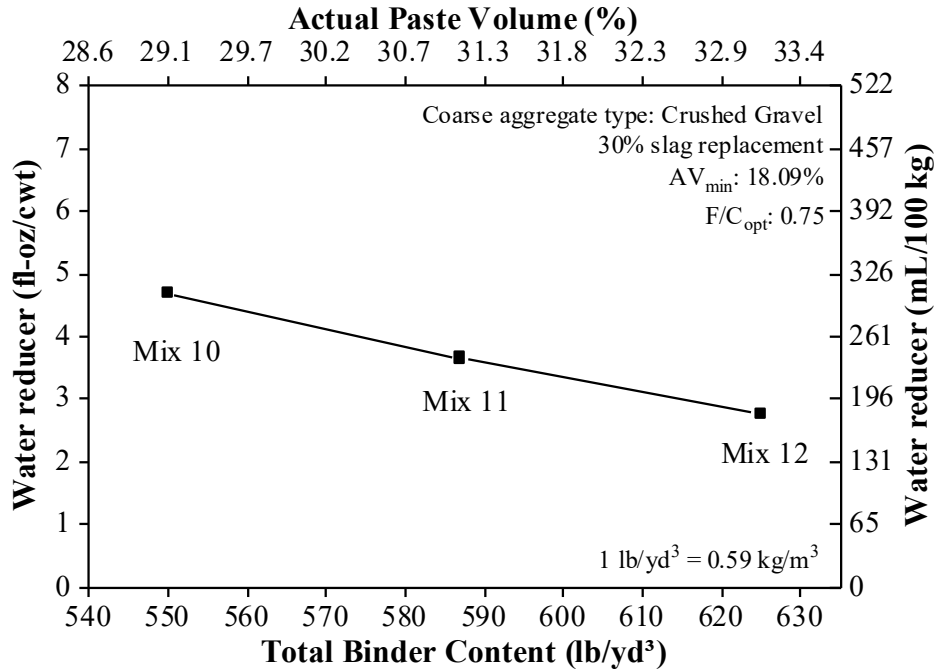


Figure 6.31: Effect of paste volume and binder content on WR dosage (Mixtures 10, 11, 12).

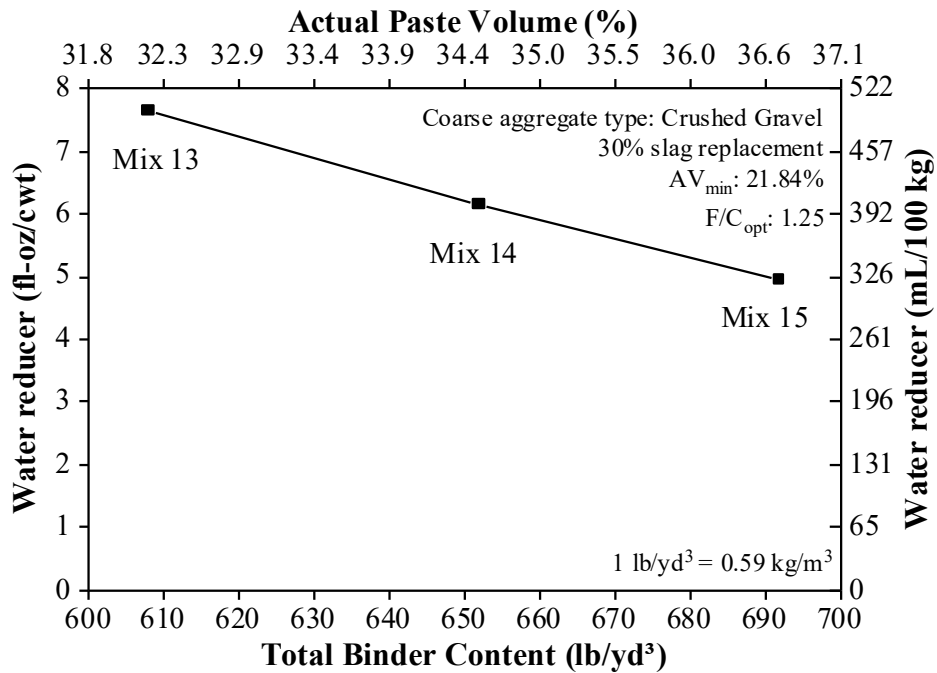


Figure 6.32: Effect of paste volume and binder content on WR dosage (Mixtures 13, 14, 15).

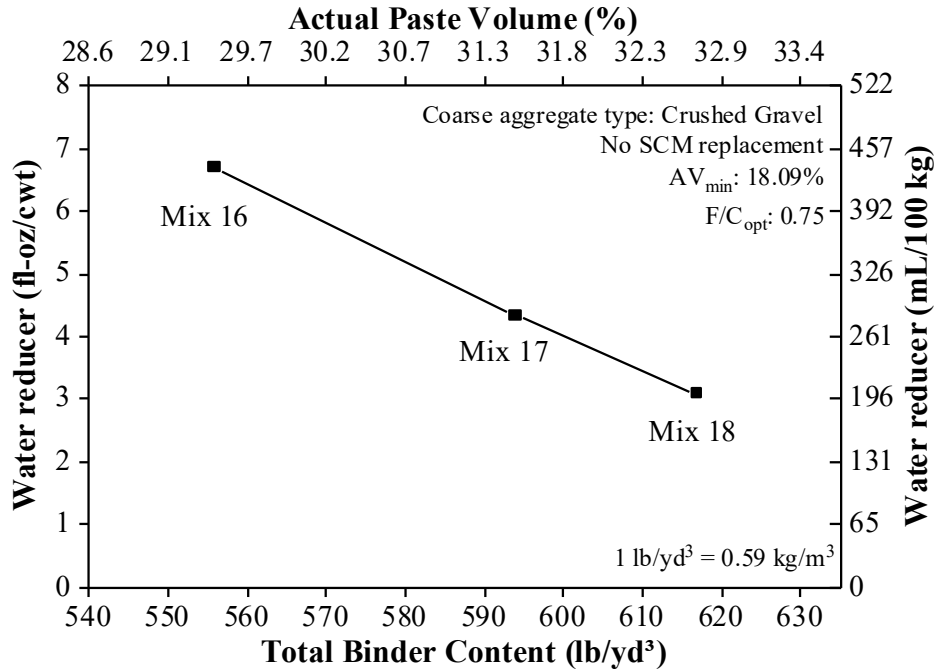


Figure 6.33: Effect of paste volume and binder content on WR dosage (Mixtures 16, 17, 18).

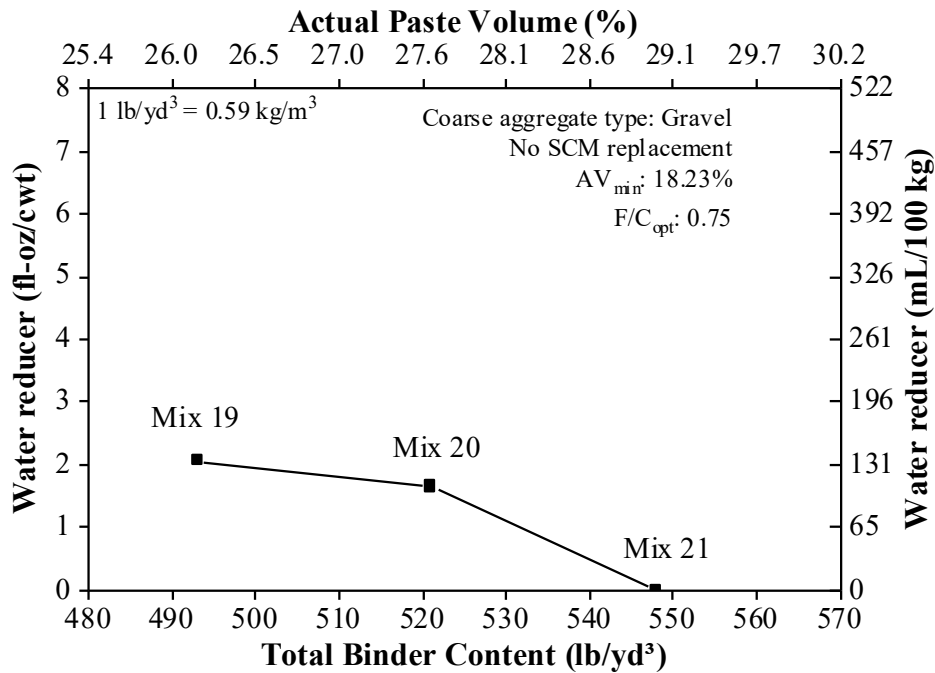


Figure 6.34: Effect of paste volume and binder content on WR dosage (Mixtures 19, 20, 21).

Overall, the general trend observed in Figures 6.28 to 6.34 is that as the total binder content increases, the need for WR decreases. This is of importance from a sustainability standpoint because these figures demonstrate that it is possible to achieve ample workability with a lower binder content and a higher WR dosage. If presented an option

to either choose a higher binder content or a higher WR dosage, it is recommended to choose a higher WR dosage because cement is the most energy intensive component of concrete. For the range of paste volumes investigated in this study for different mixtures, the maximum requirement of WR dosage fell below the 8 fl-oz/cwt (522.4 mL/100 kg) limit (for MasterPozzolith 80) commonly considered by concrete producers in Oregon for slip-form paving concrete mixtures. A survey of recent ODOT concrete mixtures for slip-form paving indicated that a total binder of 611 lbs/yd³ (362 kg/m³). Data generated in this study confirm that slip-form concrete mixtures can be potentially designed with a total binder content significantly lower than 611 lbs/yd³ (362 kg/m³), without compromising workability, if appropriate combined aggregate gradations (i.e., a coarser gradation for coarse aggregates and a sand with higher fineness modulus) and PV/AV values are considered during the mixture proportioning process. Cementitious materials contents as low as 524 lbs/cy (310 kg.m³) exhibited adequate workability when containing a WR.

6.4.2.2 Compressive strength

Figure 6.35 to Figure 6.41 compare the 28- and 56-day compressive strengths for different mixture groups as a function of paste volume and binder content. The p-values from ANOVA testing conducted to assess the effect of paste volume on compressive strength are shown in Table 6.8. As previously noted, certain mixtures exhibited lower mean 56-day strengths compared to mean 28-day strengths; however, t-tests results revealed no significant differences in mean test results. Due to the large scatter observed within some of the replicate specimens, the effect of paste volume on compressive strength was not clearly captured. This can be justified through the p-values reported in Table 6.8. Clear trends between paste volumes and compressive strength results were not observed for quarry rock mixtures (1 to 9), likely due to associated differences between workability and measured air contents. However, the mean compressive strength results recorded at 28-days for all mixtures met the minimum 28-day compressive strength limit of 4000 psi (27.6 MPa), suggesting the possibility of designing concrete mixtures with paste volumes lower than the paste volumes traditionally used in ODOT paving mixtures. Data pooled from all mixtures indicate that the 56-day compressive strength values were, on an average, 10% higher compared to 28-day strengths.

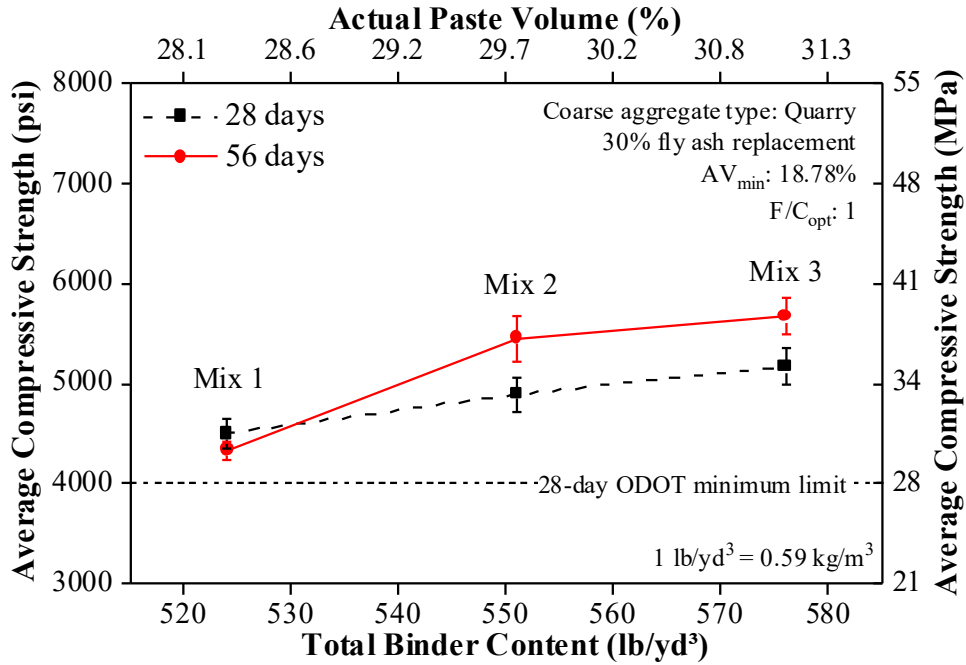


Figure 6.35: Effect of paste volume and binder content on compressive strength (Mixtures 1, 2, 3).

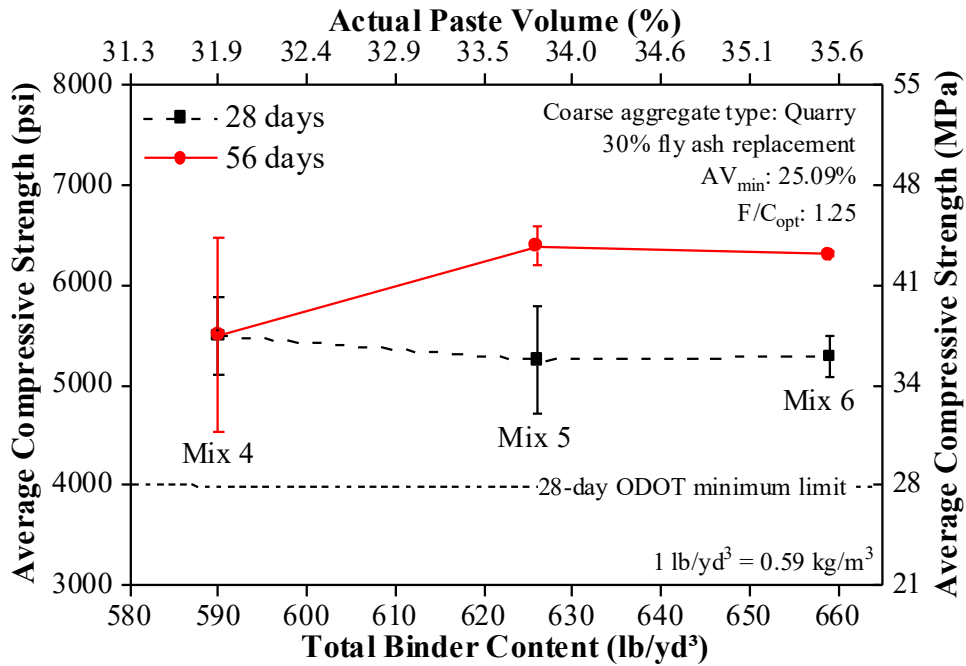


Figure 6.36: Effect of paste volume and binder content on compressive strength (Mixtures 4, 5, 6).

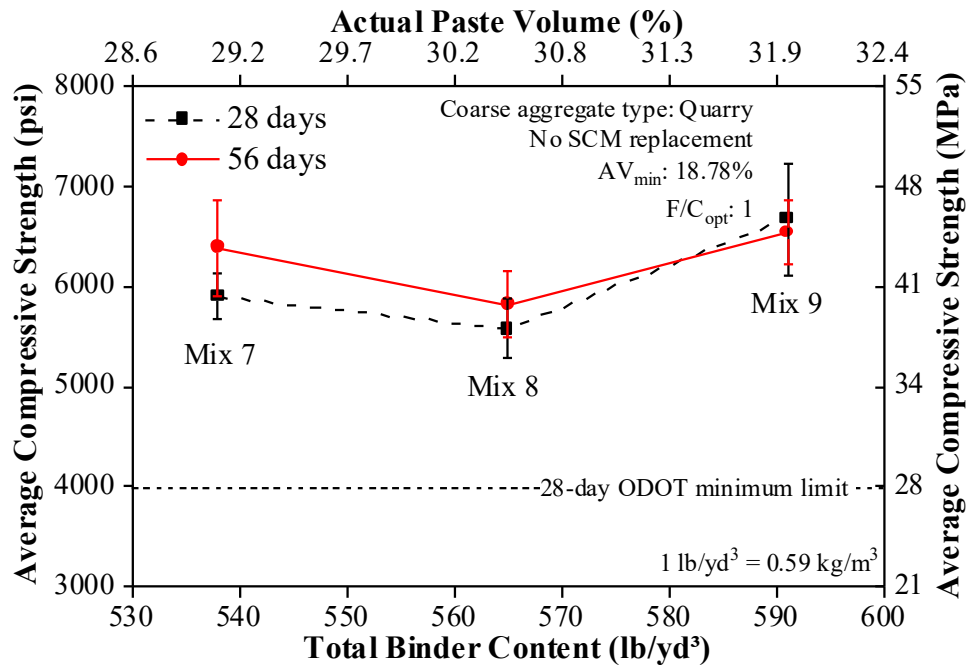


Figure 6.37: Effect of paste volume and binder content on compressive strength (Mixtures 7, 8, 9).

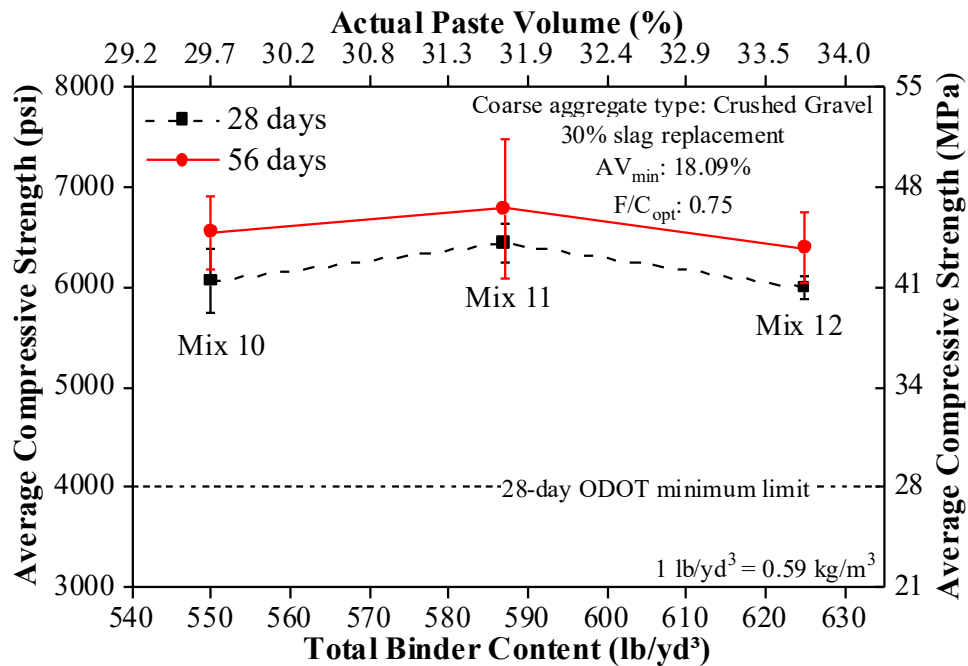


Figure 6.38: Effect of paste volume and binder content on compressive strength (Mixtures 10, 11, 12).

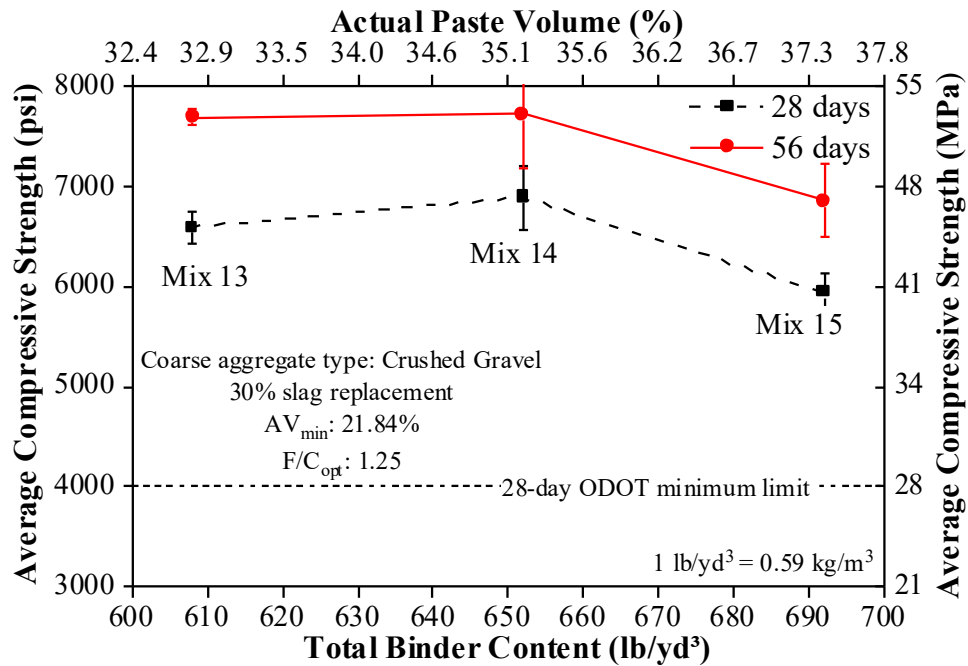


Figure 6.39: Effect of paste volume and binder content on compressive strength (Mixtures 13, 14, 15).

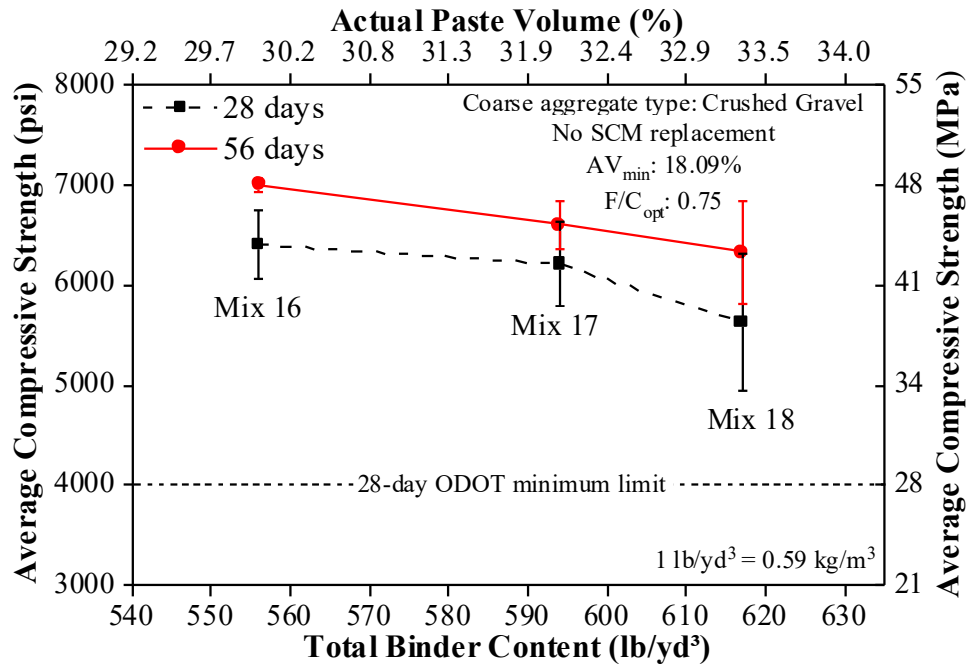


Figure 6.40: Effect of paste volume and binder content on compressive strength (Mixtures 16, 17, 18).

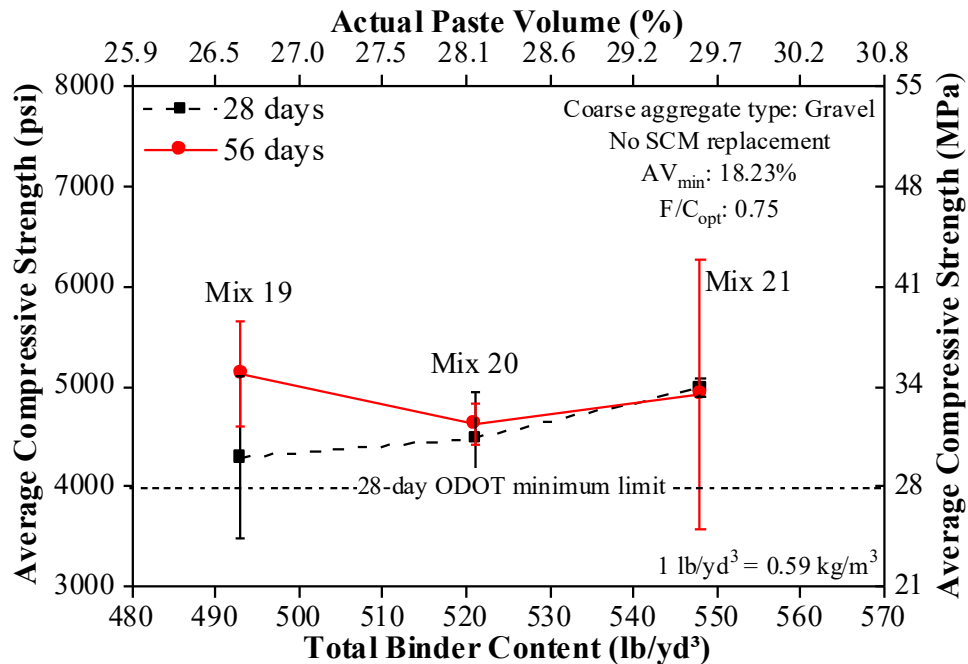


Figure 6.41: Effect of paste volume and binder content on compressive strength (Mixtures 19, 20, 21).

Table 6.8: p-values Generated from ANOVA Testing of Compressive Strength Data within Different Mixture Groups.

Mixture group	28-days	56-days
(1, 2, 3)	< 0.01	< 0.01
(4, 5, 6)	0.725	0.186
(7, 8, 9)	0.043	0.555
(10, 11, 12)	0.102	0.630
(13, 14, 15)	< 0.01	0.520
(16, 17, 18)	0.237	0.116
(19, 20, 21)	0.49	0.77

For crushed gravel mixtures with 30% slag (mixtures 10 to 15), increasing the paste volume from a low to moderate value slightly increased the mean compressive strength value, whereas increasing the paste volume from a moderate to high value decreased the mean strength value. Note that the range of paste volumes considered for mixture groups (10, 11, 12) and (13, 14, 15) are different due to differences in combined aggregate gradations. Data from mixtures 10 to 15 suggest the presence of an optimal paste volume, at which, concrete exhibits enhanced strength due to better packing of constituent materials (Yurdakul et al., 2013). For paste volumes below or above this optimal value, the distribution of concrete constituents is relatively less uniform compared to the distribution achieved at the optimal paste volume, resulting in relatively lower concrete strengths. This trend was not witnessed in data from mixture groups (1, 2, 3), (4, 5, 6), and (16, 17, 18). Data also suggests that the optimal paste volumes required to achieve a workability that is representative of slip-form paving concrete could be different from the

optimal paste volume required to produce a well-consolidated, higher slump hardened concrete.

Figure 6.42 and Figure 6.43 show scatter plots of the 28-day and 56-day compressive strength results, respectively as a function of paste volume and total binder content. It should be noted that the effects of aggregate type, gradation, and binder type on strength results are masked in the data plots shown below. A polynomial function of the second degree was fitted for both 28-day and 56-day compressive strength scatter plots. Further analysis, not shown here, revealed that the R^2 (goodness of fit) values was higher for the polynomial function when compared to the linear function. It can be observed that, at both test times, after a certain amount of binder content there is no increase in the compressive strength value.

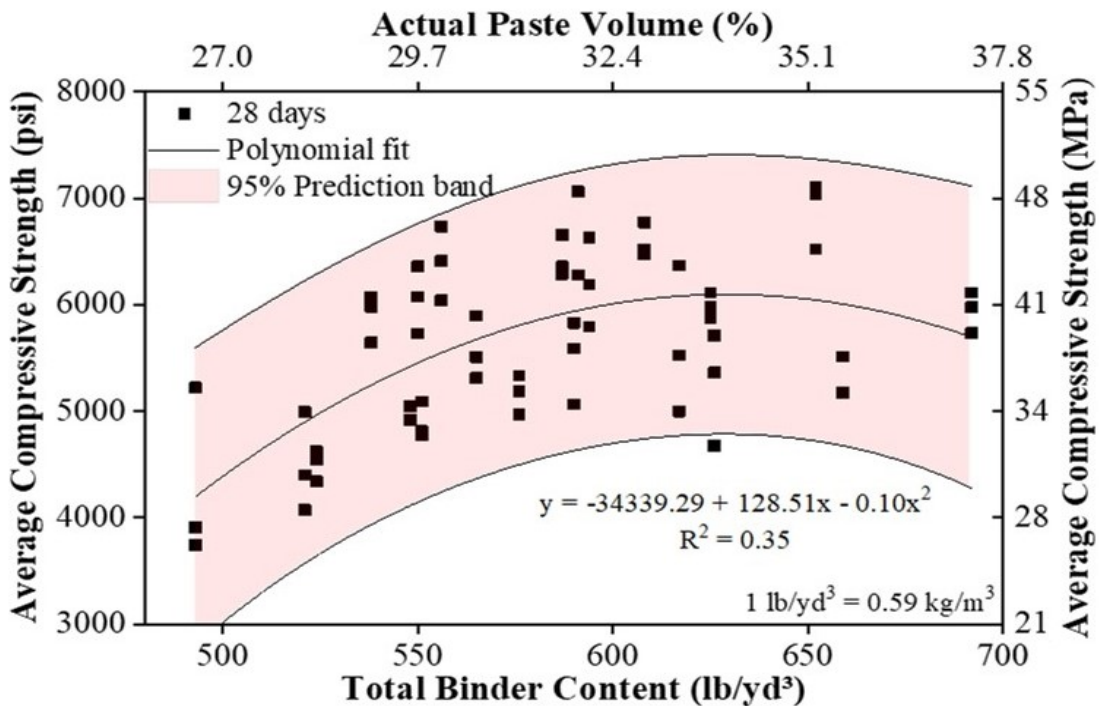


Figure 6.42: Scatter plot of 28-day compressive strength results as a function of paste volume and binder content.

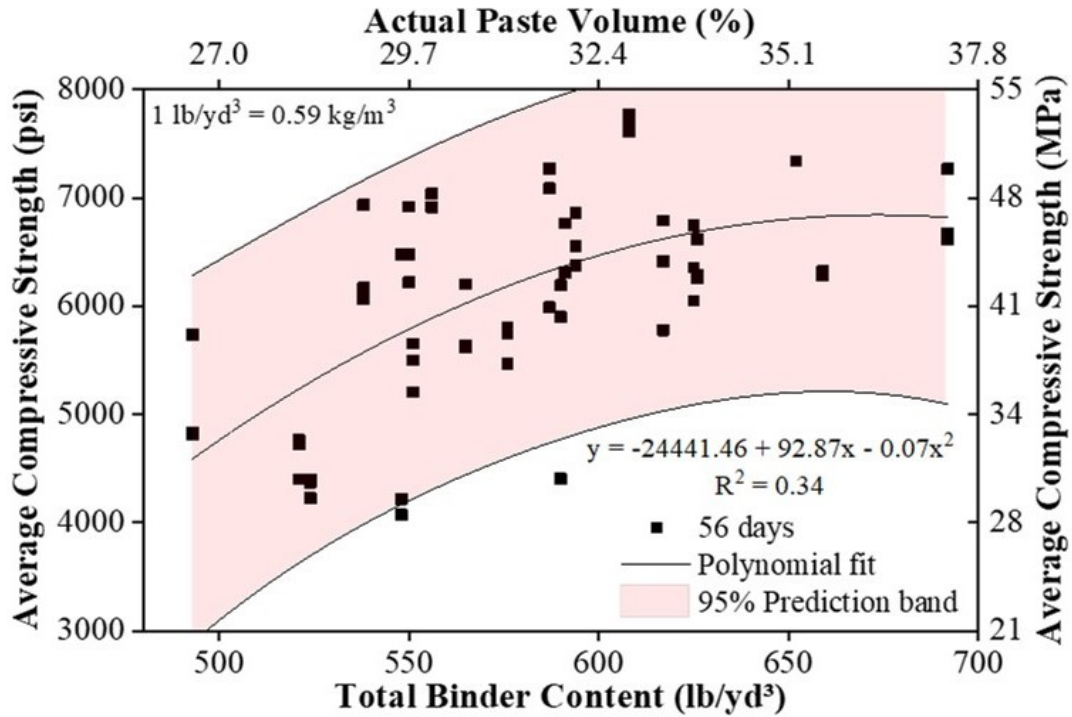


Figure 6.43: Scatter plot of 56-day compressive strength results as a function of paste volume and binder content.

6.4.2.3 Flexural strength

Figure 6.44 to Figure 6.50 show the 28- and 56-day flexural strength data recorded for mixtures of different groups as a function of paste volume and total binder content. With the exceptions of mixtures 1 and 2, data from other mixtures met the 28-day ODOT flexural strength requirement of 600 psi (4.1 MPa). No clear trends between the paste volume and flexural strength values were observed. The ratio between average flexural and compression strengths from both ages ranged between 10.2% and 18.4%, with an overall average of 13%. Data pooled from all mixtures also indicate that the 56-day flexural strengths were, on an average, 8% higher compared to flexural strengths recorded at 28 days. The ANOVA test results that compare flexural strength data between different mixtures for each of the six different groups are summarized in Table 6.9. Similar to the findings observed for compressive strength, a significant effect of paste volume on flexural strength results was not observed in the majority of cases evaluated herein. This is likely due to the variations in degree of consolidation achieved and varying air contents.

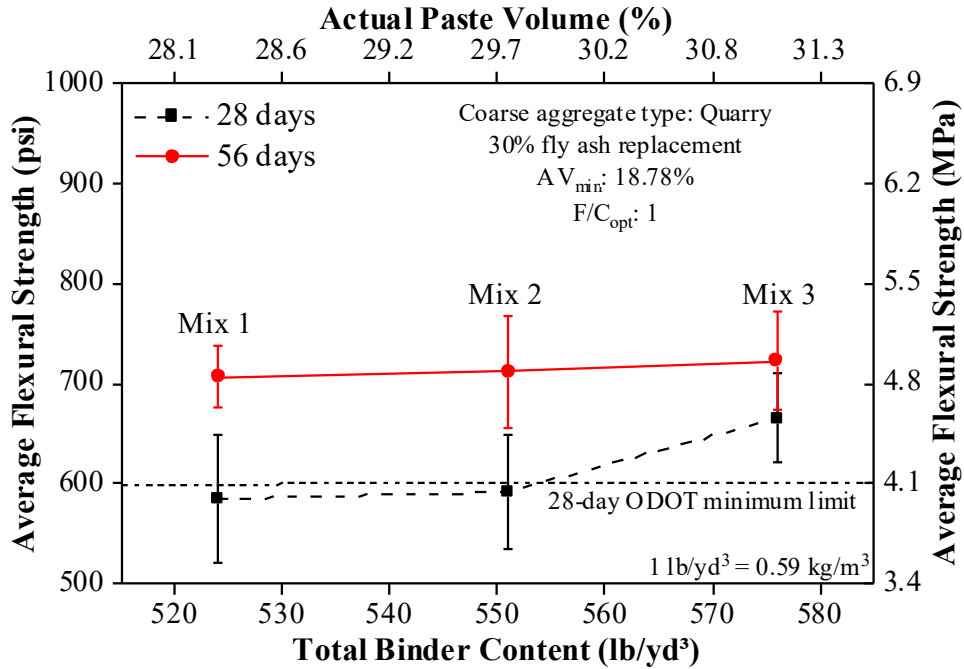


Figure 6.44: Effect of paste volume and binder content on flexural strength (Mixtures 1, 2, 3).

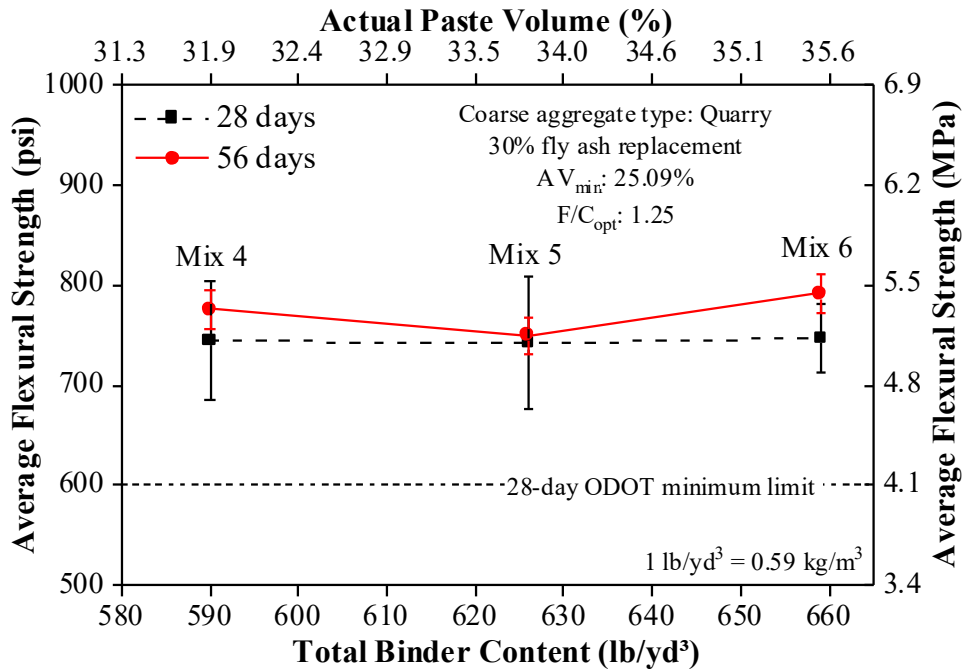


Figure 6.45: Effect of paste volume and binder content on flexural strength (Mixtures 4, 5, 6).

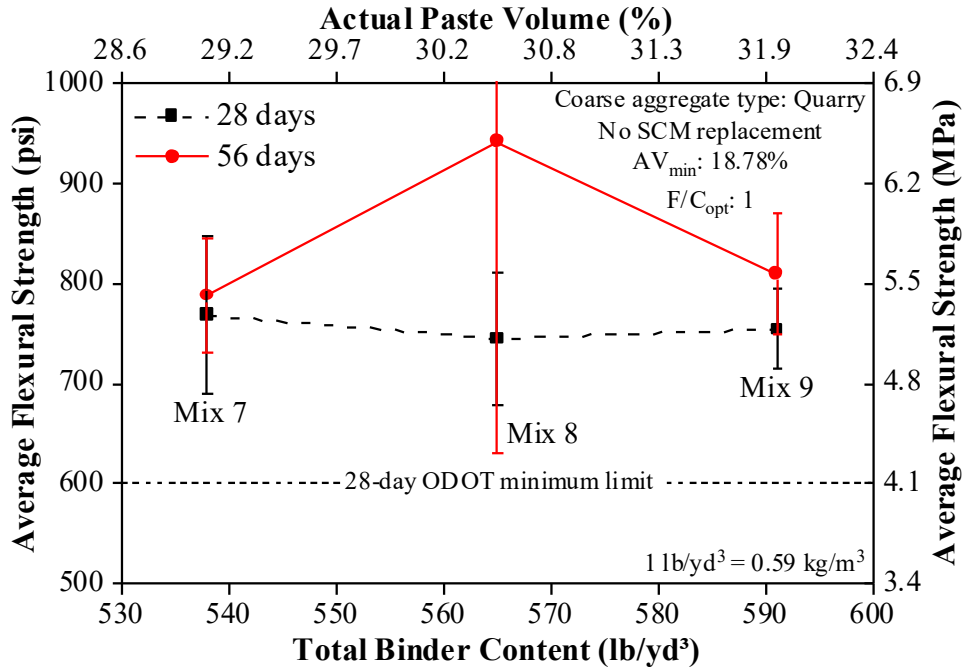


Figure 6.46: Effect of paste volume and binder content on flexural strength (Mixtures 7, 8, 9).

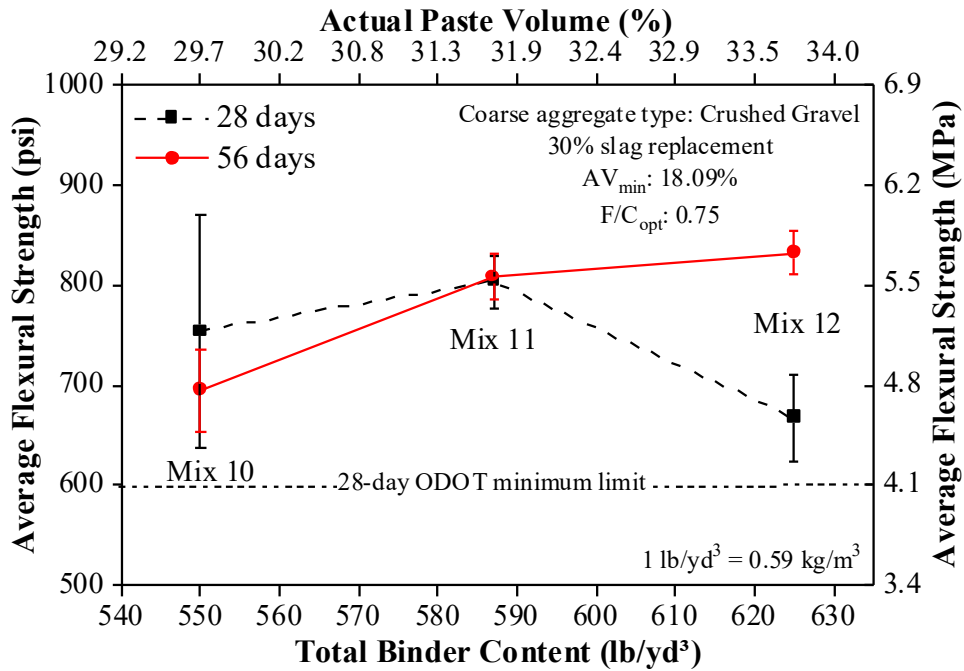


Figure 6.47: Effect of paste volume and binder content on flexural strength (Mixtures 10, 11, 12).

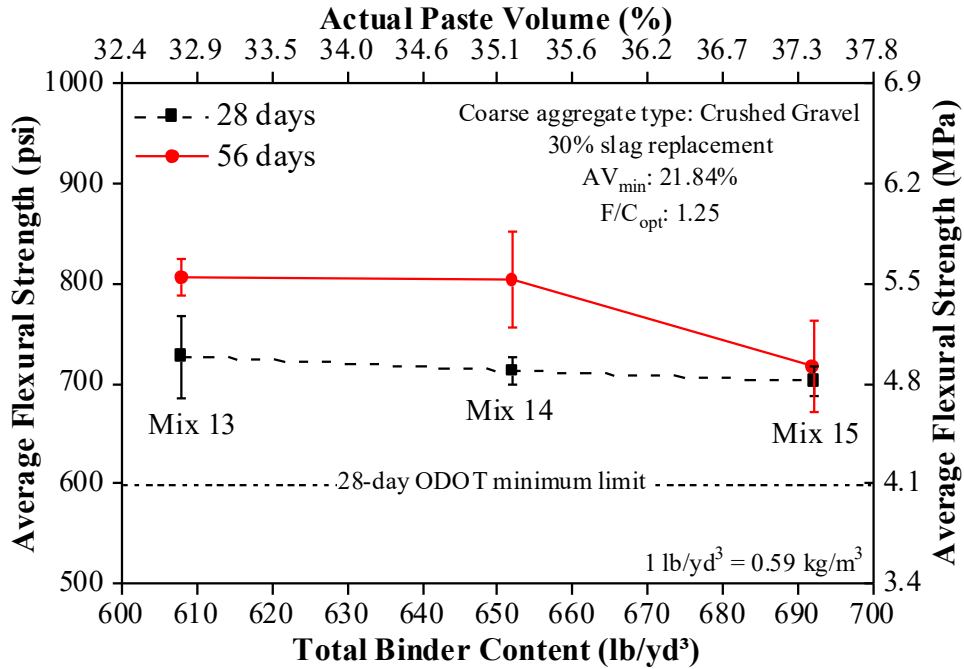


Figure 6.48: Effect of paste volume and binder content on flexural strength (Mixtures 13, 14, 15).

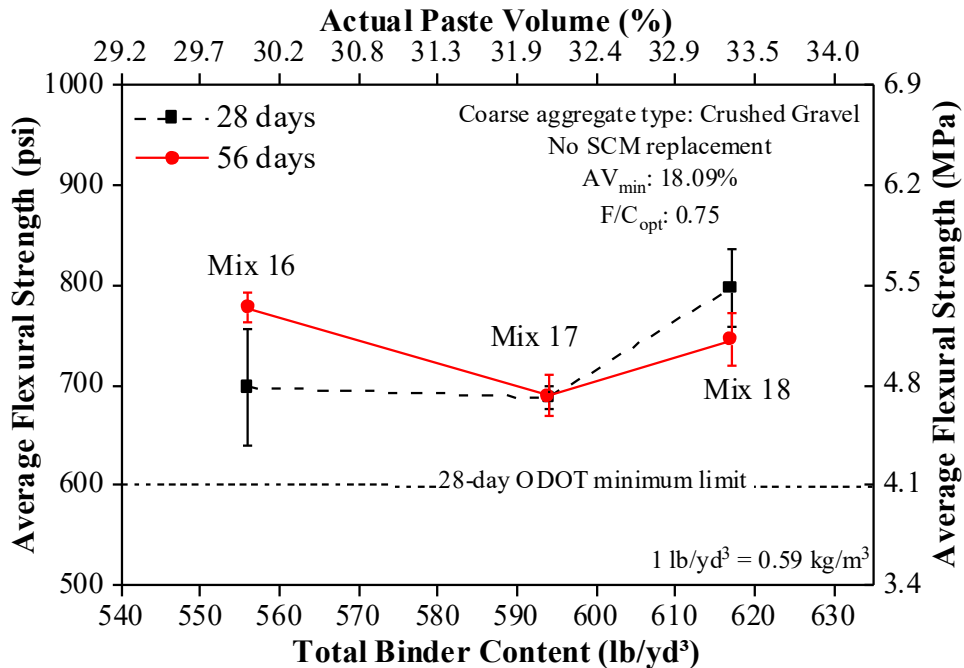


Figure 6.49: Effect of paste volume and binder content on flexural strength (Mixtures 16, 17, 18).

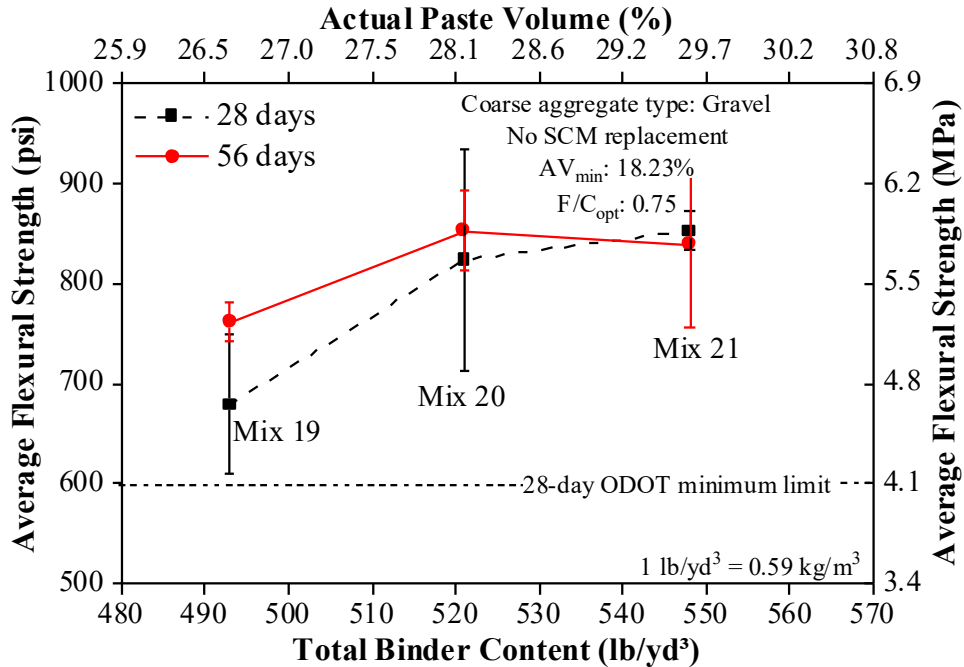


Figure 6.50: Effect of paste volume and binder content on flexural strength (Mixtures 19, 20, 21).

Table 6.9: p-values Generated from ANOVA Testing of Flexural Strength Data within Different Mixture Groups.

Mixture group	28-days	56-days
(1, 2, 3)	0.224	0.906
(4, 5, 6)	0.992	0.331
(7, 8, 9)	0.904	0.579
(10, 11, 12)	0.150	< 0.01
(13, 14, 15)	0.539	0.053
(16, 17, 18)	0.031	< 0.01
(19, 20, 21)	0.065	0.158

Figure 6.51 and Figure 6.52 show the general relationship between flexural strength values and paste volumes and binder content, at 28-days and 56-days, respectively. A comparison of these plots to Figure 6.42 and Figure 6.43 indicate that the flexural strength test outcome is less sensitive compared to compressive strength test outcome when paste volume and binder content of a mixture is varied.

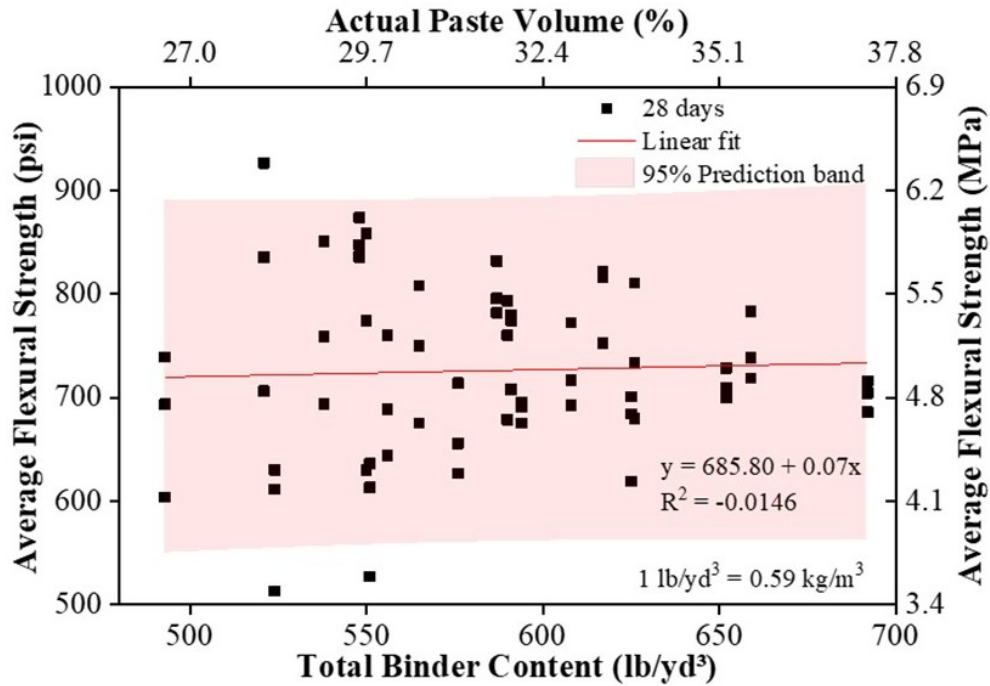


Figure 6.51: Scatter plot of 28-day flexural strength results as a function of paste volume and binder content.

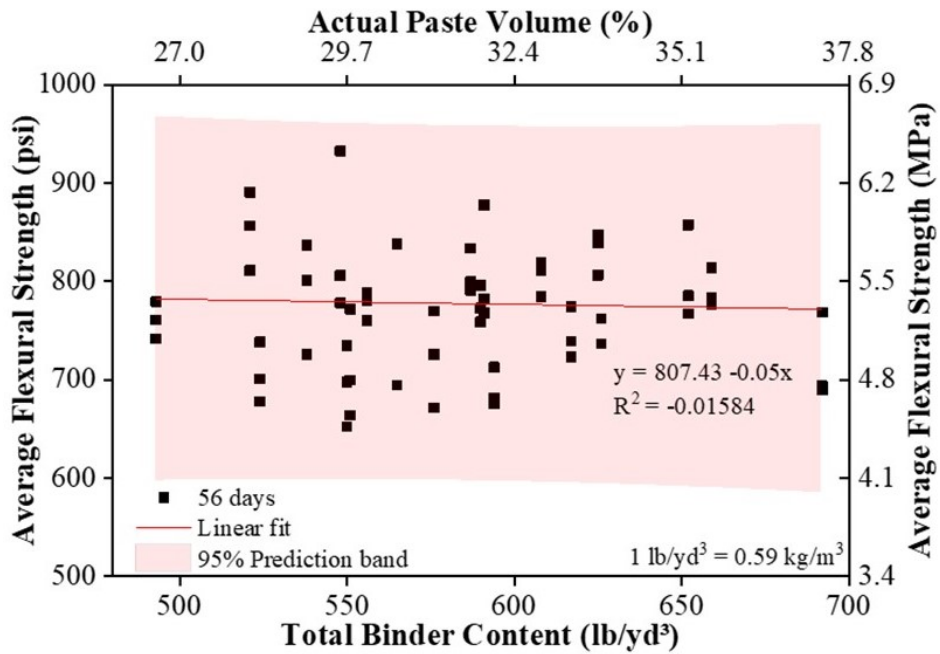


Figure 6.52: Scatter plot of 56-day flexural strength results as a function of paste volume and binder content.

6.4.2.4 Unrestrained length change

Figure 6.53 to Figure 6.59 show the drying shrinkage test results obtained from the different mixture groups as a function of paste volume and binder content. It has to be noted here that drying shrinkage was calculated based on the length change measurements at 7 and 28 days. Length change at 7 days was assumed to be the baseline and drying shrinkage, in microstrain, was calculated based on the difference in length change between 7 and 28 days. The ANOVA results obtained from testing of different data groups are shown in Table 6.10. It was initially hypothesized that an increase in paste volume would result an increase in drying shrinkage. This hypothesis was confirmed for mixture groups (7, 8, 9), (10, 11, 12), and (19, 20, 21). For certain groups of concrete mixtures made of crushed gravel, the average drying shrinkage values increased with increase in paste volume from a low to a moderate value, followed by a decrease in drying shrinkage values with increase in paste volume from a moderate to a high value. However, the variations observed in drying shrinkage values in these groups were not statistically different, indicating no significant difference in drying shrinkage with increased paste content for these specimen groups.

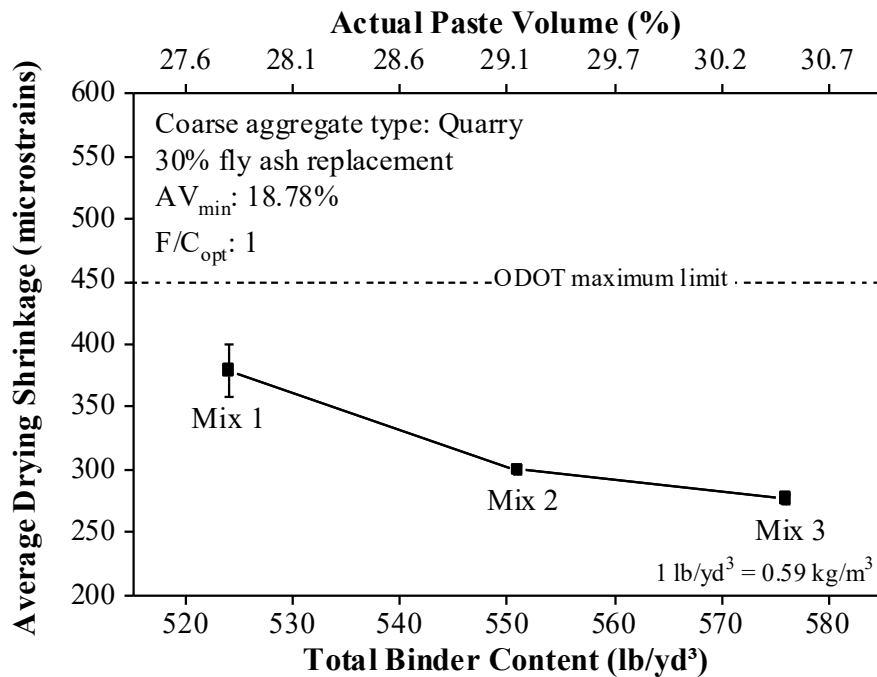


Figure 6.53: Drying shrinkage as a function of the paste volume and total binder content (Mixtures 1, 2, 3).

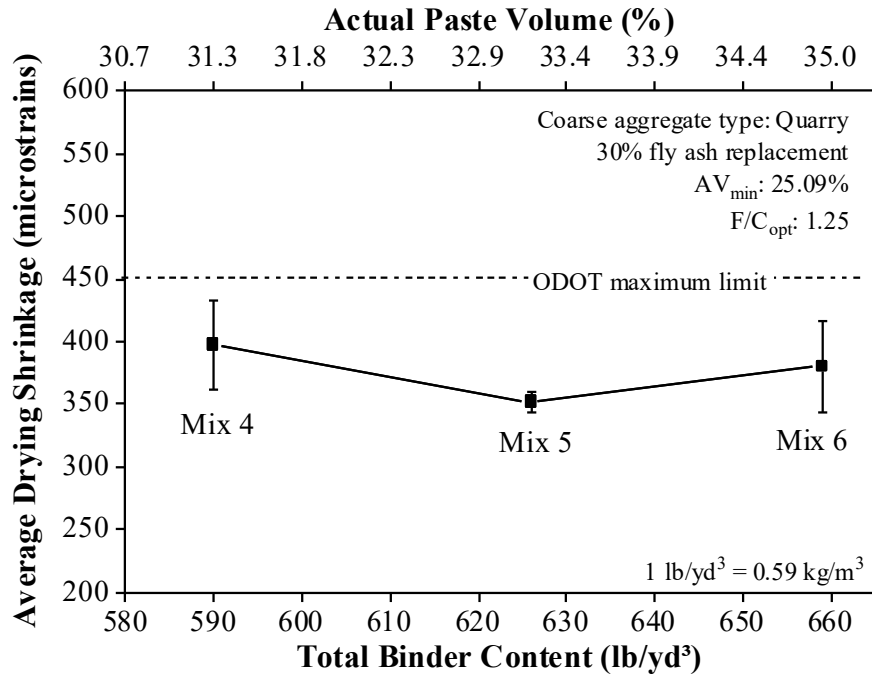


Figure 6.54: Drying shrinkage as a function of the paste volume and total binder content (Mixtures 4, 5, 6).

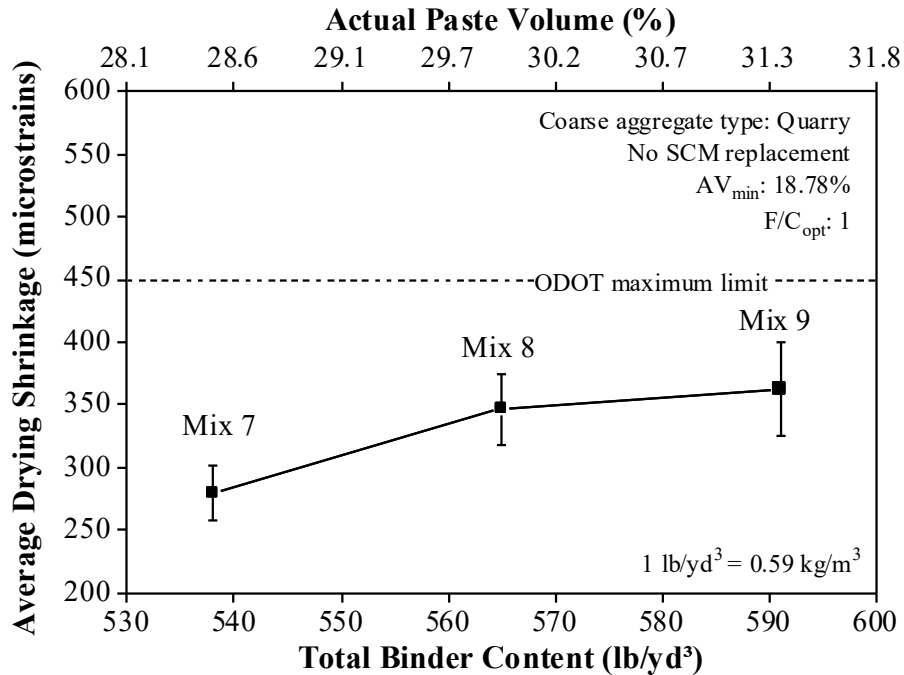


Figure 6.55: Drying shrinkage as a function of the paste volume and total binder content (Mixtures 7, 8, 9).

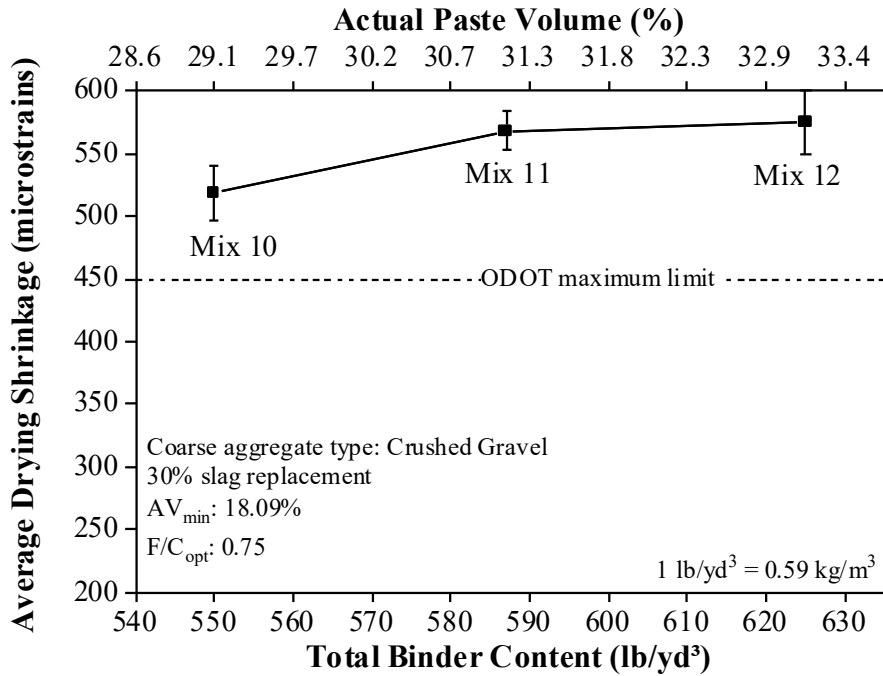


Figure 6.56: Drying shrinkage as a function of the paste volume and total binder content (Mixtures 10, 11, 12).

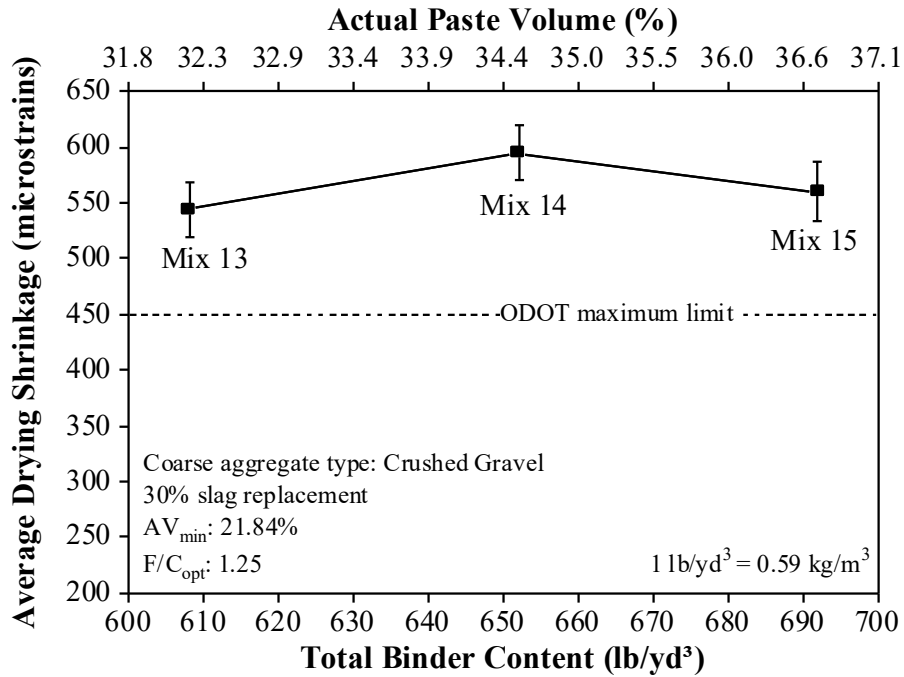


Figure 6.57: Drying shrinkage as a function of the paste volume and total binder content (Mixtures 13, 14, 15).

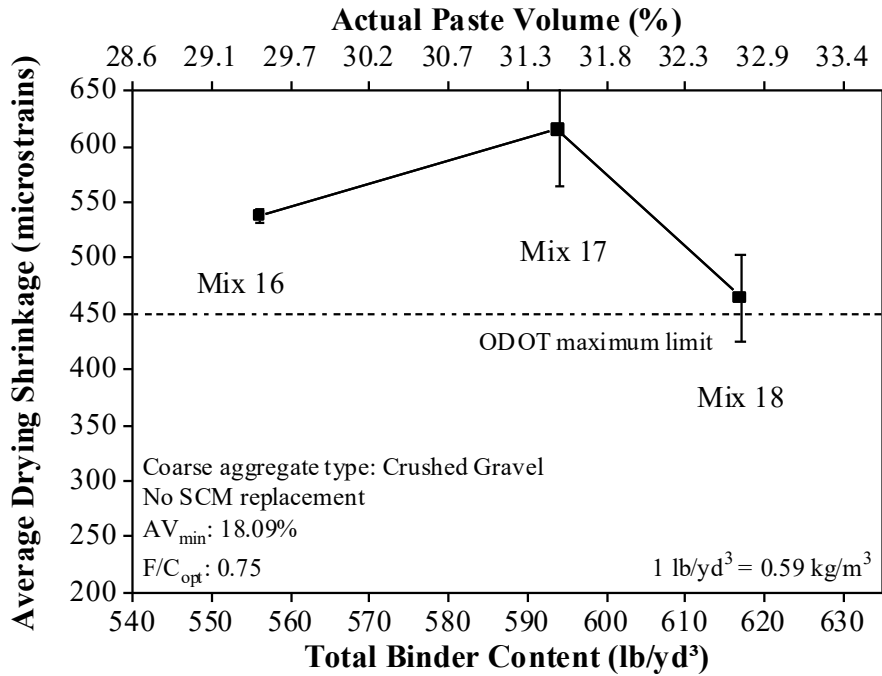


Figure 6.58: Drying shrinkage as a function of the paste volume and total binder content (Mixtures 16, 17, 18).

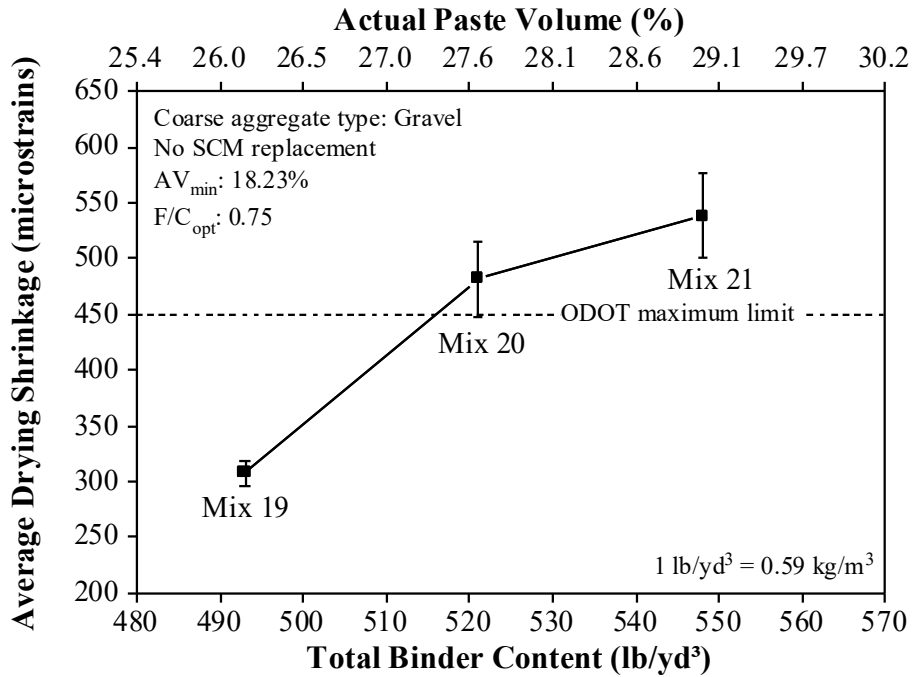


Figure 6.59: Drying shrinkage as a function of the paste volume and total binder content (Mixtures 19, 20, 21).

Table 6.10: p-values Generated from ANOVA Testing of Drying Shrinkage Data within Different Mixture Groups

Mixture group	p-value
(1, 2, 3)	< 0.01
(4, 5, 6)	0.360
(7, 8, 9)	0.069
(10, 11, 12)	0.074
(13, 14, 15)	0.197
(16, 17, 18)	0.036
(19, 20, 21)	< 0.01

Data from mixture group (1, 2, 3) indicated a decrease in mean drying shrinkage with an increase in paste volume, which was contrary to the hypothesis originally defined for the relationship between paste volume and drying shrinkage and reported in the literature. ANOVA testing also revealed significant differences in mean drying shrinkage values between mixtures 1 and 3 within this group. However, the average 28-day drying shrinkage strains for mixtures 1, 2, and 3 were below the 420-micron limit specified by AASHTO PP 84 (2020b). Because the drying shrinkage strain data for these mixtures were abnormal, mixtures 1 and 3 were evaluated for restrained shrinkage strains following modified AASHTO T 334 (2008) procedure. Results for this testing are discussed in the next section.

It has been reported that the drying shrinkage behavior of slag mixtures is dependent, among other factors, on the composition and fineness of slag, and curing duration (Tazawa, Yonekura, & Tanaka, 1989; Yuan, Lindquist, Darwin, & Browning, 2015; Zhang, Hama, & Na, 2015). Data generated in this study for slag mixtures agree with some of the experimental results reported by Zhang et al. for slag mixtures cured for 7 days. The literature indicates that an increase in curing age (7 to 28 days) will increase the resistance of slag mixtures investigated in this study for drying shrinkage. The differences in drying shrinkage strains of control, fly ash, and slag mixtures after 7-day curing observed in this study were similar to the observations made by (Yang, Wang, & Zhou, 2017). The authors attributed this behavior to the lower activity of fly ash at early ages.

6.4.2.5 Restrained shrinkage

As noted in the previous section, mixtures 1 and 3 were assessed for restrained shrinkage following modified AASHTO T 334 (2008) procedure. The modification to the method was that of the concrete ring thickness. An inner and an outer ring with radii of 6.5 in. (0.16 m) and 12 in. (0.3 m), respectively, were chosen for casting the ring specimens. This resulted in a thickness of 5.5 in. (0.14 m) instead of 3 in. (0.07 m) as required by the AASHTO T 334 (2008) standard. This was modified because of the 1.5 in. (37 mm) NMSA used in this study. The objective of this testing was to investigate whether the concrete paste volume significantly influenced the restrained shrinkage strain. Two rings were fabricated and monitored for a period of 28 days for restrained shrinkage strains and cracking.

Restrained shrinkage strains for mixtures 1 and 3 are shown in Figure 6.60 and Figure 6.61, respectively. Concrete rings from both mixtures did not exhibit any cracking during the test duration. The average 28-day restrained shrinkage strain observed in mixtures 1 and 3 were 52.8 and 70.9 microstrain, respectively. These data indicate that concrete mixtures made with higher paste volumes can exhibit larger restrained shrinkage strains compared to mixtures with lower paste volumes. These preliminary results indicate that assessing the effects of paste volume on restrained concrete shrinkage via the ring shrinkage test could be more reliable compared to unrestrained length change test. However, more research is needed to confirm this.

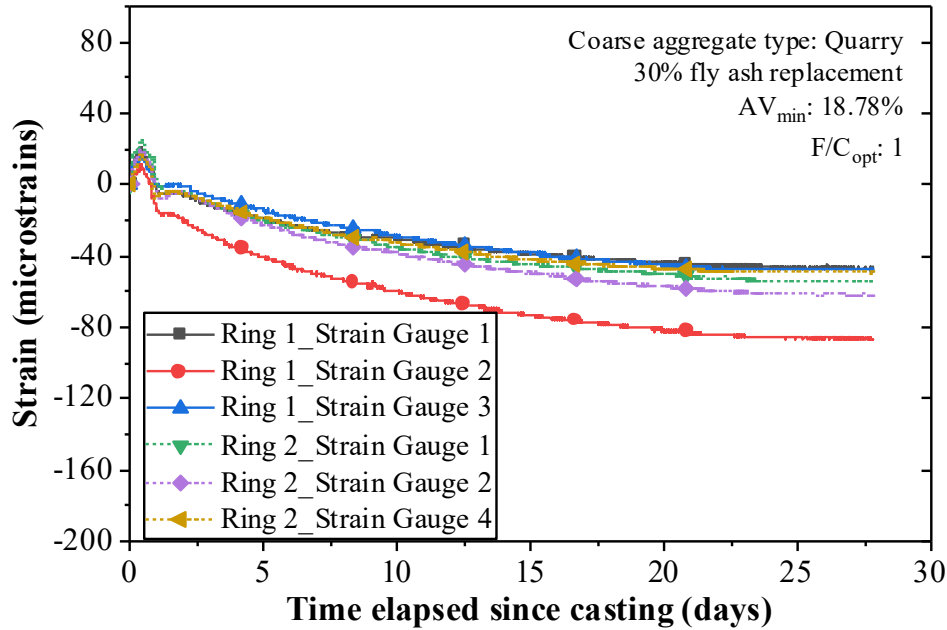


Figure 6.60: Restrained shrinkage strain for mixture 1.

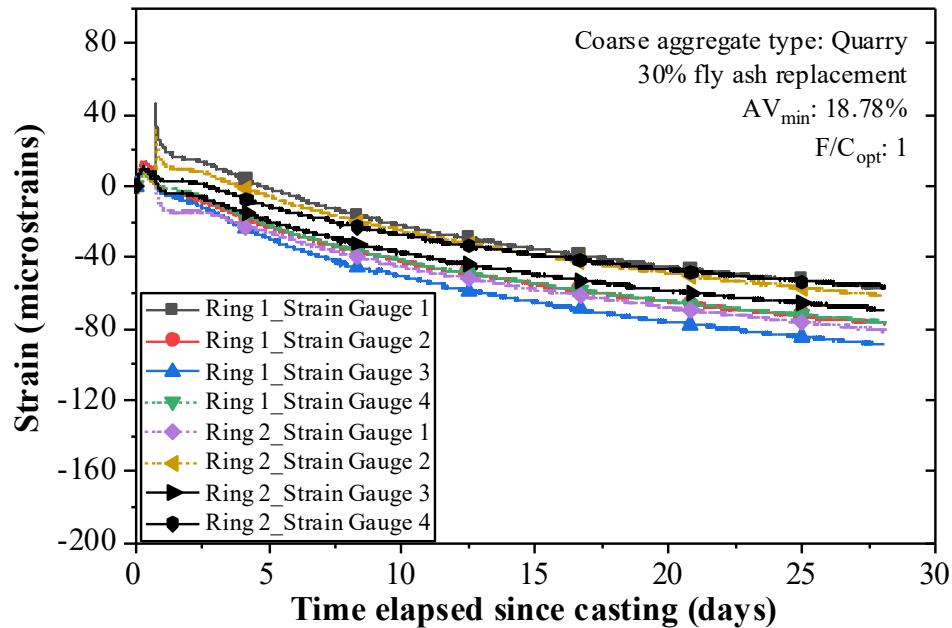


Figure 6.61: Restrained shrinkage strain for mixture 3.

6.4.3 Effect of binder type

6.4.3.1 Water reducer dosage

Figure 6.62 to Figure 6.63 show the effects of different binder types on the requirement of water-reducer dosages. The mixture number associated with the data points are adjacent to the data and shown in parentheses. Irrespective of the amount of paste volume, inclusion of fly ash or slag or a combination of both was found to reduce the demand for water-reducer in achieving a workability consistent with that of a typical slip-form paving mixture. The beneficial effects of fly ash or slag in improving concrete workability are well documented (Matthes et al., 2018; Thomas, 2007). The difference between the WR dosages of concrete mixtures with and without fly ash has been found to increase with increasing paste volume, as shown in Figure 6.64. This trend, however, was not clearly observed between the control and slag mixtures. It should be noted that mixture 18 failed to meet edge-slump requirements, due to high water-reducer dosage adopted during concrete batching.

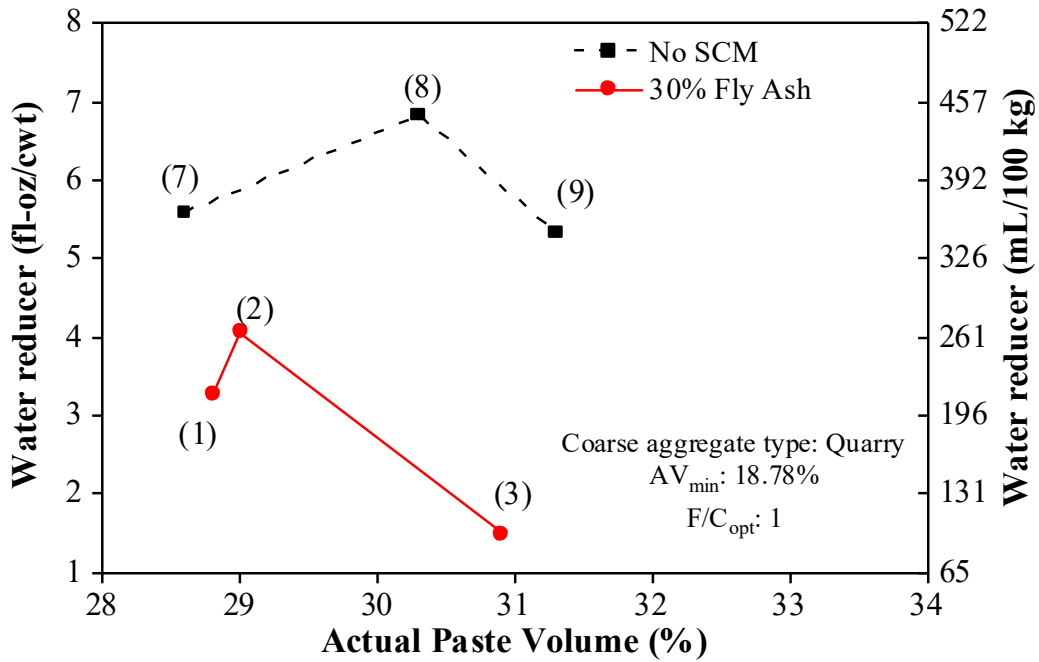


Figure 6.62: Effect of binder type on water-reducer dosage (Mixtures 1, 2, 3, 7, 8, 9).

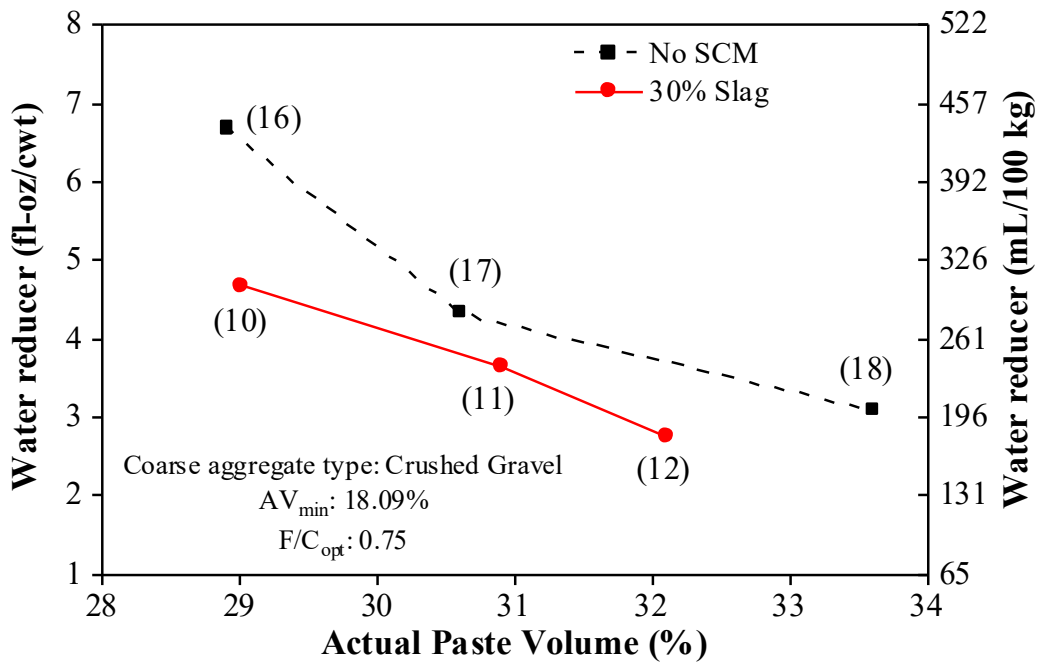


Figure 6.63: Effect of binder type on water-reducer dosage (Mixtures 10, 11, 12, 16, 17, 18).

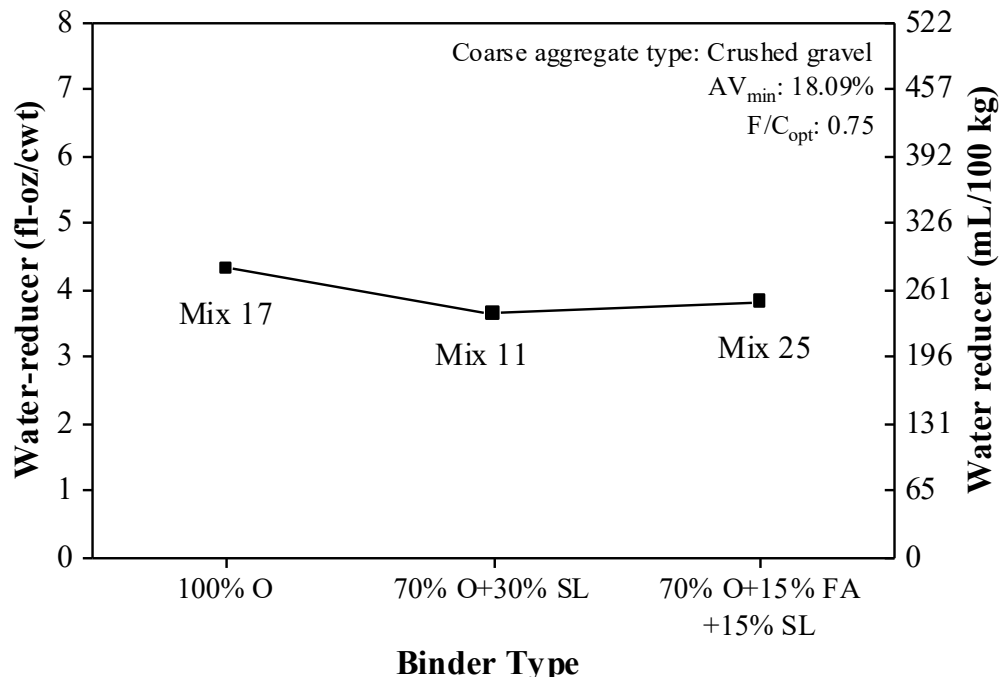


Figure 6.64: Effect of binder type on water-reducer dosage (Mixtures 17, 11, 25).

6.4.3.2 Compressive strength

Figure 6.65 to Figure 6.68 show the effects of different binder types on compressive strength results. As expected, the rate of strength gain in fly ash mixtures was comparatively lower than the strength gain in slag mixtures. Irrespective of the paste volume, concrete mixtures with fly ash were found to have lower mean strength values when compared to concrete mixtures without fly ash at both 28- and 56-days. However, it should be noted that both control and fly ash mixtures met the ODOT minimum limit on compressive strength. The relationship between the compressive strength of mixtures with and without SCM was influenced by paste volume in this study, as shown in Figure 6.69. This effect is likely skewed due to the significant differences in measured air contents of mixtures at high paste volume (i.e., 7% air for 0% slag mixture versus 4.8% air for 30% slag mixture), which in turn could have affected the compressive strength values. Data shown in Figure 6.69 clearly exhibit significant differences in compressive strength values between binary and ternary slag mixtures at 28 days, likely due to the presence of fly ash in latter. This difference, however, reduced significantly at 56 days likely due to long-term strength gain associated with fly ash mixtures.

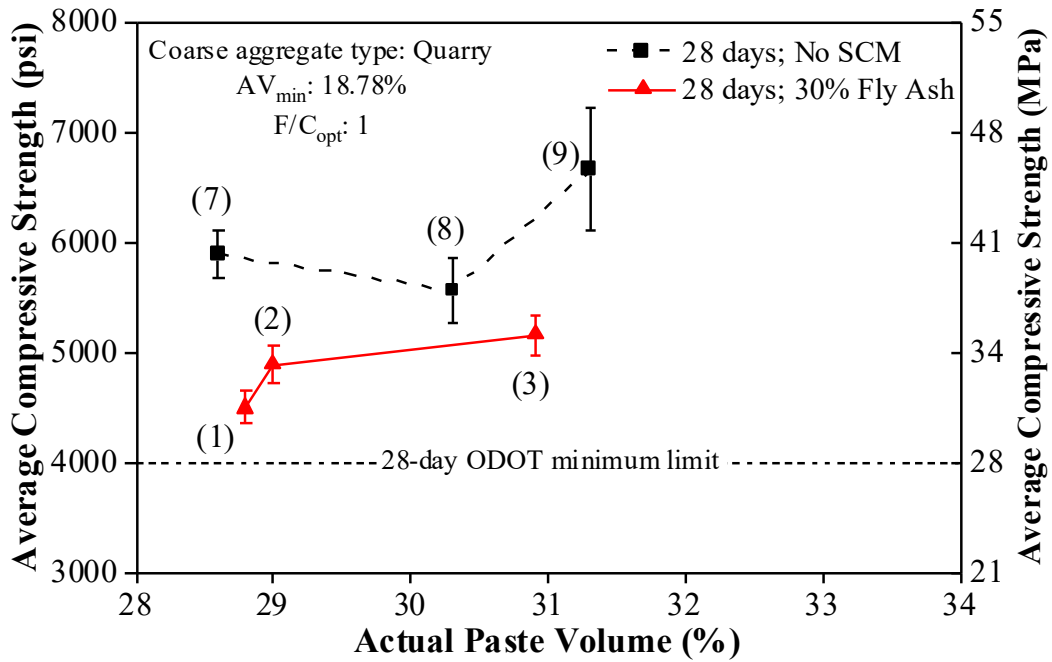


Figure 6.65: Effect of binder type on 28-day compressive strength (Mixtures 1, 2, 3, 7, 8, 9).

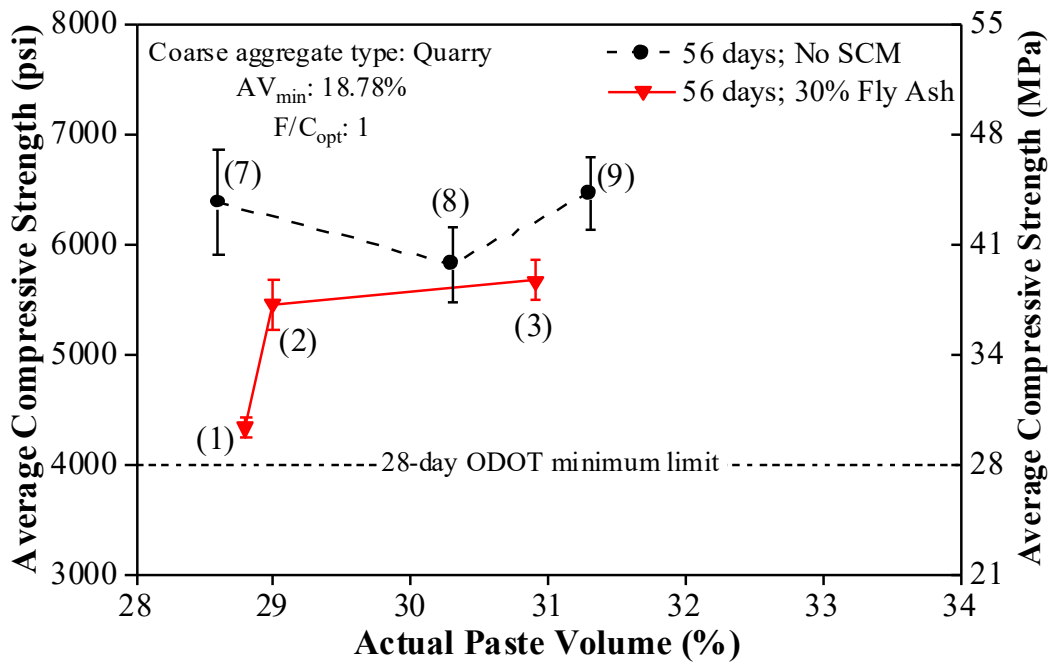


Figure 6.66: Effect of binder type on 56-day compressive strength (Mixtures 1, 2, 3, 7, 8, 9).

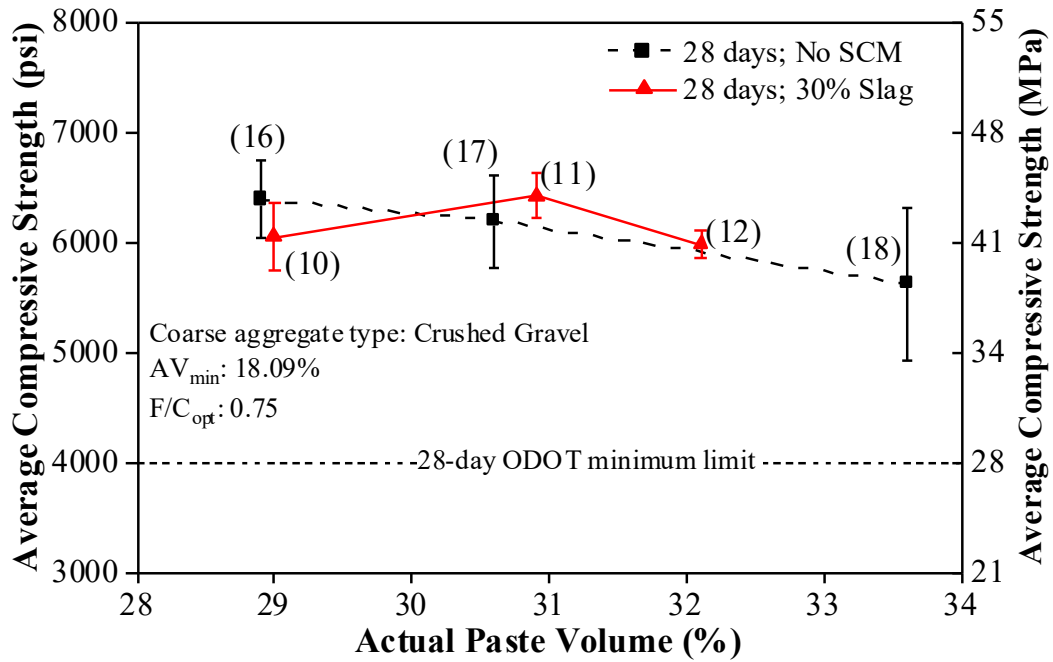


Figure 6.67: Effect of binder type on 28-day compressive strength (Mixtures 10, 11, 12, 16, 17, 18).

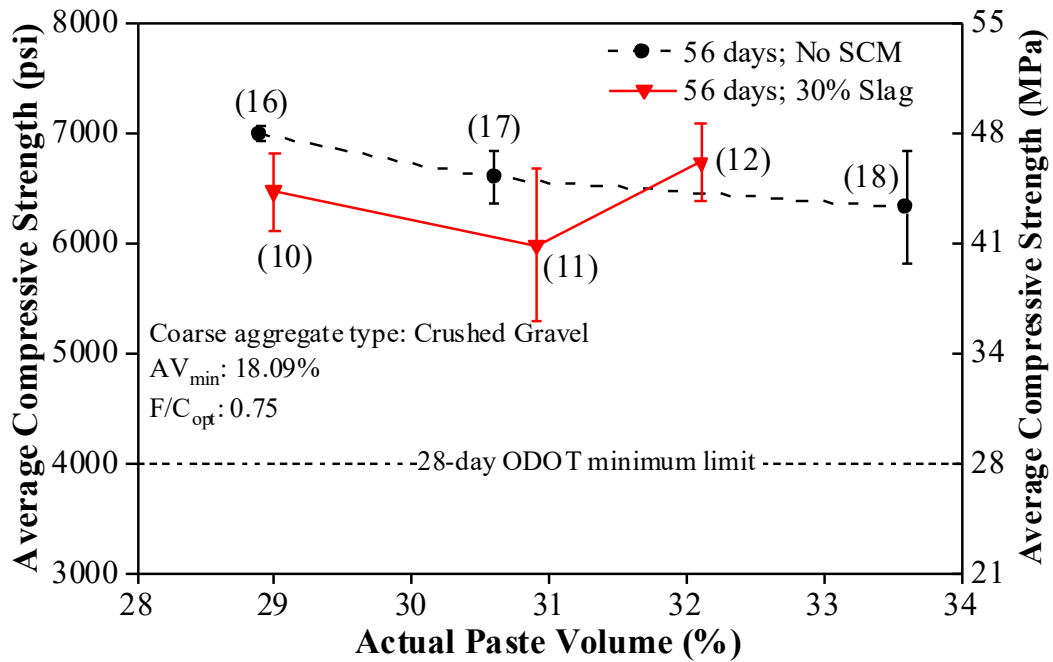


Figure 6.68: Effect of binder type on 56-day compressive strength (Mixtures 10, 11, 12, 16, 17, 18).

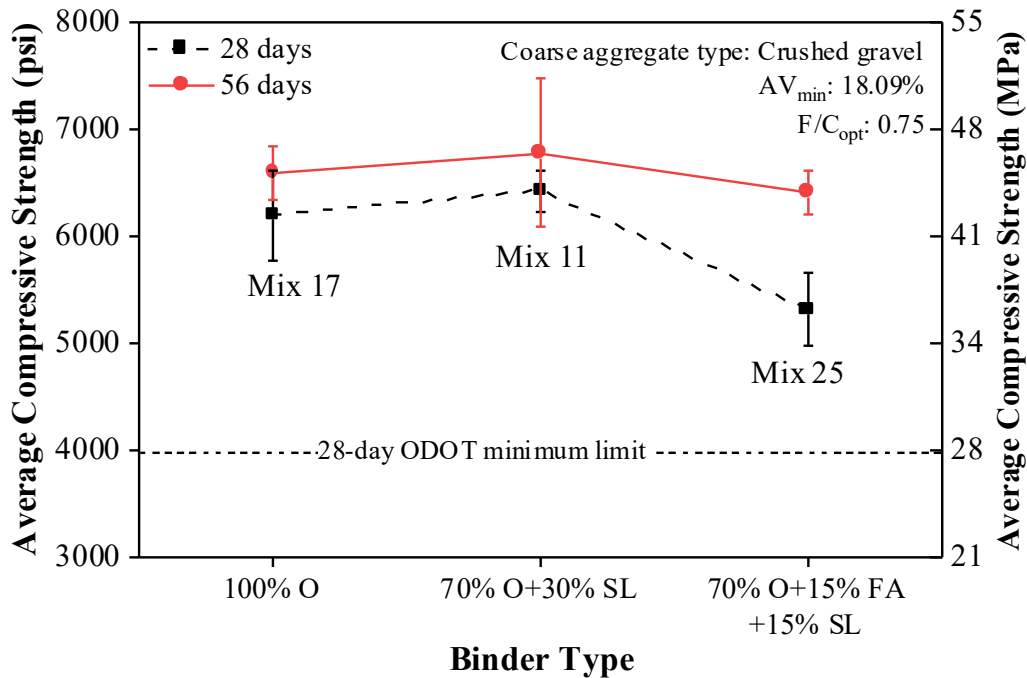


Figure 6.69: Effect of binder type on compressive strength (Mixtures 17, 11, 25).

6.4.3.3 Flexural strength

Figure 6.70 to Figure 6.73 show the effects of different binder types on flexural strength results. The relationship trends observed between the flexural strength data and binder type were similar to the trends observed in the compressive strength data shown in the previous section. Irrespective of paste volume, flexural strengths of mixtures with fly ash were lower compared to flexural strengths of control mixtures without fly ash. For mixtures with slag, flexural strengths were comparable to the strength of control mixtures at low paste volumes. However, strength gain associated with slag mixtures at 56-days was found to be greater than the control mixtures at moderate and high paste volumes. For crushed gravel mixtures with moderate paste volume, data indicated little or no flexural strength gain from 28- to 56-days for mixtures without SCMs and 30% slag, whereas the strength gain observed in ternary mixture (15% ash and 15% slag) with increasing age was determined to be significant. The 56-day results for 30% slag mixtures were comparable to the results from ternary mixtures at moderate paste volume.

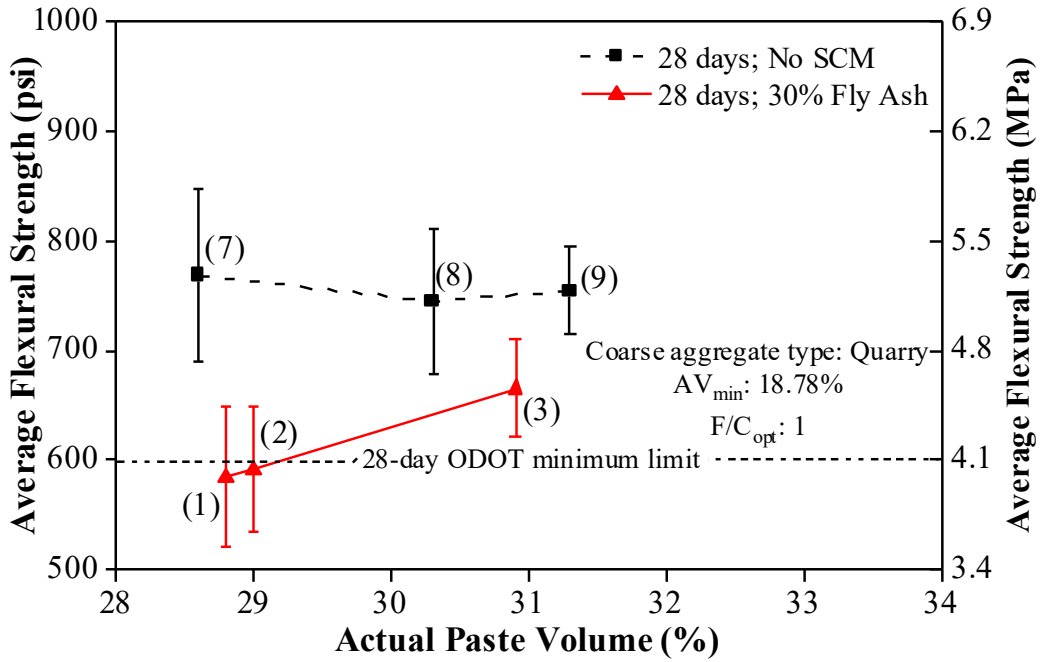


Figure 6.70: Effect of binder type on 28-day flexural strength (Mixtures 1, 2, 3, 7, 8, 9).

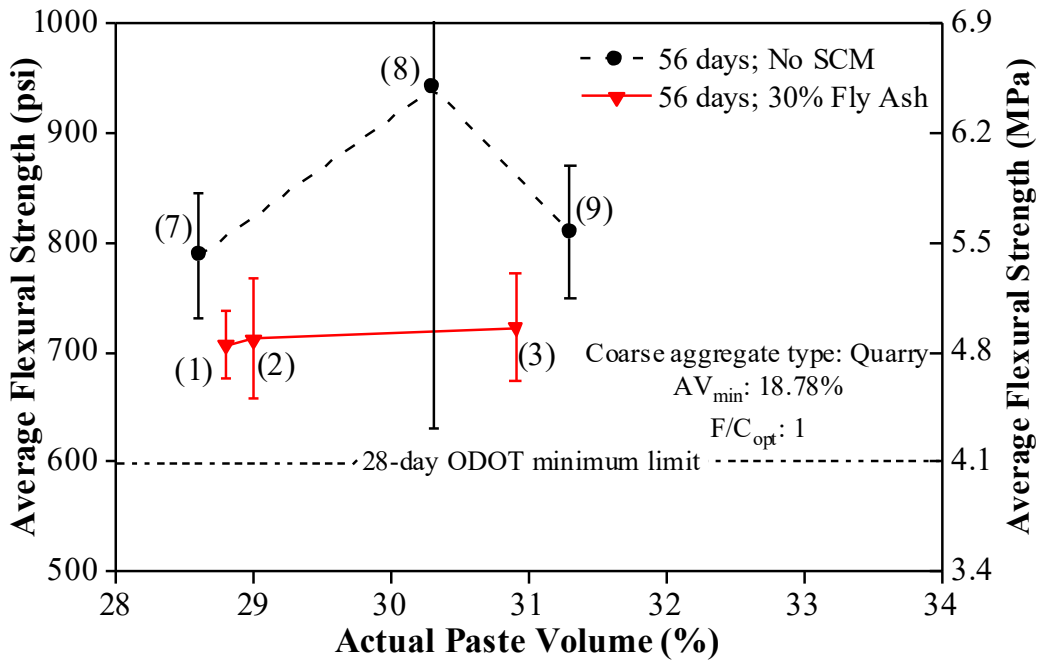


Figure 6.71: Effect of binder type on 56-day flexural strength (Mixtures 1, 2, 3, 7, 8, 9).

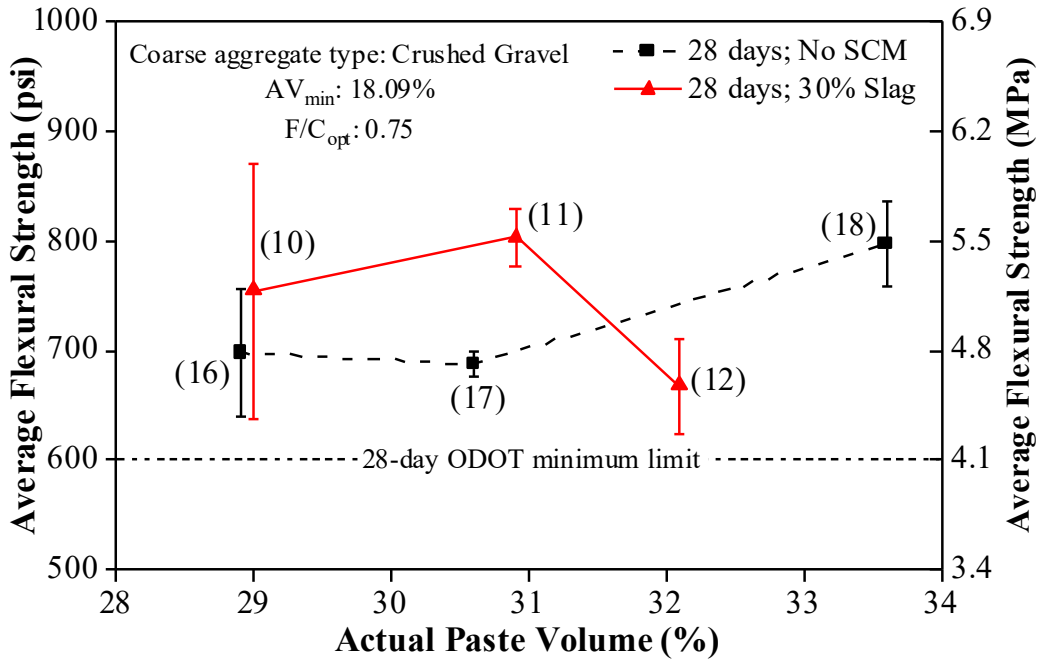


Figure 6.72: Effect of binder type on 28-day flexural strength (Mixtures 10, 11, 12, 16, 17, 18).

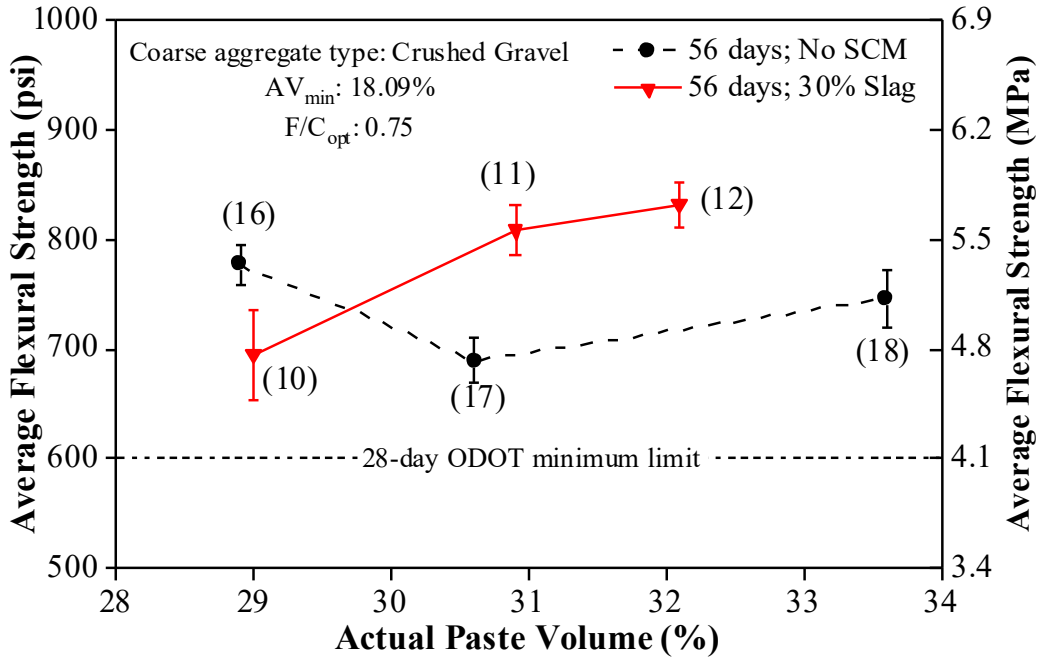


Figure 6.73: Effect of binder type on 56-day flexural strength (Mixtures 10, 11, 12, 16, 17, 18).

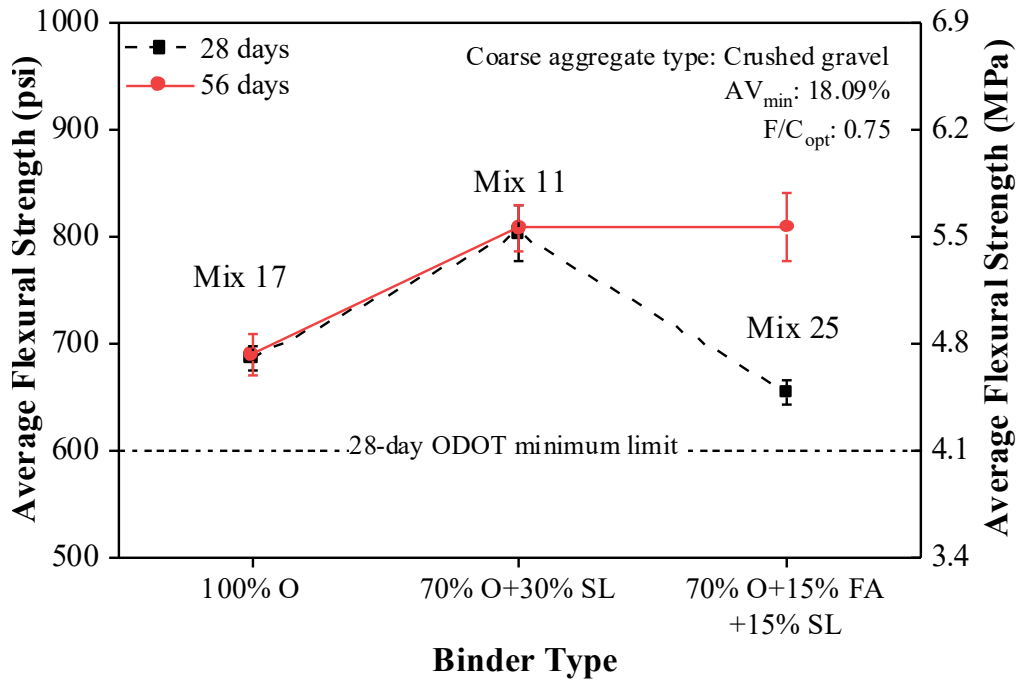


Figure 6.74: Effect of binder type on flexural strength (Mixtures 17, 11, 25).

6.4.3.4 Drying Shrinkage

Figure 6.75 to Figure 6.77 show the effects of different binder types on drying shrinkage results. Data indicates that addition of SCMs generally help in minimizing the shrinkage in most cases. The fly ash mixture at low paste volume and the slag mixture at high paste volume did not exhibit reduced shrinkage when compared to their respective control mixtures. While further testing is needed to investigate this outcome, data does show that the reduction in shrinkage is more significant in fly ash mixtures when compared to slag mixtures at 30% replacement level for the materials tested in this study. Data also indicates that shrinkage reduction is more pronounced when ternary mixtures are adopted over binary mixtures or control mixtures without SCMs.

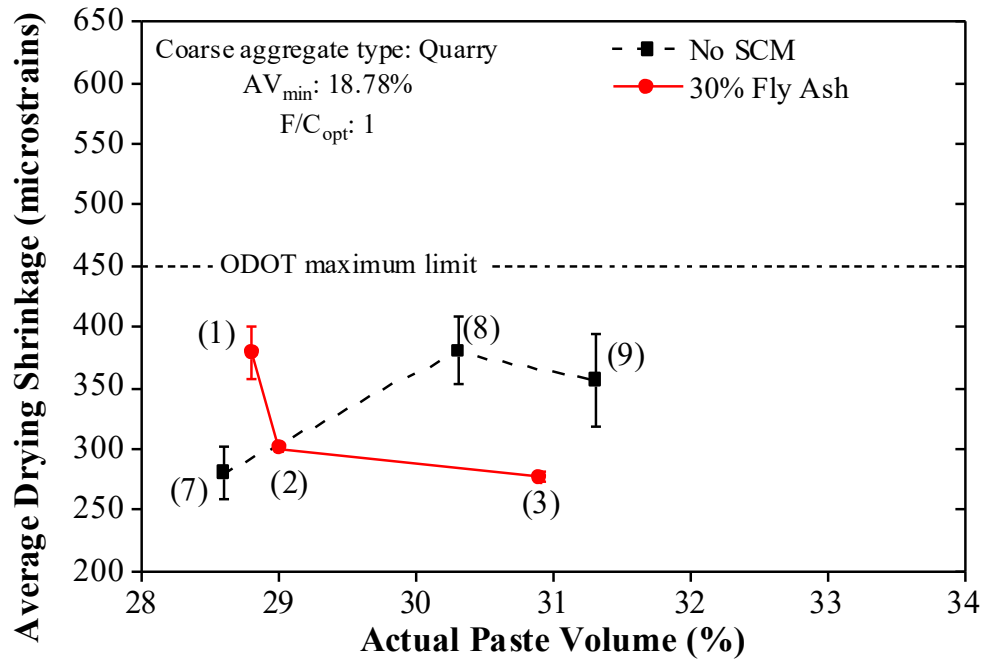


Figure 6.75: Effect of binder type on drying shrinkage (Mixtures 1, 2, 3, 7, 8, 9).

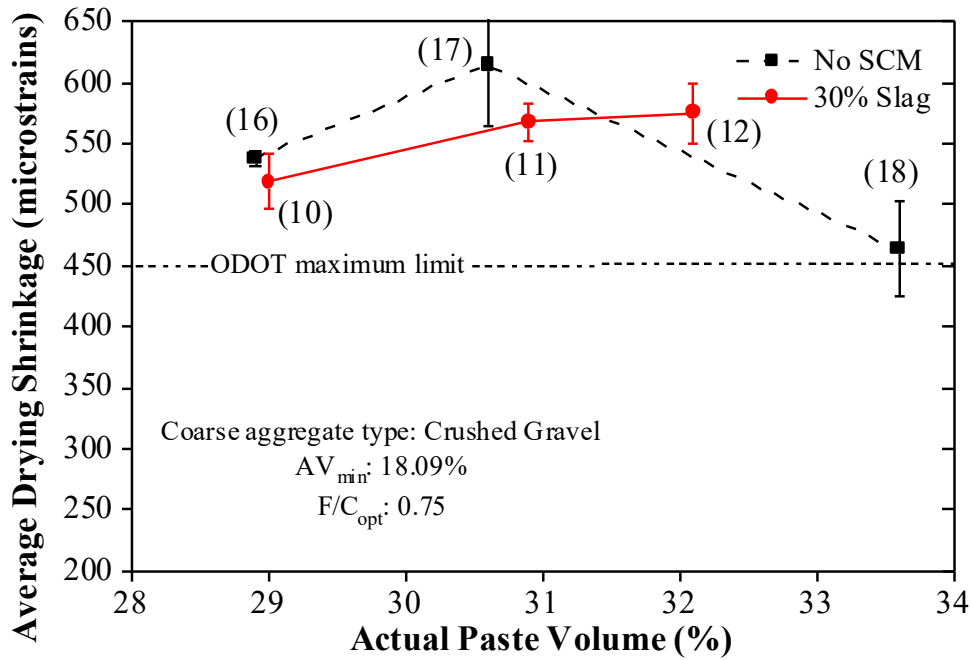


Figure 6.76: Effect of binder type on drying shrinkage (Mixtures 10, 11, 12, 16, 17, 18).

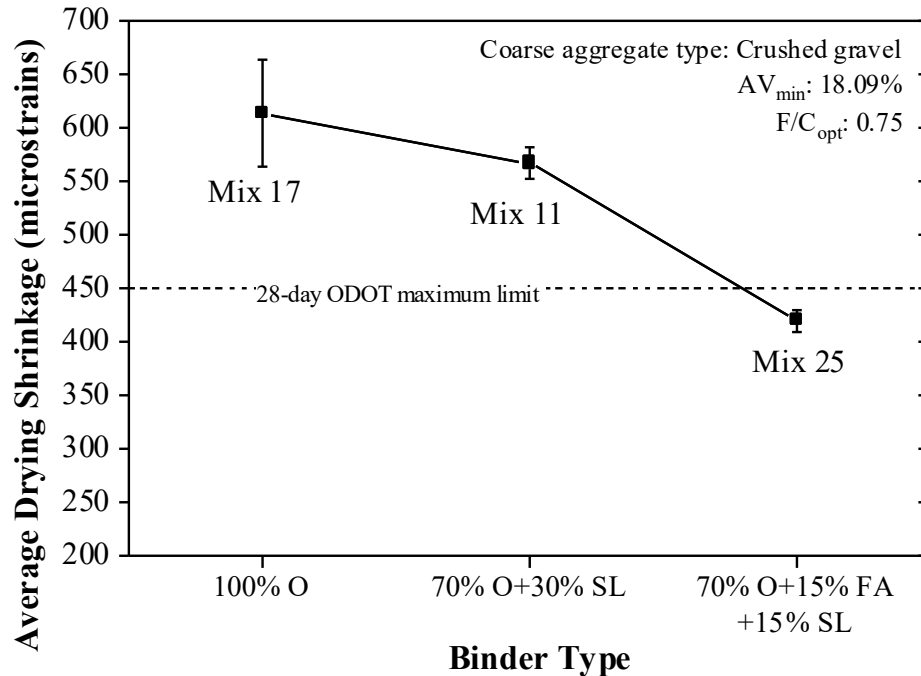


Figure 6.77: Effect of binder type on drying shrinkage (Mixtures 17, 11, 25).

6.4.4 Effect of w/cm

6.4.4.1 Water reducer dosage

Figure 6.78 shows the influence of w/cm on WR dosage requirement. Because one purpose of a WR is to reduce the water demand of concrete mixture, a decrease in w/cm would be expected to increase the dosage requirement of the WR. This trend was observed for mixtures investigated in this study.

Note that mixture 23 (w/cm = 0.44) did not meet edge-slump requirements, although the average measured edge-slump (0.31 in. (0.78 cm)) was close to the set limit value (0.25 in. (0.64 cm)). It is likely that this mixture will pass edge-slump requirements at a lower dosage of WR. However, this was not investigated and the batched concrete that did not meet edge-slump requirement was used for fabrication and testing.

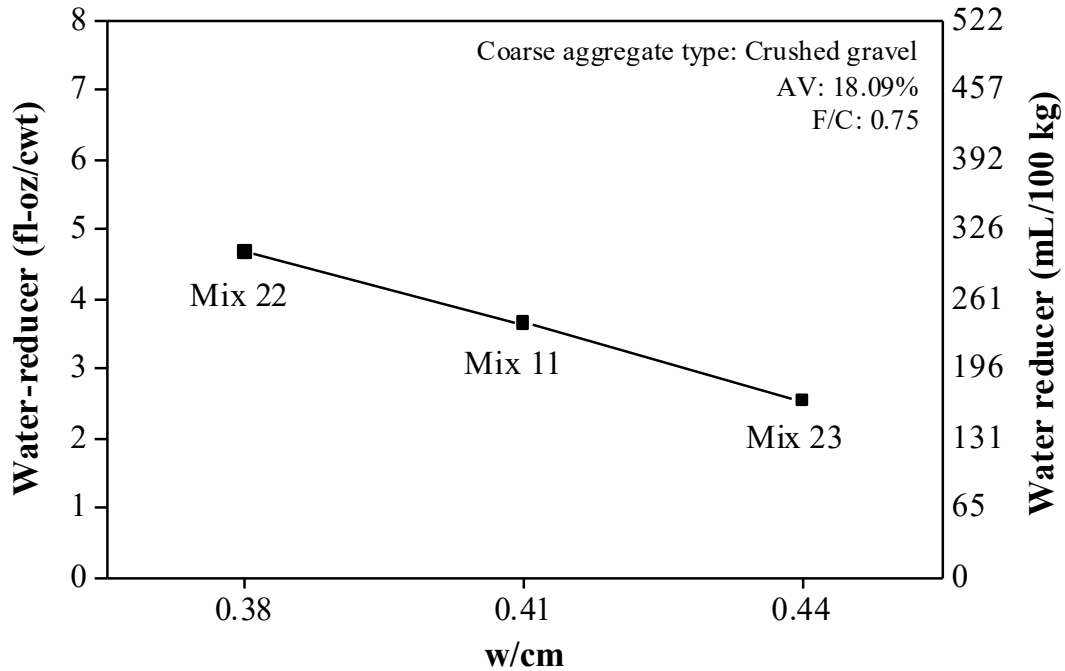


Figure 6.78: Effect of w/cm on water-reducer dosage (Mixtures 22, 11, 23).

6.4.4.2 Compressive and flexural strength

Figure 6.79 and Figure 6.80 show the effects of w/cm on compressive and flexural strength results, respectively. An increase in w/cm is expected to lower these strengths, which has been observed for the mixtures investigated in this study.

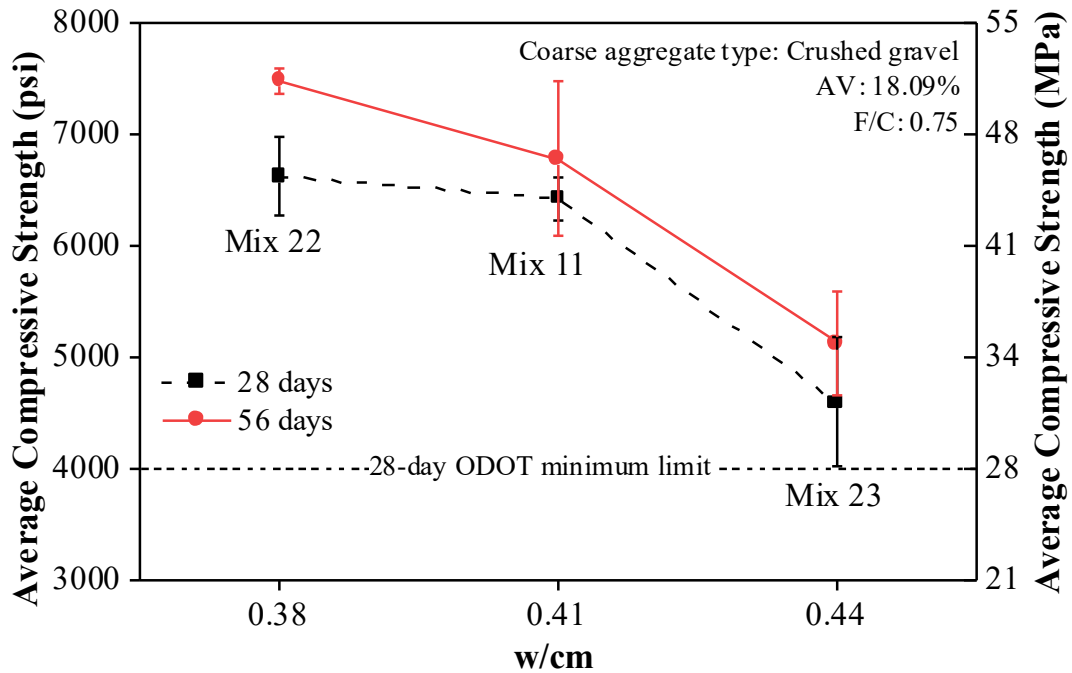


Figure 6.79: Effect of w/cm on compressive strength results (Mixtures 22, 11, 23).

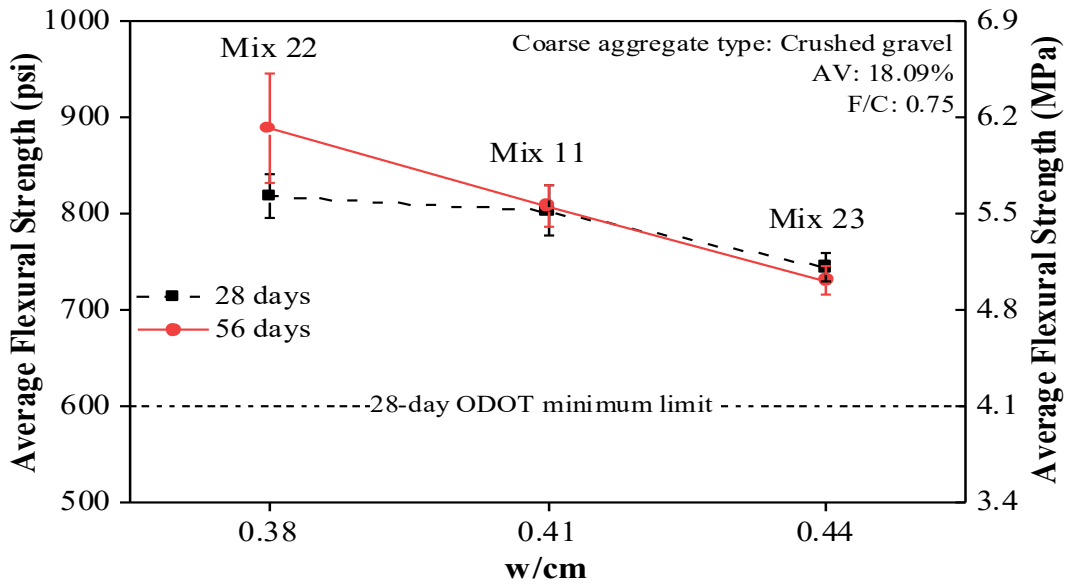


Figure 6.80: Effect of w/cm on flexural strength results (Mixtures 22, 11, 23).

6.4.4.3 Drying shrinkage

Figure 6.81 shows the effect of w/cm on drying shrinkage results. As expected, the mean drying shrinkage strain increased with increase in w/cm.

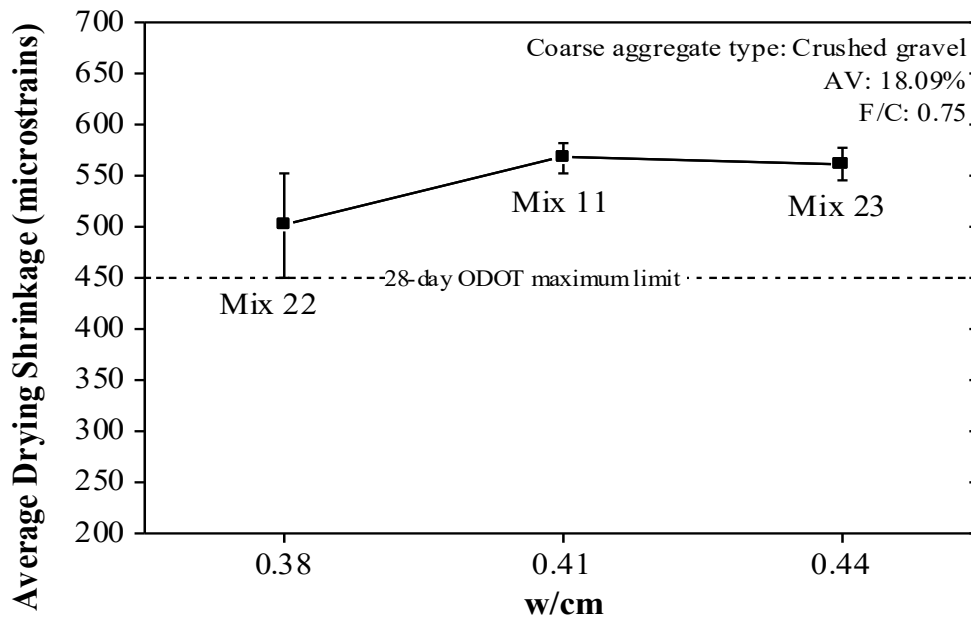


Figure 6.81: Effect of w/cm on drying shrinkage results (Mixtures 22, 11, 23).

6.4.4.4 Durability factor

Freeze-thaw testing was performed on select mixtures in accordance with the AASHTO T 161 (2017e) standards. Mixtures 10, 11, 12, 16, 17 and 18 were selected for this

assessment. The specimens were subjected to 300 freeze-thaw (FT) cycles and the transverse frequency was measured at the end of each 36th cycle. The durability factor was determined based on the formula provided in the AASHTO T 161 (2017e) standard. Results are shown in Figure 6.82 and Figure 6.83.

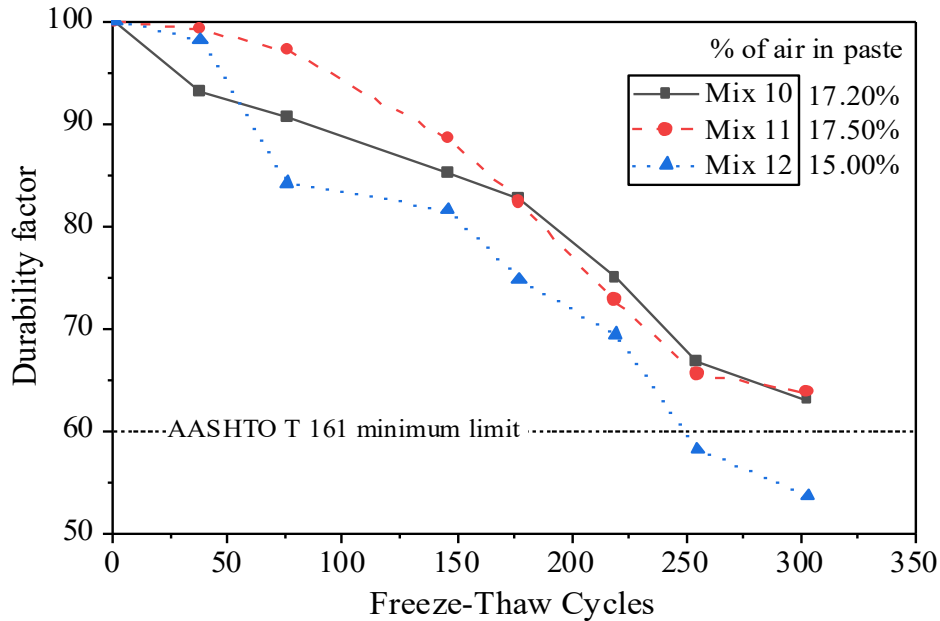


Figure 6.82: Durability factor of specimens subjected to 300 FT cycles (Mixtures 10, 11, 12).

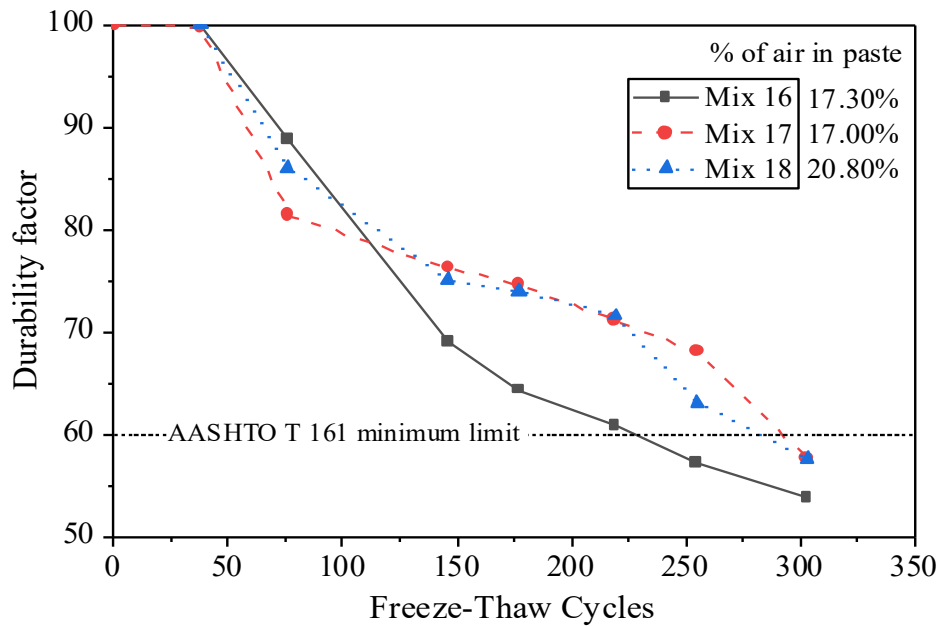


Figure 6.83: Durability factor of specimens subjected to 300 FT cycles (Mixtures 16, 17, 18).

The durability factor of four of the six mixtures dropped below 60 during the testing. As already reported, gradation and the amount of sand can have a substantial impact on the effectiveness of the air-entraining admixture and the measured air content (Bloem & Walker, 1964; Du & Folliard, 2005). As noted earlier, air content alone does not provide a complete characterization of the freeze-thaw durability of a concrete mixture. Air bubble size and spacing is a significant factor, but this was not evaluated in this research. The literature shows that, for the range of plastic air contents observed in this study, the durability factor values would typically be above 80 at the end of 300 FT cycles (Tanesi & Meininger, 2007). However, the influence of gradation and sand content on freeze-thaw performance and assessing air-bubble size and spacing was beyond the scope of this research. Additional research should be performed to assess the influence of these variables for materials available in Oregon.

6.4.4.5 Box Test

Edge slump was measured for all the mixtures using the Box Test. This test was developed as an alternative to the traditional slump test to measure the workability of slip-formed concrete pavements. Figure 6.84 shows the edge slump values as a function of the total binder content for all the mixtures considered in the study. Results indicate that on average, the edge slump increases with increasing binder content (or paste volume). However, the R^2 (goodness of fit) value associated with the linear fit line indicates that there is no statistically significant correlation between the total binder content and the edge slump values measured. It must be noted that data from various mixtures are shown in the figure and other factors, such as coarse aggregate type and gradation, water reducer dosage, SCM replacement, and w/cm are masked in this figure. There is insufficient data to statistically assess individual mixtures.

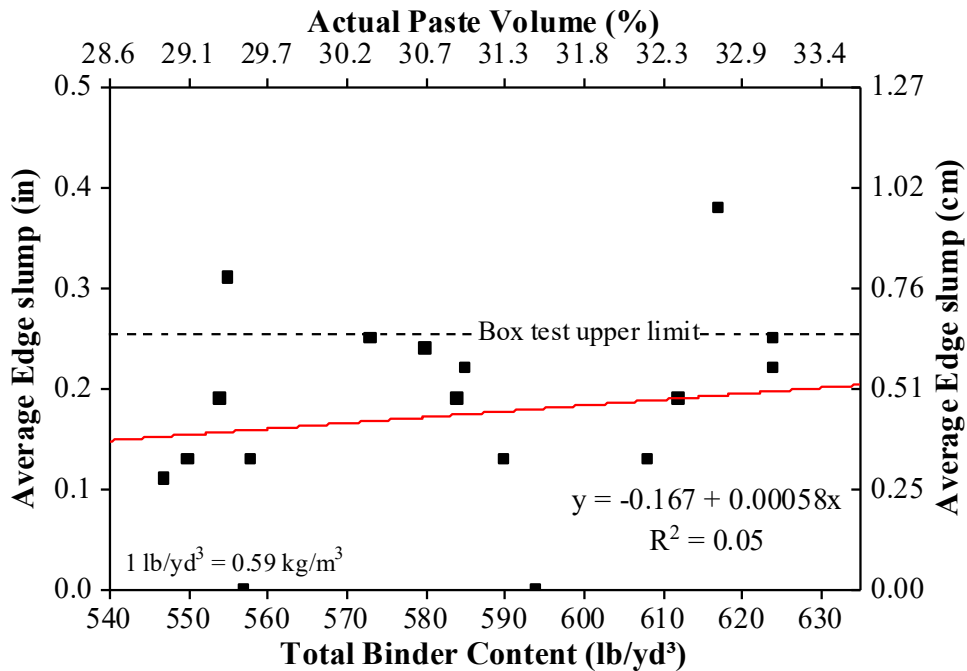


Figure 6.84: Edge slump versus binder content.

7.0 CONCLUSIONS, RECOMMENDATIONS, AND NEEDED RESEARCH

A sustainable, durable, constructible, and economical concrete can provide long-lasting pavements for Oregonians. The objective of this research program is to develop a concrete mixture proportioning method that can minimize paste content while also ensuring performance of this concrete. The premise of the new mixture proportioning method is that the required paste content for a workable concrete is dependent on the aggregates used in that concrete, and more specifically the void content of that aggregate. If the voids in the aggregate can be minimized, the paste content of the concrete, and therefore the OPC, can be minimized. This research clearly shows that the required paste content to achieve a low slump concrete for paving is dependent on aggregate void content. Minimizing the OPC can improve performance, reduce the carbon footprint, and improve economics. To identify the minimum void content of the aggregate, the aggregate must be evaluated.

The new proportioning method includes 7 steps as follows:

1. Characterization of the coarse and fine aggregates.
2. Conducting AASHTO T 19M (2014aq) test on different combined samples of coarse and fine aggregates and identifying the fine to coarse aggregate mass ratio values, F/C_{opt} , that results in the lowest aggregate void content. AV_{min} .
3. Determining whether the optimized combined gradation meets the project specification requirements or gaining approval of the out-of-specification gradation.
4. Determining a range of paste volumes for conducting trial mixtures. The total paste volume is dependent on aggregate type and FA/CA and is reported as the paste volume to aggregate void volume (PV/AV).
5. Determining the water to cementitious material ratio (w/cm) value and the type of binder required for meeting the specified prescriptive or performance requirements for concrete.
6. Determining the individual mass proportions of water, cement, SCMs, and the coarse and fine aggregates.
7. Batching trial mixtures using the estimated mass proportions and identifying a mixture that meets the requirements of the project.

The average AV_{min} of the aggregate gradations assessed in this research was 20.7%. The minimum AV_{min} was 17.57% and the maximum AV_{min} was 25.09 %. This is a difference of 7.52%, which is about 2 cubic feet in a cubic yard of concrete. These results clearly show that aggregate type and total gradation significantly influence the voids in the aggregate and therefore the required paste content.

Past research indicates that a PV/AV of 1.5 is sufficient to achieve workability (Yurdakul et al. (2013). This research indicates that the required PV for paving mixtures in Oregon is very dependent on both the coarse and fine aggregate characteristics. Concrete containing quarry rock required, on average, a PV/AV of 1.7; concrete containing crushed gravel required an average PV/AV of about 1.9; and concrete containing gravel required an average PV/AV of 1.7. Results also indicate that concrete containing sand with a finer FM required an average PV/AV of almost 1.9 and a concrete with a coarse sand required an average PV/AV of 1.55. This research clearly shows that testing of the aggregates to quantify the volume of the aggregate voids prior to mixture proportioning provides valuable information that can be used to minimize the paste content of concretes used for concrete pavements. Trial mixtures can then be mixed to identify a PV/AV to achieve required workability and performance.

Note that all mixtures assessed in this research contained a water-reducing admixture at quantities typically used in the field. Increasing water-reducer content may result in reduced OPC quantities.

This research assessed both the fresh and hardened characteristics of concretes proportioned with the new mixture proportioning methodology.

7.1 CONCLUSIONS

The following conclusions can be drawn regarding aggregate packing and minimizing air voids in the aggregates:

1. Increasing the coarse aggregates to a coarser gradation decreased the AV_{min} , irrespective of the type of sand used.
2. Using finer sand resulted in lower AV_{min} values, irrespective of the coarse aggregate type and coarse aggregate gradation.
3. When a coarser sand (higher FM) was used, the coarse aggregate type seemed to have a more pronounced influence on aggregate voids.
4. Irrespective of the coarse aggregate type, the aggregate system with the coarser coarse aggregates and the finer sand exhibited the lowest AV_{min}
5. The system with finer coarse aggregates and coarser sand had the highest AV_{min} .

The following conclusions can be drawn from the research regarding edge slump and surface voids, as determined using the Box Test, of the concretes proportioned using the new proportioning method:

1. The average edge slump increases with increasing cementitious materials content.
2. In general, the edge slump increases with increasing cementitious paste content for specific aggregate gradations and aggregate types.

3. The lowest cementitious materials content required to pass the box test was 493 lbs/cy; this is significantly lower than ODOT's current practice of using 611 lbs/cy.
4. All mixtures evaluated in Phase 2C, except mixture 24, passed the surface void requirements of the Box Test. This indicates that passing surface void requirements of the Box Test is very dependent on aggregate type, gradation, and fine to coarse aggregate ratio.

The following conclusions can be drawn from the research regarding hardened properties of the concretes proportioned using the new proportioning method:

1. All concretes met ODOT requirements for compressive strength at 28 days; 56-day strengths were on average about 10% higher than the 28-day compressive strength values.
2. Compressive strength is dependent on paste volume or cementitious materials content up to some optimum value, followed by no increase or a decrease in strength.
3. Most concretes assessed herein met ODOT's flexural strength requirement at 28 days. Only two mixtures containing fly ash did not meet the 600 psi (4.1 MPa) requirement. All concretes met the 600 psi (4.1 MPa) requirement at 56 days.
4. Results indicate that flexural strength is independent of paste content, assuming the concrete is placeable.
5. Almost 80% of the specimens passed the minimum formation factor specified in AASHTO PP 84 (2020b) (1000 units). This research used a 63-day cure time instead of the 91-day cure time specified by AASHTO PP 84 (2020b) due to time constraints. All mixtures would be assumed to meet the minimum AASHTO requirements at a 91-day cure.
6. Results from unrestrained length change testing indicates little correlation between paste content and magnitude of shrinkage; however, this may be a result of the testing protocol. Early-age length change is not assessed in this test and further research is needed. Shrinkage testing using shrinkage rings indicates shrinkage is dependent on paste content. However, only limited testing was performed in this research and additional testing is highly recommended to identify paste contents that can minimize shrinkage and concrete cracking.
7. A select number of specimens were evaluated for freeze-thaw performance. The limited testing indicated that specimens may be subject to freeze-thaw damage as 4 out of 6 mixtures exhibited durability factors of less than 60 before or at 300 cycles. It should be noted that only 6 mixtures were assessed and all mixtures contained crushed river gravel. Void spacing and void size were not assessed and further research is needed to quantify freeze-thaw performance.

7.2 RECOMMENDATIONS

This research developed a new procedure for mixture proportioning for concrete used in pavement projects. The new proportioning procedure assumes that the aggregate sources for the concrete has been identified and are available to be assessed. When the aggregates are available, the following recommendations are made:

- If possible, use coarser coarse aggregate gradations with finer sands in concrete used for pavements.
- If aggregate characteristics are not provided or known, characterize the aggregates for gradation, specific gravity, and absorption (AASHTO T 27 (2020a), AASHTO T 84 (2013a), and AASHTO T 85 (2014b))
- Evaluate different combination of fine and course aggregates to identify the F/C that results in the lowest AV (AV_{\min}); this is referred to as F/C_{opt} ;
- After identifying the F/C_{opt} and AV_{\min} , identify a range of PV/ AV_{\min} values that should provide required workability characteristics;
- Make corrections to the trial mixtures to yield 1 unit of concrete (i.e., 1 cubic yard, 1 cubic meter);
- Mix trial batches at the PV/ AV_{\min} values identified and select the mixture with the paste content that provides adequate workability at the lowest paste (and cementitious materials) content;
- Evaluate the harden properties of the concrete to ensure these meet specification requirements.

These procedures should provide a concrete mixture that minimizes OPC and paste content, which will lead to paving concrete that is more environmentally friendly, more economical, and more durable. However, because durability was only assessed for a limited number of mixtures, additional research is needed to confirm the durability of these systems.

7.3 NEEDED RESEARCH

This research focused on developing a procedure to minimize the paste (and OPC) content of concretes used for pavements. By reducing the OPC content, concrete can become more environmentally friendly and more economical. However, the benefits of having a concrete that is initially more environmentally friendly and has a lower initial cost can be lost if the concrete is not long-lasting. Durability is critical minimizing life-cycle cost and value.

This research performed some limited evaluations of concretes proportioned with the new methodology. Insufficient data were obtained on shrinkage and freeze-thaw performance of these concretes. In addition, additional performance data on potential transport rates of aggressive ions (e.g., salts) would be beneficial and valuable. It is recommended that a comprehensive assessment of concretes proportioned with the new proportioning methodology be performed. The research should include a comprehensive program to assess the shrinkage (using shrinkage

rings), freeze-thaw durability, chloride transport rates, and possibly formation factor for these concretes. Once the durability assessment is performed, lower costing, long-lasting concrete, that is more environmentally friendly, can be used for pavements in Oregon.

8.0 REFERENCES

- Aïm, R., & le Goff, P. (1968). La coordinance des empilements désordonnés de sphères. Application aux mélanges binaires de sphères. *Powder Technology*, 2(1), 1–12. [https://doi.org/10.1016/0032-5910\(68\)80027-0](https://doi.org/10.1016/0032-5910(68)80027-0)
- American Association of State Highway and Transportation Officials, (AASHTO). (1991). *Standard method of test for sampling of aggregates* (Standard No T 2). Washington, DC. Retrieved from <https://standards.globalspec.com/std/9945233/AASHTO%20T%202>
- American Association of State Highway and Transportation Officials, (AASHTO). (2008). *Standard method of test for estimating the cracking tendency of concrete* (Standard No. T 334) Washington, DC. Retrieved from <https://standards.globalspec.com/std/2028853/aashto-t-334>
- American Association of State Highway and Transportation Officials, (AASHTO). (2013a). *Standard method of test for specific gravity and absorption of fine aggregate* (Standard No. T 84). Washington, DC. Retrieved from <https://standards.globalspec.com/std/10182254/aashto-t-84>
- American Association of State Highway and Transportation Officials, (AASHTO). (2013b). *Standard test method for air-void characteristics of freshly mixed concrete by buoyancy change* (Standard No. T 348). Washington, DC. Retrieved from <https://standards.globalspec.com/std/10289655/aashto-t-348>
- American Association of State Highway and Transportation Officials, (AASHTO). (2014a). *Standard method of test for bulk density (“unit weight”) and voids in aggregate* (Standard No. T 19M). Washington, DC. Retrieved from <https://standards.globalspec.com/std/13053318/aashto-t-19m-t-19>
- American Association of State Highway and Transportation Officials, (AASHTO). (2014b). *Standard method of test for specific gravity and absorption of coarse aggregate* (Standard No. T 85). Washington, DC. Retrieved from <https://standards.globalspec.com/std/13053335/aashto-t-85>
- American Association of State Highway and Transportation Officials, (AASHTO). (2015a). *Standard method of test for electrical resistivity of a concrete cylinder tested in a uniaxial resistance test* (Standard No. TP 119). Washington, DC. Retrieved from <https://standards.globalspec.com/std/13344855/aashto-tp-119>
- American Association of State Highway and Transportation Officials, (AASHTO). (2015b). *Standard method of test for electrical indication of concrete’s ability to resist chloride ion penetration* (Standard No. T 277). Washington, DC. Retrieved from <https://standards.globalspec.com/std/13344840/aashto-t-277>

- American Association of State Highway and Transportation Officials, (AASHTO). (2017a). *Standard method of test for compressive strength of cylindrical concrete specimens* (Standard No. T 22). Washington, DC. Retrieved from <https://standards.globalspec.com/std/10159810/aashto-t-22>
- American Association of State Highway and Transportation Officials, (AASHTO). (2017b). *Standard method of test for flexural strength of concrete (using simple beam with third-point loading)* (Standard No. T 97). Washington, DC. Retrieved from <https://standards.globalspec.com/std/10159812/aashto-t-97>
- American Association of State Highway and Transportation Officials, (AASHTO). (2017c). *Standard method of test for characterization of the air-void system of freshly mixed concrete by the sequential pressure method* (Standard No. TP 118). Washington, DC. Retrieved from <https://standards.globalspec.com/std/10289591/aashto-tp-118>
- American Association of State Highway and Transportation Officials, (AASHTO). (2017d). *Standard method of test for length change of hardened hydraulic cement mortar and concrete* (Standard No. T 160). Washington, DC. Retrieved from <https://standards.globalspec.com/std/10159815/aashto-t-160>
- American Association of State Highway and Transportation Officials, (AASHTO). (2017e). *Standard method of test for resistance of concrete to rapid freezing and thawing* (Standard No T 161). Washington, DC. Retrieved from <https://standards.globalspec.com/std/10159814/aashto-t-161>
- American Association of State Highway and Transportation Officials, (AASHTO). (2018). *Standard method of test for slump of hydraulic cement concrete* (Standard No. T 119M). Washington, DC. Retrieved from <https://standards.globalspec.com/std/10289658/aashto-t-119m-t-119>
- American Association of State Highway and Transportation Officials, (AASHTO). (2019a). *Standard method of test for density (unit weight), yield, and air content (gravimetric) of concrete* (Standard No. T 121M). Washington, DC. Retrieved from <https://standards.globalspec.com/std/13344869/aashto-t-121m-t-121>
- American Association of State Highway and Transportation Officials, (AASHTO). (2019b). *Standard method of test for air content of freshly mixed concrete by the pressure method* (Standard No. T 152). Washington, DC. Retrieved from <https://standards.globalspec.com/std/13344875/aashto-t-152>
- American Association of State Highway and Transportation Officials, (AASHTO). (2019c). *Standard method of test for surface resistivity indication of concrete's ability to resist chloride ion penetration* (Standard No. T 358). Washington, DC. Retrieved from <https://standards.globalspec.com/std/13344862/aashto-t-358>
- American Association of State Highway and Transportation Officials, (AASHTO). (2020a). *Standard method of test for sieve analysis of fine and coarse aggregates* (Standard No. T

- 27). Washington, DC. Retrieved from <https://standards.globalspec.com/std/14316742/aashto-t-27>
- American Association of State Highway and Transportation Officials, (AASHTO). (2020b). *Standard practice for developing performance engineered concrete pavement mixtures* (Standard No. PP 84). Washington, DC. Retrieved from <https://standards.globalspec.com/std/14221373/AASHTO%20PP%2084>
- ASTM International. (2006). *Standard test method for index of aggregate particle shape and texture* (Standard No. D3398). West Conshohocken, PA. Retrieved from <https://www.astm.org/Standards/D3398.htm>
- ASTM International. (2013). *Standard test method for density, absorption, and voids in hardened concrete* (Standard No. C642-13). West Conshohocken, PA. Retrieved from <https://www.astm.org/Standards/C642.htm>
- ASTM International. (2016). *Standard test method for microscopical determination of parameters of the air-void system in hardened concrete* (Standard No. C457/C457M-16). West Conshohocken, PA. Retrieved from <https://www.astm.org/Standards/C457.htm>
- ASTM International. (2017). *Standard test method for bulk density (“unit weight”) and voids in aggregate* (Standard No. C29/C29M-17a). West Conshohocken, PA. Retrieved from <https://www.astm.org/Standards/C29.htm>
- ASTM International. (2021). *Standard specification for Portland cement* (Standard No. C150/C150M-21). West Conshohocken, PA. Retrieved from <https://www.astm.org/Standards/C150>
- Andrade, C. (1993). Calculation of chloride diffusion coefficients in concrete from ionic migration measurements. *Cement and Concrete Research*, 23(3), 724–742. [https://doi.org/10.1016/0008-8846\(93\)90023-3](https://doi.org/10.1016/0008-8846(93)90023-3)
- Bentz, D. P. (2007). A virtual rapid chloride permeability test. *Cement and Concrete Composites*, 29(10), 723–731. <https://doi.org/10.1016/j.cemconcomp.2007.06.006>
- Bu, Y., & Weiss, J. (2014). The influence of alkali content on the electrical resistivity and transport properties of cementitious materials. *Cement and Concrete Composites*, 51, 49–58. <https://doi.org/10.1016/j.cemconcomp.2014.02.008>
- Caltrans. (2018). *Standard specifications*. Retrieved from <https://dot.ca.gov/-/media/dot-media/programs/design/documents/f00203402018stdspecs-a11y.pdf>
- Cook, D. M., Ghaeezadeh, A., Ley, M. T., & Russell, B. W. (2013). *Investigation of optimized graded concrete for Oklahoma – Phase 1* (Report No. FHWA-OK-13-12). Oklahoma City, OK: Oklahoma Department of Transportation. Retrieved from <https://shareok.org/bitstream/handle/11244/54452/FHWA-OK-13-12%202160%20Cook.pdf?sequence=1&isAllowed=y>

- Cook, M. D., Ghazeezadah, A., & Ley, M. T. (2014). A workability test for slip formed concrete pavements. *Construction and Building Materials*, 68, 376–383. <https://doi.org/10.1016/j.conbuildmat.2014.06.087>
- Coyle, A., Spragg, R., Amirkhanian, A., & Weiss, J. (2016). Measuring the influence of temperature on electrical properties of concrete. In *International Rilem Conference on materials, systems and structures in Civil Engineering, 2016: Segment on moisture in materials and structures: Lyngby, Denmark, August 22-24, 2016*. Paris: RILEM publications.
- Coyle, A. (2017). *The Effects of temperature on electrical resistivity measurements of concrete* (Master's thesis, Corvallis, OR / Oregon State University, 2017). Corvallis: OSU.
- Cramer, S. M., & Carpenter, A. J. (1999). Influence of total aggregate gradation on freeze-thaw durability and other performance measures of paving concrete. *Transportation Research Record: Journal of the Transportation Research Board*, 1668(1), 1–8. <https://doi.org/10.3141/1668-01>
- Cramer, S. M., Hall, M., & Parry, J. (1995). Effect of optimized total aggregate gradation on Portland cement concrete for Wisconsin pavements. *Transportation Research Record*, 1478, 100–106. Retrieved from <https://onlinepubs.trb.org/Onlinepubs/trr/1995/1478/1478-013.pdf>
- de Larrard, F. (1999). *Concrete mixture proportioning: A scientific approach* (1st ed.). Boca Raton, FL: CRC Press. <https://doi.org/10.1201/9781482272055>
- Distlehorst, J. A., & Kurgan, G. J. (2007). Development of precision statement for determining air void characteristics of fresh concrete with use of air void analyzer. *Transportation Research Record: Journal of the Transportation Research Board*, 2020(1), 45–49. <https://doi.org/10.3141/2020-06>
- Du, L., & Folliard, K. J. (2005). Mechanisms of air entrainment in concrete. *Cement and Concrete Research*, 35(8), 1463–1471. <https://doi.org/10.1016/j.cemconres.2004.07.026>
- Elkey, W., & Sellevold, E. J. (1995). *Electrical resistivity of concrete* (Publication No. 80). Oslo, Norway: Norwegian Road Research Laboratory. Retrieved from <https://vegvesen.brage.unit.no/vegvesen-xmlui/bitstream/handle/11250/191626/Publication%2080.pdf?sequence=1>
- Fuller, W. B., & Thompson, S. E. (1907). The laws of proportioning concrete. *Transactions of the American Society of Civil Engineers*, 59(2), 67–143. <https://doi.org/10.1061/taceat.0001979>
- Furnas, C. C. (1929). *Flow of gases through beds of broken solids*. Washington, D.C.: U.S. Government Printing Office.
- Gaynor, R.D. (1963). Effects of Prolonged Mixing on the Properties of Concrete, *National Ready Mixed Concrete Association*, Publication 111, Washington DC, June 1963, pp. 18.

- Goltermann, P., Johansen, V., & Palbol, L. (1997). Packing of aggregates: An alternative tool to determine the optimal aggregate mix. *ACI Materials Journal*, 94(5), 435–443. <https://doi.org/10.14359/328>
- He, Z., Zhu, X., Wang, J., Mu, M., & Wang, Y. (2019). Comparison of CO₂ emissions from OPC and recycled cement production. *Construction and Building Materials*, 211, 965–973. <https://doi.org/10.1016/j.conbuildmat.2019.03.289>
- Hendrix, G. (2015). *Development of a new mixture proportioning method and assessing the influence of material characteristics on flowing concrete mixtures*. (Master's thesis, Corvallis, OR / Oregon State University, 2017). Corvallis: OSU.
- Hendrix, G., & Trejo, D. (2017). New mixture proportioning method for flowing concrete mixtures. *ACI Materials Journal*, 114(4). <https://doi.org/10.14359/51689894>
- Holland, J. A. (1990). Mixture optimization. *Concrete International*, 12(10), 10.
- Hover, K. C. (1998). Concrete mixture proportioning with water-reducing admixtures to enhance durability: A quantitative model. *Cement and Concrete Composites*, 20(2–3), 113–119. [https://doi.org/10.1016/s0958-9465\(98\)00002-x](https://doi.org/10.1016/s0958-9465(98)00002-x)
- Huang, E. Y. (1962). In-Situ stability of soil-aggregate road materials. *Journal of the Highway Division*, 88(1), 43–70. <https://doi.org/10.1061/jhcea2.0000149>
- Imbabi, M. S., Carrigan, C., & McKenna, S. (2012). Trends and developments in green cement and concrete technology. *International Journal of Sustainable Built Environment*, 1(2), 194–216. <https://doi.org/10.1016/j.ijsbe.2013.05.001>
- Illinois Department of Transportation. (2016). *Standard specifications for road and bridge construction*. Retrieved from <https://idot.illinois.gov/Assets/uploads/files/Doing-Business/Manuals-Guides-&-Handbooks/Highways/Construction/Standard-Specifications/Standard%20Specifications%20for%20Road%20and%20Bridge%20Const ruction%202016.pdf>
- Iowa Department of Transportation. (2015). *Standard specifications for highway and bridge construction*. Retrieved from <https://www.iowadot.gov/specifications/pdf/completebook.pdf>
- Jacobsen, S., & Arntsen, B. (2008). Aggregate packing and -void saturation in mortar and concrete proportioning. *Materials and Structures*, 41(4), 703–716. <https://doi.org/10.1617/s11527-007-9275-4>
- Jamkar, S., & Rao, C. (2004). Index of aggregate particle shape and texture of coarse aggregate as a parameter for concrete mix proportioning. *Cement and Concrete Research*, 34(11), 2021–2027. <https://doi.org/10.1016/j.cemconres.2004.03.010>

- Jerath, S., & Hanson, N. (2007). Effect of fly ash content and aggregate gradation on the durability of concrete pavements. *Journal of Materials in Civil Engineering*, 19(5), 367–375. [https://doi.org/10.1061/\(asce\)0899-1561\(2007\)19:5\(367\)](https://doi.org/10.1061/(asce)0899-1561(2007)19:5(367))
- Ley, T., Cook, D., & Fick, G. (2012). *Concrete pavement mixture design and analysis (MDA): Effect of aggregate systems on concrete properties* (Report No. Part of DTFH61-06-H-00011 Work Plan 25). Washington, D.C.: Federal Highway Administration. Retrieved from <https://rosap.ntl.bts.gov/view/dot/26335>
- Ley, T., & Tabb, B. (2013). *Development of a robust field technique to quantify the air-void distribution in fresh concrete* (Report No. OTCREOS9. 1-31-F). Midwest City, OK: Oklahoma Transportation Center. Retrieved from <https://rosap.ntl.bts.gov/view/dot/27051>
- Li, Z., Xiao, L., & Wei, X. (2007). Determination of concrete setting time using electrical resistivity measurement. *Journal of Materials in Civil Engineering*, 19(5), 423–427. [https://doi.org/10.1061/\(asce\)0899-1561\(2007\)19:5\(423\)](https://doi.org/10.1061/(asce)0899-1561(2007)19:5(423))
- Mamirov, M. (2019). *Using theoretical and experimental particle packing for aggregate gradation optimization to reduce cement content in pavement concrete mixtures* (Master's thesis). Lincoln, NE / University of Nebraska - Lincoln. Retrieved from <https://digitalcommons.unl.edu/cgi/viewcontent.cgi?article=1141&context=civilengdiss>
- Mangulkar, M., & Jamkar, S. (2013). Review of particle packing theories used for concrete mix proportioning. *International Journal of Scientific & Engineering Research* 4(5), 143-148.
- Matthes, W., Vollpracht, A., Villagrán, Y., Kamali-Bernard, S., Hooton, D., Gruyaert, E., . . . De Belie, N. (2018). Ground granulated blast-furnace slag. In *Properties of Fresh and Hardened Concrete Containing Supplementary Cementitious Materials* (1st ed., pp. 1–53). Springer. https://doi.org/10.1007/978-3-319-70606-1_1
- Monteiro, P. J. M., Miller, S. A., & Horvath, A. (2017). Towards sustainable concrete. *Nature Materials*, 16(7), 698–699. <https://doi.org/10.1038/nmat4930>
- Naik, T. R. (2005). Sustainability of cement and concrete industrie. In *Achieving sustainability in construction: Proceedings of the International Conference held at the University of Dundee, Scotland, UK on 5-7 July 2005*. London: Thomas Telford.
- Nokken, M. R., & Hooton, R. D. (2008). Using pore parameters to estimate permeability or conductivity of concrete. *Materials and Structures*, 41(1), 1–16. <https://doi.org/10.1617/s11527-006-9212-y>
- Park, H. M. (2009). *Comparing group means: T-tests and one-way ANOVA using Stata, SAS, R, and SPSS*. Bloomington, IN: University Information Technology Services Center for Statistical and Mathematical Computing Indiana University. Retrieved from https://scholarworks.iu.edu/dspace/bitstream/handle/2022/19735/T-tests_and_One-way_ANOVA_Using%20Stata_SAS_R_SPSS.pdf?sequence=1&isAllowed=y

- Pennsylvania Department of Transportation. (2017). *Construction specifications* (Standard No. PUB 408/2016-3). Retrieved from https://www.dot.state.pa.us/public/PubsForms/Publications/Pub_408/408_2016/408_2016_IE/408_2016_IE.pdf
- Piasta, W., & Zarzycki, B. (2017). The effect of cement paste volume and w/c ratio on shrinkage strain, water absorption and compressive strength of high performance concrete. *Construction and Building Materials*, *140*, 395–402. <https://doi.org/10.1016/j.conbuildmat.2017.02.033>
- Powers, T. C. (1968). *The properties of fresh concrete* (First Edition). Hoboken, NJ: John Wiley & Sons.
- Ramezani-pour, A. A., Pilvar, A., Mahdikhani, M., & Moodi, F. (2011). Practical evaluation of relationship between concrete resistivity, water penetration, rapid chloride penetration and compressive strength. *Construction and Building Materials*, *25*(5), 2472–2479. <https://doi.org/10.1016/j.conbuildmat.2010.11.069>
- Richardson, D. N. (2005). *Aggregate gradation optimization--Literature search* (Report No. RDT 05-001). Jefferson City, MO: Missouri Department of Transportation. Retrieved from https://scholarsmine.mst.edu/cgi/viewcontent.cgi?article=1001&context=civarc_enveng_facwork
- Riding, K. A., Poole, J. L., Schindler, A. K., Juenger, M. C., & Folliard, K. J. (2008). Simplified concrete resistivity and rapid chloride permeability test method. *ACI Materials Journal*, *105*(4), 390–394. <https://doi.org/10.14359/19901>
- Rudy, A., & J. Olek. (2012). *Optimization of mixture proportions for concrete pavements—Influence of supplementary cementitious materials, paste content and aggregate gradation* (Publication No. FHWA/IN/JTRP-2012/34). West Lafayette, Indiana: Joint Transportation Research Program, Indiana Department of Transportation and Purdue University. doi: 10.5703/1288284315038.
- Rupnow, T. D., & Icenogle, P. J. (2012). Surface resistivity measurements evaluated as alternative to rapid chloride permeability test for quality assurance and acceptance. *Transportation Research Record: Journal of the Transportation Research Board*, *2290*(1), 30–37. <https://doi.org/10.3141/2290-04>
- Sant, G., Ferraris, C. F., & Weiss, J. (2008). Rheological properties of cement pastes: A discussion of structure formation and mechanical property development. *Cement and Concrete Research*, *38*(11), 1286–1296. <https://doi.org/10.1016/j.cemconres.2008.06.008>
- Skarendahl, Å., & Petersson, Ö. (1999). *PRO 7: 1st international RILEM symposium on Self-Compacting concrete* (Vol. 7). Stockholm, Sweden: RILEM Publications.
- Snyder, K., Feng, X., Keen, B., & Mason, T. (2003). Estimating the electrical conductivity of cement paste pore solutions from OH⁻, K⁺ and Na⁺ concentrations. *Cement and Concrete Research*, *33*(6), 793–798. [https://doi.org/10.1016/s0008-8846\(02\)01068-2](https://doi.org/10.1016/s0008-8846(02)01068-2)

- Stovall, T., de Larrard, F., & Buil, M. (1986). Linear packing density model of grain mixtures. *Powder Technology*, 48(1), 1–12. [https://doi.org/10.1016/0032-5910\(86\)80058-4](https://doi.org/10.1016/0032-5910(86)80058-4)
- Tanesi, J., Kim, H., Beyene, M., & Ardani, A. (2016). Super air meter for assessing Air-Void system of fresh concrete. *Advances in Civil Engineering Materials*, 5(2), 22–37. <https://doi.org/10.1520/acem20150009>
- Tanesi, J., & Meininger, R. (2007). Freeze-thaw resistance of concrete with marginal air content. *Transportation Research Record: Journal of the Transportation Research Board*, 2020(1), 61–66. <https://doi.org/10.3141/2020-08>
- Tazawa, E., Yonekura, A., & Tanaka, S. (1989). Drying shrinkage and creep of concrete containing granulated blast furnace slag. *Special Publication*, 114, 1325-1344. doi:[10.14359/2604](https://doi.org/10.14359/2604)
- Texas Department of Transportation. (2014). *Standard specifications for construction and maintenance of highways, streets, and bridges*. Retrieved from <https://ftp.txdot.gov/pub/txdot-info/cmd/cserve/specs/2014/standard/specbook-2014.pdf>
- Thomas, M. (2007). *Optimizing the use of fly ash in concrete* (Vol. 5420). Skokie, IL: Portland Cement Association. Retrieved from https://www.cement.org/docs/default-source/fc_concrete_technology/is548-optimizing-the-use-of-fly-ash-concrete.pdf
- Tumidajski, P., Schumacher, A., Perron, S., Gu, P., & Beaudoin, J. (1996). On the relationship between porosity and electrical resistivity in cementitious systems. *Cement and Concrete Research*, 26(4), 539–544. [https://doi.org/10.1016/0008-8846\(96\)00017-8](https://doi.org/10.1016/0008-8846(96)00017-8)
- Vavrik, W. R., Pine, W. J., & Carpenter, S. H. (2002). Aggregate blending for asphalt mix design: Bailey method. *Transportation Research Record: Journal of the Transportation Research Board*, 1789(1), 146–153. <https://doi.org/10.3141/1789-16>
- Wee, T., Suryavanshi, A. K., & Tin, S. (2000). Evaluation of rapid chloride permeability test (RCPT) results for concrete containing mineral admixtures. *ACI Materials Journal*, 97(2), 221–232. <https://doi.org/10.14359/827>
- Weiss, W. J., Spragg, R. P., Isgor, O. B., Ley, M. T., & Van Dam, T. (2018). *Toward performance specifications for concrete: linking resistivity, RCPT and diffusion predictions using the formation factor for use in specifications*. In: Hordijk D., Luković M. (eds) High Tech Concrete: Where Technology and Engineering Meet. Springer, Cham. https://doi.org/10.1007/978-3-319-59471-2_235
- Welchel, D. (2012). *Determining the air-void distribution of fresh concrete with the sequential pressure method* (Unpublished master's thesis). Stillwater, OK / Oklahoma State University. Retrieved from <https://core.ac.uk/download/pdf/215260671.pdf>
- Yang, J., Wang, Q., & Zhou, Y. (2017). Influence of curing time on the drying shrinkage of concretes with different binders and Water-to-Binder ratios. *Advances in Materials Science and Engineering*, 2017, 1–10. <https://doi.org/10.1155/2017/2695435>

- Yuan, J., Lindquist, W., Darwin, D., & Browning, J. (2015). Effect of slag cement on drying shrinkage of concrete. *ACI Materials Journal*, *112*(2), 267–276.
<https://doi.org/10.14359/51687129>
- Yurdakul, E., Taylor, P. C., Ceylan, H., & Bektas, F. (2013). Effect of Paste-to-Voids volume ratio on the performance of concrete mixtures. *Journal of Materials in Civil Engineering*, *25*(12), 1840–1851. [https://doi.org/10.1061/\(asce\)mt.1943-5533.0000728](https://doi.org/10.1061/(asce)mt.1943-5533.0000728)
- Zhang, W., Hama, Y., & Na, S. H. (2015). Drying shrinkage and microstructure characteristics of mortar incorporating ground granulated blast furnace slag and shrinkage reducing admixture. *Construction and Building Materials*, *93*, 267–277.
<https://doi.org/10.1016/j.conbuildmat.2015.05.103>

APPENDIX

This appendix includes Figure A.1 through Figure A.59: Concrete finished surface after screeding and troweling (Mixture 23) which include photos taken during mixing and placing of fresh concrete during the Phase 2C study. These are presented to provide the reader with a sense of the placeability and workability of the concrete mixtures. Photos for mixtures 19, 24, and 25 were not taken and are not provided herein.

MIXTURE 1



Figure A.1: Surface-void profile for one of the sides of box test specimen (Mixture 1)



Figure A.2: Overview of box test specimen (Mixture 1)



Figure A.3: Result from slump testing (Mixture 1)



Figure A.4: Concrete finished- surface after screeding and troweling (Mixture 1)

MIXTURE 2



Figure A.5: Surface-void profile for one of the sides of box test specimen (Mixture 2)



Figure A.6: Result from slump testing (Mixture 2)



Figure A.7: Concrete finished surface after screeding and troweling (Mixture 2)

MIXTURE 3



Figure A.8: Surface-void profile for one of the sides of box test specimen (Mixture 3)



Figure A.9: Overview of box test specimen (Mixture 3)



Figure A.10: Result from slump testing (Mixture 3)



Figure A.11: Concrete finished surface after screeding and troweling (Mixture 3)

MIXTURE 4



Figure A.12: Surface-void profile for one of the sides of box test specimen (Mixture 4)



Figure A.13: Overview of box test specimen (Mixture 4)



Figure A.14: Result from slump testing (Mixture 4)



Figure A.15: Concrete finished surface after screeding and troweling (Mixture 4)

MIXTURE 5



Figure A.16: Surface-void profile for one of the sides of box test specimen (Mixture 5)



Figure A.17: Overview of box test specimen (Mixture 5)



Figure A.18: Result from slump testing (Mixture 5)



Figure A.19: Concrete finished surface after screeding and troweling (Mixture 5)

MIXTURE 6



Figure A.20: Surface-void profile for one of the sides of box test specimen (Mixture 6)



Figure A.21: Overview of box test specimen (Mixture 6)



Figure A.22: Result from slump testing (Mixture 6)



Figure A.23: Concrete finished surface after screeding and troweling (Mixture 6)

MIXTURE 7



Figure A.24: Surface-void profile for one of the sides of box test specimen (Mixture 7)



Figure A.25: Result from slump testing (Mixture 7)



Figure A.26: Concrete finished surface after screeding and troweling (Mixture 7)

MIXTURE 8



Figure A.27: Surface-void profile for one of the sides of box test specimen (Mixture 8)



Figure A.28: Result from slump testing (Mixture 8)



Figure A.29: Concrete finished surface after screeding and troweling (Mixture 8)

MIXTURE 9



Figure A.30: Surface-void profile for one of the sides of box test specimen (Mixture 9)



Figure A.31: Result from slump testing (Mixture 9)



Figure A.32: Concrete finished surface after screeding and troweling (Mixture 9)

MIXTURE 10



Figure A.33: Surface-void profile for one of the sides of box test specimen (Mixture 10)



Figure A.34: Result from slump testing (Mixture 10)



Figure A.35: Concrete finished surface after screeding and troweling (Mixture 10)

MIXTURE 11



Figure A.36: Surface-void profile for one of the sides of box test specimen (Mixture 11)



Figure A.37: Result from slump testing (Mixture 11)



Figure A.38: Concrete finished surface after screeding and troweling (Mixture 11)

MIXTURE 12



Figure A.39: Surface-void profile for one of the sides of box test specimen (Mixture 12)



Figure A.40: Result from slump testing (Mixture 12)



Figure A.41: Concrete finished surface after screeding and troweling (Mixture 12)

MIXTURE 13



Figure A.42: Surface-void profile for one of the sides of box test specimen (Mixture 13)



Figure A.42: Result from slump testing (Mixture 13)



Figure A.43: Concrete finished surface after screeding and troweling (Mixture 13)

MIXTURE 14



Figure A.44: Surface-void profile for one of the sides of box test specimen (Mixture 14)



Figure A.45: Result from slump testing (Mixture 14)



Figure A.46: Concrete finished surface after screeding and troweling (Mixture 14)

MIXTURE 15



Figure A.47: Surface-void profile for one of the sides of box test specimen (Mixture 15)



Figure A.48: Result from slump testing (Mixture 15)



Figure A.50: Concrete finished surface after screeding and troweling (Mixture 15)

MIXTURE 16



Figure A.51: Surface-void profile for one of the sides of box test specimen (Mixture 16)



Figure A.52: Concrete finished surface after screeding and troweling (Mixture 16)

MIXTURE 17



Figure A.49: Surface-void profile for one of the sides of box test specimen (Mixture 17)



Figure A.50: Result from slump testing (Mixture 17)



Figure A.51: Concrete finished surface after screeding and troweling (Mixture 17)

MIXTURE 18



Figure A.52: Surface-void profile for one of the sides of box test specimen (Mixture 18)



Figure A.53: Surface-void profile for one of the sides of box test specimen (Mixture 18)



Figure A.54: Concrete finished surface after screeding and troweling (Mixture 18)

MIXTURE 20



Figure A.55: Surface-void profile for one of the sides of box test specimen (Mixture 20)

MIXTURE 21



Figure A.60: Surface-void profile for one of the sides of box test specimen (Mixture 21)

MIXTURE 22



Figure A.61: Surface-void profile for one of the sides of box test specimen (Mixture 22)



Figure A.62: Result from slump testing (Mixture 22)



Figure A.56: Concrete finished surface after screeding and troweling (Mixture 22)

MIXTURE 23



Figure A.57: Surface-void profile for one of the sides of box test specimen (Mixture 23)



Figure A.58: Result from slump testing (Mixture 23)



Figure A.59: Concrete finished surface after screeding and troweling (Mixture 23)